

Selection of Multilateral Well Configuration on Ekofisk South

Bjørnar Nesland

Petroleum Geoscience and Engineering

Submission date: June 2013 Supervisor: Pål Skalle, IPT

Norwegian University of Science and Technology Department of Petroleum Engineering and Applied Geophysics

i. Acknowledgement

This Master Thesis has been written in cooperation with ConocoPhillips Norway (COPNO) and submitted to the Department of Petroleum Engineering and Applied Geophysics at the Norwegian University of Science and Technology.

First of all I would like to thank Jan Roger Berg, and the rest of the Well Operations group at COPNO, for giving me this opportunity and for letting me make use of COPNO's office and facilities in Stavanger.

To my supervisor at COPNO, Tove Husby, I would like to express my largest gratitude for her excellent guidance and support, quality control and assurance, and for pushing me to perform my best at all times.

I would also like to thank my academic advisor at NTNU, Pål Skalle, for advices, guidance and feedback throughout the process.

A special thank is given to Rick Watts for his expertise and experience. He has helped me increase my understanding in the subjects covered and has been important for the progression of the thesis.

In addition, a special thank is also given to Gorm Liland in Halliburton for his presentations and technical support related to multilateral junctions and systems. His knowledge has helped me to increase my understanding in the area of multilateral well technology.

In addition I would like to show my thankfulness to the following people for their help and involvement in the thesis:

Arindam Arang - Reservoir targets Helen Haneferd - Junction placement

Reki Indrawan - MLT requirements and reservoir targets

Kjell-Harry Lyngaas - Wellplan support

Thomas Mæland - Drilling Engineering support
Gunnar Namtvedt - Drilling Engineering support
Leif Inge Ramsdal - Creation of well paths

Sindre Sørensen - Various reservoir related issues

Guri Tveitnes - Junction placement Stanley Tørressen - Technical mentoring

Jan P. Vikhammar - Various reservoir related issues

Last, but not the least, I would like to thank my fellow students and good friends at the
Norwegian University of Science and Technology for their support and good spirits
during the period of study.

Trondheim, Norway
11 June 2013
Bjørnar Nesland

«Housework can't kill you, but why take the chance?»

- Phyllis Diller

ii. Abstract

In 2004 ConocoPhillips Norway (COPNO) drilled two multilateral wells in the Ekofisk field in the North Sea. These wells yielded more stable production rates, but had several issues and challenges when it came to junction stability and access to the side-branch. Due to matters related to the reservoir performance and the production rates, as well as optimized utilization of the slot spaces, the drilling of multilateral wells again has been listed as a possible future strategy for COPNO¹.

In this Master Thesis three different multilateral well options, each with a mainbore (Lateral 1) and a side-branch (Lateral 2), for the Ekofisk South area has been evaluated in order to select the optimum configuration for a possible future implementation, based on six given reservoir targets. A project scope was established, including suggestion of junction design, junction placement and well paths. Further were physical limitations and technical challenges related to the drilling of multilateral wells on Ekofisk mapped, before a simulation base representing Ekofisk South was created in the Wellplan software. Based on the results from the simulations, an evaluation of the different multilateral well technology (MLT) options were performed, and a selection of the optimum multilateral well configuration on Ekofisk South for future success optimization with regards to the drilling process was executed.

The report concludes that recommended type of multilateral for Ekofish South, based on the reservoir targets given, is the planar dual-lateral, or forked, multilateral. The junction should be placed in the overburden, 200 - 300 ft above the top of Ekofisk in a stable formation. Of the investigated three MLT options the MLT1 configuration indicates highest possibility of future success with regards to the drilling process. Further, a recommended composition of separate wellbore sections to form a new MLT option would include lateral 1 from MLT1, the 9 ½" lateral 2 section from MLT2 and the 8 ½" lateral 2 section from MLT1. A trend was that that the longer wellbores indicated more issues, and that optimization of the well paths for the wellbore sections leading to the reservoir targets for the MLT options should be performed in order to mitigate any challenges with regards to elevated ECD effects.

Future improvements involve the implementation of actual underground data to the simulation base, and an optimization of both the well paths and the BHA design used in the simulations. Simulations on junction design option 1, as well as investigations on the effects related to under reaming of the 8 %" and the 9 %" hole sections to 9 %" and 10", respectively, summarize the most important suggestions of further work in the field.

¹ Personal communication with J.R Berg. 2013. Stavanger: ConocoPhillips Norway

iii. Sammendrag

I 2004 boret ConocoPhillips Norge (COPNO) to multilaterale brønner på Ekofiskfeltet i Nordsjøen. Disse brønnene gav mer stabile produksjonsrater, men hadde flere problemer og utfordringer i forbindelse med stabilitet av brønnkrysset og tilgang til sidesteget. Som følge av grunner relatert til reservoarytelsen og produksjonsratene, i tillegg til optimal utnyttelse av brønnrammene, er boringen av multilaterale brønner igjen kommet på agendaen som en mulig strategi i fremtiden for COPNO²

I denne Masteroppgaven har tre ulike multilaterale brønnoppsett, hver med en hovedbrønnbane (Sidesteg 1) og en sidegren (Sidesteg 2), for Ekofisk Sør blitt evaluert for å velge en optimal konfigurasjon til en mulig, fremtidig implementering, basert på seks gitte reservoarmål. Et omfang over prosjektet, inneholdende forslag til design av brønnkryss, plassering av brønnkryss og brønnbaner, ble etablert. Videre ble fysiske begrensninger og tekniske utfordringer, relatert til boringen av multilaterale brønner på Ekofisk, kartlagt, før en simuleringsbase, representativ for Ekofisk Sør, ble etablert i softwaren Wellplan. Basert på resultatene fra simuleringene ble en evaluering av de ulike mulighetene for multilateral brønnteknologi utført, og en utvelgelse av den optimale multilaterale brønnkonfigurasjonen på Ekofisk Sør, med mål om å optimalisere fremtidig suksess med tanke på boreprosessen, gjennomført.

Rapporten konkluderer med at den anbefalte multilaterale brønntypen for Ekofisk Sør, basert på de gitte reservoarmålene, er en dobbel-lateral i ett plan, eller en forgrenet multilateral. Brønnkrysset bør være plassert i en stabil formasjon, 200 – 300 fot over toppen av Ekofisk. Av de tre multilaterale brønn-mulighetene som ble utredet indikerte MLT1-konfigurasjonen den høyeste sannsynligheten for fremtidig suksess i forhold til boreprosessen. Videre ville den anbefalte sammensetningen av separate brønnbaner for å danne en ny multilateral brønnmulighet bestå av sidesteg 1 fra MLT1, 9 1/2"-seksjon fra MLT2 og 8 1/2"-seksjon fra MLT1. En trend var at lengre brønnbaner gav indikasjoner om flere problemer, og at en optimalisering av brønnbanene bør bli gjennomført for å redusere utfordringene med tanke på for høye ECD-effekter.

Fremtidige utbedringer involverer implementeringen av reell undergrunnsdata for simuleringsbasen, og en optimalisering av både brønnbaner og BHA-design brukt i simuleringene. Simuleringer på brønnkryss-design alternativ 1, i tillegg til utredninger av effektene som følge av utvidelse av henholdsvis 8 1/2" og 9 1/2" hullseksjoner til 9 1/2" og 10", summerer opp de viktigste forslagene til fremtidig arbeid på området.

_

² Personlig samtale med J.R Berg. 2013. Stavanger: ConocoPhillips Norge

iv. List of Content

	List of Figures	11
	List of Tables	19
1	Introduction	23
2	ConocoPhillips and the Ekofisk area 2.1 ConocoPhillips Company 2.2 ConocoPhillips Norwas 2.3 The Greater Ekofisk Area and the Ekofisk reservoir 2.4 Why drill Multilateral Wells on Ekofisk?	25 25 25 25 32
3	The Multilateral Well Technology 3.1 Development of MLT and the introduction of the TAML standard 3.2 Junction Design and Configurations 3.3 Ongoing R&D on MLT for future, improved utilization in the oilfield	33 33 33 39
4	Setting up possible MLT configurations for Ekofisk 4.1 Reservoir targets 4.2 Designing the project scope 4.3 Geology in the area of planned MLT 4.4 Determination of Junction design and configuration 4.5 Determination of Junction placement 4.6 Well Slot 4.7 Designing the well paths 4.8 Drilling Rig 4.9 Overview of the three MLT options, with all the wellbore sections	41 42 42 45 50 52 53 54
5	Technical challenges related to the drilling of Multilateral Wells 5.1 Dog Leg Severity 5.2 Build-Up Rate 5.3 Effective Tension 5.4 Torque 5.5 Fatigue and Wear of the Drill string 5.6 Drag forces and Hook load 5.7 Minimum WOB to buckle 5.8 Hole Cleaning 5.9 Pressure Losses 5.10 Circulating Pressures and ECD-effects 5.11 Specific challenges on Ekofisk	57 59 61 63 67 68 70 73 75 78

_		_
6	Parameter simulations by using the Wellplan software	81
	6.1 Selection of two input scenarios	81
	6.2 Optimization through iterations	81
	6.3 The Wellplan software	83
	6.4 Simulations to be performed	83
	6.5 Assumptions	85
	6.6 Making of the mother wellbore from surface to the junction point	86
	6.7 Making of the nine wellbore sections for the three MLT options to be	0.5
	simulated in Wellplan	86
	6.8 Input parameters	88
7	Results	93
	7.1 Dog Leg Severity	96
	7.2 Build-Up Rate	97
	7.3 Effective Tension	98
	7.4 Torque	102
	7.5 Fatigue Ratio	104
	7.6 Hook Load	106
	7.7 Torque vs MD	109
	7.8 Minimum WOB to sinusoidal buckle	112
	7.9 Hole Cleaning	114
	7.10 Pressure Losses	117
	7.11 Circulating Pressures vs MD	120
	7.12 ECD vs MD	123
8	Evaluation	127
Ü	8.1 Wellplan results for Scenario 1 and Scenario 2 parameter values	127
	8.2 Wellplan results for suggested parameter input values	129
	8.3 Correlations in the results	130
	8.4 Suggestions to improvements	131
	8.5 Selection of the optimum MLT option based on the drilling process	132
9	Self-Assessment	139
	9.1 Applicability of the work	139
	9.2 Quality and shortcomings	140
	9.3 Possible future improvements and further work	145
10	Conclusions	147
	List of References	153
	Appendix	160

v. List of Figures

Figure 1: Location of the Greater Ekofisk Area in the North Sea (Maxwell 2013)	. 26
Figure 2: Illustration of the Ekofisk reservoir, with Ekofisk and Tor formation	
(ConocoPhillips 2013f)	. 27
Figure 3: Reservoir model of oil saturation in Ekofisk as a function of time	
(ConocoPhillips 2013h)	. 28
Figure 4: Reservoir model of water saturation in Ekofisk as a function of time	
(ConocoPhillips 2013h)	. 28
Figure 5: Top view of the Ekofisk reservoir in the top left corner. The main picture	
displays the size-relationship between the Ekofisk area and the city of Stavanger	
(ConocoPhillips 2013f)	
Figure 6: Ekofisk historical production rates, with timeline of significant events since t	
start in 1971 (ConocoPhillips 2013f)	. 30
Figure 7: Subsidence at the Ekofisk complex shown at the Ekofisk tank. From left the	
pictures are from 1974, 1985 and 2006, respectively (ConocoPhillips 2013f)	
Figure 8: Production rates of 2/4-X-02 and 2/4-X-21, two of the four wells drilled with	
MLT on Ekofisk (ConocoPhillips 2013f)	. 32
Figure 9: TAML junction classification for Multilateral Wells (Frailja, J., Ohmer, H. and Figure 9: TAML junction classification for Multilateral Wells (Frailja, J., Ohmer, H. and Figure 9: TAML junction classification for Multilateral Wells (Frailja, J., Ohmer, H. and Figure 9: TAML junction classification for Multilateral Wells (Frailja, J., Ohmer, H. and Figure 9: TAML junction classification for Multilateral Wells (Frailja, J., Ohmer, H. and Figure 9: TAML junction classification for Multilateral Wells (Frailja, J., Ohmer, H. and Figure 9: TAML junction classification for Multilateral Wells (Frailja, J., Ohmer, H. and Figure 9: TAML junction classification for Multilateral Wells (Frailja, J., Ohmer, H. and Figure 9: TAML junction classification for Multilateral Wells (Frailja, J., Ohmer, H. and Figure 9: TAML junction classification for Multilateral Wells (Frailja, J., Ohmer, H. and Figure 9: TAML junction classification for Multilateral Wells (Frailja, J., Ohmer, H. and Figure 9: TAML junction classification for Multilateral Wells (Frailja, J., Ohmer, H. and Figure 9: TAML junction classification for Multilateral Wells (Frailja, J., Ohmer, H. and Figure 9: TAML junction classification for Multilateral Wells (Frailja, J., Ohmer, H. and Figure 9: TAML junction classification for Multilateral Wells (Frailja, J., Ohmer, H. and Figure 9: TAML junction classification for Multilateral Wells (Frailja, J., Ohmer, H. and Figure 9: TAML junction classification for Multilateral Wells (Frailja, J., Ohmer, H. and Figure 9: TAML junction classification for Multilateral Wells (Frailja, J., Ohmer, H. and Figure 9: TAML junction classification for Multilateral Wells (Frailja, J., Ohmer, H. and Figure 9: TAML junction classification for Multilateral Wells (Frailja, J., Ohmer, H. and Figure 9: TAML junction classification for Multilateral Wells (Frailja, J., Ohmer, H. and Figure 9: TAML junction classification for Multilateral Wells (Frailja, J., Ohmer, H. and Figure 9: TAML junction classification for Multilateral Wells (Fra	nd
Pulick, T. et al. 2002)	
Figure 10: TAML Level 1A and Level 1B Junctions (Weatherford 2006)	. 35
Figure 11: TAML Level 2A and Level 2B Junctions (Weatherford 2006)	. 36
Figure 12: TAML Level 3 Junction (Weatherford 2006)	. 36
Figure 13: TAML Level 4A and Level 4B Junctions (Weatherford 2006)	
Figure 14: TAML Level 5 Junction (Weatherford 2006)	. 38
Figure 15: TAML Level 6A and Level 6B (6S) Junctions (Weatherford 2006)	. 39
Figure 16: Schematic of the well path configuration. Should only be used for overview	⁷ •
The figure is not to be scaled, and the shown inclinations are incorrect (Figure made by	y
this author)	. 42
Figure 17: UTM coordinates in meter for the reservoir targets for the three possible	
multilateral well designs in the Ekofisk South.	
Figure 18: Layers in the Ekofisk and Tor formations in the Ekofisk field (ConocoPhilli	ips
2011)	
Figure 19: Junction design option 1 installed and ready for production. The figure is no	
scaled, nor are the proper inclinations shown. Should be used for information purposes	
only (Figure made by this author)	
Figure 20: Junction design option 2 installed and ready for production. The figure is no	
scaled, nor are the proper inclinations shown. Should be used for information purposes	
only (Figure made by this author)	
Figure 21: Hole sizes to be drilled for all of the three MLT options for junction design	
option 2, with IWS (Figure made by this author)	. 50
Figure 22: Investigated area in the overburden in order to determine junction placemen	
(ConocoPhillips 2013h).	
Figure 23: Top view of the MLT set-up for well slot 2/4-Z-26 with junction placement	
and the three multilateral configurations s to be investigated. All positions and	

differential distances are with regards to the slot coordinates (Figure made by this author) 53
Figure 24: High DLS caused by the entering of a harder formation at inclination (Figure made by this author)
Figure 25: Examples of build-up, hold and drop for deviated and horizontal wells (Inglis 1987)
Figure 26: Convenient dividing of the drillstring for manual calculations using the discrete model (Figure made by this author)
Figure 27: Forces on a pipe section element for torque and drag analysis using the discrete model (Johancsik et al. 1984)
Figure 28: Classification of drill pipes based on wear (Figure made by this author) 67 Figure 29: Forces on a drill pipe element with pipe rotation (Figure made by this author)
Figure 30: Effect of buoyancy on buckling in form of neutral point of tension and NPB (Figure made by this author)71
Figure 31: High velocity area in a horizontal well (Figure made by this author)
Figure 33: Schematic of the step-wise iteration process for each of the wellbores in order to find the individual, suggested drilling parameter values (Figure made by this author) 83 Figure 34: Well schematic for the drilling of the 12 1/4" hole section in the mother
wellbore (Wellplan 2013a)
Figure 36: Schematic of the well path configuration. Same as Figure 16. Should only be used for overview. The figure is not to be scaled, and the shown inclinations are incorrect (Figure made by this author)
Figure 37: Hole sizes to be drilled for all of the three MLT options for junction design option 2, with IWS. Same as Figure 21 (Figure made by this author)
2013a)
2013a)
Figure 41: Effective tension for rotating on bottom with scenario 1 and 2 input parameter values for comparison case A. Left red line indicates minimum WOB to sinusoidal
buckle the drillstring, while the right blue line displays the tension limit/tensile strength for the drillstring components at different measured depths (Wellplan 2013a)
Figure 42: Effective tension for rotating on bottom with scenario 1 and 2 input parameter values for comparison case A. The left red line indicates minimum WOB to sinusoidal buckle the drillstring. As long as the effective tension values are to the right-hand side of
the minimum WOB sinusoidal buckling will not occur (Wellplan 2013a)

Figure 67: The world's first multilateral well drilled in Soviet in 1953 (E&P Magazin 2007)	
2007)	
single, long horizontal wellbore section (Frailja et al. 2002)	
Figure 69: MLT applied in a natural fractured reservoir (Frailja et al. 2002)	
Figure 70: MLT applied in a laminated, or layered, formation (Frailja et al. 2002)	
Figure 71: Reservoir with separated reservoir compartments penetrated by a multilate	
well with three branches (Frailja et al. 2002)	
Figure 72: Satellite field being drained by a multilateral well (Frailja et al. 2002)	
	1/2
Figure 73: MLT applied in a heavy oil deposit, either as producer or steam injector	172
(Frailja et al. 2002)	1/3
Figure 74: Example of a stacked horizontal well from the Austin chalk formation in	174
Texas, USA (Bosworth et al. 1998)	
Figure 76: 3D and top view of a forked/planar dual-lateral (Crouse 1996)	
Figure 77: 3D and top view of a forked/planar tri-lateral (Crouse 1996)	
Figure 78: 3D example of a chicken foot, or multibranched, multilateral well (Boswo	
et al. 1996)	
Figure 79: Top and 3D view of a radial tri-lateral, also referred to as a radial fan or	170
chicken foot ML (Crouse 1996)	176
Figure 80: Example of a planar opposed multilateral well, 3D and top view (Crouse	170
1996)	176
Figure 81: A dual opposing lateral ML design (Bosworth et al. 1996)	
Figure 82: Example of at planar, offset quadrilateral (Crouse 1996)	
Figure 83: Stacked, or inclined, tri-lateral, 3D view and top view (Crouse 1996)	
Figure 84: Step 5 – Junciton design option 1 (Figure made by this author)	
Figure 85: Step 7 – Junciton design option 1 (Figure made by this author)	
Figure 86: Step 8 – Junciton design option 1 (Figure made by this author)	
Figure 87: Step 9 – Junciton design option 1 (Figure made by this author)	
Figure 88: Step 12 – Junciton design option 1 (Figure made by this author)	
Figure 89: Step 14 – Junciton design option 1 (Figure made by this author)	
Figure 90: Step 15 – Junciton design option 1 (Figure made by this author)	
Figure 91: Step 16 – Junciton design option 1 (Figure made by this author	
Figure 92: Step 18 – Junciton design option 1 (Figure made by this author)	
Figure 93: Step 5 – Junction design option 2 (Figure made by this author)	
Figure 94: Step 7 – Junction design option 2 (Figure made by this author)	
Figure 95: Step 8 – Junction design option 2 (Figure made by this author)	
Figure 96: Step 9 – Junction design option 2 (Figure made by this author)	
Figure 97: Step 12 – Junction design option 2 (Figure made by this author)	
Figure 98: Step 13 – Junction design option 2 (Figure made by this author)	
Figure 99: Step 15 – Junction design option 2 (Figure made by this author)	
Figure 100: Step 18 – Junction design option 2 (Figure made by this author)	
Figure 101: Separation Factor (SF) (Compass 2013b)	
Figure 102: Separation plot (Compass 2013a)	
Figure 103: Picture of Mærsk Gallant (Mærsk 2013)	
Figure 104: Mother wellbore well path vertical sections to TOE (Wellplan 2013a)	

Figure 105: Geothermal gradient input in Wellplan for the mainbore (Wellplan 2013a)
Figure 106: Riser booster pump configuration for both Scenario 1 and Scenario 2 (Wellplan 2013)
Figure 107: Schematic of hole sections with drillstring for the 20" x 17 ½" drilling in mainbore (to scale) (Wellplan 2013a)
Figure 108: Overview of the hole sections at the input page in Wellplan for 20" x 17 ½" drilling in mainbore (Wellplan 2013a)
Figure 109: Drillstring design for the drilling of the 20" x 17 ½" hole section in the mainbore (Wellplan 2013a)
Figure 110: BHA Schematic for the drilling of 20" x 17 ½" hole section in mainbore (non-deviated, not to scale) (Wellplan 2013a)
Figure 111: Mud program for the drilling of the 20" x 17 ½" hole section in mainbore (Wellplan 2013a)
Figure 112: Schematic of hole sections with string for running of the 17" liner in mainbore (to scale) (Wellplan 2013a)
Figure 113: String design for the running of the 17" liner in the mainbore (Wellplan 2013a)
Figure 114: Component schematic for the running of 17" liner in mainbore (to scale) (Wellplan 2013a)
Figure 115: Schematic of hole sections with drillstring for the 16" drilling in mainbore (to scale) (Wellplan 2013a)
Figure 116: Overview of the hole sections at the input page in Wellplan for 16" drilling in mainbore (Wellplan 2013a)
Figure 117: Drillstring design for the drilling of the 16" hole section in the mainbore (Wellplan 2013a)
Figure 118: BHA Schematic for the drilling of 16" hole section in mainbore (non-deviated, not to scale) (Wellplan 2013a)
Figure 119: Mud program for the drilling of the 16" hole section in mainbore (Wellplan 2013a)
Figure 120: Schematic of hole sections with string for running of 13 5/8" casing in mainbore (to scale) (Wellplan 2013a)
Figure 121: String design for the running of the 13 5/8" casing in the mainbore (Wellplan 2013a)
Figure 122: Component schematic for the running of 13 5/8" casing in mainbore (to scale) (Wellplan 2013a)
Figure 123: Schematic of hole sections with drillstring for the 12 ¼" drilling in mainbore (to scale) (Wellplan 2013a)
Figure 124: Overview of the hole sections at the input page in Wellplan for 12 ¼" drilling in mainbore (Wellplan 2013a)
Figure 125: Drillstring design for the drilling of the 12 ¼" hole section in the mainbore (Wellplan 2013a)
Figure 126: BHA Schematic for the drilling of 12 ¹ / ₄ " hole section in mainbore (non-deviated, not to scale) (Wellplan 2013a)
Figure 127: Mud program for the drilling of the 12 ¼" hole section in mainbore (Wellplan 2013a)
·····································

Figure 128: Schematic of hole sections with string for running of 10 34" liner in maint	ore
(to scale) (Wellplan 2013a)	220
Figure 129: String design for the running of the 10 3/4" liner in the mainbore (Wellplan	n
2013a)	220
Figure 130: Component schematic for the running of 10 3/4" liner in mainbore (to scale	e)
(Wellplan 2013a)	
Figure 131: Hole sections for drilling of the 9 ½" hole from junction to TD for MLT1	
Lateral 1 (Wellplan 2013a)	
Figure 132: Drillstring design for the drilling of the 9 1/2" hole section from junction to	
TD for MLT1 Lateral 1 (Wellplan 2013a)	
Figure 133: Well schematic for the drilling of the 9 1/2" hole section from junction to 7	
for MLT1 Lateral 1 (Wellplan 2013a)	
Figure 134: Initial BHA schematic for the drilling of the 9 1/2" hole section from junct	
to TD for MLT1 Lateral 1 (Wellplan 2013a)	223
Figure 135: Well path vertical section for the drilling of 9 1/2" section from junction to	TD
for MLT1 Lateral 1 (Wellplan 2013)	
Figure 136: Well path plan view for the drilling of 9 1/2" section from junction to TD f	or
MLT1 Lateral 1 (Wellplan 2013)	225
Figure 137: Well path tortuosity input for the drilling of 9 1/2" section from junction to) TD
for MLT1 Lateral 1 (Wellplan 2013)	
Figure 138: Well path inclination with tortuosity for the drilling of the 9 1/2" section fr	
junction to TD for MLT1 Lateral 1 (Wellplan 2013)	226
Figure 139: Well path azimuth with tortuosity for the drilling of the 9 1/2" section from	1
junction to TD for MLT1 Lateral 1 (Wellplan 2013)	226
Figure 140: Geothermal gradient for the underground for drilling of the 9 ½" section	
from junction to TD for MLT1 Lateral 1 (Wellplan 2013a)	227
Figure 141: Overview of the different modules in Wellplan (Wellplan 2012)	228
Figure 142: Wellplan interface showing the general well input module. The dropdown	1
curtain under "case" is different from when other modules are selected allowing the u	ser
to input general data (Wellplan 2012)	
Figure 143: Drilling fluid properties for the drilling of the 9 ½" section from junction	to
TD in Ekofisk for MLT1 Lateral 1 (Wellpan 2013)	234
Figure 144: Torque and Drag Setup Data used for both Scenario 1 and Scenario 2	
(Wellplan 2013a)	236
Figure 145: Circulating system setup for both Scenario 1 and Scenario 2 based on Ma	ersk
Gallant specifications (Wellplan 2013)	
Figure 146: Initial bit and nozzle configuration for the drilling of all the 8 1/2" sections	in
the MLT options. For the 9 ½" section the BHA had the same design, but larger bit	
diameter, naturally (Wellplan 2013; Maxwell 2013)	239
Figure 147: Torque and Drag Setup with WOB, torque at bit and tripping speed for	
Scenario 1 (Wellplan 2013)	
Figure 148: Transport analysis data initial setup for Scenario 1 (Wellplan 2013)	
Figure 149: Torque and Drag Setup with WOB, torque at bit and tripping speed for	
Scenario 2 (Wellplan 2013)	242
Figure 150: Transport analysis data initial setup for Scenario 2 (Wellplan 2013)	243
Figure 151: Effective tension scenario 1 and 2 comparison case B (Wellplan 2013a)	

Figure 152: Effective tension scenario 1 and 2 comparison case C (Wellplan 2013a).	. 256
Figure 153: Effective tension scenario 1 and 2 comparison case D (Wellplan 2013a).	. 257
Figure 154: Effective tension scenario 1 and 2 comparison case F (Wellplan 2013a)	. 258
Figure 155: Effective tension scenario 1 and 2 comparison case G (Wellplan 2013a).	. 259
Figure 156: Effective tension suggested values comparison case C (Wellplan 2013a)	. 260
Figure 157: Effective tension suggested values comparison case D (Wellplan 2013a)	
Figure 158: Effective tension suggested values comparison case F (Wellplan 2013a).	
Figure 159: Effective tension suggested values comparison case G (Wellplan 2013a)	
Figure 160: Torque scenario 1 and 2 values comparison case B (Wellplan 2013a)	
Figure 161 Torque scenario 1 and 2 values comparison case C (Wellplan 2013a)	
Figure 162: Torque scenario 1 and 2 values comparison case D (Wellplan 2013a)	
Figure 163: Torque scenario 1 and 2 values comparison case F (Wellplan 2013a)	
Figure 164: Torque scenario 1 and 2 values comparison case G (Wellplan 2013a)	
Figure 165: Torque suggested values comparison case C (Wellplan 2013a)	
Figure 166: Torque suggested values comparison case D (Wellplan 2013a)	
Figure 167: Torque suggested values comparison case F (Wellplan 2013a)	
Figure 168: Torque suggested values comparison case G (Wellplan 2013a)	
Figure 169: Fatigue ratio scenario 1 and 2 values comparison case C (Wellplan 2013a)	
11gure 109. I augue 1au o secuario 1 ana 2 varaes comparison case e (wenpian 2013)	. 273
Figure 170: Fatigue ratio scenario 1 and 2 values comparison case D (Wellplan 2013)	
	. 274
Figure 171: Fatigue ratio scenario 1 and 2 values comparison case F (Wellplan 2013a	
1 iguie 171. I augue rado sechario 1 ana 2 varues comparison case 1 (wenpian 2013a	. 275
Figure 172: Fatigue ratio scenario 1 and 2 values comparison case G (Wellplan 2013)	
	. 276
Figure 173: Fatigue ratio suggested values comparison case C (Wellplan 2013a)	
Figure 174: Fatigue ratio suggested values comparison case D (Wellplan 2013a)	
Figure 175: Fatigue ratio suggested values comparison case F (Wellplan 2013a)	
Figure 176: Fatigue ratio suggested values comparison case G (Wellplan 2013a)	
Figure 177: Hook load scenario 1 and 2 values comparison case C (Wellplan 2013a).	
Figure 177: Hook load scenario 1 and 2 values comparison case D (Wellplan 2013a).	
Figure 179: Hook load scenario 1 and 2 values comparison case F (Wellplan 2013a).	
Figure 180: Hook load scenario 1 and 2 values comparison case G (Wellplan 2013a).	
Figure 181: Hook load suggestev values comparison case C (Wellplan 2013a)	
Figure 182: Hook load suggestev values comparison case D (Wellplan 2013a)	
Figure 183. Hook load suggestev values comparison case E (Wellplan 2013a)	
Figure 184: Pressure losses scenario 1 and 2 values comparison case C (Wellplan 20)	
E' 105 D D. (W.11-1 20	. 289
Figure 185: Pressure losses scenario 1 and 2 values comparison case D (Wellplan 20	
E' 106 D E (W-11-1 201	. 290
Figure 186: Pressure losses scenario 1 and 2 values comparison case F (Wellplan 201	
Eigene 197: Descript lesses compris 1 and 2 values comparison cost C (Wallulan 20	. 291
Figure 187: Pressure losses scenario 1 and 2 values comparison case G (Wellplan 20	
	. 292
Figure 188: Pressure losses suggested values comparison case C (Wellplan 2013a)	
Figure 189: Pressure losses suggested values comparison case D (Wellplan 2013a)	. 294

Figure 190: Pressure losses suggested values comparison case F (Wellplan 2013a)	295
Figure 191: Pressure losses suggested values comparison case G (Wellplan 2013a)	296
Figure 192: ECD for scenario 1 and 2 values comparison case C (Wellplan 2013a)	297
Figure 193: ECD for scenario 1 and 2 values comparison case D (Wellplan 2013a)	298
Figure 194: ECD for scenario 1 and 2 values comparison case F (Wellplan 2013a)	299
Figure 195: ECD for scenario 1 and 2 values comparison case G (Wellplan 2013a)	300
Figure 196: ECD for suggested values comparison case C (Wellplan 2013a)	301
Figure 197: ECD for suggested values comparison case D (Wellplan 2013a)	302
Figure 198: ECD for suggested values comparison case F (Wellplan 2013a)	303
Figure 199: ECD for suggested values comparison case G (Wellplan 2013a)	304
Figure 200: Project scope of the current ongoing development of the Ekofisk South are	ea
(ConocoPhillips 2013f)	305
Figure 201: Map showing the Ekofisk south area, with the waterflood expansion area	
marked in blue (ConocoPhillips 2013f)	306
Figure 202: Details of mudpumpt EMSCO FC-220 Triplex (American Manufacturing	
2013)	

vi. List of Tables

Table 1: Preferred requirements and needs from a reservoir and well planning persp	ective
for a MLT project on Ekofisk	44
Table 2: Junction design option 1	46
Table 3: Junction design option 2	46
Table 4: Junction placement suggestions in the overburden (Maxwell 2013)	
Table 5: Site and well slot placement and properties (Maxwell 2013)	
Table 6: Overview of the downhole depths for the different wellbores in for the ML	T
options	55
Table 7: Simulations performed in Wellplan	84
Table 8: Assumptions made for the simulations performed in Wellplan	85
Table 9: Initial input parameter values. Scenario 1 represents the lower and scenario	2 the
higher limits of the intervals recommended by Halliburton for the actual drilling of	the
2/4-Z-17, a close by well drilled in April 2013 (Maxwell 2013)	90
Table 10: Initial input parameter values and setup equal for both Scenario 1 and Sce	
2	91
Table 11: Suggested input parameter values for the nine different wellbore sections	for
the three MLT options. For each of the wellbores these were found by changing the	
different input values via manual iterations in Wellplan	
Table 12: Comparison cases for the simulation results	95
Table 13: Summary of issues by use of scenario 1 parameter input values (Wellplan	l
2013a)	
Table 14: Summary of issues by use of scenario 2 parameter input values (Wellplan	l
2013a)	129
Table 15: Summary of issues by use of suggested parameter input values (Wellplan	
2013a)	
Table 16: List of average day rates for floating rigs (WD = Water Depth) (Rigzone	2012)
Table 17: List of average day rates for jackup rigs (Rigzozne, 2012) (IC = Independ	ent
Cantilever, IS = Independent Spud, MC = Mat Cantilever, MS = Mat Supported, W	D =
Water Depth) (Dockwise 2011)	161
Table 18: TAML functionality classification – well description (Weatherford 2006)	165
Table 19: TAML functionality classification – junction description (Weatherford 20)06)
	165
Table 20: Major collision risk based on separation factor (SF)	199
Table 21: Minor collision risk based on separation factor (SF)	200
Table 22: List of specifications for Mærsk Gallant (Mærsk 2013)	201
Table 23: List of features in the Wellplan modules (Halliburton/Landmark 2008)	
Table 24: Suggested parameter values for MLT1 L1	
Table 25: Suggested parameter values for MLT1 L2 9 1/2"	245
Table 26: Suggested parameter values for MLT1 L2 8 ½"	246
Table 27: Suggested parameter values for MLT2 L1	247
Table 28: Suggested parameter values for MLT2 L2 9 1/2"	
Table 29: Suggested parameter values for MLT2 L2 8 1/2"	249
Table 30: Suggested parameter values for MLT3 L1	

Table 31: Suggested parameter values for MLT3 L2 9 ½"	252
Table 32: Suggested parameter values for MLT3 L2 8 ½"	
Table 33: The F-series mudpumps for the manufacturer EMSCO (Sunry Petro)	307

1 Introduction

Drilling for oil and gas has today become an advanced operation. From vertical and simple wellbores, in relatively easily accessible reservoirs, the industry over the last few decades has developed technical and innovative solutions in order to reach and produce hydrocarbons from more complex reservoirs and in challenging locations. One of these inventions is the Multilateral Well Technology, also known simply as MLT. Even though first used in Russia as far back as in 1953 (E&P Magazine 2009) it is not until recently, via progresses in the industry and the creation of new well construction techniques and completion methods, this way of drilling and producing wells has been taken into consideration as a possible solution when planning the development of a field. And by creating these types of wells the companies, in many cases, are able to save money while gaining other valuable benefits³.

In 2004 ConocoPhillips Norway (COPNO) started a project with these types of wells in the Ekofisk field in the Norwegian sector of the North Sea. The wells drilled, 2/4-X-02 and 2/4-X-21, yielded more stable production rates, but had several issues and challenges when it came to junction stability and access to the side-branch. Today, due to reservoir and production related matters, as well as optimization of the slot utilization, the drilling of multilateral wells again has been listed as a possible future strategy for COPNO⁴. However, no formal work on the area has been done in the years from 2004 until today within the organization. Therefore, in order to optimize the possibility of future success for the drilling of multilateral wells on Ekofisk South, six different reservoir targets were determined to be analyzed and evaluated based on the drilling performance and process⁵.

This Master Thesis will evaluate three different multilateral well options, each with a mainbore (Lateral 1) and a side-branch (Lateral 2), to select the optimum configuration for a possible future implementation on Ekofisk, based on the reservoir targets given. In cooperation with COPNO employees a project scope, including suggestion of junction configuration, determination of junction placement and creation of the well paths, will be made. Further, technical challenges and physical limitations related to drilling of multilateral wells on Ekofisk will be addressed and presented. A simulation base representing the Ekofisk South area will be built in the Wellplan software, and sets of input parameters will be determined in order to perform adequate simulations on the drilling of the different wellbore sections in the MLT options to be investigated. Finally, based on the simulation results, an evaluation of the different MLT options will be performed, and a selection of the optimum multilateral well configuration on Ekofisk South for future success optimization with regards to the drilling process will be executed.

³ Personal communication with R. Watts. 2013. Stavanger: ConocoPhillips Norway

⁴ Personal communication with J.R Berg. 2013. Stavanger: ConocoPhillips Norway

⁵ Personal communication with A. Arang. 2013. Stavanger: ConocoPhillips Norway

2 ConocoPhillips and the Ekofisk area

2.1 ConocoPhillips Company

With more than 16 000 employees and activities in nearly 30 countries ConocoPhillips is one of the largest independent exploration and production companies in the world. Even though the history of the company can be traced all the way back to 1875 and 1917, with the founding of Continental Oil Company, or simply Conoco, and Phillips Petroleum, respectively, the company as it appears today was established in 2003 when these two companies merged (ConocoPhillips 2013a; ConocoPhillips 2013b). Three years later the leading marketer and producer of natural gas, Burlington Resources, was acquired forming ConocoPhillips as it is known throughout the industry today (ConocoPhillips 2013c).

2.2 ConocoPhillips Norway

ConocoPhillips, branded in Norway as ConocoPhillips Norway AS, also simply known as COPNO, is one of the largest foreign operators on the Norwegian Continental Shelf. In 1969 the company found the giant oil and gas field Ekofisk in the Norwegian part of the North Sea, and in 1971, two years later, they became the first operator to produce hydrocarbons in this area (Norwegian Oil and Gas Association 2013). The company is headquartered in Tananger, just outside the city of Stavanger, and has more than 1900 employees, both on- and offshore. The company has over the last 40 years played a significant role in the development of Norway as both an oil nation and a welfare society (ConocoPhillips

2.3 The Greater Ekofisk Area and the Ekofisk reservoir

The area where the Ekofisk field was discovered today consists of the four adjacent fields Ekofisk, Eldfisk, Embla and Tor, together forming the Greater Ekofisk Area. The location is around 300 km southwest of the city of Stavanger, as presented in Figure 1. COPNO, holding an interest of 35.11 %, is the operator of the combined fields, with Total E&P Norge, Eni Norge, Statoil Petroleum AS and Petoro as the other license owners in the area (ConocoPhillips 2013d).

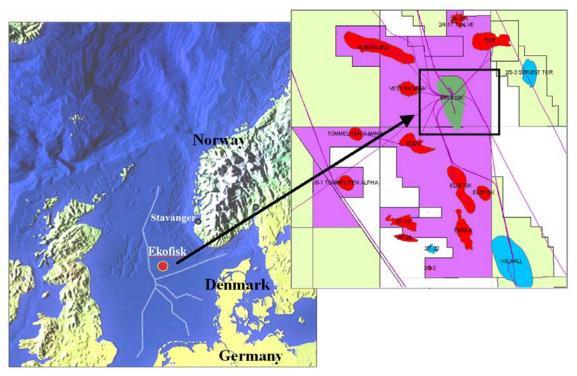


Figure 1: Location of the Greater Ekofisk Area in the North Sea (Maxwell 2013)

2.3.1 The Reservoir

The Ekofisk reservoir itself, with production license (PL) 018 and block 2/4, contains a 600 to 1000 feet tall oil column, located mostly in fractured chalk of late Cretaceous and early Paleocene age. The field, measuring 10 x 5.5 km, consists of the Ekofisk and Tor formation, divided by a tight zone in-between, as shown in Figure 2. A top view, with the scale of the development compared to the city of Stavanger, is displaced in Figure 5. From the seabed, approximately 250 feet below main sea level, it is between 9500 and 10700 feet down to the top of the reservoir (ConocoPhillips 2013f). In 1969, as one of the largest offshore oil and gas field ever found, Ekofisk had recoverable reserves of 3.349 billion bbls of oil, 5529.745 billion Scf of gas and 14.5 million metric tons of NGL (NPD 2010). Today the field has been on production for more than 40 years and is considered a mature field. The remaining reserves, as of the end of 2009, are 0.745 billion bbls of oil, 663.916 billion Scf of gas and 2.0 million metric tons of NGL (NPD 2010).

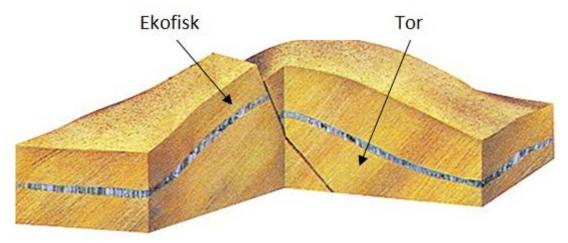


Figure 2: Illustration of the Ekofisk reservoir, with Ekofisk and Tor formation (ConocoPhillips 2013f)

Compared to the relatively high matrix rock porosity of 25 – 45 % the permeability in the area is low, varying from 1-2 mD. The initial extraction strategy was by pressure depletion only, and production during the first years yielded a recovery factor of around 17 %. After a rapid increase from the start in 1971 the production rate dropped guite dramatically around 1977, see Figure 6. During the 1980's COPNO therefore decided to initiate a water injection program, as well as restricted gas injection (this was however terminated around year 2000) to increase both the recovery and rates. From the first water injection pilot in 1981 the injection has been expanded in several stages. Figure 3 displays a reservoir model of Ekofisk with oil saturation as a function of time made in the Petrel software. The snapshot from 1984 is in the starting phase of this water injection program. Until today the water saturation, shown in Figure 4, has increased dramatically due to the heavy waterflooding the past decades. As a result the oil has been displaced yielding a current saturation of around 0.3. Despite this, large quantities of hydrocarbons still can be found in Ekofisk, and COPNO presently are developing Ekofisk South, a project that possibly can increase the lifetime of Ekofisk with another 40 years, see Figure 200 and Appendix R (ConocoPhillips 2013f). The drilling of multilateral wells might be a potential technology to utilize in this area to help increase the ultimate recovery, while reducing the cost.

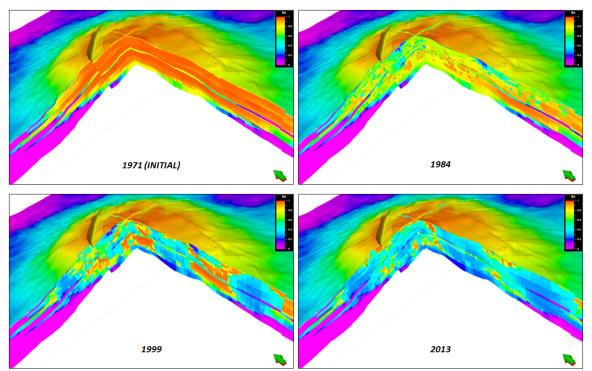


Figure 3: Reservoir model of oil saturation in Ekofisk as a function of time (ConocoPhillips 2013h)

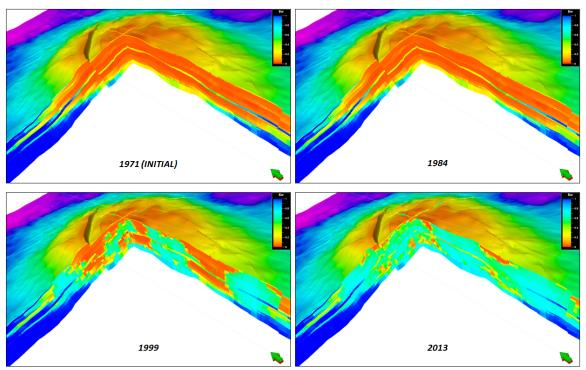


Figure 4: Reservoir model of water saturation in Ekofisk as a function of time (ConocoPhillips 2013h)

Today the water injection program, together with an extensive chemical treatment of the chalk formation, compaction of the reservoir and solution gas drive, is crucial for Ekofisk and has increased the recovery factor to around 50 % (ConocoPhillips 2013f). In addition the production rates have somewhat stabilized, also due to the drilling of new wells, and are today approximately at 176 000 bopd, 60.741 million scf/d and 0.23 million metric tons NGL per day (NPD 2010).

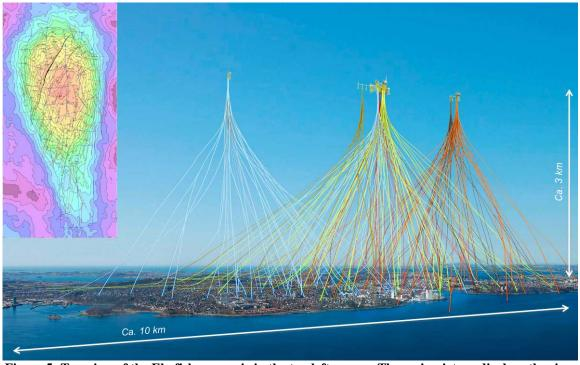


Figure 5: Top view of the Ekofisk reservoir in the top left corner. The main picture displays the size-relationship between the Ekofisk area and the city of Stavanger (ConocoPhillips 2013f)

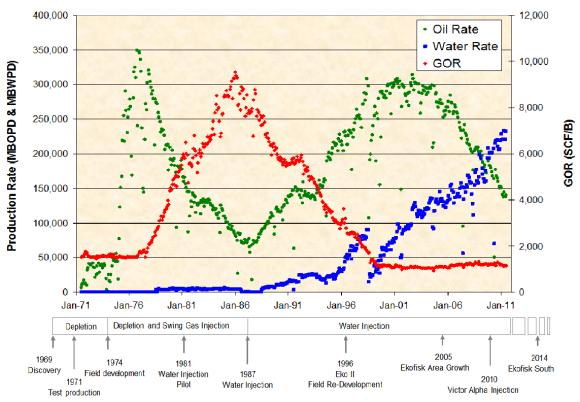


Figure 6: Ekofisk historical production rates, with timeline of significant events since the start in 1971 (ConocoPhillips 2013f)

2.3.2 Subsidence and compaction

Ekofisk has ever since the production start in 1971 experienced compaction of the reservoir, with a following subsidence at the seabed. The chalk formation being produced is a fairly weak rock matrix and collapses when the supporting pressure from the fluid inside disappears due to the extraction. In the years from 1971 to 1984, when the subsidence was discovered, the Ekofisk complex had sunk more than 10 feet, as shown in Figure 7. This was due to the heavy pressure depletion of the field. In 1987 COPNO, as a result of this, decided to jack up the installations in the Ekofisk complex to save them from sinking (NY Times 1987). The water injection project the same year was in addition initiated not only to recover more of the hydrocarbons, but also to repressurize the reservoir to terminate the issue. Despite this the compaction in the waterflooded areas continued, mostly due to what is called water weakening of chalk. When the injected water gets in contact with the rock matrix at the inter-grain contact the chalk re-dissolves and re-deposits in a structure with lower porosity (Austad et al. 2008). Today the compaction in the Ekofisk reservoir is around 36 feet, with a following subsidence at seabed of about 30 feet. New installations in the field are all, due to this issue, designed with longer than normal jackets to mitigate the subsidence challenges⁶.

⁶ Personal communication with J.R. Berg. 2013. Stavanger: ConocoPhillips Norway

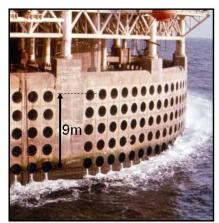






Figure 7: Subsidence at the Ekofisk complex shown at the Ekofisk tank. From left the pictures are from 1974, 1985 and 2006, respectively (ConocoPhillips 2013f)

2.3.3 Challenges related to drilling in the Ekofisk field

The overburden between the Ekofisk reservoir and the seabed is divided into three groups, namely the Nordland, Hordaland and Rogaland compartments. When the pressure in the reservoir decreases, the weight of the overburden is too heavy for the reservoir matrix rock and crushes the reservoir. This vertical overburden movement leads to challenges related to buckling of downhole equipment. In addition, the subsidence experienced at the seabed as a result of this creates shear movements on the rim of the subsidence bowl directly above the center of Ekofisk. These shear forces can lead to movement, deformation and collapse of the wells penetrating the area, and all new wellbores drilled in the area are therefore planned with paths avoiding this rimpart (Midtgarden 2010).

In addition to the stretching in the outer top parts there are also challenges with water intrusion and gas migration into the overburden. The area between the reservoir and the overburden consists of several fractured and faulted zones, giving the injected water, as well as the solution gas, a path from Ekofisk and into the overburden. This migration has led to a high pressured water zone and a shallow Miocene gas pocket, causing challenges for the drilling of new wells. The Miocene gas, consisting of both insitu and migrated, cannot be produced, and instead creates a seismic obscured area directly above the center of the Ekofisk reservoir (Midtgarden 2010).

2.4 Why drill Multilateral Wells on Ekofisk?

To prevent a future decline the drilling of new wells are essential in the Ekofisk area. Large investments, topside and subsea, the last few years have increased the expected lifetime of the Greater Ekofisk Area with more than forty years, and installation of new platform facilities are currently ongoing⁷. A possible future part of this strategy is multilateral wells. This type of well design, described more in details in Appendix D, can increase reservoir exposure while saving slot spaces, increase the recovery factor, be beneficial in areas with layered reservoirs and in reservoirs with separated pockets of hydrocarbons. For Ekofisk especially the first factor, increased wellbore and reservoir interaction while utilizing each slot, is important⁸. In addition, previous two-branched multilateral wells drilled by Halliburton in the North Sea have yielded up to 85 % of the production rate, but shown significantly increased lifetime, and thus higher ultimate recovery, compared to two, separate wells drilled to TD. Two examples of this can be seen in Figure 8, presenting X-02 and X-21, the two multilateral well drilled in Ekofisk in 2004. Compared to other wells in the area the decline curves are gentler, thus leading to a more stable production and longer lifetime. Even though these two specific wells, due to technical issues, ended up too expensive to be economically justifiable, a multilateral well in the North Sea on average is only 1.3 times more expensive than a single well. If topside equipment, casing strings, tubing, wellhead, stimulation and workover equipment is also included the number can be as low as 1.15 times a lone wellbore cost. Finally, a successful drilling and completion of such a multilateral well with two branches in the North Sea on average save around 15 to 17 rig-days compared to the drilling of two, fully separated wellbores to TD⁹. With this in mind it is clear that a successful implementation of multilaterals in the Ekofisk field potentially may have significant economic upsides, while increasing the recovery factor and maintaining the production rates.

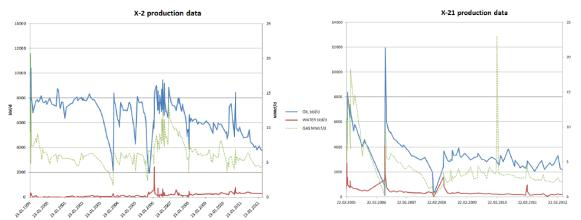


Figure 8: Production rates of 2/4-X-02 and 2/4-X-21, two of the four wells drilled with MLT on Ekofisk (ConocoPhillips 2013f)

⁷ Personal communication with I. Blaauw. 2013. Stavanger: ConocoPhillips Norway AS

32

⁸ Personal communication with J.R. Berg. 2013. Stavanger: ConocoPhillips Norway AS

⁹ Personal communication with G. Liland. 2013. Stavanger: Halliburton Scandinavia AS

3 The Multilateral Well Technology

3.1 Development of MLT and the introduction of the TAML standard

The first patent on a well similar to what today is considered a multilateral was filed as early as 1929 in the USA (E&P Magazine 2007). However, the world's first true multilateral well, presented in Figure 67 in Appendix B, was not drilled until 1953, when the Soviet petroleum engineer Alexander Grigoryan constructed a multilateral with nine branches in the Soviet Union (E&P Magazine 2009). Despite producing 17 times more and costing only 1.5 as much as the surrounding well, it was not until the development of Logging While Drilling (LWD) in the 1970 that the development of MLT accelerated. The LWD tool replaced wireline and introduced the possibility of accurate real-time downhole steering, which ultimately made multilateral well a more feasible solution in many cases (E&P Magazine 2009; Colombia University 2008).

In the years and decades to follow the research and advance in MLT continued, and in 1997 the industry launched the Technical Advancements of Multi Laterals, or TAML, a classification system defining the complexity and functionality of different junction types and designs for a multilateral well (E&P Magazine 2009). The different categorizations are listed in whole in Appendix C. During the 90's both the industry and the different governing authorities accepted TAML as the new classification standard, and since then a common effort has been made to develop and utilize multilateral well technology across companies and countries (E&P Magazine 2009). For more details regarding the history and development of MLT see Appendix B.

3.2 Junction Design and Configurations

Today, as presented more in detail in Appendix F, there are several different multilateral well configurations utilized in the industry. The design of the mainbore, as well as the lay-out of the branches, is a function of the reservoir properties, pay-zone area, desired drainage, production rates and more. However, what all different configurations have in common is the need of a junction in the mother wellbore where the laterals diverge. With the introduction of the TAML standard in 1997 the industry, led by the service companies, started to develop more advanced junction systems and designs that could meet the most challenging conditions. Today there are several systems available in the market, from general configurations to customized design.

3.2.1 The TAML classification

TAML classification standard was established after an industry initiative, mainly North Sea operators, in the early 1990's in order to create a knowledge database, establish a network of contacts, common goals for further development in the area and guidelines for the various governing authorities (E&P Magazine 2007). TAML divides the complexity

of the junctions into six levels, level 1 being the simplest and level 6 being the most sophisticated, as presented in Figure 9. The level of a multilateral well, if more than one junction, corresponds to the junction with the highest level of complexity (TAML 2002). The lower two levels dominated the industry in the years to follow after the first multilateral well in Soviet in 1953. These are fairly simple junction types and describe an openhole sidetrack or unsupported junction (Level 1) and openhole sidetrack from a cased and cemented mother wellbore (Level 2). The latter can also contain a drop-off liner, a liner not connected to the main wellbore, in the lateral.

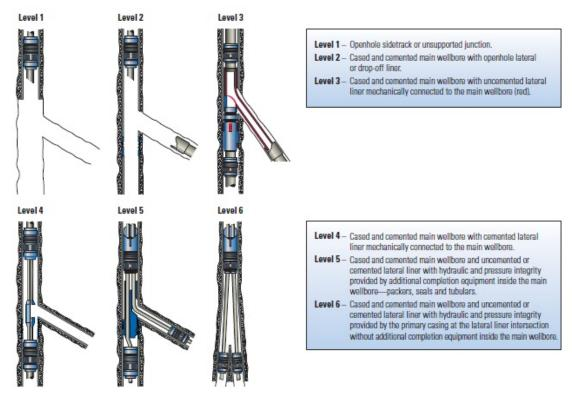


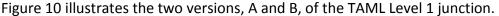
Figure 9: TAML junction classification for Multilateral Wells (Frailja, J., Ohmer, H. and Pulick, T. et al. 2002).

It was not until the mid-1990's more complex junction types were presented to the industry. With increased TAML level normally also functionality of the multilateral well completion, junction technical complexity and cost increases (Weatherford 2006). In 1993 and 1994 Shell established and installed the world's first level 3 and level 4 junctions, respectively. The year after BP created the first level 5 junction in the Gulf Of Mexico, with level 6 established in California by AERA Energy in 1999. The years between then and now more steps continuously have been taken, and limits have been moved to create level 5 and 6 junctions in deepwater areas, implement IWS to the branches and flotation of liners to establish junctions, to mention some of the milestones (E&P Magazine 2007).

3.2.2 TAML Level 1 Junction

TAML Level 1 is the open, or unsupported, junction level. This is the simplest type of junction and is characterized by:

- A) either a barefoot mother-bore and slotted liner hung off in both mother-bore and lateral after the junction, or
- B) a barefoot mother-bore and lateral (Weatherford 2006)



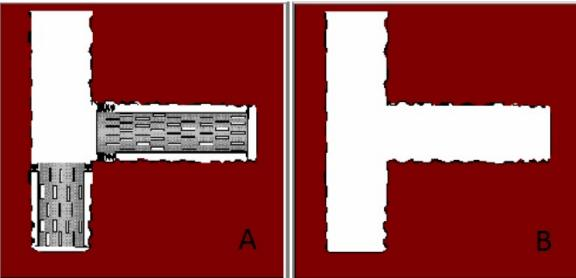


Figure 10: TAML Level 1A and Level 1B Junctions (Weatherford 2006)

3.2.3 TAML Level 2 Junction

From level 1 to level 2 the complexity of the junction increases. Here the mother-bore is cased and cemented. The lateral then can have (TAML 2002)

- A) either a slotted liner in the openhole, or
- B) be openhole, also called barefoot

Figure 11 shows the two options for TAML Level 2A and 2B.

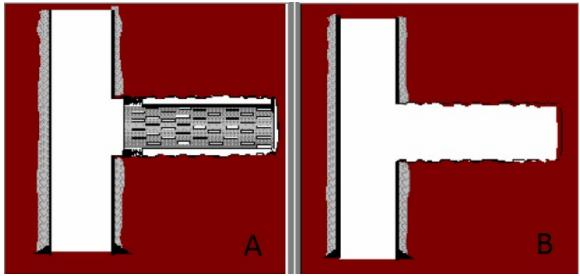


Figure 11: TAML Level 2A and Level 2B Junctions (Weatherford 2006)

3.2.4 TAML Level 3 Junction

As for the level 2 junction the mother-bore for a level 3 junction is also cased and cemented. The difference for this level, however, is that the lateral now is cased, although not cemented, as seen in Figure 12. The liner in the lateral branch is connected to the main wellbore with some kind of anchoring device, for instance a liner hanger (Weatherford 2006; TAML 2002).

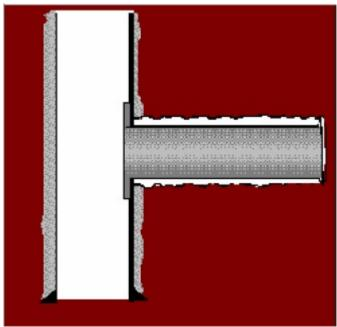


Figure 12: TAML Level 3 Junction (Weatherford 2006)

3.2.5 TAML Level 4 Junction

From level 3 to level 4 the main difference is that now both the main wellbore and the lateral are cased and cemented. The lateral can also contain a slotted liner, as indicated in Figure 13, picture A. Both the mother-bore and the lateral branch are cemented at the junction (Weatherford 2006).

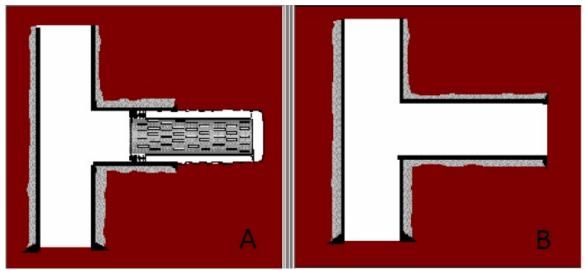


Figure 13: TAML Level 4A and Level 4B Junctions (Weatherford 2006)

3.2.6 TAML Level 5 Junction

The junction levels from 1 to 4 have one thing in common; no accepted pressure integrity. This is changed with the introduction of level 5. Here the junction is required to have full pressure integrity. For this manner cement is not considered acceptable, so the pressure integrity is achieved via the completion of the junction (Weatherford 2006). Most often this is done by the use of either mechanical seals in the casing or straddle packers, as illustrated in Figure 14 (TAML 2002). Both the mother-bore, junction itself and the lateral are cased and cemented.

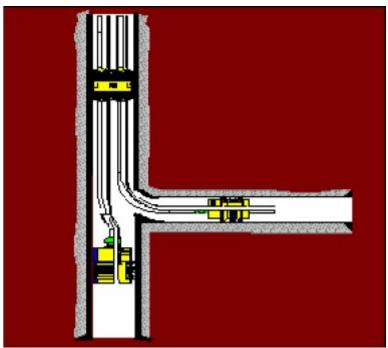


Figure 14: TAML Level 5 Junction (Weatherford 2006)

3.2.7 TAML Level 6 Junction

For level 6 junctions, presented in Figure 15, there is also a requirement of pressure integrity at the junction. For this level, however, the integrity is achieved via a casing string, and not through the completion. As for level 5 the mother-bore and the lateral branch are both cased and cemented, but again the cement itself is not considered an acceptable mean to obtain the required pressure integrity (Weatherford 2006).

Another version of the level 6 junction is the split junction, as seen in Figure 15, picture B. Here the lateral is created by the installation of a large casing string in the main wellbore with a splitter attached to the bottom. This is also known as TAML Junction Level 6S, where "S" represents either a surface or a downhole split.

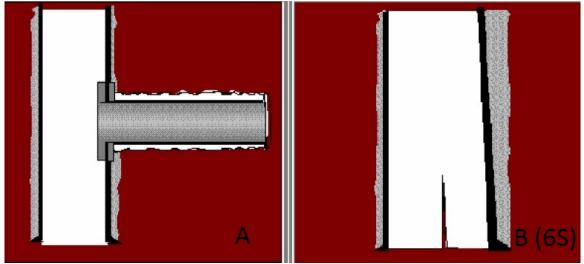


Figure 15: TAML Level 6A and Level 6B (6S) Junctions (Weatherford 2006)

3.3 Ongoing R&D on MLT for future, improved utilization in the oilfield

With a lot of mature fields around the globe new multilateral wells are today drilled every week in order to exploit well slots, access the remaining hydrocarbons and get maximum return on investments. As presented more in detail in Appendix E, the modern aspects of these types of wells are mainly in natural fractures reservoirs, heavyoil formations, thin layer reservoirs and reservoirs with separated hydrocarbons compartments. Based on the TAML classification as a backbone the industry today spend most of their effort within multilateral well-technology to develop software programs, intervention and workover tools, field development models and economic calculation programs on cost vs. value in return for multilateral wells contra conventional, single-wellbore developments (E&P Magazine 2009). In addition the Intelligent Well System (IWS), quite recently introduced to the industry, is subject to major research and effort in order to be implemented to the branches in multilateral wells. An IWS completion divides the pay zone into compartments, up to seven with today's technology, separated with packers, valves and mechanisms makes it possible to remotely control the inflow to each of these compartments. This way of completion a reservoir can be beneficial in areas where early water breakthrough is an issue, such as in the Ekofisk field. The biggest challenges as of today when it comes to IWS implementation into the branches of a multilateral well are equipment size for IWS components versus drift diameter of junction, pressure integrity requirements in the junction, and access and the ability to seal of the different branches in the junction for IWS control¹⁰.

¹⁰ Personal communication with R. Watts. 2013. Stavanger: ConocoPhillips Norway AS

_

Even though MLT has a history all the way back to the first patent in the late 1920's, the industry considers this well construction method a young technology still in the starting phase. The major service companies, such as Halliburton, Baker Hughes and Schlumberger, all have their respective technologies and equipment on multilaterals ready to be customized for the different customers. The focus on R&D within this area increased rapidly after the TAML initiative in 1997, and the amount of multilateral wells drilled worldwide increases every year. Halliburton, for instance, has since the end of the 1990's drilled 177 multilaterals only in the Norwegian part of the North Sea, with the vast majority of these the last few years. However, challenges still remain within MLT, especially with the junction design. The service companies continuously work together with the major oil companies to come up with new solutions and products that can improve important junction-related factors such as pressure integrity rating, access to the laterals for stimulation, workovers and installation of equipment, stability and installation 11.

-

¹¹ Personal communication with G. Liland. 2013. Stavanger: Halliburton Scandinavia AS

4 Setting up possible MLT configurations for Ekofisk

In order to evaluate the three possible multilateral candidates to be drilled on Ekofisk, given the six reservoir targets, as mentioned in the introduction, a configuration, with overview of the project scope, suggestions of junction placement and design, and well paths, had to be established. It was early in the planning process decided that this configuration would have to have the Ekofisk field as the backbone, meaning that the model had to be realistic in terms of reservoir properties, layers and layout in order to perform accurate investigations and reflections regarding the feasibly of possible multilaterals in the area. It was therefore important to define the perimeters, determine the requirements and lay out goals for a possible MLT utilization on Ekofisk as early as possible in the process.

4.1 Reservoir targets

The reservoir targets were determined by the reservoir group in CONO to be placed in Ekofisk South. An assumption was given that each of the six targets would result in identical reservoir exposure and performance. The reservoir targets would be in the Ekofisk South, an area currently being developed for the future with a new wellhead platform, 2/4-Z, for 36 new production wells, 2/4-VB, for 8 new water injection wells, and a new hotel, 2/4-L, for more than a total of 27 billion NOK (see also Appendix R) (ConocoPhillips 2013f). It was further suggested that the different multilateral wells to be investigated should be drilled from slot 2/4-Z-26, which would be on the new production platform.

For the reservoir group it was desired to look at three different MLT options, MLT1, MLT2 and MLT3. Each of these configurations would have a mainbore, also called Lateral 1, or L1, and a sidestep, referred to also as Lateral 2, or L2. A better overview and explanation of this naming can be seen in Figure 16 (it should be noted that the selection of the junction depth at 9958 ft TVD is presented in section 4.5). Each of the different MLT options would share the same mother wellbore from the rig down to a common junction point. From there each of the options would be unique. For each MLT option the Lateral 1 would hit one target and the Lateral 2 another target, as presented in Figure 17. For MLT1 it was decided that both L1 and L2 would go to different targets in the EA3 layer, thus making the MLT1 option a so-called forked, or planar dual-lateral, as presented in Figure 76 in Appendix F. The L2 for MLT2 option, on the other hand, would go to a target in the EL1 formation, with the L1 going to a target in EA3. MLT2, by that reason, would therefore be a stacked horizontal multilateral well, due to the vertical differences between the target layers (see Figure 18, as well as Figure 74 in Appendix F). The last option, the MLT3, would have both L1 and L2 in the EL2 layer.

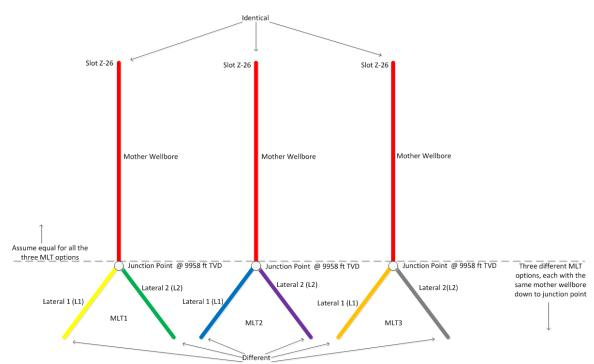


Figure 16: Schematic of the well path configuration. Should only be used for overview. The figure is not to be scaled, and the shown inclinations are incorrect (Figure made by this author)

Well Nr./Name	Lateral Nr.	x	Y	Z	Unit in 'metres'	Layer Name
MLT-1	1	514294	6262263	3100.33	Entry Point	EA3
		514225	6261748	3102.44		EA3
		514204	6261522	3109.54		EA3
		514153	6261232	3125.08		EA3
		514226	6260861	3138.25	TD	EA3
	2	514294	6262263	3100.33	Entry Point	EA3
		514294	6262264	3109.48		EA3
		514615	6261032	3123.25	TD	EA3
MLT-2	1	513306	6263262	3082.26	Entry Point	EA3
		513429	6263420	3082.26		EA3
		513432	6263419	3092.1		EA3
		512915	6262692	3128.56	TD	EA3
	2	513306	6263262	3139.74	Entry Point	EL1
		513149	6263039	3151.51		EL1
		512989	6262649	3164.16	TD	EL1
MLT-3	1	514564	6263379	3139.13	Entry Point	EL1
		514565	6263380	3153.98		EL1
		514281	6263234	3150.35		EL2
		514104	6262946	3153.95		EL2
		513992	6262850	3162.85	TD	EL2
	2	514564	6263379	3139.13	Entry Point	EL1
		514582	6263213	3151.94		EL2
		514339	6262565	3164.28	TD	EL2

Figure 17: UTM coordinates in meter for the reservoir targets for the three possible multilateral well designs in the Ekofisk South.

str	flow units		
		EA1_U	Layer 1
	~	EA1_M EA1_L	
_	JPPER	EA2	Layer 2
EKOFISK formation	5	EA3_U	Layer 3
Ĕ		EA3_M	
for		EA3_L	Layer4
×	ш	EM1	Layer 5
Ë	占	EM2	Layer6
8	MIDDLE	EM3	Layer 7
		EM4	
	LOWER	EL1	Layer 8
		EL2	Layer 9
		EL3	Layer 10
TIGHT zo	ne	EE	Layer 11
		TA_A	Layer 12
		TA_B	Layer 13
- E	ΤĀ	TA_C	Layer 14
aţi		TA_D	Layer 15
E		TA_E	
FOR formation	_	TB_U	Layer 16
Ř	쁘	TB_M	Layer 17
-		TB_L	Layer 18
	ည	TC_U	Layer 19
		TC_M	

Figure 18: Layers in the Ekofisk and Tor formations in the Ekofisk field (ConocoPhillips 2011)

These three MLT options would be simulated and investigated with regards to drillability in order to select the one option that would have the highest probability for success in a possible future implementation on Ekofisk. It was therefore a challenge that the three different options in reality probably would have un-equal reservoir exposure and possible production rates. As a simplification, and as mentioned, but important to stress, an assumption was therefore given that all the three different MLT options, and all the different, respective Laterals, would have identical exposure to the pay-zone and identical production rates. In other words, for this thesis it was decided that from a reservoir perspective there would be nothing separating the three MLT options. The recommended solution would therefore be the one yielding the highest probability of success based on factors such as drillability, issues and challenges, feasibility of the drilling operation and rig constraints.

4.2 Designing the project scope

The designing of the project scope started with meetings with the reservoir and well planning group in COPNO in order to discuss and come up with goals for the project. These gatherings led to a list of preferred requirements and needs for a MLT project, presented in Table 1. These requirements would lay the basis for the further progress and work in order to create a possible multilateral well setup for Ekofisk.

Table 1: Preferred requirements and needs from a reservoir and well planning perspective for a MLT project on Ekofisk

No.	MLT Requirements	Required/expected specifications
1	Expected and/or required	About 2000' – 6000' MD laterals
	horizontal section length	
2	Entry point into the Ekofisk for	Junction within the reservoir, or casing shoe
	both legs or the horizontal	in Våle formation
3	Data gathering during drilling	Standard, including LWD suite
4	Isolation requirements for each	Preferred for each branch of type. Check
	branch	valves
5	Stimulation methodology	Fully completing, selective stimulation, high
		pressure stimulation
6	Access requirements to each leg	Preferred in both legs, but at least in
		mainbore
7	Water shut-off	Preferred
8	IWS	Preferred in mainbore
9	Scale squeeze needs	Yes
10	Production rate expected	1.5 times a single, horizontal well in the
		area
11	Gas lift efficiency	Needed
12	Future monitoring	Down hole gauge preferred, tracers
13	P&A – containment assurance	Standard

4.3 Geology in the area of planned MLT

The possible MLT configurations to be investigated were decided to be placed in the Ekofisk South area, drilled from slot Z-26 and with targets as given in Figure 17. A challenge related to this was the relatively unexplored subsurface in the area of the different reservoir targets. As no wells in reality had been drilled in the specific area there was limited accurate information regarding the geology. Based on this assumptions were made that the lack of information regarding the geology for the area where the MLT wells in this thesis would be placed could be represented with data from measurements and surveys prior, and during, the drilling of nearby wells, mostly 2/4-Z-17 and 2/4-VB-05. This, together with actual overburden surveys in the designated area

carried out in March 2013, made it possible to get a rough picture of the downhole situation for the planned MLT options.

4.4 Determination of Junction design and configuration

Based on the initial requirements presented in Table 1 the oil service company Halliburton was contacted to evaluate possible solutions and technical challenges related to junction placement, design and installation. One of the biggest challenges for COPNO in 2004, first and last time MLT was utilized on Ekofisk, was the junction design with regards to access and stability. The two wells drilled then, 2/4-X-02 and 2/4-X-21, were non-pressure tight junctions, so-called TAML Level 4 (see Figure 13), and the necessary high pressure stimulation required in the Ekofisk was achieved by a one-time packing off, for then to run completion while leaving the junction exposed to the formation. The hydraulic integrity at the junction was provided by cement and formation strength¹². If this strength is not sufficient, as suspected for X-02 and X-21, there is a high possibility of movement of the sidestep, or Lateral 2, attachment position related to the mainbore, or Lateral 1, as a result of production and thermal forces¹³, which can make later access into the lateral impossible.

It was therefore early in the process with Halliburton decided to either go for a pressure tight junction (TAML Level 5), or to place the junction in an area where the formation strength would be sufficient and use a TAML Level 4 non-pressure tight system. An initial suggestion was made to have a junction with pressure integrity set in the reservoir, with Intelligent Well System (IWS) in Lateral 1. The Lateral 2 would then be treated as one, long stimulated perforation via a surface controlled valve in the junction. However, the minimum size of the casing or liner containing the junction system from Halliburton would be 9 5/8", a size that would be too large to meet the production requirements for Ekofisk¹⁴. In addition, the drift diameters in the pressure tight Level 5 junction would be a challenge for a solution with IWS in Lateral 1¹⁵. For this type of completion a non-pressure tight Level 4 junction would be the best option.

Due to the non-pressure tight junction for installation of IWS it was therefore decided to look at the possibility of placing the junction in the overburden, in an area where the formation strength would be sufficient to overcome re-stimulation pressure requirements. It was decided to look at two different junction design options, one pressure tight Level 5 solution without IWS and one non-pressure tight Level 4 solution with IWS in the mainbore. These two junction design options are presented in Table 3 and Table 2.

45

¹² Personal communication with G. Liland. 2013. Stavanger: Halliburton Scandinavia AS

¹³ Personal communication with R. Watts. 2013. Stavanger: ConocoPhillips Norway

¹⁴ Personal communication with S. Sørensen. 2013. Stavanger: ConocoPhillips Norway

The formation demands on Ekofisk require a casing string to be set 2/3 into Våle, the last formation at Top Of Ekofisk (TOE) before entering the reservoir. Today's casing design on Ekofisk, based on the formations in the overburden, is a 13 5/8" casing set at 5000 ft TVD as a basis, with a 10 ¾" casing, or liner, set to TOE in Våle, as mentioned. A re-evaluation of the casing design in order to be able to place the junction in the reservoir would not be an option for this MLT project due to cost and rig layout 16. Therefore, the 10 ¾" string had to contain the junction itself.

Table 2: Junction design option 1

Junction in overburden, 200-300 ft above
TOE
No IWS
Pressure tight junction (TAML Level 5)
Halliburton FlexRite MA

Table 3: Junction design option 2

rusie et dunetion design option 2					
Junction in overburden, 200-300 ft above					
TOE					
IWS in mainbore/Lateral 1					
No pressure tight junction (TAML Level 4)					
Halliburton LatchRite MLT system					

Together with Halliburton possible installation sequences for the two junction design options were put together. The last step of each of these sequences can be seen in Figure 19 and Figure 20. Summarized both of the cases would have a 13 5/8" casing string set at 5000 ft TVD. Then a 12 % hole would be drilled to just above TOE, with a 10 % liner set 2/3 into the Våle formation above the reservoir. From there a 9 % hole would be drilled to TD in Ekofisk, with a 7 5/8" liner post-run. The sidestep, or Lateral 2, would for both of the options be drilled after the mainbore/Lateral 1. For the junction scenario 1 a 8 % hole would be kicked off through the pre-milled window in the 10 % liner at the junction point and drilled to TOE. A 7 % liner would then be set 2/3 into Våle, but not tied all the way back to the junction. Then a 6 % hole would be drilled to TD in Lateral 2, with a 5" liner installed. For the junction option 2, with IWS, a 9 % hole would be kicked off through the pre-milled window in the 10 % liner at the junction point and drilled to TOE. A 8 5/8" expandable liner would then be set 2/3 into Våle at TOE and expanded to 9.555" OD, 8.6" nominal ID and 8.514" drift diameter. The reason for this expandable liner was the desire to drill 8 % hole in the reservoir for lateral 2.

1

 $^{^{\}rm 16}$ Personal communication with T. Husby. 2013. Stavanger: ConocoPhillips Norway

Due to size limitation for the string to be run through the pre-milled window in the junction the running of an expandable was considered to be the best solution to overcome this challenge. Then the $8\,\%$ " hole would be drilled to TD for lateral 2, with a 7 5/8" liner set at TD, tied back to the junction point in the $10\,\%$ " liner. The $8\,5/8$ " expandable would in the end be pulled, as this string only provided the integrity needed to drill the $8\,\%$ " hole to TD in lateral 2.

The complete process of installing the two different junction design options, with all the steps, is presented in whole in Appendix G for option 1 and Appendix H for option 2.

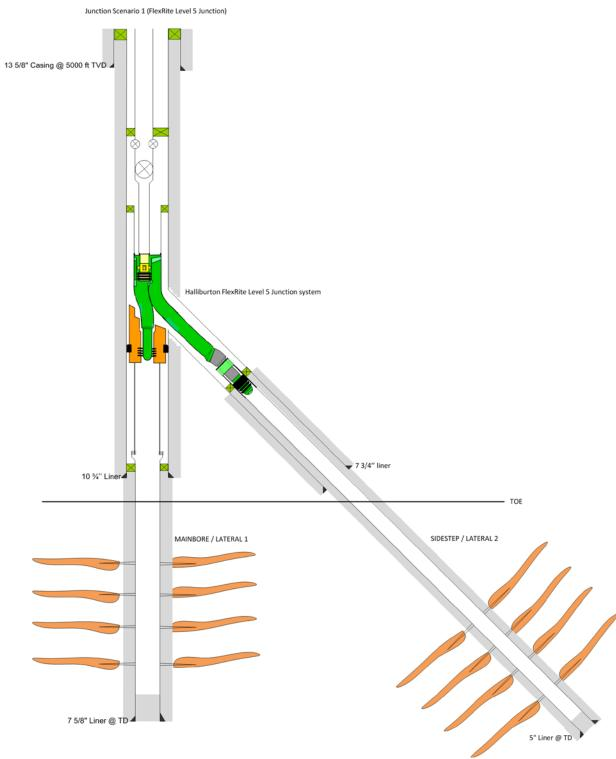


Figure 19: Junction design option 1 installed and ready for production. The figure is not scaled, nor are the proper inclinations shown. Should be used for information purposes only (Figure made by this author)

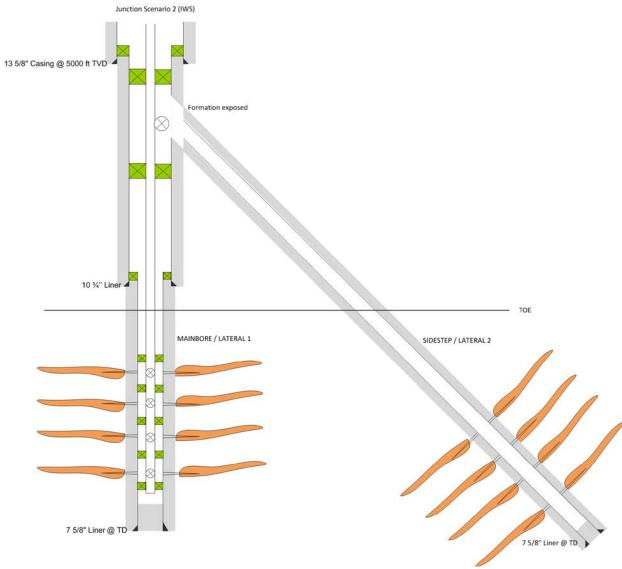


Figure 20: Junction design option 2 installed and ready for production. The figure is not scaled, nor are the proper inclinations shown. Should be used for information purposes only (Figure made by this author)

For COPNO the junction design option with IWS, presented in Table 3 and Figure 20, was decided to be more interesting to evaluate than the option without, despite having a non-pressure tight junction. As presented in Chapter 2 there are currently large water injection programs on Ekofisk, leading to issues with early water breakthrough in certain areas. The implementation of IWS, where each zone can be remotely controlled via signal cables from surface, is therefore currently being performed. By having such a system the zones with early water breakthrough can be shut-in with the rest of the well producing as before, rather than shutting the whole well down, as used to be the case

when the water cut got too high¹⁷. A future MLT option on Ekofisk should therefore have IWS, or a similar system, installed.

The selection of only investigating the junction design option 2, with IWS, then led to the hole sizes as presented in Figure 21 for each of the three MLT options. This figure is based on, and similar, to Figure 16, but focuses on the reservoir part of each of the MLT's (again it should be noted that the selection to come up with the presented junction depth of 9958 ft TVD is presented in section 4.5). As it can be seen the lateral 1 for each of the MLT would be drilled with a 9 ½" bit to TD from the last shoe, the 10 ¾" liner, set 2/3 into Våle at TOE. For Lateral 2 for each of the MLT options the lateral 2 would be kicked off from the pre-milled window in the 10 ¾" liner at a certain length above TOE. Therefore a need of an additional casing point at TOE, 2/3 into Våle, had to be established. This first, short section, from the junction point to TOE would for the junction design option 2 be drilled with a 9 ½" bit, while the reservoir would be continued with an 8 ½" bit to TD.

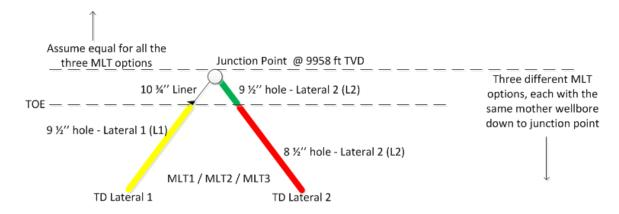


Figure 21: Hole sizes to be drilled for all of the three MLT options for junction design option 2, with IWS (Figure made by this author)

4.5 Determination of junction placement

In order to make it possible to install the junction design option 2, where the junction would be exposed to the formation, a suited place in the overburden, with sufficient formation strength with regards to production effects and re-stimulation pressures of around 5000 psi, had to be found. Together with overburden geologists in COPNO, Helen Haneferd and Guri Tveitnes, evaluations of the overburden in the area of the planned reservoir targets were performed. An interval of 200 – 300 ft TVD above TOE was looked at. The interval is marked with blue, dotted horizontal lines on the logs in Figure 22.

-

¹⁷ Personal communication with T. Husby. 2013. Stavanger: ConocoPhillips Norway

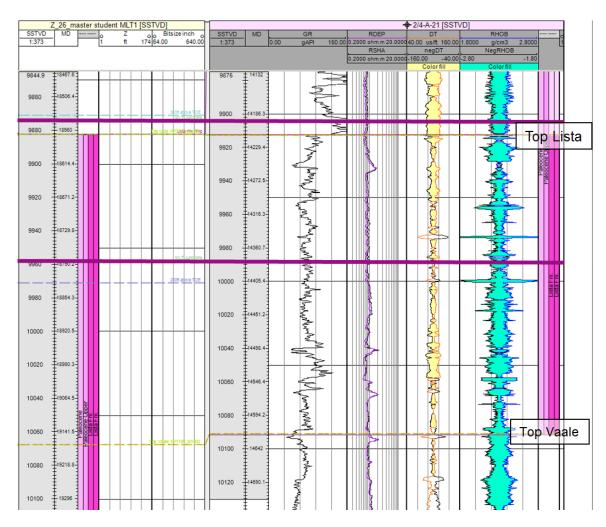


Figure 22: Investigated area in the overburden in order to determine junction placement (ConocoPhillips 2013h).

Based on this information, log data and seismic, two possible depths were proposed, marked with solid, horizontal, purple lines in

Figure 22. The geomechanical model output from the wellbore stability survey from March 2013 indicates no significant failures in the interval selected.

The depths and coordinates for the two possible junction placement proposals are found in Table 4. Of the two suggested junction placement depths, the one at the bottom, at 9958 ft TVD, was selected due to indications of slightly higher formation strenght¹⁸. The table shows the X and Y coordinates of the junction placement in the UTM coordinate system, with distance in meters, and the Z coordinate as TVD in feet from the rig's depth reference point (Rotary Kelly Bushing, or RKB).

1

¹⁸ Personal communication with H. Haneferd. 2013. Stavanger: ConocoPhillips Norway

Table 4: Junction placement suggestions in the overburden (Maxwell 2013)

Well identifier	Surface	X	Υ	Z	MD
Z_26_master student MLT1	MLT Junctions	514322.5	6262563	-9874	18544
Z_26_master student MLT1	MLT Junctions	514321.2	6262495	-9958	18784

4.6 Well Slot

As mentioned the possible MLT options would be drilled from slot 2/4-Z-26 in the Ekofisk South. The coordinates, in both Polar (Longitude and Latitude) and UTM (Northing and Easting) for the well slot, is presented in Table 5.

Table 5: Site and well slot placement and properties (Maxwell 2013)

Well Position Position Uncertainty	Z-26 - Slot Z26 +N/-S +E/-W	16.27 ft 31.92 ft 0.00 ft		6,266,835.4 513,945.8		Latitude: Longitude: Water Depth:	56° 32' 39.855 N 3° 13' 36.457 E 260.20 ft
Site Position: From: Position Uncertainty:		0.00 ft	Northing: Easting: Slot Radius:	6,266,830.520 m 513,936.090 m 0.000 in	Latitud Longit Grid C		56° 32' 39.696 N 3° 13' 35.887 E 0.19 °
Site	Ekofisk Z						

The rig set-up and slot position, with location of the junction and the three different multilateral well options to be investigated and simulated, from a top-view perspective based on the positions in Table 4 and Table 5, is presented in Figure 23.

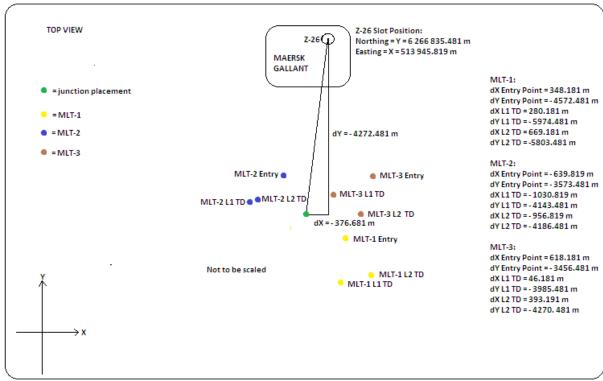


Figure 23: Top view of the MLT set-up for well slot 2/4-Z-26 with junction placement and the three multilateral configurations s to be investigated. All positions and differential distances are with regards to the slot coordinates (Figure made by this author)

4.7 Designing the well paths

Once the well slot, junction placement and reservoir targets were determined the well paths could be designed. The concept of planning a well is an integrated task, especially on Ekofisk with so many well drilled over the years, and interaction between various work groups were made in order to finalize the all the wellbores to be simulated for this thesis. More about wellplanning on Ekofisk can be found in Appendix I. As mentioned there would be three different multilateral well options to be investigated (MLT1, MLT2 and MLT3). For each of the three there would be a mainbore/Lateral 1 and a sidestep /Lateral 2, giving a total of six wellbores. Each of the lateral 2, again, as shown in Figure 21, would be divided into two sections, a 9 ½" from junction point to TOE, and a 8 ½" from TOE to TD in Ekofisk. All in all a total of six wellbore, with nine different wellbore sections had to be created for simulation.

As presented there would be a common mother wellbore from the slot at surface down to the junction point. This would mean that all three different MLT options would be identical from the slot down to the junction point. From there the three different configurations would be distinguished by each having their own pair (Lateral 1 and Lateral 2) going to dissimilar reservoir targets, as already presented in Figure 16.

Together with Leif Ramsvik in Halliburton the Landmark software Compass was used to create and lay out a common mother wellbore, as well as the six different well paths for each of the wellbores. The complete survey details of all the wellbores can be provided by the author upon request. For this report the survey data was decided not to be put in the appendix due to the excessive amount of data points.

4.8 Drilling Rig

The drilling rig currently being used in the Ekofisk Z area is the Mærsk Gallant. This is a jack-up built in 1993 and classified under the Lloyd's Register of Shipping. For the MLT options to be investigated in this master thesis it was assumed that this rig would be used also for future drilling of slot Z-26. More details and information about Mærsk Gallant can be found in Appendix J.

4.9 Overview of the three MLT options, with all wellbore sections

Based on the decision of only investigating the junction design option with IWS (option 2), the hole sizes would be as presented in Figure 21. The common mother wellbore would go from the rig down to the junction point at 9958 ft TD. For the well path created for this wellbore that depth would correspond to 18150 ft MD, which would be the junction measured depth for all the three MLT options. From there the lateral 1 and lateral 2 for each of the options would be individual, leading to different reservoir targets. As the TOE is not a horizontal straight plane a result of this would be that the L1 and L2 for the different MLT options would reach the TOE at different TVD's. The requirement of having the last casing setting point 2/3 into Våle before entering Ekofisk would be valid for all the MLT options. Table 6 presents an overview of the depths for the wellbores for the three MLT options. It should be noted that for all L2 the last casing shoe for the top 9 ½" section (see Figure 21) would be the 10 ¾" liner in form of the premilled window at 18150 ft MD. Please refer to Figure 21 for schematic of the hole sizes for the different wellbore sections. These wellbore sections will be valid for all the MLT options, but with individual differences in well path from the junction point to the target the measured depths will not be the same for equal TVD, as seen in table.

Table 6: Overview of the downhole depths for the different wellbores in for the MLT options

MLT1		ML	.T2	MLT3		
Lateral 1	Lateral 2	Lateral 1	Lateral 2	Lateral 1	Lateral 2	
Junction @	Junction @	Junction @	Junction @	Junction @	Junction @	
9958 ft TVD	9958 ft TVD	9958 ft TVD	9958 ft TVD	9958 ft TVD	9958 ft TVD	
/ 18150 ft	/ 18150 ft	/ 18150 ft	/ 18150 ft	/ 18150 ft	/ 18150 ft	
MD	MD	MD	MD	MD	MD	
10 ¾" Liner	8 5/8" Liner	10 ¾" Liner	8 5/8" Liner	10 ¾" Liner	8 5/8" Liner	
shoe @	shoe @	shoe @	shoe @	shoe @	shoe @	
10076 ft	10076 ft	10060 ft	10060 ft	10123 ft	10123 ft	
TVD / 18600	TVD / 18600	TVD / 18550	TVD / 18550	TVD / 18790	TVD / 18790	
ft MD	ft MD	ft MD	ft MD	ft MD	ft MD	
TOE @	TOE @	TOE @	TOE @	TOE @	TOE @	
10135 ft	10135 ft	10104 ft	10104 ft	10163 ft	10163 ft	
TVD / 18800	TVD / 18800	TVD / 18700	TVD / 18700	TVD / 18900	TVD / 18900	
ft MD	ft MD	ft MD	ft MD	ft MD	ft MD	
TD @ 10467	TD @ 10246	TD @	TD @ 10552	TD @ 10548	TD @ 10553	
ft TVD /	ft TVD /	10437.29 ft	ft TVD /	ft TVD /	ft MD /	
24280 ft MD	23950 ft MD	TVD/	29116.78 ft	30592.58 ft	32941.66 ft	
		29778.94 ft	MD	MD	MD	
		MD				

5 Technical challenges related to the drilling of Multilateral Wells

Compared to a conventional single wellbore well there are not many differences for a MLT system. As for any other wells drilled the challenges for a multilateral well are related to wellbore geometry such as Dog Leg Severity (DLS) and Build-Up Rate (BUR), Torque and Drag, such as effective tension, rotary torque, fatigue, hook load and minimum WOB to buckle and Hydraulics, in form of hole cleaning, pressure losses and circulating pressures and ECD-effects. More drilling related challenges could be mentioned, but for this master thesis it was decided to focus only on the effects stated here. In addition, and separating a multilateral well from a conventional one, there are challenges related to kicking off from the mother wellbore to create the sidestep, as well as the installation process of the junction itself. In this report field units are used due to COPNO guidelines and policies.

5.1 Dog Leg Severity

The DLS, measured in degrees per 100 ft, is a measurement of change in direction in the three dimensional space of the well path as a function of length (Wojtanowicz 2012). The most critical doglegs most often occur as a result of un-wanted events during drilling, leading to rapid changes and tight bends in the wellbore geometry. An example of this can be if the bit enters a harder formation at an inclination. If the inclination is below 30 degrees from the vertical the bit has a tendency to want to stay in the soft formation leading to sharp direction changes in the hole is the bit weight is continued. If the layer is above 30 degrees inclined compared to the vertical the bit often has no other choice than to enter the harder formation, but the side of the bit first encountering the harder formation will get reduced penetration rate resulting in a turning effect towards the side touching the harder rock (Wojtanowicz 2012). Simple schematics of this example can be seen in Figure 24.

Any well drilled that have directional changes will have doglegs present. Even though the uncontrolled doglegs most often cause the ones with the highest DLS sometimes the well path is planed with high doglegs in order to hit desired targets given a range of constraints. For most drilling operations today a maximum DLS is considered to be around 3.0 degrees per 100 ft (Wojtanowicz 2012), even though new tools and equipment might make it possible to increase this number to 5, and even 6, for hole sizes of 8 ½" to 9 7/8" (Hummus et al 2011). The 3.0 number is based on the ability of running tubulars, casings and other downhole equipment of certain lengths through the dogleg. If the DLS gets to high it might be impossible to get to the desired depths through the tight curves and rapid changes in hole geometry. In addition the fatigue and wear issues increases with increased DLS (Wojtanowicz 2012). Cyclic rotations of the drillstring through high doglegs are critical for the integrity of the tool joints between

the pipe segments, and might ultimately lead to failure of the threads in the TJ's. On top of this the running of pipe and tubulars, as well as drilling ahead and tripping in/out, will be experience higher frictional forces, and thus increased wear, for higher DLS. On the other hand, however, doglegs can help reduce the hook load by creating bends for the drillstring to "rest" on, thereby taking some of the weight otherwise felt by the rig. But for the general case the DLS should be kept as low as possible to avoid issues with running of equipment and to mitigate fatigue and wear issues. It should be noted that the shallower the dogleg, the worse (Wojtanowicz 2012).

The DLS for maximum excessive wear of tool joints caused by contact between the wall of the hole and the TJ, as given by Lubinski, can be calculated by Eq. 1 (Wojtanowicz 2012). For this Eq. the F is the maximum lateral force on the TJ, given in lbf, the $w_{\it mud}$ is the buoyed weight of the drillstring below the dogleg, units in lbf, and the $L_{\it half}$ is the half-distance between the tool joints. The applied constant of 34400 is an empirical ratio applied in order to get the units for the DLS in degrees per 100 ft.

$$DLS = 34400 * \frac{F}{L_{half} * w_{mud}} \tag{1}$$

For DLS with regards to the ensuring of running of next casing string and tubular Eq. 2 (Sangesland 2012) can be utilized. The parameter φ is the dogleg angle, found from Eq. 3, given in degrees, and the L is the difference in measured depth in feet between two following survey points. In Eq. 3 the parameter α is the inclination and the parameter β the azimuth angle. The subscript 1 and 2 denotes the values at two following survey stations.

$$DLS = 100 * \frac{\varphi}{L} \tag{2}$$

$$\varphi = \cos^{-1} \left[\cos(\alpha_1) * \cos(\alpha_2) + \sin(\alpha_1) * \sin(\alpha_2) * \cos(\beta_1 - \beta_2) \right]$$
(3)

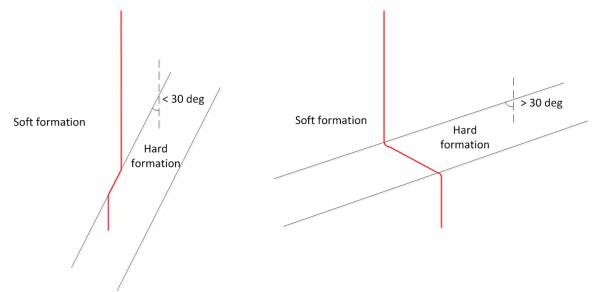


Figure 24: High DLS caused by the entering of a harder formation at inclination (Figure made by this author)

5.2 Build-Up Rate

The BUR is closely related to the DLS. The build-up rate describes the rate, in degrees per 100 ft, which the well path builds inclination. A smaller BUR will result in a longer well path interval required in order to obtain the desired hole-inclination, and vice versa. The BUR can be both positive and negative. For positive values of the build-rate the inclination increases, while for negative values it decreases. The latter is also known as drop, as presented in Figure 25. A section of the wellbore where the BUR is zeo is often referred to as the hold section. Compared to the DLS the BUR only considers the inclination changes in the well path, and not the azimuth changes. Said in another way the BUR is two-dimensional, while the DLS is three-dimensional. A high BUR will therefore result in a high DLS, but a high DLS does not necessarily mean a high BUR. Normally the BUR is lower than the DLS and is most often used to describe the desired changes in the well path in order to, for instance, hit the target in the best possible manner (Sangesland 2012). In most cases the BUR is investigated for a larger section of the well. As mentioned in the previous sub-chapter, the DLS, on the other hand, is often negatively used for undesired, rapid bends and corners in the well path, and is analyzed in smaller portions of the well path.

The calculation of the rate of build-up is pure geometrical. The calculation of BUR is given by Eq. 4. The L here is the well path length between two survey stations. This length is dependent on how the wellbore is modeled, and will therefore influence the output value of BUR. The most commonly used methods to find L is the tangential method, balanced tangential method, radius of curvature method and the minimum curvature method (Sangesland 2012). Of these is the latter the most accurate and the

one most often used for directional survey calculations. It should be mentioned that these methods described here today are being utilized by advanced computing programs build-in to the different survey tools to yield decreased levels of uncertainty for the calculations by dividing the well path into more fragments. Still, however, the most advanced tools in the marked today still have a given inaccuracy giving an ellipsis of uncertainty around the calculated wellbore position. The actual position will be somewhere inside this ellipsis (Sangesland 2012).

$$BUR = 100 * \frac{\alpha_2 - \alpha_1}{L} \tag{4}$$

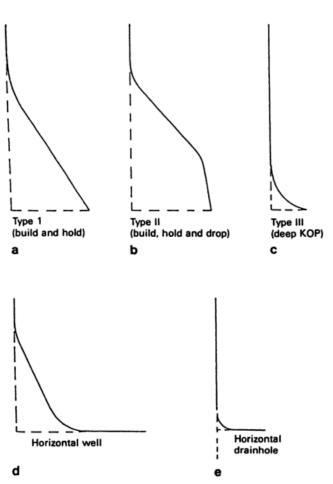


Figure 25: Examples of build-up, hold and drop for deviated and horizontal wells (Inglis 1987)

The trade-off when it comes to benefits versus negative effects with high BUR for drilling of wells is often a challenge. In the United States, where onshore lease lines at surface imagined to go vertically down in the subsurface dictates the cube the operator is allowed to drill within in the underground, a high BUR is often desired in order to get as much exposure to the pay zone as possible (Hummus et al. 2011). In other areas a high build-rate might be necessary in order to avoid other wellbores, or desired in order

to enter the reservoir in an optimum way. A high BUR might also result in a shorter overall well path, leading to less equipment having to be used for the well. On the other side, the higher the BUR the larger the challenges with fatigue, wear and passing of tubulars and strings. The ultimate constraint when it comes to maximum BUR, just as for DLS, is given by the ability of running casings, drillstring and other downhole tools through the build-section. However, in modern drilling operations the BUR is often limited by the inclination-change capabilities in the BHA (Hummus et al 2011).

5.3 Effective Tension

The effective tension is the tension, adjusted for all other load effects, felt in the pipe at any depth at any time in the well during a drilling operation. These load effects can be tension from the hook at the rig, torque due to rotation of the pipe, bending stresses due to doglegs and pressure differentials between inside and outside of the drillstring (Wojtanowicz 2012).

During normal operations the highest tension is felt by the pipe elements closest to the rig floor during tripping out when the bit just leaves bottom. For rotation on bottom the effective tension at surface will be lower due to the bottom part of the string being in compression as weight is applied to the bit. The weight felt at the rig during drilling ahead will therefore only be the buoyed weight of drillstring from the neutral point of tension and upwards. For tripping out the top DS element feel the buoyed weight of the whole string below all the way down to TD, plus friction and acceleration effects (Wojtanowicz 2012). In addition wellbore geometry will impact the effective tension in form of bends and corners where the drillstring can "rest" or get "hung-up". In events such as a stuck pipe, overpull often has to be exerted to the string resulting in higher effective tension than for tripping out. However, the critical combined loads are normally considered to be during fishing operations (Wojtanonwicz 2012).

If the effective tension in the string gets too high the string elements might suffer from yield failure. The yielding of the drillstring will not occur as long as the equivalent, or effective, stress is lower than the yield strength of the string element. The maximum values for yield strength can be found in drilling tables specified for different drill pipes and other downhole equipment. However, these tabulated values are valid only for uniaxial state of stress, meaning that the yield strength values in the tables only are valid for no other stress state than tension. This never happens in reality, and combined stress, such as internal pressure in addition to tensional force, will influence the tabulated yield strength. It is therefore important always to consider the combined loads in order to find the effective maximum yield strength for a pipe element for a given situation. Alternatively the maximum yield strength from the tables can be kept, and instead adjusting the stresses in the pipe for combined loads to find the effective, or equivalent, stresses exerted on the drillstring. This can for instance be performed by using the von Mises Eq., presented in Eq. 5, to find the equivalent stress for a string. This

Eq. takes into account the combined stresses acting on the drillstring, and gives as an output the equivalent stress acting on the pipe. The pipe is indicated to fail if the von Mises stress, V, exceeds the yield limit given for the pipe. It should be mentioned that Eq. 5 is a general Eq., meaning the in the case of a failure the reason cannot be determined. In other words, if the combined stress of pressure and torque are acting on a drillstring, and the calculations show that the pipe is likely to fail given by the von Mises stress, it cannot be determined whether the pipe will fail due to the pressure or the torque (Wojtanowicz 2012).

$$2V_2 = \left[\left(S_a - S_r \right)^2 + \left(S_t - S_r \right)^2 + \left(S_a - S_t \right)^2 \right] + 6 \left[T_t^2 + T_r^2 + T_z^2 \right]$$
 (5)

In the von Mises Eq. the S_a is the axial stress in the wall of the drill pipe, given in psi, the S_r is the radial stress in the wall of the DP, also given in psi, the S_t is the tangential stress in the wall of the drill pipe, given in psi, the T_t is the tangential shear stress normal to the longitudinal axis of the DP, units in psi, the T_t is the radial shear stress normal to the longitudinal axis of the DP, while the T_z is the axial shear stress parallel to the longitudinal axis of the drill pipe, also given in psi. Said differently the T_t represents the torque applied to the string and the T_z is the additional forces due to bending. The T_t is typically set to zero for simplification (Wojtanowicz 2012). For the sake of this report the different parameters in the von Mises Eq. will not be discussed in detail any further. For more information regarding the calculation of equivalent stress for a drillstring please refer to Wojtanowicz (2012), page 231 – 237.

The effective tension in the string, on the other hand, measured in lbf, can be calculated using Eq. 6. Here the OP is the overpull in lbf, the P_i the internal pressure inside the drillstring at given depth, given in psi, P_o the external, or outer, pressure outside the drillstring, also given in psi, A_i the cross-sectional area inside the pipe, units in inches squared, and A_o the cross-sectional area outside the pipe, also given in inches squared, or in other words between the borehole wall and the OD of the drill pipe (Wojtanowicz 2012). The internal pressure in the pipe can be found from Eq. 7, while the outside pressure can be found utilizing Eq. 8. The $P_{i,surf}$ and $P_{o,surf}$, both in psi,are the pressure at the surface for inside and outside of the string, respectively. The T_{real} , given in lbf, is the sum of the actual hook load of the string submerged in mud and the internal pressure area force acting on the end of the DP. This value can be found by using of Eq. 9. The bouancy factor, BF, can be calculated by Eq. 10. The $W_{DS,air}$ is the weight of the drillstring in air, while the L_{DS} is the length of drillstring below the surface, or depth. For calculations at the rig the last part of Eq. 9 therefore can be neglected (Wojtanonwicz 2012).

$$T_{eff} = T_{real} - (P_i * A_i) + (P_o * A_o) + OP$$

$$\tag{6}$$

$$P_{i} = 0.052 * \rho_{mud} * D_{TVD} + P_{i,surf}$$
 (7)

$$P_o = 0.052 * \rho_{mud} * D_{TVD} + P_{o,surf}$$
 (8)

$$T_{real} = Hookload + P_{surf} * A_i - W_{DS,air} * BF * L_{DS}$$
(9)

$$BF = 1 - \frac{\rho_{mud}}{\rho_{steel}} \tag{10}$$

5.4 Torque

The top drive at the rig, or in some cases the rotary table, provides rotary torque for the drilling operation. For Mærsk Gallant the maximum torque that can be applied is 60000 ft-lbf. However, most string component have their respective make-up torque recommended values lower than this, often ranging in the area between 20000 and 45000 ft-lbf, dependent on size, grade and class (Wojtanowicz 2012). It is important that the experienced rotary torque in the string at any depth never exceeds the make-up torque for the given component in the string at that depth. For DP the make-up torque corresponds to the maximum load capacity of the TJ. If the actual torque applied is higher than this maximum additional tensional stress will be applied to the pipe, and the load capacity in the TJ will be reduced. Therefore, in order for the tabulated strength and maximum load values for a DP to be valid it is important that the correct make-up torque, listed in the same tables, is always applied (Wojtanowicz 2012). For DC's it is likewise crucial to follow the make-up torque directions found in the data tables. The recommended torque for drill collar connections is to keep the seal on the shoulders of the collars intact. If the make-up torque is too low the shoulders may separate during bending and rotation, leading to leakage of drilling fluid from the inside of the pipe to the annulus. The shoulders are kept together by a compressive force at the shoulder face created by a sufficient load. It is the make-up torque that applies this back-up load, and an insufficient connection torque therefore can lead to shoulder separation between to following collars. On the other hand, if the DC make-up torque is higher than the tabulated recommendation it can, just as for the DP, create an additional tensional force in the DC, and the number of cycles before experiencing fatigue failure of the pin in the connection, as a result of this, can be reduced (Wojtanowicz 2012; Sangesland 2012).

Eq. 11 gives the maximum value of rotary torque, in in-lbf, that can be applied at surface to a drillstring with a given working tension load (Wojtanowicz 2012) without yielding of the pipe. This working tension load is given as the actual tension felt at surface, $\sigma_{y,applied}$, in psi, times the cross-sectional area of the drillstring, A_{cross} , in inches squared. The result of the multiplication of these will have units in lbf. The $\sigma_{y,table}$ is the tabulated maximum tensile strength of the pipe. Z is the polar module of the DP, given by Eq. 12, with units in inches cubed. The J in Eq. 12 is the polar moment of inertia, given in inches raised to the fourth power, and can be calculated by use of the outside and inside diameter of the DP from Eq. 13.

$$T_{\text{max}} = \frac{Z}{A_{cross}} * \sqrt{\frac{\left(\sigma_{y,table} * A_{cross}\right)^2 - \left(\sigma_{y,applied} * A_{cross}\right)^2}{3}}$$
 (11)

$$Z = \frac{2J}{OD_{DP}} \tag{12}$$

$$J = \frac{\pi}{32} \left(OD_{DP}^{4} - ID_{DP}^{4} \right) \tag{13}$$

For calculations of torque due to friction Eq. 14 can be used. Here F is the friction force between the pipe and the borehole wall acting in the opposite direction of pipe rotation. This force can be pictured by use of N, the normal force acting on the drill pipe from the borehole wall, and μ , the friction factor. The last parameter, r, is the radius of the pipe.

$$T_{friction} = F * r = N * \mu * r \tag{14}$$

In order to find the total torque at surface due to downhole friction, and hook load, as will be discussed in section 5.6, there are often two models considered, namely the analytical friction model and the discrete model (Sangesland 2012). For smooth curved hole sections the analytical model is the most suitable to use, while the discrete is better for holes with continuous changes in inclination and azimuth. In reality most wellbores are not smooth and therefore the discrete model most often has to be utilized. The discrete model divides the wellbore into sections, where the calculations performed on each section add up to the total value for the wellbore. A common method to perform these calculations is to start at TD and end up at surface. The number of sections divided into will influence the value at the surface, and most computer software will make use of thousands of steps. For manual calculations a convenient method is to divide between vertical section and build/drop sections (see Figure 25), and between build/drop sections and hold sections. An example of this is showed in Figure 26.

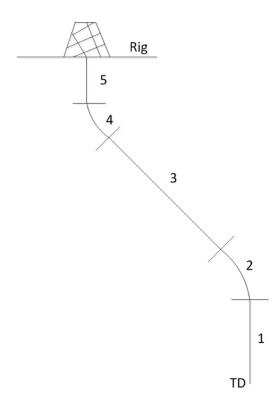


Figure 26: Convenient dividing of the drillstring for manual calculations using the discrete model (Figure made by this author)

For the discrete model the torque due to friction at a given depth in the well is found by using Eq. 15. This Eq. says that the torque at the end of a section of the pipe in the well (here denoted T_2), going from bottom and upwards, as described, is the sum of the torque at the start of the pipe section, T_1 , plus the torque due to friction caused by the length of the pipe section between the two depths. An illustration of this can be seen in Figure 27. This torque due to friction of the pipe section is the last part of Eq. 15, same as Eq. 14. The normal force, N, for a pipe in a borehole can be calculated using Eq. 16 (Johancsik et al. 1984). Here the F_1 is the force pulling on the lower side of the pipe due to the weight of the drill pipe below this point, see Figure 27. The $\Delta\phi$ is the change in azimuth in radians, and for zero changes the Eq. for N simplifies to Eq. 17. $\Delta\theta$ is the change in inclination, also given in radians. It should be noted that the $\overline{\theta}$ is the average inclination for the pipe section given in degrees, not radian. The calculation of change in azimuth and inclination, as well as average inclination, is found in Eq. 18, Eq. 19 and Eq. 20, respectively. Finally, the w in Eq. 16 is the buoyed weight of the pipe section and can be calculated using Eq. 21. The BF is the buoyancy factor found from Eq. 10. By performing calculations on the torque at the end of each of the pre-defined pipe sections the torque at surface can be found as the $T_2 = T_{surface}$ for the top section.

$$T_2 = T_1 + \mu * r * |N| \tag{15}$$

$$N = \sqrt{\left(F_1 * \Delta \phi * \sin(\overline{\theta})\right)^2 + \left(w * \sin(\overline{\theta}) + F_1 * \Delta \theta\right)^2}$$
 (16)

$$N = w * \sin(\overline{\theta}) + F_1 * \Delta\theta \tag{17}$$

$$\Delta \theta = \theta_2 - \theta_1 \tag{18}$$

$$\Delta \phi = \phi_2 - \phi_1 \tag{19}$$

$$\overline{\theta} = \frac{\theta_2 + \theta_1}{2} \tag{20}$$

$$w = m_{pipe} * L_{pipe} * BF (21)$$

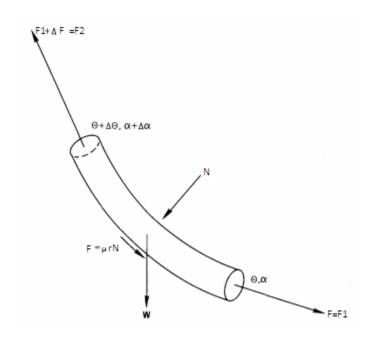


Figure 27: Forces on a pipe section element for torque and drag analysis using the discrete model (Johancsik et al. 1984)

5.5 Fatigue and Wear of the Drillstring

Fatigue of the drillstring can occur if the wear, forces or loads experienced get too extensive. During a drilling operation the downhole equipment will continuously wear out, and changes have to be done in order to ensure that the integrity in the string and other crucial elements are intact at all times. If the drillstring gets exposed to cyclic rotations in doglegs with high severity, as mentioned in section 5.1, the fatigue ratio increases rapidly (Wojtanowicz 2012). In addition the normal operations such as drilling, tripping in/out, tension in the string, rotary torque applied, make-up torque applied, pipe handling, transportation of the string, and more, will influence the fatigue ratio negatively¹⁹.

According to Wojtanowicz (2012) there are four major pipe classes, based on wear of the pipe, presented in Figure 28. These are new, premium, class 2 and class 3. The new class assumes no wear and 100 % nominal wall thickness. For the premium class the pipe is given the torsional and tensile maximum tabulated strength values, as well as the collapse and internal pressure resistance, based on an assumed 20 % uniform wear of the pipe walls compared to a new pipe, meaning that the minimum pipe wall thickness is 80 % of a new. For class 2 also a uniform wear of 20 % is assumed, but the minimum wall thickness is reduced to 65 % of new, meaning that 35 % eccentric wear can be found. The last class, class 3, assumes a uniform wear of 37.5 %, with eccentric wear of up to 45 %, meaning that the minimum wall thickness, compared to a new pipe, might be as low as 55 %. Naturally, a class 3 pipe will reach the fatigue limit faster than a premium class pipe, if all other conditions are kept constant. To apply an additional safety factor against wear and fatigue most pipes used in the industry are classified as premium as soon as they leave the factory, even though never used (Wojtanowicz 2012).

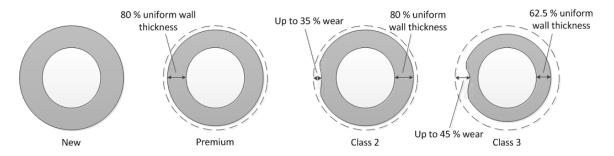


Figure 28: Classification of drill pipes based on wear (Figure made by this author)

-

¹⁹ Personal communication with P. Skalle. 2013. Trondheim: NTNU

5.6 Drag forces and Hook Load

The hook load is a function of wellbore length (or drillstring length really), drillstring composition, drilling fluid density, wellbore geometry and drag forces. Normally the tripping out operation yields the largest hook load for normal operation. When the bit just leaves the bottom at TD the maximum hook load is experienced at the surface, a value that often is referred to as the pick-up force (Sangesland 2012). For issues, such as stuck pipe and fishing operations the values might get higher (Wojtanowicz 2012).

As mentioned in section 5.4 the forces in the drill pipe can be calculated using either the analytical or the discrete model. The hook load can be found by using the discrete model and by dividing the drillstring into pre-defined sections, as suggested in Figure 26. The force required to pull on the top side of the pipe section, F_2 , as displayed in Figure 27, is given by Eq. 22. The \pm in Eq. 22 indicates the difference between pulling and lowering of the pipe. For pulling out of the hole the friction force will work against the pulling, giving an additional force required to pull the pipe. The plus sign should therefore be used for POOH. For lowering of the drillstring the drag force working against the direction of motion of the pipe will reduce the hook load, therefore the minus sign has to be used (Sangesland 2012). The F_1 is the force pulling on the lower side of the pipe section due to the buoyed weight of the drillstring below. The w is the weight of the pipe section itself, as given in Eq. 21, the $\overline{\theta}$ the average inclination for the section, calculated by Eq. 20, μ the friction factor and N the normal force acting on the side of the pipe from the borehole wall, as presented in Eq. 16. The hook load can, as for the torque, be found by performing calculations from bottom and upwards for each of the pipe sections. For the top DP section the F_2 equals the hook load (Sangesland 2012).

$$F_2 = F_1 + w + \cos\left(\overline{\theta}\right) \pm \mu * N \tag{22}$$

It should be mentioned that Eq. 22 is given for no rotation of the pipe. If rotational speed is applied the drag forces will be reduced significantly, resulting in a reduced hook load. The forces on a pipe element, if seen from top, can be displayed as showed in Figure 29. For pulling out of the hole in the x-direction the pipe will have a velocity, V_x , in that direction, with a resulting frictional force, F_x , acting against the direction of movement. With the introduction of rotation of the pipe a velocity, V_y , is applied to the DP. This velocity in the y-direction will result in a frictional force, F_y , acting against the direction or rotation. Based on this the resultant friction, F_{res} , and velocity, V_{res} , will be as showed in the figure. The resultant velocity can be described by use of Eq. 23, while the resultant frictional force can be calculated using Eq. 24.

$$V_{res}^{2} = V_{x}^{2} + V_{y}^{2} \tag{23}$$

$$F_{res}^{2} = F_{x}^{2} + F_{y}^{2} = const.$$
 (24)

For Eq. 24 the F_x again can be described as in Eq. 25, where F_N is the normal force acting from the borehole wall on the pipe element.

$$F_{x} = \mu * F_{N} * \frac{V_{x}}{V_{res}} \tag{25}$$

Given that the resultant velocity can be written as in Eq. 23, Eq. 25 then becomes as presented in Eq. 26. This Eq. indicates that if the velocity in the y-direction, the rotational velocity of the pipe, goes towards infinity, the frictional forces in the x-direction goes against zero.

$$F_{x} = \mu * F_{N} * \frac{V_{x}}{\sqrt{V_{x}^{2} + V_{y}^{2}}}$$
 (26)

The velocity in the y-direction can again be described with revolutions per minute by transforming the expression for V_y into Eq. 27. Here n is the revolutions per minute of the drillstring and r the pipe radius. With this Eq. 26 then becomes as given in Eq. 28. This Eq. shows the effect of rotation of the DP on the drag effect, or frictional force acting in the opposite direction of pipe movement in the x-direction, F_x (Sangesland 2012). As an example, for a rotation of 100 RPM, and otherwise constant parameters, the drag force will be reduced by 25 % contra no pipe rotation.

$$V_{y} = \frac{2 * \pi * n}{60} * r \tag{27}$$

$$F_{x} = \mu * F_{N} * \frac{V_{x}}{\sqrt{V_{x}^{2} + \left(\frac{2 * \pi * n}{60} * r\right)^{2}}}$$
 (28)

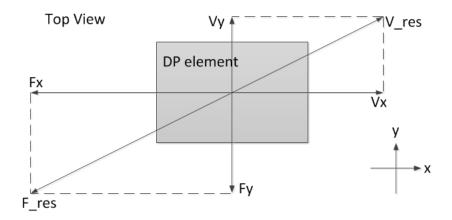


Figure 29: Forces on a drill pipe element with pipe rotation (Figure made by this author)

5.7 Minimum WOB to buckle

The minimum WOB to buckle is the critical bit weight applied that will make the drillstring buckle. For a vertical borehole, with no weight on the bit, the drillstring will remain straight. As soon as the bit reaches the bottom the applied weight on bit will increase until the desired level is reached. At this point the bottom part of the drillstring will be in compression, applying weight to the bit, while the upper part of the string will be in tension, creating a positive hook load at the rig. The point in the drillstring where the net tensional force is zero is called the neutral point of tension (Wojtanowicz 2012). It is important to stress to difference between the neutral point of tension and the neutral point of buckling (NPB). Lubinski defined this point in the drillstring as "the point at which compressive stress is equal to hydrostatic pressure of the surrounding fluid" (Wojtanowicz 2012). In other words, the NPB is at the top of the portion of drillstring that actually produces bit weight, and if the string is cut here there will be no change of stress, and WOB will be identical as before. The NPB can also be described as the point at which the stability force, found by Eq. 29, equals the compressive load. In this Eq. the A_i and A_a represents the inner and outer cross-sectional area of the pipe, while the P_i and P_o describes the pressure inside and outside the pipe, respectively.

$$F_{S} = (A_{i} * P_{i}) - (A_{o} * P_{o})$$

$$\tag{29}$$

The difference between the neutral point of tension and NPB then becomes the length of string that is in compression due to the upwards hydrostatic pressure, or buoyancy force, of the drilling fluid, but does not apply any weight to the bit. That section of pipe will not be felt as tension at the surface; neither will it add weight to the bit (Wojtanowicz 2012). This is displayed in Figure 30. For a pipe hanging in air the neutral point of tension will be at the bit, marked with an A. The whole DP will for this condition be in tension. As the hole is filled with mud (as it naturally always is) a compressional

force is applied to the bit and the neutral point of tension shift upwards to point B in the figure. As WOB then is applied to the bottom for drilling ahead the neutral point of tension continues upwards the string to point C. If the effects of mud surrounding the pipe had not been taken into account the point would have been at D in the figure, due to the lower start point given in point A. The length difference between point C and D represents the difference between the NPB and the neutral point of tension. The length of drillstring below the NPB in D will add weight to the bit, while the section of string between C and D will represent the compression due to the buoyancy effect (Wojtanowicz 2012).

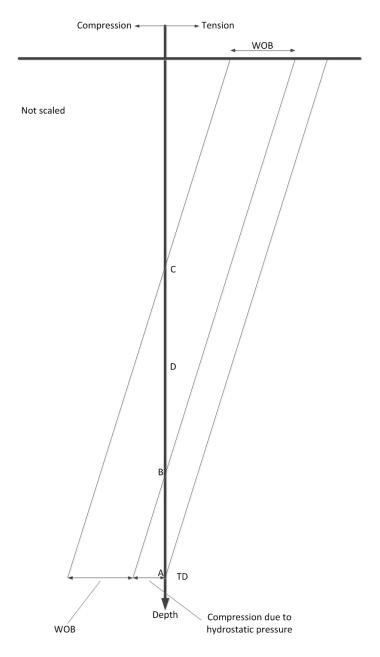


Figure 30: Effect of buoyancy on buckling in form of neutral point of tension and NPB (Figure made by this author)

Normally the drillstring is designed to have the NPB in the BHA in order to prevent buckling of the drill pipe. If the NPB falls in the DP instead of the BHA the possibility of buckling increases as the buckling resistance, or minimum WOB for buckling, is lower for the DP than the BHA (Wojtanowicz 2012). In order to achieve that, the minimum length of DC's must be calculated. This can be achieved by using Eq. 30. The w_{DC} is the average unit weight of the BHA in air. The BF is the buoyancy factor, presented in Eq. 10, while the θ is the hole inclination. It should be noted that Eq. 30 does not take into account the circulating pressures or the torque applied to the bit. In addition the WOB as measured on surface might be different from the actual downhole WOB due to wall friction and other errors in the readings. A safety factor, SF, should therefore be multiplied to the minimum length in order to account for these sources of errors (Wojtanowicz 2012). According to Bourgoyne et al. (1986c) this factor should be at least 1.3.

$$L_{BHA} = \frac{WOB}{W_{BHA} * (1 - BF) * \cos(\theta)} * SF$$
(30)

In addition the stiffness factor ratio between the last DP and the top DC, or any two following string sections, should be kept within the maximum considered value of 3.5 given by the International Association of Drilling Contractors (IADC). This ratio can be calculated using Eq. 31. The subscript 1 denotes the lower of two following sections (for example the DC) and 2 the upper (for example the DP).

$$SFR = \frac{OD_1^4 - ID_1^4}{OD_2^4 - ID_2^4} * \frac{OD_2}{ID_1}$$
(31)

If the neutral buckling point falls in the drill pipe above the BHA, where the buckling resistance, or minimum WOB to buckle, is much smaller, the string is likely to buckle as weight is applied to the bit (Wojtanowicz 2012). Normally there are two conditions considered, namely the sinusoidal buckling (S-buckling) and helical buckling (H-buckling). If the compressional force applied to a string element exceeds the minimum WOB the pipe element will deform and contact the borehole wall. That is 1st degree buckling, or sinusoidal buckling. At this point the string is still able to transfer part of the the applied weight to the bit. For continued increased compression to the string the pipe will buckle a second time and touch the borehole wall at two points, a condition better known as 2nd degree buckling, or helical buckling. At this point the string will fail to transfer any more weight to the bit, and if the compressional force is further increased the string will continue to buckle to form a shape similar to a helix. The buckling of the drillstring is undesired as it can lead to several challenges. In addition to unsuccessful transferring of the weight applied to the bit, the rotation of a buckled pipe will fatigue the TJ quickly

and the integrity of the pipe might fail (Bourgoyne et al. 1986). On top of that can a buckled drillstring lead to issues when pulling out, as the helical shape might be difficult to get through high doglegs in the wellbore (Wojtanowicz 2012).

The minimum WOB in order to buckle for the drillstring will be dependent on string composition and design, mud weight, as well as wellbore geometry. A small annulus between the pipe and the borehole wall might support the string if buckling should occur, preventing further buckling from occurring. The mud weight provides a specific buoyancy factor, an effect that must be included in the NPB calculations. The drilling fluid will provide hydrostatic pressure to the drill string from the annulus, as well as a stability force (see Eq. 29) as a result of fluid pressure inside the string. In addition the circulation of the mud will affect the fluid frictional forces between the string and the mud (Bourgoyne et al. 1986). The composition of the string will affect the buckling resistance as different pipe sections, with different grades and classification, will have different minimum WOB to buckle. The length of the BHA and DC's should be designed in order to prevent any buckling issues (Wojtanowicz 2012).

5.8 Hole Cleaning

In order to ensure successful drilling ahead it is important to sufficiently clean the wellbore. The bit-rock interaction will result in cuttings that need to be transported away from the bottom of the hole and up to the surface in the annulus. If the hole does not get cleaned in a proper manner a lot of different issues can occur. Not only can there be challenges with the running of the next casing string due to excessive amount of cutting bed in the hole, insufficient cleaning can also wear the bit out faster due to the cutting of the same rock twice. This latter will also result in slower rate of penetration. If the amount of cuttings in the hole gets too large the pipe might get stuck, of the hole packed-off, leading to expensive extra-work to get it free. A severe result of packing off the hole might be lost circulation due to the increased pressure and resulting fracturing of the formation caused by the pack-off²⁰. On top of that inadequate hole cleaning can lead to increased level of torque and drag due to increased friction due to the cuttings bed in the annular annulus and the drillstring. If the torque and drag issues get too severe there might be issues with make-up torques exceeded and tensile failures of the string due to high levels of effective tension when pulling out. In addition, bad hole cleaning can lead to elevated levels of Equivalent Circulating Density (ECD) as the frictional pressure losses in the annulus will be higher due to the large amount of cuttings needing to be moved. This is especially a challenge for long, horizontal wells. The additional cuttings will increase the surface area encountered by the drilling mud, increasing the overall friction between the fluid and the rock, which will result in higher pressure losses. The formula for ECD is given in Eq. 42. If the ECD gets too high, the fracture gradient might be exceeded, leading to fracturing of the formation rock at the bit. That again might lead to lost circulation, as mentioned for packing-off, a condition

_

²⁰ Personal communication with S. Tørressen. 2013. Lindesnes: Acona Wellpro

that can have severe consequences in form of a kick, or even a blowout. Finally, insufficient hole cleaning can cause issues when cementing due to higher possibilities of bad bond between the casing and the formation (Wojtanowicz 2012).

Saasan (1998) showed that the pressure loss due to friction in the annulus is the largest contributor to cleaning of the wellbore for a deviated well. In other words the pump rate for the mud pumps must be selected so that the resulting frictional pressure loss in the annulus is high enough to obtain the required hole cleaning. In addition the cleaning is dependent on the cutting bed consolidation, cutting density and shape, annular velocity and mud properties in form of lifting capacities (Saasan 1998). For horizontal wells it can be a challenge to obtain a sufficient hole cleaning, as mentioned. As the TVD remains more or less constant, but the measured depth increases, the ECD will increase, while the fracture gradient will remain constant, something that can cause challenges with regards to fracturing of the formation. Also, for long horizontal sections the gravity will pull the cuttings down to the lower side of the wellbore, and a cuttings bed might be established along the lower side of the hole. As the DP for such a horizontal wellbore will be resting on the lower side of the hole the major drilling fluid flow will occur in a concentrated area in the upper, central part of the wellbore. This concept is described in Figure 31. Therefore it is important to get the cuttings into this "conveyor belt" in order to achieve a better cuttings transport. This is most often achieved by increasing the rotational speed of the drillstring, so that the frictional forces between the drilling fluid and the side of the cuttings will move the rock up from the lower sides of the wellbore (next to the DP) into this high-velocity stream (Sangesland 2012).

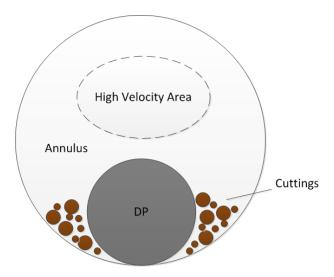


Figure 31: High velocity area in a horizontal well (Figure made by this author)

If the hole cleaning for a well being drilled is insufficient issues with the running of the next casing string might occur, as described earlier. That might happen if the penetration rate is too high resulting in excessive amounts of produced cuttings

compared to the lifting capacity of the mud at given pump rate for the given wellbore. As described by Nesland (2012), the effect of hydraulics, or bit jet impact force, on Rate of Penetration (ROP) is determined either by the flounder point or the hydraulic erosion. The latter is valid for soft formation, but studies have not yet been able to get the full overview of this effect. For hard formations the flounder point, which is the point where the cuttings are created faster than they are removed, as described, gives the bit jet impact force effect on ROP (Bourgoyne et al. 1986; Wojtanowicz 2012). This means that if more jet impact force is applied to the bit, more WOB and a higher ROP will be obtained before reaching the flounder point (Bourgoyne et al. 1986). Eckel performed in 1968 a correlation between the Reynolds number, $N_{\rm Re}$, and ROP. The Reynolds number, described more in detail in section 5.9, is a value used to determine the flow regime in the different parts of the well (Bourgoyne et al. 1986c). These studies showed that ROP really is function of the Reynolds number, and that for most cases by increasing the Reynolds number the ROP also will increase (Bourgoyne et al. 1986). In other words, if the penetration rate is so high that the cuttings are not removed properly a bed height might arise in the wellbore, leading to smaller effective drift diameter of the openhole section. If that drift is smaller than the OD of the next casing to be run, time consuming mud circulations have to be performed in order to clean the hole sufficiently for the string to be run successfully²¹. Going back a decade or two the norm in the industry was to obtain as high as possible penetration rate for the drilling of a new section. The different rig crews were often measured up against each other based on the average ROP for a section. That often led to bad hole cleaning, which resulted in expensive cleaning of the hole for the successive rig crew. Today the overall average penetration rate for the whole well is more in focus, meaning that the openhole sections are drilled more carefully to ensure sufficient cleaning of the hole, so that the next casing string can be run without any issues. In the long run, for most cases, that will be more efficient and lead to overall shorter time from casing point to casing point for the well²².

5.9 Pressure Losses

It is important to address and control the pressure losses during drilling. From the outlet of the mud pumps the mud will go through the surface equipment, down the inside of the drill pipe, through the bit nozzles, up the annulus to transport the cuttings, back through the surface equipment to finally end up in the mud tanks again (Bourgoyne et al. 1986b). During this whole journey frictional forces acting on the side of the fluid, in the opposite direction of fluid movement, will result in pressure losses along the way. The overall pressure losses, from surface, trough the circulating system, and back to the surface again, are for this report called the system pressure losses. If the system pressure losses get to high the mud pumps might fail to pump the drilling fluid at the desired rate around the circulating loop.

_

²¹ Personal communication with G. Namtvedt. 2013. Stavanger: ConocoPhillips Norway

²² Personal communication with S. Tørressen. 2013. Lindesnes: Acona Wellpro

The system pressure losses in the well are made up of smaller, sectional pressure losses. For this report these are considered to be surface pressure losses, drillstring pressure losses, bit pressre losses and annulus pressure losses. The size of each of these sectional pressure losses, summing up the total pressure losses for a well, is dependent of a lot of complex factors. First of all a rheology model has to be selected that will fit the properties of the actual drilling fluid used. The most commonly used models are the Newtonian, Bingham Plastic, Herschel-Bulkley and the Power-Law models. Each of these models gives their own sets of Eq.s, with specific dependencies, for pressure loss calculations. For the Bingham-Plastic model, for instance, the first task is to find the mean velocity in both the pipe and the annulus. The velocity in the pipe, given by Eq. 32, is a function of flow rate, q, in gpm and inner diameter of the DP, given in inches. For the annulus the mean velocity (Eq. 33) is dependent also on the flow rate, but now given a flow area between the hole, or casing, diameter, ID_{hole} , and outer diameter of the DP, OD_{DP} . The constant of 2.448 is applied in order to get the velocities in ft/s. Further, these velocities will determine the flow regimes, laminar or turbulent.

$$\overline{V_{DP}} = \frac{q}{2.448 * ID_{DP}^{2}} \tag{32}$$

$$\overline{V_{annulus}} = \frac{q}{2.448 * \left(I D_{hole}^{2} - O D_{DP}^{2}\right)}$$
(33)

Again there are several criteria Eq.s to choose between, but the most commonly used is the Reynolds number. In the DP this number is found by using Eq. 34. In this Eq. the 928 is a constant applied in order to get the Reynolds number unit free. The ρ_m is the mud weight in ppg, and the μ_p is the plastic viscosity of the mud, given in centipoise. For the annulus Eq. 35 must be used. The 757 value is also here a constant applied in order to get the Reynolds number unit free. The values found for the $N_{\rm Re}$ can then be used to determine whether there is laminar or turbulent flow in the different parts of the well. The values are different for the different rheological models. According to Bourgoyne (1986c) the limit between laminar and turbulent flow is at the Reynolds number of 2100. Any value below this indicates laminar flow regime, while any number above indicates turbulent low. Often a transitional flow regime, representing the transformation from laminar to fully turbulent flow, is considered to lie in the interval from 2000 – 4000, but for the calculation purposes given in the Eq.s in this sub-chapter the border limit of 2100 represents a significant switch in flow regime (Bourgoyne et al. 1986c).

$$N_{\rm Re} = \frac{928 * \rho_m * \overline{v_{DP}} * ID_{DP}}{\mu_p}$$
 (34)

$$N_{\text{Re}} = \frac{757 * \rho_m * \overline{v_{annulus}} * (ID_{hole} - OD_{DP})}{\mu_p}$$
(35)

Given the Reynolds number the flow regime can be determined, and the following pressure losses can be calculated. For laminar flow the frictional pressure losses for the string and annulus can be calculated using Eq. 36 and Eq. 37, respectively. The τ_y for these Eq.s is the yield point of the mud, given in lbf/ $100\,ft^2$.

$$\frac{dP_f}{dL} = \frac{\mu_p * \overline{\nu_{DP}}}{1500 * ID_{DP}^2} + \frac{\tau_y}{225 * ID_{DP}}$$
(36)

$$\frac{dP_f}{dL} = \frac{\mu_p * \overline{v_{annulus}}}{1000 * (ID_{hole} - OD_{DP})^2} + \frac{\tau_y}{200 * (ID_{hole} - OD_{DP})}$$
(37)

If the flow is indicated to be turbulent by the Reynolds number Eq. 38 and Eq. 39 have to be used for frictional pressure losses in the DP and annulus, respectively. The constants of 1800 and 1396 are given in order to end up with units in psi/ft for the two Eq.s. To find the total pressure loss of a portion of the well the results from the Eq.s have to be multiplied with section length, in ft, in order to get frictional pressure losses in psi (Bourgoyne et al. 1986c).

$$\frac{dP_f}{dL} = \frac{\rho_m^{0.75} * \mu_p^{0.25} * (\overline{\nu_{DP}})^{1.75}}{1800 * ID_{DP}^{0.125}}$$
(38)

$$\frac{dP_f}{dL} = \frac{\rho_m^{0.75} * \mu_p^{0.25} * (\overline{v_{annunlus}})^{1.75}}{1396 * (ID_{hole} - OD_{DP})^{1.25}}$$
(39)

For a complete overview of the Eq.s for pipe and annulus pressure losses for the other rheological models, as well as presentations of other methods to find the flow regimes in the well, please refer to Bourgoyne et al. (1986c), page 127 - 184, with summary of the Eq.s used in this report, and more, on page 155.

In addition to frictional pressure losses in the drillstring and the annulus, the system pressure losses in this report is considered to also contain the surface equipment pressure losses and the pressure loss across the bit nozzles, as mentioned. For simplicity the surface pressure loss is often assumed to be a constant value, for this report 100 psi. Normally the frictional pressure losses at the surface are so small compared to the rest

that they many time also simply are neglected 23 . The bit pressure loss is calculated using Eq. 40. The A_i is the total flow area across the bits, given in inches squared, while the C_d is the discharge coefficient correcting for the assumption of friction-free flow of mud through the bit nozzles (Bourgoyne et al. 1986c). According to Wojtanowicz (2012) this coefficient usually range between 0.7 and 0.95, dependent on nozzle type.

$$\Delta p_{bit} = \frac{8.311 * 10^{-5} * \rho_m * q^2}{C_d^2 * A_t^2} \tag{40}$$

5.10 Circulating Pressures and ECD-effects

The system pressure losses introduced in section 5.9 are mostly important in a well control perspective. As the mud exits the bit nozzles the circulating pressure, the pressure given by the drilling fluid at any point in the well during circulation created by the mud pumps, should, for conventional overbalanced drilling, be within the drilling window, an interval defined by the pore pressure at the lower end and the fracture gradient at the upper side. If the circulating pressure falls below the pore pressure, the well becomes underbalanced and influx of formation fluid might occur, a condition better known as a kick. On the other hand, if the pressure from the mud gets too high crossing the fracture limit, lost circulation of mud might happen, possibly leading to a reduction in the hydrostatic height of the mud column. That again can reduce the BHP also leading to underbalance and influx of formation fluids. In order to ensure a safe drilling operation the circulating system, and properties, therefore have to be designed so that the circulating pressure always falls within the drilling window for a conventional, overbalanced operation where the mud weight is the primary barrier element dictating the BHP to the largest extent. It should be noted that today several other drilling techniques are found, yielding slightly different approaches of controlling the circulating pressure conventional overbalanced drilling, as used in the simulations in this report, including underbalanced drilling (UBD), dual gradient drilling and managed pressure drilling (MPD), without describing these methods any further.

Often the pore pressure and fracture gradient limits are given as equivalent densities rather than in pressure, by use of Eq. 41 (Bourgoyne et al. 1986c). The P in that Eq. is the pressure at given true vertical depth in the well. This is often a more convenient method because it is easier and faster to check if the selected mud weight will fall within the drilling window. Since the mud weight density normally is given for static conditions, the equivalent circulating density has to be calculated in order to include the increased BHP due to frictional pressure losses in the annulus during circulation (Wojtanowicz 2012). It is this ECD that has to be within the drilling window, rather than the static mud weight.

_

²³ Personal communication with S. Tørressen. 2013. Lindesnes: Acona Wellpro

Eq. 42 shows the calculation of ECD from the initial mud weight, $\rho_{\scriptscriptstyle m}$. The numerator in the Eq. is the frictional pressure losses in the annulus.

$$\rho_e = \frac{P}{0.052 * D_{TVD}} \tag{41}$$

$$ECD = \rho_m + \frac{\Delta P_{f,annulus}}{0.052 * D_{TVD}} \tag{42}$$

It should be noted that a smaller overbalance above the pore pressure normally will lead to a faster penetration rate, so the ECD should be designed, if possible, to fall as close to the pore pressure line, but with a trip margin in between to act as a safety margin against the lowered BHP due to the swabbing effect when the pipe is pulled out (Bourgoyne et al. 1986e). By using of Eq. 41 this trip margin can be calculated using Eq. 43. The Δp_{safety} is here the desired safety margin in pressure above the pore pressure in order to mitigate the swabbing effects. Other suggestions make use of Eq. 44 for trip margin calculations (Drilling Formulas 2013). The τ_y is the yield point of the mud given in lbf/ $100\,ft^2$. For both Eq. 43 and Eq. 44 the trip margin, TM, given in ppg, has to be added to the mud weight in order to find the needed mud weight in order to mitigate any swabbing effects during tripping (Bourgoyne et al. 1986). In many drilling operations the trip margin is simply set to around 0.5 ppg above the pore pressure equivalent density, or 200-300 psi above the pore pressure (Hyne, N.J. 1991;Bourgoyne et al. 1986e). For more information regarding the swab effect please refer to Bourgoyne et al. (1986), page 164.

$$TM = \frac{\Delta p_{safety}}{0.052 * D_{TVD}} \tag{43}$$

$$TM = \frac{\tau_{y}}{11.7 * (ID_{hole} - OD_{DP})}$$
 (44)

In the same way as a trip margin is set to prevent the ECD to decrease below the pore pressure line during tripping, a kick margin is determined in order to add a safety margin for the kill weight mud (KWM) during a kick. This is done by saying that the maximum ECD is a certain value lower than the fracture gradient. As for the trip margin a normal kick margin is often set to around 0.5 ppg below the fracture gradient (Bourgoyne et al. 1986e). At the casing depth, if no margin against kick is present, a fracturing of the formation will occur KWM is pumped down to the bottom, leading to a possible underground blowout (Bourgoyne et al. 1986e). The calculation of the kick margin and the KWM can be found in numerous well control manuals and literature.

5.11 Specific challenges on Ekofisk

As mentioned in chapter 2 the compaction of the Ekofisk reservoir, and the following subsidence at the seabed, lead to several challenges for well planning and drilling in the area. The compaction in the overburden increases the risk of buckling failure, presented in section 5.7, for the wells penetrating the area. The subsidence bowl in addition yield elevated shear forces at the rim of the bowl, creating movement, deformation and collapses of the wellbores. In addition, the existence of fractured and faulted zones in the area creates challenges with regards to migrating injection water and solution gas from the reservoir into the overburden, influencing the downhole pressure regimes (Midtgarden 2010). Finally, the large amount of existing wells is a challenge for any new drilling operation in the Ekofisk field, and proper planning must be performed in order to achieve a successful result.

6 Parameter simulations by using of the Wellplan software

In order to evaluate the drillability of the three different multilateral well configurations, presented in Figure 16 and Figure 17, the Wellplan software was used in order to perform simulations of different effects during drilling. As mentioned in Section 4.4 only the junction design option with IWS (option 2) would be investigated. The simulation process is step-wise presented in Figure 32. A mother wellbore from surface to junction point was first created in the software, using data and setup from well 2/4-Z-17 nearby. No simulations were performed on this wellbore, thus assuming the drilling of this would occur without any issues. The mother wellbore would make up the top section from surface down to the junction point for all of the investigated MLT options. From there the drilling of these three options (MLT1, MLT2 and MLT3) would be studied. For each of the three there would be a mainbore/Lateral 1 (L1) and a sidestep/Lateral 2 (L2), each L2 with a 9 ½" and a 8 ½" section (see Figure 21), adding up to a total of nine different possible wellbore sections from the junction point to be simulated. For each of the nine a background setup for the simulations were established, presenting hole sections, drillstring, with BHA design, and well path.

6.1 Selection of two input scenarios

When the establishment of the wellbores was done two different initial sets of drilling parameter values were determined based on real data from the drilling of the nearby well 2/4-Z-17. Prior to the drilling of the 8 ½" section in that well Halliburton set up intervals for each of the humanly manipulative drilling parameters to place the actual values within. For this thesis it was decided, for simplicity, only to consider WOB, RPM, ROP (in form of block position) and flow rate as the adjustable parameters for the two initial parameter value-scenarios. The two parameter sets for the simulations performed in this thesis would represent the lower and higher limits of the recommended intervals for Z-17. The fluid properties would therefore be equal for both of the scenarios. By doing this two scenarios, each with four constant parameter values, were created. All the six possible wellbores would then first be simulated with the values from scenario 1, then with values from scenario 2. The thoughts behind doing two such comparisons, each with equal parameter values for all of the six different wellbores, were to relatively compare the six different wellbores with each other with regards to issues and challenges during drilling. In addition an early indication of which junction configuration that would lead to least problems in a drilling-technical perspective could be found.

6.2 Optimization through Iterations

After the initial process it was decided to execute iterations on each of the two wellbores for each of the three different MLT options. This was done in order to remove

any issues revealed when using either scenario 1 or scenario 2 values, and to find the best practice, or suggested drilling parameter values, for each of the six wellbores with regards to possible actual constraints while drilling. The iteration process is presented in Figure 33. Here more than just the four previously defined changeable parameters (WOB, RPM, ROP and flow rate) could be changed if necessary. When the iterations were executed for all of the wellbores the individual results from the simulations on torque and drag, and hydraulics, with the suggested parameter values, were laid out. In the end the initial simulation results, with the two sets of constant drilling values for each of the six wellbores, and the second results, with suggested parameter values for each of the six wellbores, were compared and analyzed. This was done in order to find the MLT option that would have highest probability for future success with regards to drillability and the drilling process.

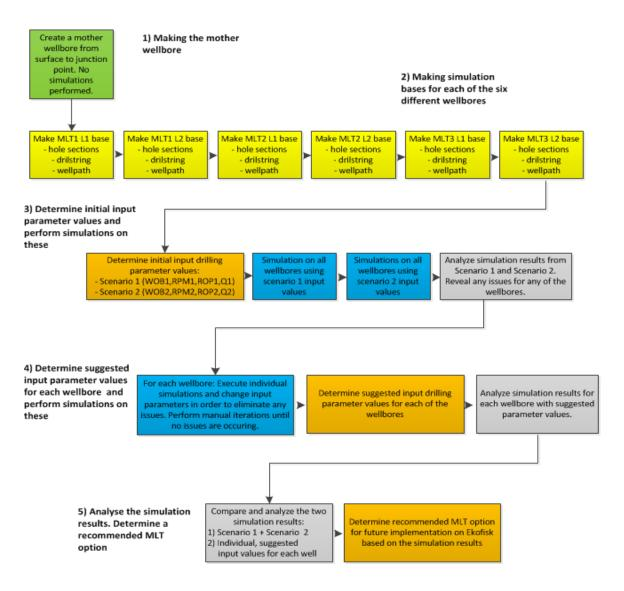


Figure 32: Step-wise process of the simulations performed in Wellplan (Figure made by this author)

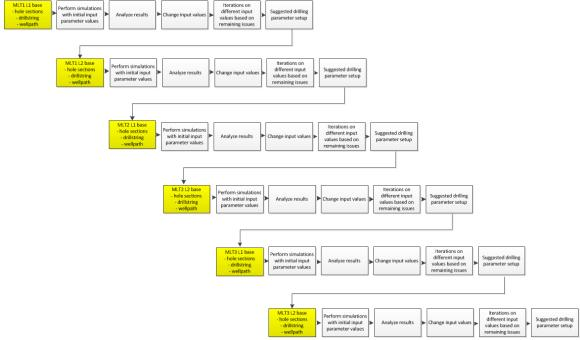


Figure 33: Schematic of the step-wise iteration process for each of the wellbores in order to find the individual, suggested drilling parameter values (Figure made by this author)

6.3 The Wellplan software

Wellplan, developed by the Halliburton owned Landmark, as described by Nesland (2012), is an extensive software for analysis and simulation to use in well operations optimization. The software has a set of comprehensive engineering tools to use in both drilling and completions, and it can be used together with other Landmark software in the Engineer's Data Model (EDM) platform to perform a more complete analysis (Halliburton 2012b). The software suite is based on seven different modules, all designed to perform analysis for different scenarios the well will experience in the drilling phase. In Appendix M these modules as presented more in detail.

6.4 Simulations to be performed

After the mother wellbore from surface to junction point, as well as all the nine different wellbore sections for the three different MLT options, had been created in the Wellplan software, the simulations on drillability were performed. As mentioned in the previous section the Wellplan software consists of seven different modules. For this report only two of these were used, namely the Torque and Drag, and Hydraulics module. A summary of the simulations performed on the three MLT options can be seen

in Table 7. The results from these simulations are presented in Chapter 7, with following evaluation in Chapter 8.

Table 7: Simulations performed in Wellplan

Table 7: Simulations performed in Wenplan			
● Ef	ffective tension		
• To	orque along the drillstring – bit on bottom		
● Fa	atigue ratio		
• H	ook load		
• To	orque at bit – bit depth from surface to TD		
• N	linimum WOB to sinusoidal buckle		
• N	linimum flow rate required for sufficient hole		
cl	eaning		
• Sy	ystem pressure losses		
• Ci	irculating Pressure vs depth		
• E(CD vs depth		
• Sy	ystem pressure losses irculating Pressure vs depth		

6.5 Assumptions

For the simulations performed in this reports several assumptions were made. These were qualitatively determined in order to make the simulation process as realistic as possible. However, for software simulations there will always be various sources of errors compared to reality, based on both assumptions and calculating models utilized in the program. The assumptions made for the simulations performed in this report are summarized in Table 8, and evaluated in Chapter 8.

Table 8: Assumptions made for the simulations performed in Wellplan

- The targets for all the three MLT options yield the same reservoir performance in form of exposure and production rate
- Geological data from wells 2/4-Z-17, 2/4-A-21 and 2/4-VB-05 assumed to be valid for the area investigated
- Identical mother wellbore from surface to the junction point for all the three MLT options
- Soft string model valid
- BHA identical, except bit size, for 8 ½" and 9 ½" hole sections
- Pressure losses in TJ ignored
- Bed porosity equal to average on Ekofisk of 36 % (Maxwell 2013)
- Constant friction factors of 0.18 for both open and cased hole sections
- Underground data equal for the nine wellbores for the three MLT options, identical to well 2/4-VB-05
- Constant torque at bit of 2500 ft-lbf
- Sheave friction correction irrelevant
- Buckling limit of value 1.0
- Contact force normalization length of 31.0 ft
- Bending stress magnification valid
- No viscous torque and drag
- Max overpull using yield of 90 %
- Cuttings diameter of 0.125"
- No issues with regards to running of casing and liner string (this was not simulated)
- Nominal wall thickness of DP to be 80 % of new (premium pipe)
- Mud pump volumetric efficiency of 85 %

6.6 Making of the mother wellbore from surface to the junction point

As mentioned in the introduction of this chapter, in order to perform simulations on each of the nine different wellbore sections for the three MLT options the mother wellbore from surface down to the junction point had to be created in Wellplan. This mother wellbore would be common for the MLT options, as shown in Figure 16. Further it was assumed that the drilling and installation of this section of the well would not lead to any issues, and therefore no simulations on the mother wellbore were performed.

Figure 34 shows a well schematic of the drilling of the 12 ½" section for the mother wellbore. (It should be noted that this particular case is for the MLT3 L1, where TOE is at 18900 ft MD, as presented in Table 6.) The well schematics for the other sections in the mother wellbore, as well as overview of the BHA, drillstring and fluid properties, can be found in Appendix K.

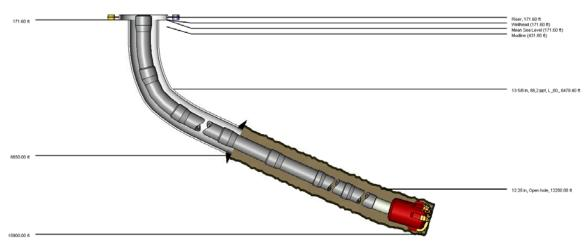


Figure 34: Well schematic for the drilling of the 12 ¼" hole section in the mother wellbore (Wellplan 2013a)

6.7 Making of the nine wellbore sections for the three MLT options to be simulated in Wellplan

When then mother wellbore had been created in Wellplan the nine different wellbore sections for the three MLT options had to be made. To sum up these were the MLT1 L1 (9 ½"), MLT1 L2 9 ½" section, MLT1 L2 8 ½" section, MLT2 L1 (9 ½"), MLT2 L2 9 ½" section, MLT2 L2 8 ½" section, MLT3 L1 (9 ½"), MLT3 L2 9 ½" section and MLT3 L2 8 ½" section, as presented in Figure 21.

The well schematic for the MLT1 L1 is shown in Figure 35. For this MLT option this section would be drilled out through the $10 \, \frac{3}{4}$ " liner shoe set at 18600 ft MD at TOE in the mother wellbore to TD at 24280 ft MD in Ekofisk. The $9 \, \frac{1}{2}$ " section was created with the same hole sections above the $10 \, \frac{3}{4}$ " liner shoe as for the mother wellbore, meaning

a riser from the rig to the sea bottom, a 13 5/8" casing set to 5000 ft TVD / 6650 ft MD and a 10 ¾" liner to 18600 ft MD, as mentioned. It was assumed that the BHA would be identical for all the nine different wellbore sections to be simulated, except for the bit size, based on the actual strings used when COPNO drilled the close by 2/4-Z-17 well. In addition to the bit size the only difference in the drillstring between the wellbore section would be the length of the top DP in order to reach to each of the nine wellbores respective TD. The drillstring used for the MLT1 Lateral 1 drilling, as well as a presentation of the rest of the simulation base for MLT1 L1 can be found in Appendix L. For the other eight wellbore section, as described in Appendix L.2, the process of creating the simulation bases were quite similar to the MLT1 L1. For simplicity, and to reduce the amount of figures used in this report, the complete simulation bases, with hole sections, wellbore schematic, BHA schematic, string design, and more, can be provided by the author upon request.

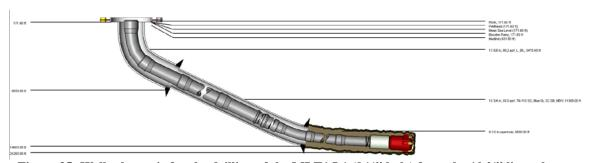


Figure 35: Well schematic for the drilling of the MLT1 L1 (9 $\frac{1}{2}$ " hole) from the 10 $\frac{3}{4}$ " liner shoe to TD (Wellplan 2013a)

6.8 Input parameters

As soon as the simulation bases, with hole sections, drillstring and well path, was created for each of the nine wellbore sections to be simulated the input parameter values had to be determined. As mentioned in the introduction of this chapter it was decided to initial set up two sets of input values based on the recommended drilling values for the neighboring well Z-17, drilled in April 2013 (Maxwell 2013). In addition was underground data from the offset well 2/4-A-21 used for validation. The two sets of input values would be named Scenario 1 and Scenario 2, and an overview of the initial input parameter values for each of the cases can be found in Table 9, with a detailed process found in Appendix O.

Then iterations and changes would be performed on each of the six wellbores with start parameters as in Scenario 1. The values from this scenario was used as a base for the iteration process, and was selected based on the less extreme values compared to Scenario 2. However, Scenario 2 values probably would have yielded the same set of suggested values, but the steps in the iterations would probably have been more. Manual changing of the input values and setup configurations were done until no issues were indicated in the simulation results, thus yielding the suggested drilling parameter values to be used for each wellbore. These suggested values are summarized in Table 11. The complete iteration processes for each of the wellbores with manually changing the input parameters and setup to end up with the suggested input values and configuration are found in Appendix P. The six wellbores, and nine wellbore sections, would then be compared both with regards to the results from Scenario 1 and Scenario 2 parameters and with the set of suggested values.

6.5.1 Drilling fluid properties

The drilling fluid properties for both of the initial scenarios was set based on the underground data from well 2/4-A-21, a closely offset well, as well as experience from the drilling of Z-17²⁴. For both Scenario 1 and Scenario 2 a mud weight of 12.4 ppg was selected as the initial suggestion for the simulations to be performed. Details regarding the mud properties can be found in Appendix O, with overview in Figure 143.

6.5.2 WOB

The WOB for rotating on bottom and slide drilling was set to 10 klbf for Scenario 1 and 25 klbf for Scenario 2. These values represent the lower and higher recommendations from Halliburton prior to the actual drilling of the neighboring well Z-17. For both scenarios the torque at bit while rotating on bottom and slide drilling was assumed to be 2500 ft-lbf, according to suggestions by Midtgarden (2010). Studies performed by both Gazaniol (1987) and Maidla and Haci (2004) showed that increased WOB gives

²⁴ Personal communication with G. Namtvedt. 2013. Stavanger: ConocoPhillips Norway

increased torque at bit, followed proportionally after the tangential force vector to the bit rotation. Excessive torque in the string may lead to a crossing of the make-up torque limit for any element in the drillstring. In order for the strength and maximum load values for a DP, or any other element, listed in drilling tables to be valid the experienced torque at any point in the drillstring should not exceed the make-up torque (Wojtanowicz 2012). A constant torque at bit might be a simplification compared to reality, but was set in order to be able to compare the different wellbore sections with each other. Summaries of the WOB and Torque at bit values for Scenario 1 and Scenario 2 for all sections to be simulated are shown in Figure 147 and Figure 149, respectively, in Appendix O.

6.5.3 Rotational Speed

For scenario 1 the string rotary speed was set to 140 RPM, while the value was determined to be 195 RPM for scenario 2. For well Z-17 the higher limit was 250 RPM, but the top drive on Mærsk Gallant, the rig currently drilling on Ekofisk Zulu, has a limitation of 195 RPM at maximum torque (ECU 2006), and therefore this value was set at the highest possible to obtain for all simulations (this was also a constraint for the suggested parameter values found through the iterations).

6.5.4 Penetration Rate

In Wellplan the penetration rate is an input parameter, rather than output. In reality the ROP will come in return based on selection of WOB, RPM, bit type, bit configuration, mud weight and properties, flow rate and a lot of other manipulative parameters, as well as the properties of the non-manipulative parameters such as formation type, downhole pressures, bit and bearing wear to mention some (Wojtanowicz 2012). By having ROP as an input parameter Wellplan instead give as an output some of the other input parameter values that are needed in order to achieve that desired penetration rate (Nesland 2012).

For this report the ROP for scenario 1 was determined to be 25 ft/hr and 40 ft /hr for scenario 2. These values were based on common interval values experienced during drilling of the $8 \frac{1}{2}$ " and $9 \frac{1}{2}$ " sections on Ekofisk²⁵.

6.5.5 Flow rate

The flow rate recommendation for well Z-17 was between 450 and 650 gpm, values that therefore would define scenario 1 and scenario 2, respectively (Maxwell 2013).

²⁵ Personal communication with G. Namtvedt. 2013. Stavanger: ConocoPhillips Norway

6.5.6 Other configurations

In addition to the WOB, rotational speed, ROP and flow rate, a set of input parameters that were equal for both scenario 1 and scenario 2 were defined. These were mud weight, as described, set to 12.4 ppg, tripping in/out speed of 60 ft/min, tripping in/out rotational speed of 0 RPM, torque at bit of 2500 ft-lbf, as mentioned, friction factor of 0.18 for both cased and open hole, as well as the rig constraints of maximum pump pressure of 5000 psi and maximum SPP of 5500 psi.

The tripping in and tripping out speed was set based on default settings in the Wellplan software. The friction factors for both openhole and casing were set based on work performed by Midtgarden (2010), where it was showed, via reverse-calculations data from actual drilling on Ekofisk, that a friction factor of 0.18 was appropriate for both cases. This value was therefore assumed to be valid also for the simulations to be performed in this thesis. In reality there are a lot of factors influencing the actual friction factors, and to model them as a constant for a hole section might yield inaccurate results. In many cases the friction factors are suggested to be a function of depth, wall material and other properties. Some of these are pipe stiffness effects, viscous drag forces, cutting beds, lubricity, contact area between pipe and wall, hole geometry and tortuosity, and hole cleaning (Samuel 2010).

For complete overview and description of all the different input parameters and setup for the three variuos MLT options please see Appendix O (Scenario 1 and Scenario 2 values) and Appendix P (Suggested values).

6.5.7 Summary of the input parameters values used in scenario 1 and scenario 2

Table 9 summarizes the input parameter values for scenario 1 and scenario 2 for better overview. These were the initial values used in the simulations for all the nine different wellbore sections for the three MLT options. The input values that were set equal for both scenarios, such as the mud weight to mentioned one, are presented in Table 10. A more complete overview of the selection of these parameters can be found in Appendix O.

Table 9: Initial input parameter values. Scenario 1 represents the lower and scenario 2 the higher limits of the intervals recommended by Halliburton for the actual drilling of the 2/4-Z-17, a close by well drilled in April 2013 (Maxwell 2013)

Scenario 1	Scenario 2	
$WOB_1 = 10 \text{ klbf}$	$WOB_2 = 25 \text{ klbf}$	
$RPM_1 = 140$	$RPM_2 = 195$	
$ROP_1 = 25 \text{ ft/hr}$	$ROP_2 = 40 \text{ ft/hr}$	
$Q_1 = 450 \text{ gpm}$	$Q_2 = 650 \text{ gpm}$	

Table 10: Initial input parameter values and setup equal for both Scenario 1 and Scenario 2

Tripping in/out speed = 60 ft/min			
Tripping in/out rotational speed = 0 rpm			
Torque at bit = 2500 ft-lbf			
$\rho_{mud} = 12.4 \text{ ppg}$			
Friction factor cased hole = 0.18			
Friction factor openhole = 0.18			
Max pump discharge pressure = 5000 psi (rig specific)			
Max SPP = 5500 psi (rig specific)			

6.5.8 Summary of the suggested input parameter values for the different MLT options

Via the iteration processes performed in Wellplan for each of the nine wellbore sections for the three MLT options a set of suggested parameter input values were determined for each of the sections. These are summarized in Table 11. For the details regarding the iterations performed in Wellplan please refer to Appendix P.

Table 11: Suggested input parameter values for the nine different wellbore sections for the three MLT options. For each of the wellbores these were found by changing the different input values via manual iterations in Wellplan

	manual iterations in Wellplan					
	MLT1					
2 5777 5	Lateral 1 (9 ½")	Lateral 2 (9 ½")	Lateral 2 (8 ½'')			
MW [ppg]	11.2	12.1	11.1			
WOB rot.on bot [klbf]	25	25	25			
RPM	195	195	195			
ROP [ft/hr]	25	25	25			
Q [gpm]	680	620	640			
Bit nozzles	3x (18/32)"	3x (18/32)"	3x(18/32)"			
Tripping in/out [ft/hr]	60	60	60			
Tripping in/out [RPM]	0	0	0			
WOB slide [klbf]	25	25	15			
Other						
		MLT2				
	Lateral 1 (9 ½'')	Lateral 2 (9 ½'')	Lateral 2 (8 ½")			
MW [ppg]	10.5	12.1	10.8			
WOB rot.on bot [klbf]	25	25	25			
RPM	195	195	195			
ROP [ft/hr]	25	25	25			
Q [gpm]	640	620	640			
Bit nozzles	3x(18/32)"	3x(18/32)"	3x(18/32)"			
Tripping in/out [ft/hr]	60	60	60			
Tripping in/out [RPM]	120	0	0			
WOB slide [klbf]	10	25	3			
Other			New BHA			
	MLT3					
	Lateral 1 (9 ½'')	Lateral 2 (9 ½'')	Lateral 2 (8 ½")			
MW [ppg]	10.5	12.1	10.7			
WOB rot.on bot [klbf]	25	25	25			
RPM	195	195	195			
ROP [ft/hr]	25	25	25			
Q [gpm]	640	610	500			
Bit nozzles	3x(18/32)"	3x(18/32)"	3x(18/32)"			
Tripping in/out [ft/hr]	60	60	60			
Tripping in/out [RPM]	0	0	120			
WOB slide [klbf]	5	25	0 (not possible)			
Other		1				

7 Results

As mentioned in the last chapter simulations in Wellplan were performed on each of the six wellbores (see Figure 36) with input parameter values as from scenario 1, scenario 2, and finally with the suggested values, found via the iteration process. For each set of input parameters a total of ten drilling effects were investigated, as described in section 6.4. To sum up, these were the effective tension when bit at TD, torque when bit at TD, fatigue ratio for bit rotation on bottom at TD, hook load, torque and minimum WOB, all as a function of MD for different bit depths, as well as the hydraulic effects of minimum flow rate for hole cleaning, system pressure losses and circulating pressures and ECD versus depth. These ten effects would then be simulated for each of the three MLT options. As mentioned previously in this report every one of the MLT options would consist of two wellbores, a Lateral 1 and a Lateral 2, as presented in Figure 36. On top of this each Lateral 2 for each of the three MLT options would consist of two hole sections, one 9 ½" and one 8 ½", shown in Figure 37. In other words a total of 9 wellbore sections would be simulated for all of the ten effects for three different input parameter sets, making the total sum of individual simulation results 270.

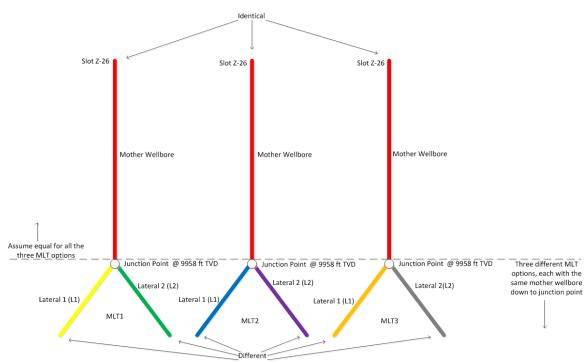


Figure 36: Schematic of the well path configuration. Same as Figure 16. Should only be used for overview. The figure is not to be scaled, and the shown inclinations are incorrect (Figure made by this author)

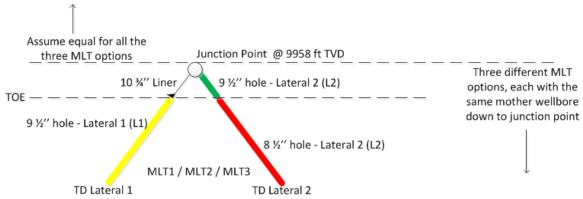


Figure 37: Hole sizes to be drilled for all of the three MLT options for junction design option 2, with IWS. Same as Figure 21 (Figure made by this author)

In order to make it easier to keep overview of the 270 different results and to better compare the six different wellbores (or effectively nine sections, as explained) for the three input value sets, seven different comparison cases were made. These were named from A to G. In case A all the MLT L1's were gathered. In other words, in this case only the Lateral 1 in each of the three MLT options (see Figure 37) would be compared. In case B all L1's going to layer EA3 (see Figure 17) were compared. Case C was decided to compare all L2 8.5" sections, and nothing else, while in case D all the L2 9.5" sections were compared. Further, case E would compare all the 8.5" L2's going to target in the EL-layer (see Figure 17). The two last cases would compare all the wellbores having targets in the same, respective layer. For case F that would mean that only the wellbores going to layer EA3 would be compared, while for case G all the wellbores going to layer EL would be gathered. A summary of these comparison cases can be seen in Table 12. For better overview of the different wellbores and sections, refer to Figure 36 and Figure 37. The targets and layers are presented in Figure 17.

Table 12: Comparison cases for the simulation results

Comparison Case:	Description:	Wellbores compared:	
Α	All L1 compared	MLT1 L1	
		MLT2 L1	
		MLT3 L1	
В	All L1 going to layer EA3	MLT1 L1	
	compared	MLT2 L1	
С	All L2 8.5" sections	MLT1 L2 8.5"	
	compared	MLT2 L2 8.5"	
		MLT3 L2 8.5"	
D	All L2 9.5" sections	MLT1 L2 9.5"	
	compared	MLT2 L2 9.5"	
		MLT3 L2 9.5"	
E	All L2 8.5" sections going to	MLT2 L2 8.5"	
	layer EL compared	MLT3 L2 8.5"	
F	All wellbores going to layer	MLT1 L1	
	EA3 compared	MLT1 L2 8.5"	
		MLT2 L1	
G	All wellbores going to layer	MLT2 L2 8.5"	
	EL compared	MLT3 L1	
		MLT3 L2 8.5"	

For each comparison case the individual simulation results from each of the wellbore sections compared would be plotted in the same graph. Each comparison case would then be checked twice, once with Scenario 1 and Scenario 2 parameter values combined, and one with only suggested values. For comparison case A, for example, this would mean that for each of the ten drilling effects (effective tension, torque etc) there would be one graph presenting the results from MLT1 L1, MLT2 L1 and MLT3 L1 together for Scenario 1 and 2, and one graph with the results with suggested values for the same wellbores. In other words, each comparison case would have 20 different result graphs, 10 graphs with the results from the combined Scenario 1 and 2, and 10 graphs for the suggested values. By doing these comparison cases and by joining results from different wellbore sections into same graphs, the number of individual output charts were reduced from 270 to 140. In chapter 8 two evaluation summary sheets, one for Scenario 1 and 2 combined, and one for the suggested values, of the seven comparison cases can be found. These two evaluation sheets would then be compared again in order to draw the conclusions presented in chapter 10.

For the simplicity and due to still a large amount of result charts only the results from comparison case A, all L1's compared, for Scenario 1 and 2 combined, as well as for the suggested values, are presented in this chapter. The results from the other comparison cases are somewhat similar to the ones in case A, and the analysis and evaluation

performed of the graphs to end up with the evaluation summary sheets in chapter 8 are comparable. The rest of these result graphs for all the other comparison cases can be found in Appendix Q.

7.1 Dog Leg Severity

As mentioned in section 5.1 is it beneficial to keep the DLS as low as possible in order to avoid issues with regards to running of casing or downhole equipment. For comparison case A, and for all other of the comparison cases, the well paths for each of the sections making up the three MLT options were constant for scenario 1, scenario 2 and the suggested input parameter values. For the investigations performed the DLS in the mother wellbore, making up the common wellbore from surface down to the junction point (see Figure 36), was not considered for any of the MLT options due to the assumption declared in section 6.2 of no issues while drilling that section. Therefore only the unique wellbore sections from the junction point to TD for each of the MLT options were decided to be presented and analyzed in this report.

In Figure 38 the DLS for the wellbores gathered in comparison case A is shown. The MLT3 L1 and MLT2 L1 indicated identical highest severity of 6.42 degrees per 100 ft at 18810 ft MD, while the peak for MLT1 L1 is 3.75 degrees per 100 ft from 23040 ft MD to 23970 ft MD. The MLT2 L1 (red line in the graph) displayed a trend of having a higher DLS from junction point to TD than the two other wellbores. For all the sections the maximum dogleg severity is quite high and above the recommended maximum of 3.0 degrees per 100 ft (Wojtanowicz 2012).

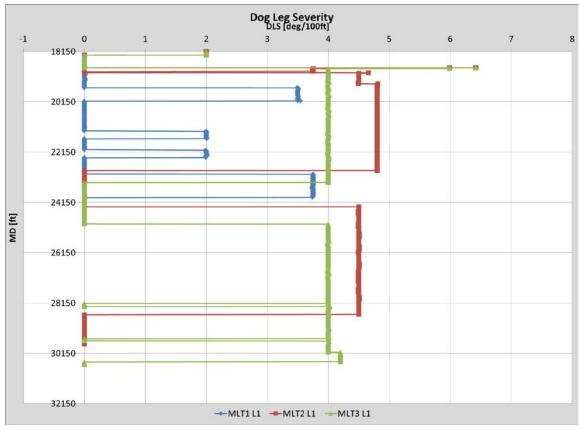


Figure 38: DLS for the wellbore sections compared in comparison case A (Wellplan 2013a)

7.2 Build-Up Rate

As mentioned in chapter 5.2 the BUR describes the wells change in inclination per well path length, with units in degrees per 100 ft. A positive BUR represents an increase in inclination, for example from vertical to deviated, while a negative sign means a drop in inclination.

For the wellbore section gathered in comparison case A the maximum BUR was indicated to be for the MLT1 L1, with 3.5 degrees per 100 ft at 19980 ft MD, when only considering the well path from the junction to TD (for the same reason as for the DLS as well). The second largest build-rate was for the MLT2 L1, with 3.36 degrees per 100 ft at 18840 ft MD. A trend for the wellbores in comparison case A was that the MLT3 L1 had slightly smaller values of BUR than the two others, with a peak of -2.02 at 27960 ft MD. It should be noted that all of the investigated well paths for comparison case A had quite large BUR. As mentioned for DLS, a value of 3.0 degrees per 100 ft normally is considered the maximum for running of tubulars, casing strings and other downhole tools. In addition, BHA's often have limitations when it comes to high build-rates, although some modern Rotary Steerable drilling Systems (RSS) can go as high as 6 – 7 degrees per 100 ft (Hummus et al 2011).

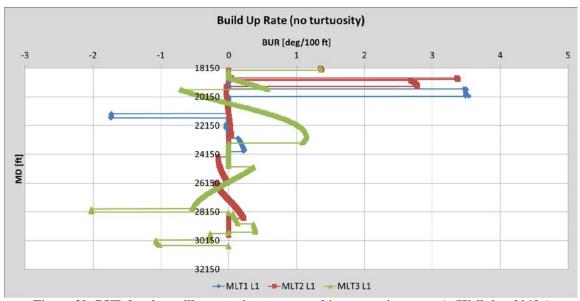


Figure 39: BUR for the wellbore sections compared in comparison case A (Wellplan 2013a)

7.3 Effective Tension

The first simulation to be performed for all the different sections to be drilled for the three various MLT configurations was the effective tension for when the bit was at each respective TD. "At TD" means that the results and graphs presented in this sub-chapter for all the MLT options are all when the bit is on bottom. Parameters plotted as a function of depth therefore show the situation along the string from surface to TD when the bit is at TD. For COPNO, and normally for drilling operations, a lower effective tension is beneficial. As mentioned in section 5.3, if the effective tension in the string gets too high the string elements might suffer from yield failure. Therefore it is important to check that the effective tension in the string for any of the wellbore sections to be drilled does not yield values that are above the max yield strength of any of the downhole string elements (Wojtanowicz 2012).

7.3.1 Comparison case A (all L1 compared) – Scenario 1 and Scenario 2

The effective tension for comparison case A, for both scenario 1 and 2, is presented in Figure 40. There are six lines, MLT1 L1, MLT2 L1 and MLT3 L1 for scenario 1 and scenario 2 input parameter values. For scenario 1 the WOB was set to 10 klbf, while for scenario 2 the bit weight was determined to be 25 klbf, as shown in Table 9. The WOB is represented for each line in the left lower corner at each wellbore sections representative TD. As it can be seen all the wellbores have for scenario 1 a -10 klbf effective tension and for scenario 2 a – 25 klbf effective tension value. The negative sign indicates compression, in other words effective weight on bit.

For both scenario 1 and scenario 2 the MLT1 L1 has the least effective tension, while the MLT3 L1 yields the most for bit rotating at bottom. The MLT2 L1 is between the two. The maximum effective tension at surface for bit rotating at TD is 251.7 klbf for MLT3 L1 scenario 1. However, the drillstring used in the simulations has a minimum effective tensile strength of around 500 klbf, with 882 klbf (S-135000 pipe, 6.625" OD, 5.965" ID) for the DP in the top section where the effective tension in the string is worst, as seen in Figure 41. The rig capacity is 1650 klbf, well above the expected maximum effective tension. Therefore no issues with regards to yield failure or lifting capacity by the rig should were indicated by the simulations. Sinusoidal buckling, on the other hand, was signposted to happen for MLT1 L1 Scenario 2, MLT2 L1 Scenario 2 and MLT3 L1 Scenario 1 and 2 during slide drilling. For rotating on bottom no indications of buckling were present, see Figure 43. There the left, red line is the minimum WOB for sinusoidal buckle. If that line is crossed the compressional force in the drillstring is so large that the pipe will sinusoidal buckle, a state it is beneficial to avoid. If the pipe suffers under S-buckling the applied weight will only partly be transferred to the bit, as some of the weight will be absorbed by the buckling of the pipe. If the compressional forces increases further helical buckling might occur, a condition where more applied weight only will result in more buckling of the string, and no weight will be transferred to the bit for further penetration (Wojtanowicz 2012). The minimum WOB to buckle is presented more in detail in chapter 5.7.

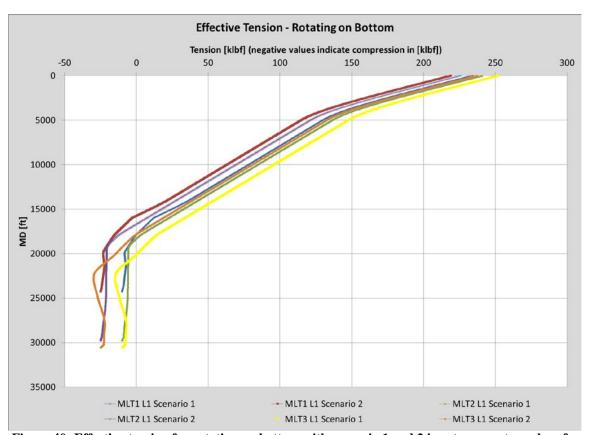


Figure 40: Effective tension for rotating on bottom with scenario 1 and 2 input parameter values for comparison case A (Wellplan 2013a)

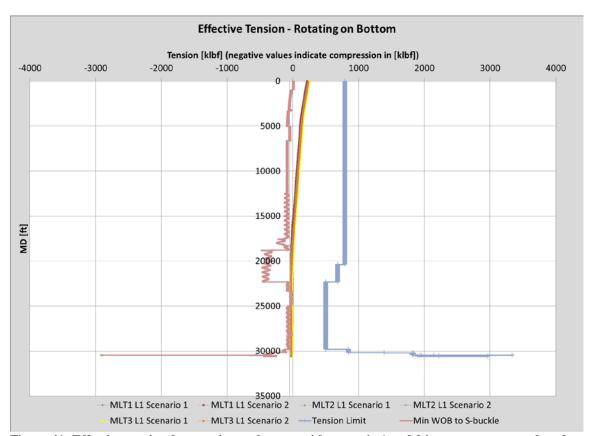


Figure 41: Effective tension for rotating on bottom with scenario 1 and 2 input parameter values for comparison case A. Left red line indicates minimum WOB to sinusoidal buckle the drillstring, while the right blue line displays the tension limit/tensile strength for the drillstring components at different measured depths (Wellplan 2013a)

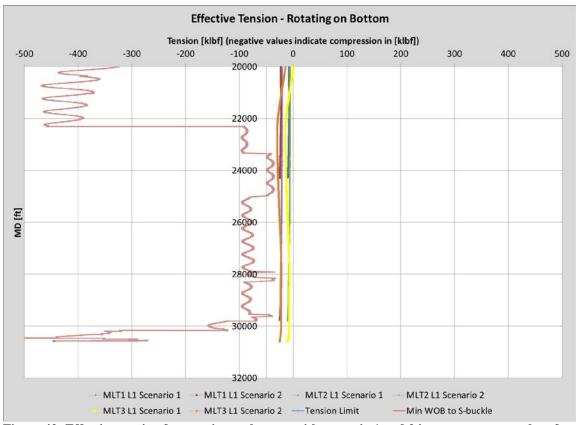


Figure 42: Effective tension for rotating on bottom with scenario 1 and 2 input parameter values for comparison case A. The left red line indicates minimum WOB to sinusoidal buckle the drillstring. As long as the effective tension values are to the right-hand side of the minimum WOB sinusoidal buckling will not occur (Wellplan 2013a)

7.3.2 Comparison case A (all L1 compared) – Suggested Values

For the suggested input values the highest effective tension at surface when rotating on bottom was indicated to be for the MLT3 L1 at 243.3 klbf, as seen in Figure 43. This values is lower than the maximum value for scenario 2, but higher than the maximum value for scenario 1. The lowest effective tension at surface for bit rotating on bottom was for the MLT1 L1, while the middle value was indicated for the MLT2 L1. As the drillstring was kept unchanged from the Scenario 1 and 2 simulations the tensional strength limit was not signaled to be exceeded for any of the wellbore sections for the suggested input values for comparison case A. For the suggested parameter values also the issues with sinusoidal buckling while slide drilling for MLT1 L1 Scenario 2, MLT2 L1 Scenario 2 and MLT3 L1 Scenario 1 and 2 were mitigated, and no indications of any buckling of any kind were present for any of the drilling modes.

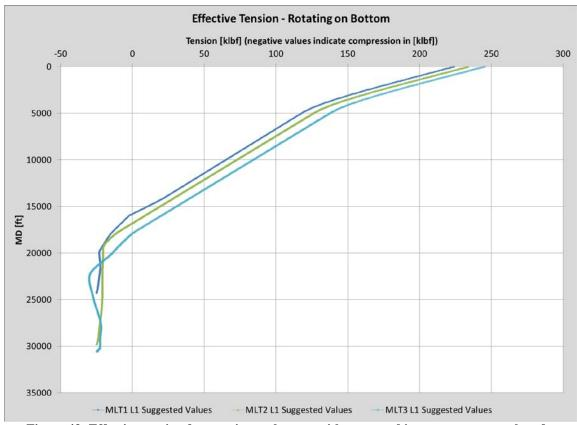


Figure 43: Effective tension for rotating on bottom with suggested input parameter values for comparison case A (Wellplan 2013a)

7.4 Torque

In chapter 6.5 it was mentioned that the torque at bit for both scenario 1 and 2 was set to 2500 ft-lbf. As the bit depth increases the torque in the string gets larger due to frictional forces acting against the direction of rotation in the deviated holes for investigated in this report (Gazaniol 1987). The highest maximum torque that can be applied to the string is limited by the make-up torque for the TJ for the different elements in the pipe, as presented in section 5.4.

7.4.1 Comparison case A (all L1 compared) – Scenario 1 and Scenario 2

For rotation of the bit on bottom the highest torque experienced at surface, displayed in Figure 44, was 47782 ft-lbf for the MLT3 L1 scenario 2. The second and third largest values, yielding almost identical torque values at the rig, were from the MLT2 L1 scenario 2 and MLT3 L1 scenario 1. The blue and purple lines to the left in the figure is the torque in the string for MLT1 L1 scenario 1 and 2, respectively. That wellbore, for both scenarios, showed to draw significantly less torque that the two others.

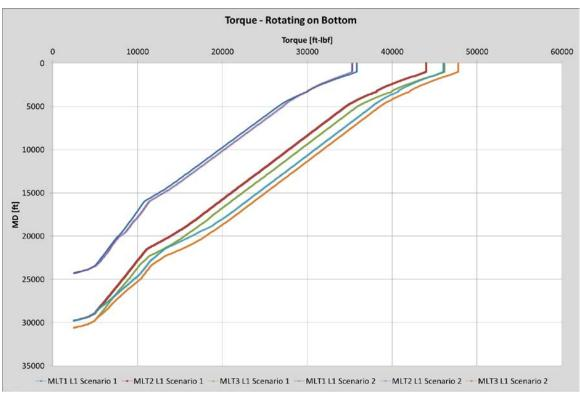


Figure 44: Rotary torque in the drillstring for bit rotating on bottom for scenario 1 and 2 input parameter values for comparison case A (Wellplan 2013a)

7.4.2 Comparison case A (all L1 compared) – Suggested values

For the suggested input parameter values the largest torque at surface for rotation of bit at TD was for the MLT3 L1, as presented in Figure 45. However, for this set of values the MLT2 L1 resulting torque at the rig was indicated to be almost as high, thus getting closer to the MLT3 L1 than for both scenario 1 and scenario 2 values. Again, the wellbore showing the least amount of torque at surface for bit rotation on bottom was the MLT1 L1.



Figure 45: Rotary torque in the drillstring for bit rotating on bottom for the suggested input parameter values for comparison case A (Wellplan 2013a)

7.5 Fatigue Ratio

In Wellplan the fatigue ratio for rotation on bottom for each of the MLT options was investigated. The ratio describes the total fatigue of the pipe, zero being new pipe and 1.0 being the failure-limit (Wellplan 2013b). As mentioned in section 5.5 the fatigue ratio is influenced by the pipe condition (new, premium, class 2 and class 3), where a class 3 pipe will reach the fatigue ratio limit faster than the new pipe given otherwise identical conditions. For the simulations in Wellplan a drillstring condition of premium was assumed, as mentioned in section 6.2. In reality the pipes often are classified as premium as soon as they leave the factory, even though they might never have been used. By doing this an additional safety factor is for fatigue and wear is applied (Wojtanowicz 2012).

7.5.1 Comparison case A (all L1 compared) – Scenario 1 and Scenario 2

For scenario 1 and scenario 2 input parameter values the indications from the simulations were that the MLT2 L1 scenario 2 yielded that highest fatigue ratio. That wellbore, with scenario 2 parameters, peaked at 0.498 at 1440 ft MD and 0.497 at 3330 ft MD when the bit was rotating on bottom, as shown by the green line in Figure 46.

Further down in the string the simulations showed that the MLT2 L1 scenario 2 for the most part gave the largest fatigue ratio. In the other end of the scale was the MLT1 L1, for both scenario 1 and 2. The red line in the figure displays the scenario 1 for that wellbore, and it can be seen that the ratio of fatigue generally is lowest throughout the whole string for rotation of bit at bottom, with the lowest peak of 0.394 at 23325 ft MD.

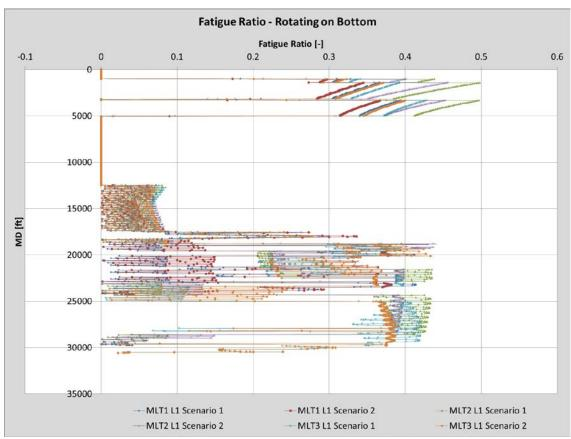


Figure 46: Fatigue ratio for comparison case A with scenario 1 and scenario 2 input parameter values (Wellplan 2013a)

7.5.2 Comparison case A (all L1 compared) – Suggested values

The simulations by use of the suggested input parameter values (Figure 47) showed, as a trend, that the worst wellbore, with regards to fatigue, were the MLT2 L1, the same result as for scenario 1 and 2 combined. The peak for that section was 0.476 at 1440 ft MD, followed by 0.472 at 3330 ft MD. These were the same depths as the scenario 1 and 2, something that was expected due to identical wellbore and drillstring in the simulations for the different input values. The second largest fatigue ratio is for the MLT3 L1, with a peak of 0.411 at 3330 ft MD, with MLT1 L1 indicating the lowest peak of 0.39 at 23325 ft MD. That wellbore, as can be seen in the graph (blue line), showed as a trend the lowest fatigue ratio for all depths along the drillstring as the bit was rotating on bottom at TD.

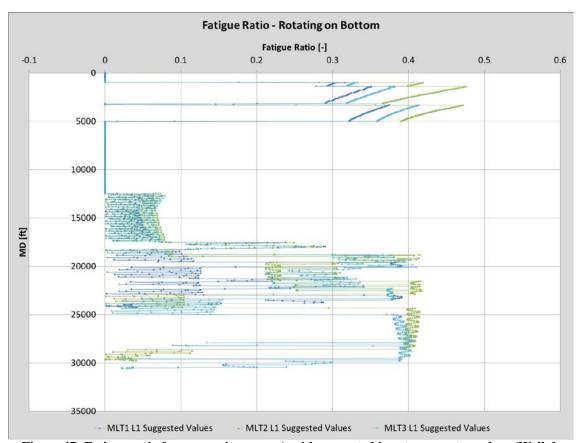


Figure 47: Fatigue ratio for comparison case A with suggested input parameter values (Wellplan 2013a)

7.6 Hook Load

The hook load was investigated by using the torque and drag module in Wellplan and selecting the drag chart-mode. That mode presents the output graph as a function of bit MD, in other words when the bit is at different depths in the well. So where the previous three effects (effective tension, torque and fatigue ratio) presented result-values in the string at different depths along the wellbore with the bit on bottom, the hook load output-graph showed the result-values experienced at surface when the bit was at different depths in the well.

As described in chapter 5 the hook load is a function of wellbore length (or drillstring length really), drillstring composition (overall average weight per foot and individual component OD) drilling fluid density, wellbore geometry and drag forces. For the simulations performed in this report only the tripping out operation was investigated as this normally yields the largest hook load (given no issues like stuck pipe or similar). When the bit just leaves the bottom at TD the maximum hook load is experienced at the surface, a value that often is referred to as the pick-up force (Sangesland 2012). The string was assumed to not be rotated while tripping out for any of the scenario 1 and scenario 2 simulations, but a few of the suggested values, found through the iterations,

had issues with tensile failures when the string was not rotated while tripping out, and a rotary speed for this operation was therefore determined for the particular wellbore sections. For all simulations, as presented in Table 10 in chapter 6, the friction factor for both openhole and cased hole was assumed to be 0.18 (Midtgarden 2010).

7.6.1 Comparison case A (all L1 compared) – Scenario 1 and Scenario 2

For scenario 1 and scenario 2 input parameter values the hook load output in Wellplan yielded the same results for running of the string from surface and down to the junction point at 18150 ft MD (9958 ft TVD), see Figure 48. This was expected as the properties, namely mud weight, wellbore geometry, well path and drillstring length, drillstring composition and design, were the same for both scenarios down to that point in the well, thereby giving the same drag frictional forces and hook load. Below the junction these parameters were no longer identical, except for the drillstring composition and mud weight.

The pick-up force indicated to be largest for the wellbores investigated in comparison case A was the one for the MLT3 L1. The hook load at surface just when the bit left the bottom was shown to be 469.8 klbf. The second largest overall hook load was for the MLT2 L1 of 455.3 klbf. Smallest hook load expected, shown by the simulations, was for the MLT1 L1, with 388.7 klbf pick-up weight. The output for scenario 1 and 2 input parameter values were expected based on differences in the well path length for the investigated welbores in comparison case A.



Figure 48: Hook load at surface for bit at different measured depths for the wellbores in comparison case A with scenario 1 and 2 input values (Wellplan 2013a)

7.6.2 Comparison case A (all L1 compared) – Suggested values

For the suggested values there were differences in the hook load all the way from surface to TD for different bit depths for the different wellbores, as seen in Figure 49. This was also expected due to the changing of the mud weight in the iterations, which again would influence the buoyancy effect, and thus the hook load at surface, for the different sections. The largest pick-up weight for the suggested parameter values for the wellbores gathered in comparison case A was for the MLT3 L1 of 484.2 klbf. Compared to the scenario 1 and 2 output this was 14.4 klbf larger. It should be noted that the smallest pick-up weight for the suggested values was indicated to be MLT2 L1, not MLT1 L1 as for scenario 1 and 2. The MLT2 L1 for scenario 1 and scenario 2 had almost the same hook load as MLT3 L1 for when the bit just left TD, which was expected due to almost equally long well paths. For the suggested values, however, the pick-up force for MLT2 L1 was indicated to be 315.9 klbf, a reduction of 139.4 klbf compared to scenario 1 and 2. The hook load for this wellbore section was also smaller than the one for MLT1 L1, a wellbore that is around 5500 ft shorter. A probable reason for that was that the

simulation of tripping out for MLT2 L1 indicated issues with sinusoidal buckling in the DP. It was therefore decided to apply a rotation of 120 RPM to the drillstring for the tripping out operation for MLT2 L1. Therefore the hook load results for this wellbore section really cannot be compared with the two others. It should also be mentioned that the suggested mudweigth for MLT2 L1 and MLT3 L1 was set to 10.50ppg, while it for MLT1 L1 was changed to 11.20ppg, from the initial 12.40ppg for scenario 1 and 2. Therefore the MLT1 L1 experienced more buoyancy effect resulting in less effective string weight (refer to Eq. 10).

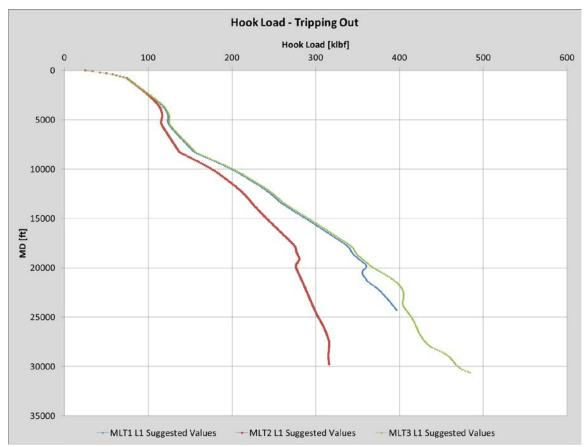


Figure 49: Hook load at surface for bit at different measured depths for the wellbores in comparison case A with suggested input values (Wellplan 2013a)

7.7 Torque vs MD

The torque as a function of measured depth displays the torque measured at surface for bit rotation on bottom for different depths along the wellbore. Or in other words the surface torque for bit rotation on bottom for different TD's along the wellbore for each section investigated. Compared to the torque simulation results in section 7.4 the output values will be the same for bit rotation on bottom. However, the lines in Figure 44 and Figure 45 display the torque in the string from bit at TD to the surface, while the

graphs presented in this sub-chapter, as mentioned, presents the surface torque for different bit depths along the well path.

7.7.1 Comparison case A (all L1 compared) – Scenario 1 and Scenario

For scenario 1 and 2 the MLT3 L1 drew most torque when bit was at TD, as seen in Figure 50. Rotation of bit on bottom yielded 47782 ft-lbf for that wellbore section, see the orange line in the figure, the same as indicated in Figure 44, as expected. The rest of the torque results for bit rotation on bottom were the same as shown in Figure 44, with MLT1 L1 as the section drawing the least surface torque. For bit depths shallower than the junction depth at 18150 ft MD the different wellbore sections indicated the same amount of surface torque for same scenario. This was expected due to equal well path and properties for the wellbores for the same scenario.

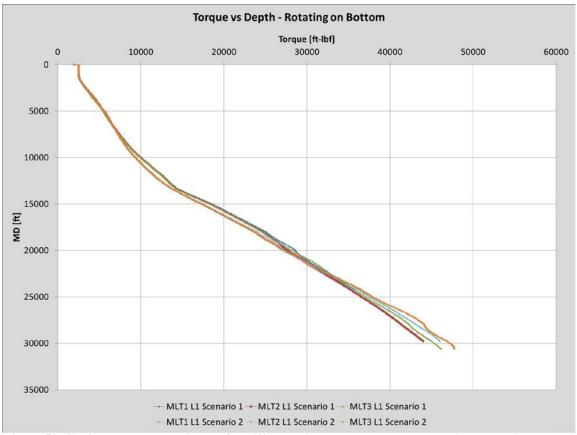


Figure 50: Surface torque experienced for different bit depths as each wellbore in comparison case A is drilled to TD with scenario 1 and 2 input parameter values (Wellplan 2013)

7.7.2 Comparison case A (all L1 compared) – Suggested values

By use of the suggested parameter input values the result was as presented in Figure 51. The green line shows the MLT3 L1 torque, the red the MLT2 L1 and the blue the MLT1 L1. As it can be seen the most torque for bit rotation at TD for the comparison case A was for the MLT3 L1, as for scenario 1 and 2 input values. That section indicated a torque of 49029 ft-lbf as maximum, while the lowest maximum was for the MLT1 L1 at 35883 ft-lbf at its respective TD of 24280 ft MD. In the figure it can be seen that from the junction point at 18150 ft MD and up towards the surface the torque appears to be quite similar. However, as mentioned in section 7.6.2 the mud weight, which affects the torque via Eq. 21, for the three different wellbore sections investigated in comparison case A is not identical. For MLT1 L1 it was set to 11.20ppg, while for MLT2 L1 and MLT3 L1 is was determined to be 10.50ppg. The two latter wellbores therefore showed the same torque from the junction to the surface due to identical drillstring design and hole friction factor, while the MLT1 L1 gave a slightly lower result because of the smaller buoyancy factor, and thus a smaller normal force acting between the drillstring and the hole wall, see the Eq. 16. However, as seen in the figure, the difference between MLT1 L1, and the pair of MLT2 L1 and MLT3 L1, is hardly distinguishable. As an example, for bit depth of 10000 ft MD the MLT1 L1 indicated a torque of 9564 ft-lbf, while the two others yielded the slightly higher 9659 ft-lbf, a difference of only 95 ft-lbf.

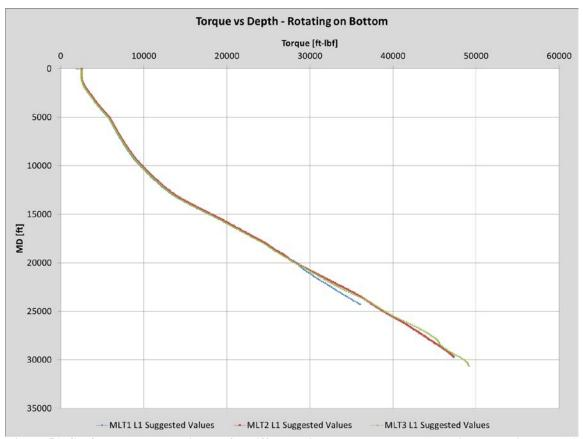


Figure 51: Surface torque experienced for different bit depths as each wellbore in comparison case A is drilled to TD with suggested parameter values (Wellplan 2013)

7.8 Minimum WOB to sinusoidal buckle

Chapter 5.7 presents the minimum WOB in order to experience buckling in the string. For this report only the sinusoidal buckling was determined to be investigated, as this is the first order of buckling that will occur in the string if the buckling resistance at any point in the string is exceeded.

7.8.1 Comparison case A (all L1 compared) – Scenario 1 and Scenario

In Figure 52 the minimum bit weight to experience S-buckling in the drillstring is presented for scenario 1 and scenario 2 input parameter values for comparison case A. For bit at bottom the minimum WOB to buckle is given by the mother wellbore. Almost at top the buckling resistance was the lowest, at 12.5 klbf. However, by neglecting the top sections; When bit was at TD the MLT3 L1 indicated the smallest buckling resistance of 28.4 klbf at 26700 – 27100 ft MD. In other words, if the WOB would exceed 28.4 klbf the string would buckle of 1st degree at this depth. The second lowest resistance against buckling was for the MLT1 L1, with a bit weight of 35.9 klbf to buckle the string at 22000

ft MD. The largest buckling resistance is for the MLT2 L1, with minimum WOB of 39.7 klbf at 24200 ft MD.

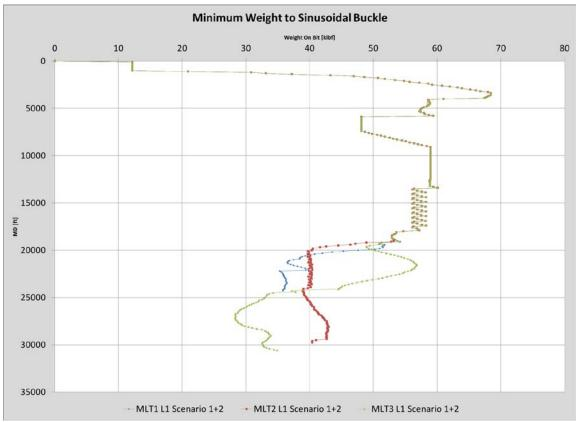


Figure 52: Minimum WOB to sinusoidal buckle for the wellbore sections gathered in the comparison case A for scenario 1 and scenario 2 input parameter values (Wellplan 2013a)

7.8.2 Comparison case A (all L1 compared) – Suggested values

For comparison case A with the suggested parameters the values are the same as for equation 1 and equation 2 for MLT1 L1 due to identical wellbore geometry and drillstring design.

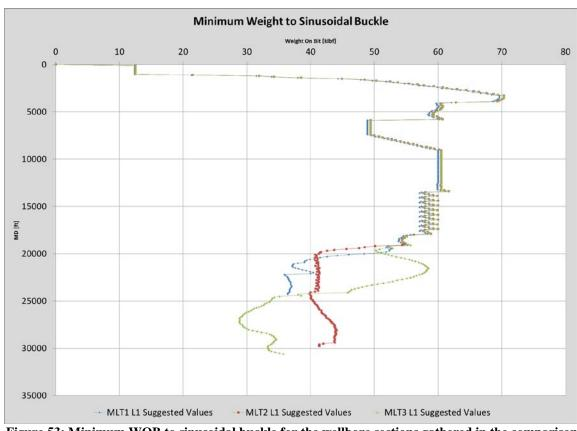


Figure 53: Minimum WOB to sinusoidal buckle for the wellbore sections gathered in the comparison case A for scenario 1 and scenario 2 input parameter values (Wellplan 2013a)

7.9 Hole Cleaning

In order to ensure successful running of the next casing string, and to mitigate issues with packing off and to make sure the drilling operation is as efficient as possible, sufficient hole cleaning is important, as mentioned in chapter 5.8. The setup in Wellplan included three EMSCO FC-2200 triplex mud pumps in parallel, each with a horsepower rating of 2200 HP, maximum discharge pressure of 5000 psi and maximum flow rate capacity of 348.7 gpm at 105 spm. The volumetric efficiency was assumed to be 85 %. Together these three pumps yielded a maximum flow rate capability of 1046.1 gpm, maximum total horsepower of 6600 HP, with a maximum system pressure loss of 5000 psi. The maximum SPP was set to 5500 psi, meaning that the mud pumps were considered the limiting factor for maximum allowable surface pressure. This setup is the same as for Mærsk Gallant, the rig currently drilling on Ekofisk Zulu. More information about both the rig can be found in Appendix J, with the mud pumps presented in Appendix S.

7.9.1 Comparison case A (all L1 compared) – Scenario 1 and Scenario

For the wellbores investigated in comparison A the minimum flow rate needed to sufficiently clean the hole can be seen in Figure 54. The largest minimum rate for all the wellbore sections was given to be in the 13 5/8" annulus from 5000 – 6700 ft MD. That is in the mother wellbore, which is common for all the simulated MLT options. As expected, the minimum flow rate was the same for same scenario in the mother wellbore. In the 13 5/8" casing annulus a mud rate of 590.2 gpm was required to transport the cuttings out of the hole for scenario 2, while the number for scenario 1 was 618.4 gpm. The lower value for scenario 2 is probably due to the higher rotational speed of 195 RPM, compared to 140 RPM for scenario 1 (see Table 9). Towards the bottom the wellbores and well paths for each of the MLT options are different, leading to differences in the minimum flow rate to adequately clean the hole. However, it is the largest minimum rate that dictates the requirement for the mud pumps, here given by the 13 5/8" annulus, as described.

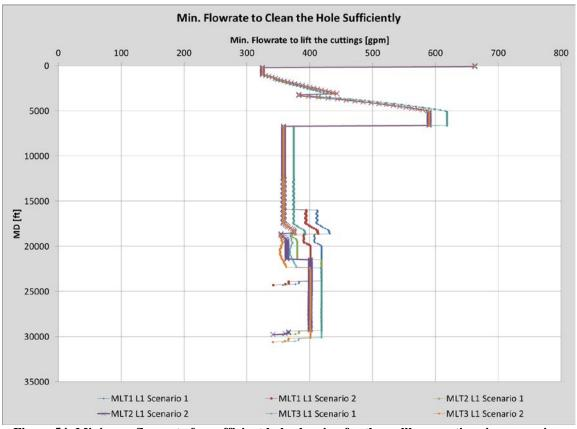


Figure 54: Minimum flow rate for sufficient hole cleaning for the wellbore sections in comparison case A with scenario 1 and 2 input parameter values (Wellplan 2013a)

7.9.2 Comparison case A (all L1 compared) – Suggested values

The trend for the suggested input parameter values is the same as for scenario 1 and 2. The minimum flow rate needed to clean the hole was for all the three wellbores

gathered in comparison case A given by the 13 5/8" annulus from 5000 – 6700 ft MD, showed in Figure 55. MLT1 L1 indicated the largest minimum flow rate requirement of 667.3 gpm, while both MLT2 L1 and MLT3 L1 showed 625.5 gpm. The reason for the difference is probably the suggested mud weight of the MLT1 L1 of 10.5 ppg, a value that is 11.20 ppg for the two others, leading to less flow rate needed to yield the same cleaning effect for otherwise similar parameters. As mentioned in chapter 5, Saasan (1998) showed that the pressure loss due to friction in the annulus is the largest contributor to cleaning of the wellbore for a deviated well. In other words the pump rate for the mud pumps must be selected so that the resulting frictional pressure loss in the annulus is high enough to obtain the required hole cleaning. In addition the cleaning is dependent on the cutting bed consolidation, cutting density and shape, annular velocity and mud properties in form of lifting capacities (Saasan 1998).

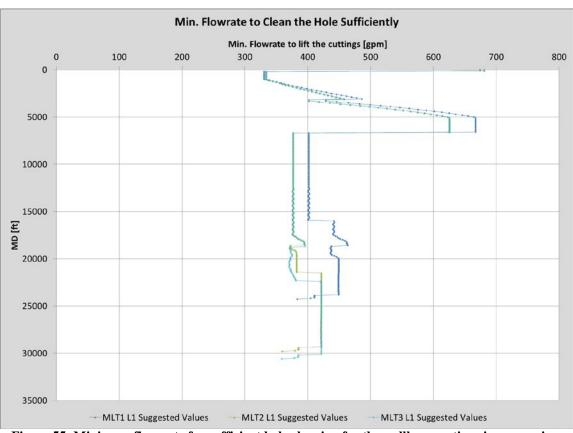


Figure 55: Minimum flow rate for sufficient hole cleaning for the wellbore sections in comparison case A with suggested parameter values (Wellplan 2013a)

7.10 Pressure Losses

As mentioned in chapter 5.9 the system pressure losses should not exceed the maximum allowable surface pressure for the given pump rate. For the simulations performed in this report the maximum pressure at surface was given by the maximum discharge pressure of the mud pumps of 5000 psi. The pressure losses in the well should be designed so that the annulus pressure losses give an ECD within the drilling window (window between pore pressure and fracture gradient lines), as well as a bit jet impact force adequate to remove the rock being cut, without exceeding the maximum allowable surface pressure, given either by the pumps or the SPP (Wojtanowicz 2012).

7.10.1 Comparison case A (all L1 compared) – Scenario 1 and Scenario

For scenario 1 and 2 input parameter values the system pressure losses as a function of pump rate are shown for the wellbores in comparison case A in Figure 56. TJ losses are not included. A trend was that the overall pressure losses for MLT2 L1 and MLT3 L1 were slightly above the values for MLT1 L1, for all variations of pump rate. The highest pressure losses were seen for the MLT3 L1, however only 5-20 psi above the values for MLT2 L1, dependent on pump rate. The results are as expected as the MLT3 L1 has the longest total well path, followed by MLT2 L1 and MLT1 L1. The MLT2 L1 and MLT3 L1 has a difference in measured depth of 813.64 ft, a length that in theory should not give too high pressure loss differences with all other parameters constant. The MLT3 L1 and MLT2 L1 had for scenario 1 and 2 input parameter values a maximum pump rate of 487.5 gpm in order to not exceed the maximum surface pressure of 5000 psi. Put together with the result in Figure 54, which gave a minimum flow rate of 590.2 gpm for scenario 2 and 618.4 gpm for scenario 1 to clean the hole, it could be determined that for scenario 1 and 2 parameter input values the hole would not be sufficiently cleaned due to the pump rate limitations based on maximum allowable surface pressure. For MLT1 L1 the maximum flow rate without exceeding the mudpump discharge pressure was 506.3 gpm, also well below the required numbers given for hole cleaning. Otherwise it can be seen than the system pressure losses were identical for both scenario 1 and scenario 2, naturally, due to same values for the parameters making up the input values in the Eq.s for pressure losses presented in chapter 5.9.

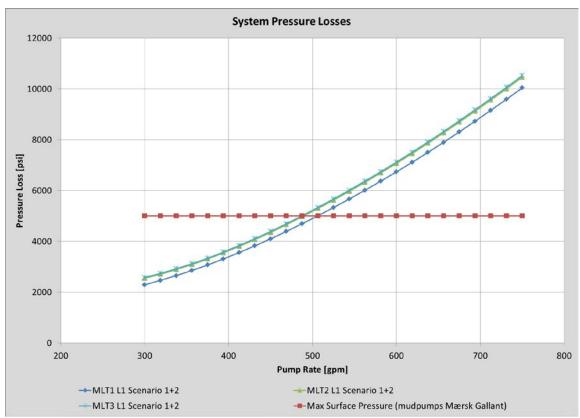


Figure 56: System pressure losses for wellbores in comparison case A with scenario 1 and scenario 2 parameter input values (Wellplan 2013a)

7.10.2 Comparison case A (all L1 compared) – Suggested values

The system pressure losses, excluded the losses in the tool joints, for the suggested input parameter values for comparison case A is presented in Figure 57. The MLT3 L1 indicated the highest losses for all of the pump rates. The small difference between MLT3 L1 and MLT2 L1 from scenario 1 and 2 now had increased to between 50 and 70 psi, dependent on flow rate. Again the MLT1 L1 showed system pressure losses significantly below the two others. Compared to scenario 1 and 2 input values the overall pressure losses had been reduced by use of the suggested values for all the wellbores. MLT1 L1 now showed a maximum flow rate of 750 gpm before exceeding the maximum surface pressure, while MLT2 L1 and MLT3 L1 had a maximum of roughly 690 gpm. A reason for this might be the decreased mudweigh from 12.40 ppg to 11.20 ppg for MLT1 L1, and from 12.40 ppg to 10.50 ppg for both MLT2 L1 and MLT3 L1. In addition the rotary speed for all the wellbores were set to maximum of 195 RPM, which will help clean the hole and reduce the frictional pressure losses in the annulus. Finally the bit nozzles were changed from 3x(12/32)" to 3x(18/32)" to reduce the pressure losses across the bit. That action, on the other hand, would decrease the jet impact force for the bit, but it was a necessary trade-off in order to reduce the elevated surface pressures (Bourgoyne et al. 1986c). For the suggested values the maximum possible

flow rate without exceeding the mudpump discharge pressure would be above the minimum flow rate given for hole cleaning given in Figure 55. For MLT1 L1the minimum pump rate needed for hole cleaning with the suggested parameter values was 667.3 gpm, while the pressure loss graph indicated a maximum pump rate of 750 gpm at 5000 psi pressure loss. For MLT2 L1 and MLT3 L1 the flow rate requirement for cleaning was 625 gpm, while the highest pump rate before exceeding the maximum surface pressure now showed a value of circa 690 gpm for both.

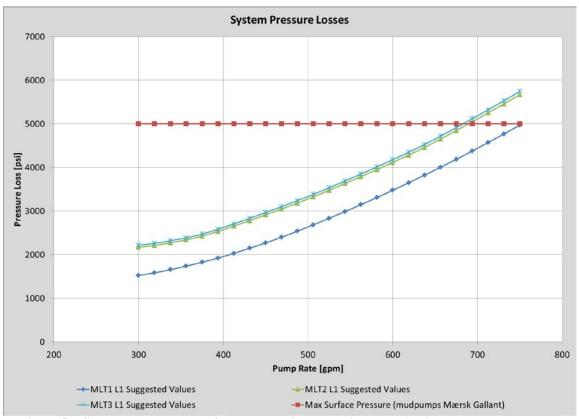


Figure 57: System pressure losses for wellbores in comparison case A with suggested parameter input values (Wellplan 2013a)

7.11 Circulating Pressures vs MD

The circulating pressure is the pressure at any point in the well exerted by the flowing mud from the mud pumps at surface, as presented in section 5.10. For a conventional, overbalanced drilling operation the circulating pressure should be within the drilling window as the mud exits the bit nozzle. Further is the rate of penetration and the bitrock interaction dependent of the pressure loss across the bit, and nozzle size selection is important in order to optimize the bit pressure loss for optimized ROP (Bourgoyne et al. 1986d).

In Wellplan the only option for the y-axis in the circulating pressure graph is measured depth, rather than TVD. The pore pressure and fracture gradient lines were for the simulations kept constant for all of the different wellbores for the three MLT options, and for graphs plotted against TVD the PP and FG would have been constant. As the wellbores do not have the same well paths, the measured depth will not correspond to the same TVD for the different wellbores. The pore pressure and fracture gradient lines will therefore not be the same for same MD for the different wellbore sections, and the three wellbores in comparison case A could therefore not be plotted in the same plot, as they have been so far. In order to reduce the number of graphs presented in this chapter it was therefore decided to only show the output from the simulation for MLT1. The rest of the wellbores for the comparison case A, as well as the output for all of the six other comparison cases, are found in Appendix Q.

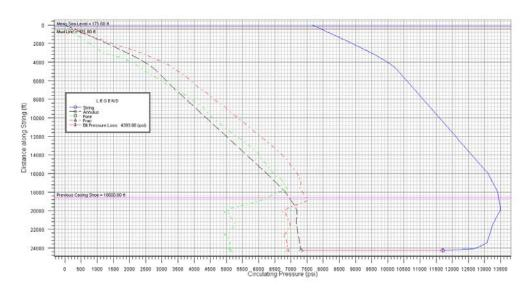
7.11.1 Comparison case A (all L1 compared) – Scenario 1 and Scenario

The circulating pressures for MLT1 scenario 1 and scenario 2 are presented in Figure 58 and Figure 59, respectively. The green, dotted line in the figures is the pore pressure, while the red is the fracture gradient. The blue line is the circulating pressure inside the string, the red, sold line the bit pressure loss, and the black, dotted one the annulus circulating pressure. The horizontal, purple/pink line indicates the measured depth of the last casing/liner string.

For MLT1 L1 scenario 1 the SPP was indicated to be 4097 psi, while for scenario 2 the value was 7764 psi, 2764 psi above the maximum allowed surface pressure. For scenario 2, with the constraint of 5000 psi pressure loss, the pump rate would maximum could be set at 506.3 gpm, below the required 590.2 gpm to sufficiently clean the hole (refer to Figure 54 and Figure 56). Otherwise it can be seen that for both MLT1 L1 scenario 1 and scenario 2 the circulating pressure in the annulus was above the fracture gradient line for most of the openhole part, a condition that should be avoided for conventional, overbalanced drilling, as mentioned.



Figure 58: Circulating pressure for MLT1 L1 for scenario 1 parameter input values (Wellplan 2013a)



Pump Flow Rule. (850.0 gpm F Include Mod Temperature Effects

Time of Circulations 200 No

Stord Pipe Pleasure 776539 psi

Figure 59: Circulating pressure for MLT1 L1 for scenario 2 parameter input values (Wellplan 2013a)

7.11.2 Comparison case A (all L1 compared) – Suggested values

Circulating pressures for MLT1 L1 with the suggested parameter input values are shown in Figure 60. The SPP was for this wellbore section with these input values indicated to be 4237 psi, below the maximum of 5000 psi. The pump rate for this wellbore section was set to 680 gpm, a value above the minimum required 667.3 gpm for hole cleaning, as given in Figure 55. Further it can be seen that the circulating pressure now fell within the drilling window for the whole part of the openhole section, despite getting quite close to the PP at the last casing shoe at 18600 ft MD. Between the scenario 1 and 2, and the suggested values, the bit nozzles for MLT1 L1 was changed from 3x(12/32)" to 3x(18/32)", decreasing the pressure loss across the bit from 2106 psi (scenario 1) and 4394 psi (scenario 2) to 858 psi.

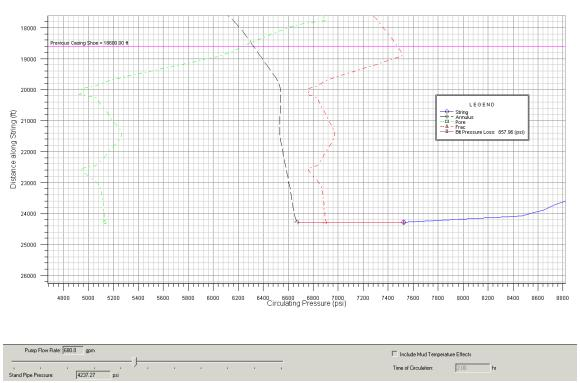


Figure 60: Circulating pressure for MLT1 L1 for suggested parameter input values (Wellplan 2013a)

7.12 ECD vs MD

As for the circulating pressures the ECD in Wellplan can only be plotted against MD, not TVD. Of the same reason as mentioned for circulating pressures in section 7.11 the three wellbores in comparison case A could therefore not be plotted in the same plot. In order to reduce the number of graphs presented in this chapter it was therefore decided to only show the output from the simulation for MLT1. The rest of the wellbores for the comparison case A, as well as the output for all of the six other comparison cases, are found in Appendix Q.

7.12.1 Comparison case A (all L1 compared) – Scenario 1 and Scenario

The ECD for MLT1 L1 with scenario 1 parameter input values can be seen in Figure 61, with scenario 2 input values presented in Figure 62 for the same wellbore section. As for the circulating pressure graphs the green, dotted line represents the pore pressure, now in equivalent density, and the red, dotted line the fracture gradient, also in equivalent density. The pink/purple horizontal line shows the last casing shoe. The simulation results, similarly to the circulating pressures, as expected, an indicated on that both of the scenarios would result in an ECD above the fracture limit for most of the openhole section, a condition that should be avoided.

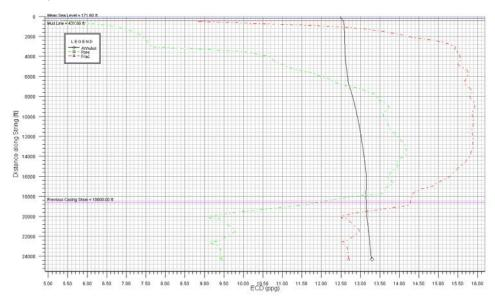


Figure 61: ECD vs MD for MLT1 L1 scenario 1 input values (Wellplan 2013a)

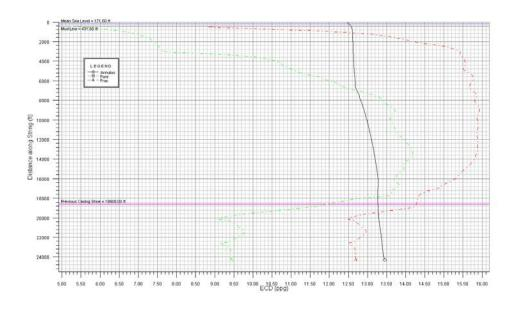


Figure 62: ECD vs MD for MLT1 L1 scenario 2 input values (Wellplan 2013a)

7.12.2 Comparison case A (all L1 compared) – Suggested values

The ECD vs MD for MLT1 L1 with the suggested parameter input values are presented in Figure 63. By introducing the changes from scenario 1 and 2, as described in section 7.11.2, the ECD now fell within the drilling window. At the last casing shoe the trip margin between the ECD and the PP is around 0.16 ppg, a value that is lower than the often used 0.5 ppg trip margin (Hyne, N.J. 1991). By using of the theory from section 5.10 the safety margin between the pore pressure and the ECD at last casing shoe (18600 ft MD / 10076 ft TVD for MLT1 L1) becomes only 83.83 psi.

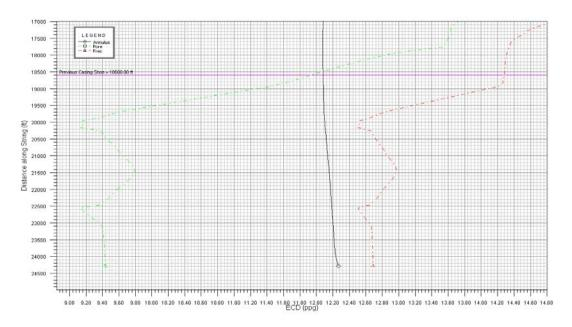


Figure 63: ECD vs MD for MLT1 L1 suggested input values (Wellplan 2013a)

8 Evaluation

8.1 Wellplan results for Scenario 1 and Scenario 2 parameter values

8.1.1 Scenario 1

The simulation results for the different drilling effects by use of scenario 1 input parameter values were gathered in output graphs and analyzed. For rotation on bottom none of the nine different wellbore sections with scenario 1 values indicated issues for effective tension, torque, fatigue ratio, hook load or buckling. For effective tension all of the wellbore sections investigated yielded values that were below the tensional limits for the drillstring, as well as below the maximum tension given by the rig. The torque values at surface for drilling on bottom gave results for all wellbore sections that were below both the make-up torque and the top drive limitation. Further was the maximum hook load rating for the rig of 1650 klbf static load not exceeded by any of the MLT options. In addition, no buckling was indicated by use of scenario 1 values for rotation on bottom.

However, for slide drilling some of the wellbore sections indicated challenges. For MLT3 L1, MLT3 L2 9.5" and MLT3 L2 8.5" sinusoidal buckling were indicates when using the scenario 1 parameter input values, as presented in Table 13. In addition, for MLT2 L1, the yield failure limit for tension was exceeded for tripping out operations. All of the wellbore sections indicated larger DLS values than the recommended maximum of 3.0 degrees per 100 ft, a condition that is undesirable due to possible issues of running casing strings and tubulars to TD. The well paths and DLS for each of the wellbore sections are evaluated in detail in section 8.7. This issue was the same, and will be the same, for all values of input parameters as the DLS only is a function of well geometry. When it came to hole cleaning all the wellbore sections indicated issues. None of the MLT options, with scenario 1 input values, gave enough flow rate to sufficiently clean the hole. This might lead to challenges with raised circulating pressure and ECD, as well as packing of due to excessive cuttings occupying the annulus. Ultimately the increased pressures due to pack-offs from cuttings might lead to fracturing of the formation and lost circulation. Finally, all the wellbores except all the MLT L2 9.5" sections, indicated problems with the ECD for the openhole section. The reason for no issues for the L2 9.5" sections was probably due to the relatively short section length, varying between 400 and 640 ft, resulting in small increases in the ECD due to frictional pressures, as well as a relatively large drilling window compared to larger TVD's. Overall, a trend for scenario 1 was too large values of ECD compared to the fracture gradient, leading to fracturing of the formation. Again this might cause lost circulation, which can result in a kick or underground blowout (Bourgoyne et al. 1986c).

Table 13: Summary of issues by use of scenario 1 parameter input values (Wellplan 2013a)

				-					
	Scenario 1								
Wellbore ->	MLT1 L1	MLT2 L1	MLT3 L1	MLT1 L2 9.5"	MLT2 L2 9.5"	MLT3 L2 9.5"	MLT1 L2 8.5"	MLT2 L2 8.5"	MLT3 L2 8.5"
S-buckling	-	-	X (slide)	-	-	X (slide)	-	-	X (slide)
H-buckling	-	-	-	-	-	-	-	-	-
Yield failure		X (trip o)	-	-	-	-	-	-	-
Fatigue failure	-	-	-	-	-	-	-	-	-
DLS above 3.0	X	X	X	X	X	X	X	X	X
Hole Cleaning	X	X	X	X	X	X	X	X	X
ECD issues	X	X	X	-	-	-	X	X	X

Based on the simulation results and issues summarized in Table 13, it was concluded that scenario 1 input parameter values were not recommended for any of the wellbore sections for the three MLT options. The issues with regards to buckling and yield failure of the pipe can be dealt with by changing the drillstring configuration. In addition is slide drilling not likely to take place for the drilling of the MLT options on Ekofisk South²⁶. Therefore these issues will probably not lead to any large consequences with regards to the drilling process. The challenges with hole cleaning and ECD, on the other hand, might lead to severe significances in form of fracturing of formation, kick, underground blowout, and ultimately danger for human lives. A summary of all the output results for all the different wellbores by using of the scenario 1 parameter values can be found in Appendix Q.

8.1.2 Scenario 2

For the simulations by using the scenario 2 parameter input values there were, as for scenario 1, no indications of issues for rotation of bit on bottom with regards to effective tension, torque, fatigue, hook load or buckling. As for scenario 1 the introduction of slide drilling yielded challenges with sinusoidal buckling. Due to the increased WOB compared to scenario 1 now more of the wellbore sections indicated this issue, see Table 14. Only MLT1 L2 9.5" and MLT2 L2 9.5" showed no signs of buckling for slide drilling. For tripping out operations only wellbore MLT2 L1 indicated issues with yield failure. This was the same for scenario 1. Due to identical well path for all the wellbore sections for both scenario 1 and 2 the DLS challenges were the same as for scenario 1. The flow rate for scenario 2 was increased from 450 gpm to 650 gpm for all the MLT options. This led to a mitigation of the hole cleaning issues present for scenario 1. On the other hand, this resulted in large system pressure losses for all the different MLT options investigated. All the nine wellbore sections indicated a SPP above the maximum allowable surface pressure of 5000 psi given by the mud pumps. The larger flow rate and pressure losses resulted in increased ECD for all the wellbores, except the MLT L2 9.5" sections (as for scenario 1), pushing the circulating pressures even more above the fracture limit.

²⁶ Personal communication with Thomas Mæland. 2013. Stavanger: ConocoPhillips Norway

Table 14: Summary of issues by use of scenario 2 parameter input values (Wellplan 2013a)

	Scenario 2								
Wellbore ->	MLT1 L1	MLT2 L1	MLT3 L1	MLT1 L2 9.5"	MLT2 L2 9.5"	MLT3 L2 9.5"	MLT1 L2 8.5"	MLT2 L2 8.5"	MLT3 L2 8.5"
S-buckling	X (slide)	X (slide)	X (slide)	-	-	X (slide)	X (slide)	X (slide)	X (slide)
H-buckling	-	-	-	-	-	-	-	-	-
Yield failure	-	X (trip o)	-	-	-	-	-	-	-
Fatigue failure	-	-	-	-	-	-	-	-	-
DLS above 3.0	X	X	X	X	X	X	X	X	X
Hole Cleaning	-	-	-	-	-	-	-	-	-
ECD issues	X	X	X	-	-	-	X	X	X

Compared to scenario 1 the overall indications by use of the scenario 2 input parameter values were that the issues with hole cleaning were mitigated. On the other hand, the increased pump rate for scenario 2 introduced even larger challenges with the ECD at the open hole section for all the nine different wellbores investigated, except MLT1 L2 9.5". This increased ECD can lead to even larger lost circulation issues than for scenario 1. In addition more problems with buckling for slide drilling operations were shown. A conclusion were made that the scenario 2 values were more extreme than the scenario 1 values yielding overall larger challenges due to the increased circulating pressures, despite giving sufficient flow rate for adequate hole cleaning. In conflict with the conclusion for scenario 1 parameter values, the simulations showed that for MLT1 L2 9.5" and MLT2 L2 9.5" the scenario 2 numbers successfully could be utilized without any issues, except for a high DLS, an issue common for all the wellbore sections. Other than that the scenario 2 input parameter values should not be used as a combination of input values in any of the wellbores for the three MLT options. A summary of all the output results for all the different wellbores by using of the scenario 2 parameter values can be found in Appendix Q.

8.2 Wellplan results for suggested parameter input values

Through iteration processes in Wellplan, as described in section 6.2, a set of suggested, individual input parameter values were determined for each of the wellbore sections for the three MLT options investigated. As seen in Table 15 by use of these values the simulation results indicated no issues, other than the well path specific high DLS, for most of the wellbores. From scenario 1 and scenario 2 the bit nozzle selection was changed from 3x(12/32)" to 3x(18/32)" in order to reduce the challenges with high pressure losses and large ECD values in the open hole portion of the well for all the MLT options. However, for MLT2 L2 8.5" and MLT3 L2 8.5", the challenges related to circulating pressures and ECD were unsuccessfully mitigated. For both of these wellbore the BHA used in all of the other simulations gave even larger issues with respect to the ECD in form of large values above the fracture gradient in the openhole portions, and a combination of pump rate, mud weight and bit nozzle selection was not found that reduced the circulating pressures towards TD. A change of BHA, with overall smaller OD's, was therefore tried for both of the wellbore sections. This reduced the ECD in the annulus outside the BHA for both MLT2 L2 8.5" and MLT3 L2 8.5", but still the best combination of input parameters with the given setup found by this author did not fully mitigate the issues with regards to the ECD. As a result both of the wellbore sections yielded an ECD below the fracture gradient for the whole length of the open hole portion, but below the pore pressure just below the last casing shoe. This is undesirable as it might lead to lost circulation, leading to severe concerns as kick and even blowout.

Table 15: Summary of issues by use of suggested parameter input values (Wellplan 2013a)

					<u>, , , , , , , , , , , , , , , , , , , </u>		-			
	Suggested values									
Wellbore ->	MLT1 L1	MLT2 L1	MLT3 L1	MLT1 L2 9.5"	MLT2 L2 9.5"	MLT3 L2 9.5"	MLT1 L2 8.5"	MLT2 L2 8.5"	MLT3 L2 8.5"	
S-buckling	-	-	-	-	-	-	-	-	-	
H-buckling	-	-	-	-	-	-	-	-	-	
Yield failure	-	-	-	-	-	-	-	-	-	
Fatigue failure	-	-	-	-	-	-	-	-	-	
DLS above 3.0	X	X	X	X	X	Х	X	X	X	
Hole Cleaning	-	-	-	-	-	-	-	-	X	
ECD issues	-	-	-	-	-	-	-	X	X	

In should be mentioned that the issues experienced in the simulation results with circulating pressures falling outside the drilling window for any of the input parameter values might not be the case in reality. As mentioned in chapter 4 and 6 the lack of underground data information available in the area where the well paths for the MLT options investigated in this report led to an assumption that the pore pressure and fracture gradient could be taken from the nearby wells 2/4-Z-17 and 2/4-VB-05. Therefore the drilling window in reality will not exactly be as presented in this report, and for some of the wellbore sections for the MLT options the ECD issues might be terminated in a real life situation. However, by use of the same underground data for all of the MLT options a picture of the circulating pressure effects for all of the wellbores could be established, independent of pore pressure and fracture gradient lines assumed.

8.3 Correlations in the results

For the three sets of input parameter values used in Wellplan a correlation of challenges with regards to circulating pressures and large ECD values towards the total depth were indicated. Even though the suggested parameter values to a certain extent mitigated these issues, also for these cases there were challenges in order to obtain a sufficient trip and kick margin of 0.5 ppg, as described in section 5.10. Naturally the results might not be the same by use of the actual pore pressure and fracture gradient values, but all of the wellbore sections, for all of the three input sets of parameter values, gave quite large pressure losses, with a resulting high SPP and elevated ECD values in the openhole portion of the well. A possible reason for this might be the long well paths for all the MLT options, as discussed further in section 8.7. As given by the formulas for frictional pressure losses, presented in section 5.9, the length of the wellbore will influence the value of the pressure losses. In addition, the well paths for all of the sections are more or less horizontal for almost the whole openhole portions. This results in stable values of

the pore pressure and fracture gradient, due to the small increase in TVD, but continuously increased ECD because of the increase in annular frictional pressure loss due to increased measured depth. Eq. 42 describes this.

A reason for the large pressure losses and challenges with the elevated ECD are partly due to the need of the relatively large flow rate in order to clean the 13 5/8" annulus, as described in section 7.9. For all of the wellbore sections for all of the MLT options the cleaning in the annular section of the well dictated the minimum flow rate in order to sufficiently clean the hole. A reduction in the largest minimum flow rate would lead to lower frictional pressure losses in the annulus, and probably partly mitigation of the issues with excessive ECD values in comparison with the fracture gradient.

8.4 Suggestions to improvements

The casing design on Ekofisk is given by the formation, based on pressure regimes and shallow gas zones in the underground. A change in the design for a possible future MLT project was decided to not be economical or beneficial with regards to standardization of rig design to fit the present setup²⁷. A solution, however, that would fit the casing program used today on Ekofisk would be to tie back the 10 ¾" liner, set at TOE, to surface. By doing this the cross-sectional area in the annulus would decrease, leading to lower minimum flow rate for cleaning in the upper sections of the wells. A simulation for scenario 1 parameter values for the MLT1 L1 wellbore with the 10 ¾" liner tied back to surface indicated a reduction in the minimum flow rate to clean the hole from 618.4 gpm, as presented in Figure 54, to 410 gpm, for otherwise identical setup. This is a reduction of around 34 %. However, a tying back of the 10 ¾" liner would lead to increased cost due to increased material and necessary rig time, and might not be economical for the project as a whole.

Another possible action that probably would help mitigate the large ECD values in the openhole sections would be to under ream the holes. By opening the 9 $\frac{1}{2}$ " hole sections to 10" and the 8 $\frac{1}{2}$ " to 9 $\frac{1}{2}$ " the annular velocity in the annulus of these sections would decrease, leading to a lowering of the frictional pressure losses and resulting ECD. This can be seen by the Eq. for annular velocity given in Eq. 33, which for increased ID of the hole will result in lower output values of the velocity. This will again influence the selection of flow regime, and finally reduce the frictional pressure losses, also dependent on the hole diameter, as shown in Eq. 36 – Eq. 39. Compared to the tying back of the 10 $\frac{3}{4}$ " liner the under reaming of the open hole sections would be both faster and less expensive to perform, resulting in overall better project economics.

_

²⁷ Personal communication with T. Husby.. 2013. Stavanger: ConocoPhillips Norway

8.5 Selection of the optimum MLT option based on the drilling process

As mentioned in Chapter 7 the simulations in Wellplan yielded a total of 270 different simulation results. In order to easier be able to compare and evaluate the outputs a total of seven comparsion cases were made, as discussed in chapter 7, shown in Table 12. Spreadsheets were then made to compare the different wellbore sections gathered in each of the comparison cases, as presented in Figure 64 and Figure 65. In these evaluation summary sheets each of the wellbore sections in the same comparison case were compared against each other and evaluated for each of the ten drilling effects (effective tension, torque, fatigue ratio, hook load, torque vs MD, minimum WOB to buckle, hole cleaning, pressure losses, circulating pressures and ECD). In addition were the wellbore geometry, in form of DLS and BUR, compared. The wellbore section that for each of the effects in each of the comparison cases gave least indications of issues was given a green color and 3 points. The wellbore section that gave simulation results with the most signals of challenges was colored red and given 1 point. The wellbore section in between would get a yellow color and 2 points. This would lead to a sum of points for the ten drilling effects given for each of the wellbore sections for a given comparison case. It should be noted that the circulating pressure and ECD were weighted with 0.5 each due to description of the same effect. Added to this sum was the evaluation of DLS and BUR. Since these two parameters are well path dependent, and might lead to inability of the drilling of a wellbore section, the weighting was doubled for these two effects. The best wellbores section (lowest DLS for example) would be given 6 points rather than 3 point due to the importance of control of the DLS. Finally the sum from the ten first drilling effects and the two wellbore geometry parameters were added together to form the total score for each wellbore section for all of the comparison cases, as presented in Figure 64 and Figure 65.

The idea behind the comparison cases and the distribution of points based on number and severance of the issues indicated by the simulation results was to better compare the different wellbore sections for the three MLT options. The comparison cases, by dividing the wellbore sections based on different criteria, made it possible to easier select an optimum MLT option as a whole, as well as a suggestion to wellbore section composition to form a new MLT option. The first were made by comparing each L1, each L2 9.5" and each L2 8.5", and select the MLT options with highest overall score for all of the three wellbore sections making up the MLT configuration. The suggestion of a new MLT configuration were based on the evaluation of the separate wellbore sections, where the L1, L2 9.5" and L2 8.5" with the highest score would be selected to form the new MLT option.

A drawback with an evaluation of the wellbores by using the evaluation sheets in Figure 64 and Figure 65 is the lack of qualitative judgment. Even though certain evaluations of the results were made in order to give the scores, the winning wellbore section would not be guaranteed to be a "good" section. In addition, the issues indicated for different

drilling effects might not be equally severe. By giving an equal weighting to all the parameters, except the DLS, BUR and circulating pressures and ECD, critical problems might come in the shadow of less crucial issues, but still be given the same amount of point. Finally, the best, middle, worst score setting camouflage the true difference between the severity of the issues for the same drilling effect indicated by the simulation results. For instance, for comparison case C, the MLT2 L2 8.5" is for all the drilling effects given the middle score of 2 points. In the end, the sum of point for this wellbore section is 19, versus the 27 for the comparison case C winner MLT1 L2 8.5". By first eyesight the MLT1 L2 8.5" appears to be much better, or yield significantly less issues, than the MLT2 L2 8.5". However, the truth might have been that wellbore MLT2 L2 8.5" indicated exactly the same issues as MLT1 L2 8.5", only with slightly higher degree of severity. A result of this would have been that the difference between the two wellbore sections would have been small, even though the evaluation sheet score would indicate a large difference. With these considerations in mind, the evaluation sheets in Figure 64 and Figure 65 should therefore be used with care and be read with a critical eye. All the simulation results for both scenario 1 and scenario 2 input values, as well as suggested input parameter values, can be found in Appendix Q.

8.4.1 Scenario 1 and Scenario 2 results

The evaluation summary sheet for scenario 1 and 2 for all the wellbores for the three MLT options is presented in Figure 64. For comparison case A, where only the L1's are compared, the simulation results indicated that the highest score would be for the MLT1 L1. The scores (best, middle, worst) were found from the output results presented in chapter 7. For example, the scores for the drilling effect number 3, the fatigue ratio for bit rotation on bottom, were found from Figure 46. Here, and as presented, the worst fatigue ratio as a trend was for the MLT2 L1. Therefore this wellbore section was given a red color and 1 point in Figure 64. For the drilling effects MLT 1 L1 were given the best score, except for the minimum WOB for sinusoidal buckling. In addition, the DLS were the lowest for MLT1 L1, even though the BUR was the highest.

For comparison case B, only evaluation the L1's going to reservoir target in layer EA3 (see Figure 17), again the MLT1 L1 gave the highest score, naturally. By only looking at the L2 8.5" sections the highest score was given to MLT1 L2 8.5in, while for comparison case D, where all the L2 9.5" sections were gathered, the best wellbore section was indicated to be the MLT2 L2 9.5". For case E, giving the best L2 8.5" section going to layer EL, the highest score was given for MLT2 L2 8.5". Considering all the wellbore sections going to layer EA3 (case F), the best to drill would be MLT1 L2 8.5". For comparison case G, gathering all the wells leading to layer EL, the highest score was given to MLT2 L2 8.5". However, the MLT3 L2 8.5" section is only 1 point behind, and in addition that wellbore indicated the least issues with regards to DLS and BUR. The selection of the best wellbore for comparison case G would therefore be difficult to declare based on the number give in Figure 64.

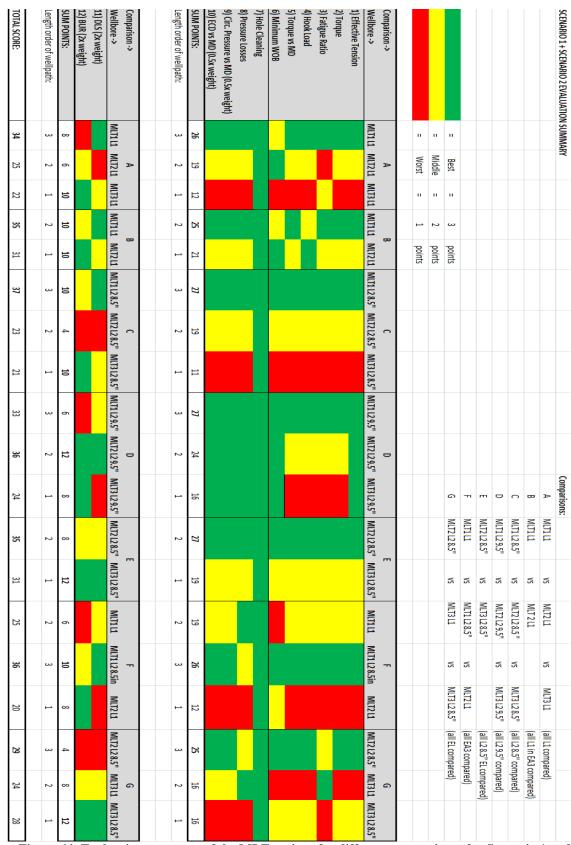


Figure 64: Evaluation summary of the MLT options for different comparisons for Scenario 1 and Scenario 2 input values

It was decided that any conclusions from scenario 1 and scenario 2 parameter input values would be difficult to make alone as both of these sets of values gave various issues for most of the different wellbores. However, the overall MLT option that got most points for scenario 1 and 2 values were MLT1 with 104 point. This value was found by adding the scores for each of the wellbore sections (case A, C and D) in the MLT1. Second came MLT2 with 84 points and last was MLT3 with 67 point. Comparing this conclusion with the issues listed for MLT1, MLT2 and MLT3 for scenario 1 and 2 values in Table 13 and Table 14 it can be seen that MLT indicated fewer overall issues than MLT2 and MLT3, supporting the conclusion made. For a new optimum composition of single wellbore section to create a new MLT option the conclusion, by use of scenario 1 and 2 comparisons, L1 from MLT1, L2 9.5" from MLT2 and L2 8.5" from MLT1, based on comparison cases A, C and D winners.

8.4.2 Suggested parameter values results

For the suggested parameter values the evaluations of the different wellbore sections for each of the MLT options can be seen in Figure 65. The method of giving points was made in the same manner as for scenario 1 and 2 in Figure 64. Here, the highest score for comparison case A, all L1's compared was for MLT1 L1. For comparison case B, naturally, the winner was the same. The optimum L2 8.5" section was found to be MLT1 L2 8.5", while the highest score for the L2 9.5" sections (case D) was for MLT2 L2 9.5". For comparison case E, all L2 8.5" sections going to layer EL, the highest score was given to MLT2 L2 8.5". By considering all wellbores leading to EA3, the evaluation yielded MLT1 L2 8.5" as the optimum wellbore. Finally, for comparison case G, just considering all the wellbores going to layer EL, the best to drill would be the MLT3 L2 8.5". However, for both MLT2 L2 8.5" and MLT3 L2 8.5" sections, as discussed in section 8.2 and showed in Table 15, both of these two wellbore section indicated issues with the ECD leading to underbalance just below the last casing shoe. Therefore, none of these wellbores would be recommended to drill, even with the suggested parameter values. For comparison case G the recommended wellbore would therefore be MLT3 L1.

A summary of the conclusions that could be drawn from the evaluation of the results for the suggested parameter values was as listed below:

- The optimum overall MLT option would be MLT1. By adding the scores from comparison case A, C and D, this option gave a total score of 98 points, versus 83 for MLT2 and 70 for MLT3.
- A new optimum MLT option based on a composition of the wellbore sections with the highest scores in comparison case A, C and D, would be L1 from MLT1, L2 9.5" section from MLT2 and L2 8.5" section from MLT1.

- For a stacked horizontal multilateral configuration (one target in layer EA3 and one in layer EL) the optimum solution would be L1 from MLT3 (going to EA3) and MLT1 L2 8.5" (going to EL). The optimum L2 9.5" section would be the winner from comparison case D, the MLT2 L2 9.5" section.
- The longer the wellbore, the larger the issues. A trend was that the shortest
 wellbore for each of the comparison cases would yield the highest score.
 Compared to reality this is often the case, even though the results also depend
 on a range of other factors.

These two first conclusions were in correlation with the results from the evaluation of scenario 1 and scenario 2 parameter input values. The latter, however, would for the scenario 1 and 2 evaluation yield MLT2 L2 8.5" as the best section to drill to the target in the EL layer.

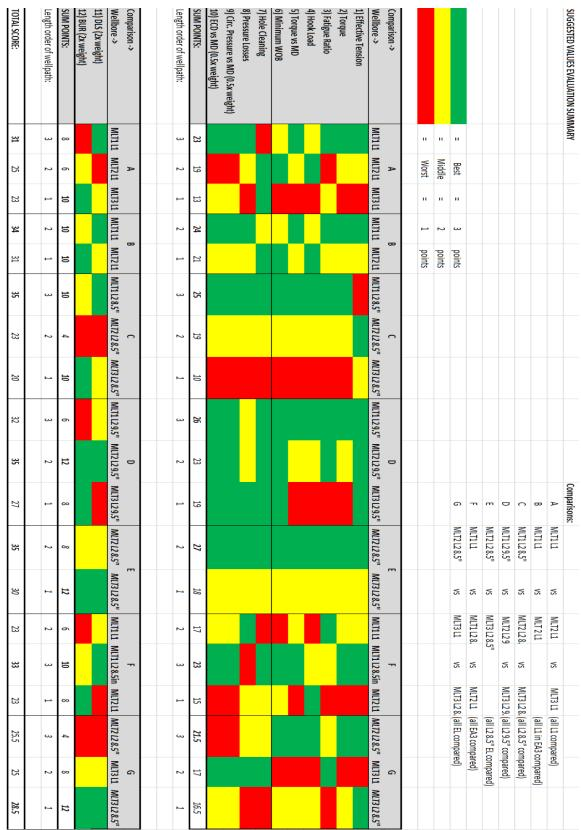


Figure 65: Evaluation summary of the MLT options for different comparisons for suggested parameter input

9 Self-Assessment

9.1 Applicability of the work

9.1.1 Application of the simulation

The performed simulations have applicability in order of providing a picture of expected issues and challenges for a possible future drilling of the wellbores in the three MLT options. Any signs of problems can be dealt with before they even occur. Further, the simulation results give paths of directions on whether any of the MLT options for this report should be followed or rejected. Finally, the output from the Wellplan simulation can give indications on where to perform changes in the project scope and setup, for instance with regards to the well planning, based on issues and challenges indicated.

9.1.2 Practical applicability

As mentioned in the introduction the drilling of multilateral wells has again been listed as a possible future strategy for COPNO due to reservoir and production related matters, as well as improved slot space utilization. Through the work with this report several people and groups within COPNO have been put to work in order to make contributions and perform studies on topics important for multilateral well implementation on Ekofisk. In addition, continuous interaction with the service company Halliburton were made in order to evaluate and determine possible junction design options to be used in a future, possible MLT project on Ekofisk. By the deadline of this report the cooperation with regards to the details around a possible, future MLT project on Ekofisk is still ongoing between COPNO and Halliburton, a collaboration that was initiated based on the work with this report. In other words, the work with this report has been of practical applicability to COPNO in order to get ideas and thoughts on paper around a possible future strategy out in reality in form of involvement of both COPNO employees and contractors. In addition the work with this report has led to interaction between different internal organizations within COPNO to come up with more united goals and directions for a future, possible project revolving multilateral wells on Ekofisk.

9.2 Quality and shortcomings

9.2.1 Assumptions used in the simulations

The assumptions taken in the simulations performed prior to the creation of this report are listed in section 6.2. As mentioned, these were qualitatively determined in order to make the simulation process as realistic as possible. However, for software simulations there will always be various sources of errors compared to reality, based on both assumptions and calculating models utilized in the program.

From the reservoir group in COPNO six different targets were given. For the task given for this report it was assumed that the targets would give the same reservoir performance and production rates. This was done is order to more easily being able to compare and evaluate the drillability of the nine different wellbores in the three MLT options. In reality the comparison of different well paths, with different geometry and length, will be difficult, as there is no simulation base to compare with. Also, the selection of the MLT option would for a real case be made based mostly on economics, in form of net present value calculations for the project as a whole, meaning that wellbore reservoir exposure and expected production rates probably would be given a higher importance. The drilling process, with optimum MLT option based on the highest possibility of success rate, would be built into this selection, but only to consider the drilling operation, with constraints and limitations as given in this report, is a simplification.

The simulation results presented in this report is dependent further on a range of assumed values. A change in the assumptions would change the results, based on degree of dependence. The most significant changes would probably be for the ECD effects, evaluated with respect to the pore pressure and fracture gradient from the nearby wellbores 2/4-Z-17 and 2/4-VB-05. These are not the actual PP and FG lines for the underground area for the three investigated MLT options, and the conclusions from the evaluations on issues for drilling, as presented in Table 13, Table 14 and Table 15, as well as Figure 64 and Figure 65, might change for changed values of pore pressure and fracture gradients.

To assume the same BHA for 9 $\frac{1}{2}$ " and 8 $\frac{1}{2}$ " sections, only with different bit sizes, was a simplification. The ECD, as given by frictional pressure loss in the annulus, is dependent of the annular cross-sectional area. The OD of the components in the BHA for the two hole sized would be somewhat different, resulting in different values for parameters dependent on cross-sectional area in the annulus. Dependent on hole section length this assumption might yield more or less significant errors to the calculations.

The assumed friction factors of 0.18 for both open and cased hole sections might be a source of error. Simulations were performed for increased friction factors, 0.3 for open

hole and 0.25 for cased hole (Wellplan default values), and most of the wellbore sections that indicated no buckling conditions or yield failures for the 0.18 value now showed issues. It should be pointed out that the correct friction factors are hard to determine, and that to assume a constant value for a section in the well in most cases is a simplification (Samuel 2010). The value of 0.18 used in the simulations performed in this report was based on previous reverse-calculations performed on Ekofisk by Midtgarden (2010).

Finally, for the hydraulic simulations performed in Wellplan no tool joint pressure losses were included. Dependent on hole size in comparison with OD of the TJ and cuttings diameter the expulsion of TJ losses might or might not give significant sources of errors. For the 8 ½" sections test-simulations were performed, where the outer diameter of the tool joints were set to 8.25". For cuttings diameter of 0.125" the increase in ECD due to frictional pressure losses in the annulus were quite significant. For simplification means the TJ effect was neglected for the simulations performed in this report.

9.2.2 Simulations performed

In Wellplan only simulations by use of the Torque and Drag, and Hydraulics, module were performed. A more complete analysis should probably have been done, also using the other built-in modules in the software, in order to get a more complete picture of the issues and challenges related to the drilling of the wellbore sections for the three MLT options investigated.

9.2.3 Input parameters in the Wellplan software

For the initial simulations with scenario 1 and scenario 2; to only consider two sets of parameter values, one with all lower limit values and one with all higher values, was a simplification. In reality there would be 16 different combinations for a setup with four adjustable parameters (WOB, RPM, ROP and flow rate) and two different values for each parameter. However, to investigate 16 different scenarios for nine different wellbore sections on ten different drilling effects would result in 1440 separate simulation outputs only for scenario 1 and 2, which would have resulted in an extensive amount of graphs and data to analyze. It was therefore, for this report, decided to check only two scenarios, one with only lower limit values and one with only higher limit values.

In addition it would probably not have been necessary to perform simulations on both parameter sets (scenario 1 and scenario 2). The results indicated the same trends for both scenarios, yielding that the conclusions and evaluations would have been more or less the same if the simulations had been done only for one set of parameter values initially. At the same time the two-set simulation verified that trends, and the scenario 2 values backed up the results from the initial simulations with scenario 1 input parameter values.

9.2.4 Iterations in Wellplan to find the suggested input drilling parameter values

The iterations in Wellplan were performed by using the Torque and Drag, and Hydraulics, modules only. If the other modules, presented in Appendix N, had been utilized as well, a better picture of the value for the suggested parameters could probably have been established. The decision of only using the two modules mentioned was therefore a simplification. In addition it should be noted that the suggested values only are what they are, namely suggested, and that other input values also might work. The result might be different for slightly other sets of parameter values.

For the iterations to find the suggested input parameter values the bit nozzle size were changed for all wellbores in order to reduce the surface pressure. The bit nozzle size selection was based experiences from well 2/4-Z-17, and on the constraint of max surface pressure of 5000 psi. According to Bourgoyne et al. (1986c) the jet nozzle selection can be optimized in a lot of ways, one being to select nozzle size so the SPP gets equal to max surface pressure (5000 psi for Mærsk Gallant). For this thesis more or less two different settings were used, either 3x12 or 3x18, dependent on what would give SPP less than, but closest to, maximum surface. So the bit nozzle size was optimized to a certain point, but could, as a further work, be optimized more.

9.2.5 Investigated drilling effects

The twelve investigated effects for drilling, as presented in chapter 7, were selected mainly due to the possibility of simulating these in Wellplan. By use of different software the selected parameters could have changed to include more, or less, effects than investigated in this report. In addition, not all of the effects in reality probably will have equally high importance for the drilling process.

9.2.6 Using of the Wellplan software for simulation of multilateral wells

For the simulations performed in this report in order to come up with the results presented in chapter 7 and to perform the evaluation in this chapter, the Wellplan software was used. Over the last years, as described by Nesland (2012) the industry has been introduced to a lot of powerful drilling simulation software, including the Wellplan suite. These programs can be very useful in detecting problems with the well design and/or the planned drilling of a well before they even occur.

A challenge with using Wellplan as a tool for simulation of multilateral wells was the lack of possibility to get rate of penetration as an output. Backwards simulation, where a desired output of ROP was set, therefore was performed. By doing this, the required input values to reach this penetration rate could be determined, a method that seemed a bit unrealistic at the time of simulations. Another issue was the challenge with regards to tying on the side branch, or lateral 2. The last casing shoe for the 9.5" section in L2 would be the pre-drilled hole in the 10 ¾" liner at 18150 ft MD. However, an actual

casing shoe would not be set at this depth. In Wellplan, however, the only method of displaying the lateral 2 was to add a casing shoe at depth of 18150 ft MD. On the other hand, by knowing that this shoe in fact would be the window in the 10 \(\frac{3}{4}'' \) liner, the software didn't cause any issues with regards to the simulations other than graphical. Also, since the Wellplan software is not created to perform simulations on MLT configurations the whole multilateral has to be created in three separate cases in the software; one for the mother wellbore, one for lateral 1 and one for lateral 2. There is no build-in function that enables the user to create a MLT setup in the very same case. This is really not an issue, but causes some challenges with regards to overview and comparison of the different wellbore sections for the MLT option. Finally the Wellplan lacks the possibility of comparing different wellbore sections from different wells in the same graphs for the same drilling effects (effective tension, torque etc.). The only method of comparing two, or more, representative wellbore sections, as for instance MLT1 L1, MLT2 L1 and MLT3 L1, is to manually copy the numbers behind the graphs in Wellplan over to Excel, or similar mathematical software. This is time-consuming and it is easy to lose track of data. In addition, the complexity of the program and the range of different modules also made it challenging to exploit all the functions with the limited training, and technical support, that was provided.

In order for Wellplan to be more convenient to use for simulations of MLT configurations a function, making it able to compare similar wellbore sections, for different wells should be implemented. In addition an own MLT module should be created, making it possible to evaluate different junction designs and to create hole sections and setup specifically for multilateral wells. With that said, from the work performed in Wellplan during the preparations to this report it was concluded that the use of Wellplan was useful for detecting of problems for the planned drilling operations, and to investigate the possible MLT options in order to come up with an optimum option based on evaluations.

9.2.7 Applied Well paths

As mentioned previously in this chapter challenges with the circulating pressures and ECD effects were experienced for the simulations performed. For long horizontal, or high-inclination, wells the ECD will increase for increased measured depth due to increased annular frictional pressure losses, see Eq. 42 and section 5.2. For the same wells the TVD will remain more or less constant, resulting in the same values for pore pressure and fracture gradient. For long horizontal sections issues with regards to fracturing might occur to the elevated ECD effect. This was probably the issue for the wellbore sections investigated in this report. Compared to other well drilled in the area in Ekofisk the wellbores for the three MLT options are quite long (Maxwell 2013), ranging between 23950 ft MD and 32942 ft MD. Normally, as the length of a well increases, the issues and challenges increases accordingly²⁸.

-

²⁸ Personal communication with T. Husby. 2013. Stavanger: ConocoPhillips Norway

In addition to the length of the wellbores the DLS levels of all the wellbore sections probably will represent challenges. As mentioned earlier the maximum dog leg severity is often considered to be around 3.0 degrees per 100 ft, even though larger values sometimes can be applied due to the use of special equipment and new technology. The DLS for the wellbores applied in this report ranges from around 4 to 6.42 degrees per 100 ft, values that normally are considered too high. Even though well planning on Ekofisk is a challenge due to issues mentioned in section 5.11, as well as a lot of already existing wells, the well paths for the three MLT options for the simulations in this report, both with regards to length and geometry in form of DLS, probably should be optimized further in order to reduce the total length.

9.2.8 Comparison of the MLT options based on the point system in the evaluation

As mentioned in section 8.4, to determine which wellbore is good and which is not based on point system might yield some errors. The points were given based on qualitative analysis, but by giving a set amount of points for best, middle and worst, there can be some errors that are might not that big if only compared qualitatively, without giving points. In addition, by giving equal weighting to all the parameters, except the DLS, BUR and circulating pressures and ECD, critical problems might come in the shadow of less crucial issues, but still be given the same amount of points. With these considerations in mind, the evaluation sheets in Figure 64 and Figure 65 should therefore be used with care and be read with a critical eye.

9.2.9 The work process

A lot of the early work with this report was done in cooperation with employees in both COPNO and Halliburton. In a hectic industry it was often challenging to be able to gather the necessary resources in order to discuss important factors and topics for this report. Therefore, in order to keep a continuously flow of the work process, shortcuts and assumptions sometimes had to be taken, leading to more or less significant sources of errors.

9.2.10 Simulations of junction design option 1 (FlexRite Level 5)

As mentioned in chapter 4.4 the decision was made to only investigate junction option 2, with IWS. Ideally the simulations performed in Wellplan, that was for this junction design, should have been done also on junction design option 2, and should be included as further work.

9.3 Possible future improvements and further work

9.3.1 Future improvements

There are several future, possible improvements for the work performed in this report. First of all the list of assumptions in section 6.2 could be shortened. The maybe most important there is to obtain the actual underground information, including pore pressure and fracture gradient, in order to perform more accurate simulations and evaluations on hydraulic effects.

In addition, the different Wellplan modules can be utilized better in order to include more factors and effects to the investigations and evaluations. The optimization process for the suggested values, including bit nozzles and BHA design, can also be improved in the future. Finally, an optimization of the well paths is needed in order to create more realistic wellbore sections for the MLT options.

9.3.3 Further Work

In addition to the future improvements mentioned in the previous sub-chapter future work include simulations on the wellbores for the different MLT options also with junctino design option 1 (FlexRite Level 5). This design will give slightly different hole sizes compared to junction design option 1 for the wellbore sections in lateral 2, as presented in Figure 19, including 8 $\frac{1}{2}$ " from junction to TOE and 6 $\frac{1}{2}$ " in the reservoir. A comparison between the two junction design options with regards to simulation results should be done.

The completion, stimulation and intervention requirements for a MLT option on Ekofisk should be investigated. This should be put in light of what junction design option that could be selected, and how that would influence the requirements.

Based on the issues presented in chapter 8 with regards to circulating pressures and elevated ECD effects, future simulations should include both the effect of tying back the 10 $\frac{3}{4}$ " liner to surface and of under reaming the 9 $\frac{1}{2}$ " sections to 10" and the 8 $\frac{1}{2}$ " sections to 9 $\frac{1}{2}$ ".

Finally, further work could include an economic analysis on the net present value, and discuss the feasibility of different MLT options, as well as the one recommended in this report, based on the drilling process, as well as reservoir performance, production rates, investment cost, project organization and management and other factors.

10 Conclusions

Based on the work preparing this report, as well as from the progress of making it, some major conclusions were established. These describe, in majority, the simulation results from Wellplan and the following evaluations, in addition to the achievements obtained through the work process, as well as recommendations to future improvement and suggestions to further work in the field.

- The recommended type of multilateral based on the reservoir targets given would be a planar dual-lateral, or forked, multilateral, as shown in Figure 70. A setup with a horizontal, stacked multilateral indicated a smaller possibility of future success with regards to the drilling process, given the well path design and configurations used in this report.
- Based on the non-pressure tight junction design the junction placement should be in a stable formation in the overburden, 200 – 300 ft above TOE. In cooperation with the overburden group in COPNO the junction depth was determined to be 9958 ft TVD.
- Based on simulation results from the Wellplan software the optimum multilateral well configuration based on the given six reservoir targets was indicated to be MLT1. This option yielded the least amount of issues during drilling. In addition, based on the shorter well path for both lateral 1 and lateral 2, this MLT option would probably lead to lower cost and faster drilling of the well compared to MLT2 and MLT3.
- A recommended composition of separate wellbores to form a new MLT option would include lateral 1 from MLT1, the 9 ½" lateral 2 section from MLT2 and the 8 ½" lateral 2 section from MLT1. These wellbore sections indicated fewer challenges with regards to the drilling process than the comparable sections for the same hole sections.
- The longer the wellbore, the larger the issues. A trend for the results from the simulations was that the shorter wellbores indicated fewer issues, with smaller significance, compared to the longer ones. This conclusion point was expected based on analysis of data from previous, actual drilling operations.
- For all the MLT options challenges with regards to large annular circulating
 pressures and ECD effects were encountered. The well designs and well path
 lengths, for all of the three MLT options, put together with casing setting depths
 and sizes to give minimum flow rate for hole cleaning, induced large
 requirements of pump rate, leading to issues with elevated ECD and challenges
 with regards to fracturing of the formation. In addition the DLS for all the

wellbore sections was higher than the 3.0 degrees per 100 ft that normally is considered the maximum allowed. Optimization of the well paths for the wellbore sections leading to the reservoir targets for the MLT options should be performed in order to mitigate any challenges with regards to elevated ECD effects and DLS.

- Together with Halliburton a possible junction design option was created to perform simulations on, involving a non-pressure tight junction (TAML Level 4) and IWS in the mainbore/lateral 1.
- For the selection of a stacked, horizontal multilateral configuration (one target in layer EA3 and one in layer EL), the optimum wellbore sections to drill, based on the results from the Wellplan simulations, would be L1 from MLT3 (going to EA3) and MLT1 L2 8.5" (going to EL). The optimum L2 9.5" section would be the MLT2 L2 9.5" section.
- The Wellplan software can be utilized to simulate the drilling process of a multilateral well configuration. However, certain challenges were encountered, leading to a recommendation of certain future improvements and implementation to the software. These can be summarized as the adding of a function that makes it possible to compare similar wellbore sections, implementation of an own MLT module for junction design evaluations and the transformation of ROP as an input parameter to an output parameter value.
- The work with this report has led to increased involvement and initiation around a possible, future project including multilateral well technology in the Ekofisk field.
- Future improvements includes the implementation of actual underground data to the simulation base, optimization of the created well paths and BHA design, as well as utilization of the different Wellplan modules in order to perform a better evaluation of the simulation results.
- Suggestions to further work involve the simulations on the junction design option 1 for the three MLT options. In addition, the effects of under reaming the 9 ½" sections to 10" and the 8 ½" to 9 ½" could be investigated. Mapping of the completion, stimulation and intervention requirements for a future multilateral well options should be performed, and a final economic analysis could be executed in order to find the finances revolving the drilling process for a MLT option, with regards to reservoir performance, production rates and junction design.

Nomenclature

Roman

Symbo	ol	Unit, Field (SI)
m	Mass	[M], $lbf(kg)$
n	Revolutions of pipe	$\left[T^{-1} ight], rpmig(-ig)$
q	Flow rate	$[L^3/T]$, $gpm(lpm)$
r	Radius	[L], ft(m)
\boldsymbol{A}	Area	$[L^2]$, $in^2(m^2)$
A_{i}	Cross-sectional area inside pipe	$[L^2]$, $in^2(m^2)$
A_{o}	Cross-sectional area in annulus	$[L^2]$, $in^2(m^2)$
A_{t}	Flow area across bit nozzles	$[L^2]$, $in^2(m^2)$
C_d	Discharge coefficient	-
\boldsymbol{F}	Lateral force on TJ	$[ML/T^2]$, $lbf(N)$
F_{N}	Normal force	$[ML/T^2]$, $lbf(N)$
F_{s}	Stability force	$[ML/T^2]$, $lbf(N)$
F_{x}	Force in x-direction	$[ML/T^2]$, $lbf(N)$
F_{y}	Force in y-direction	$[ML/T^2]$, $lbf(N)$
L	Length	[L], ft(m)
$L_{\it half}$	Half-length between TJ's	[L], ft(m)
N	Normal force	$[ML/T^2]$, $lbf(N)$
$N_{ m Re}$	Reynolds number	-
P_f	Frictional pressures losses	$[M/LT^2]$, $psi(Pa)$
P_{i}	Pressure inside pipe	$[M/LT^2]$, $psi(Pa)$
$P_{_{O}}$	Pressure outside pipe	$[M/LT^2]$, $psi(Pa)$
S_a	Axial stress	$[M/LT^2]$, $psi(Pa)$
S_r	Radial stress	$[M/LT^2]$, $psi(Pa)$
S_{t}	Tangential stress	$[M/LT^2]$, $psi(Pa)$
T	Tensile strength	$[ML/T^2]$, $lbf(N)$
$T_{\it eff}$	Effective tension in the pipe	$[ML/T^2]$, $lbf(N)$

T_{real}	Real tension in th pipe	$[ML/T^2]$, $lbf(N)$
T_{t}	Tangential shear stress	$[M/LT^2]$, $psi(Pa)$
T_r	Radial shear stress	$[M/LT^2]$, $psi(Pa)$
T_z	Axial shear stress	$[M/LT^2]$, $psi(Pa)$
V	von-Mises equivalent stress	$[M/LT^2]$, $psi(Pa)$
V_{DP}	Drillpipe velocity	[L/T], ft/hr (m/s)
V_{res}	Resultant velocity	[L/T], ft/hr (m/s)
V_{x}	Velocity x-direction	[L/T], ft/hr (m/s)
V_y	Velocity y-direction	[L/T], ft/hr (m/s)

Greek

Symbol		Unit, Field (SI)	
α	Inclination	[deg], deg (rad)	
β	Azimuth	[deg], deg (rad)	
μ	Friction factor	-	
μ_p	Plastic viscosity	[M/TL], cp(Pa*s)	
φ	Dog-leg angle	[deg], deg (rad)	
ρ	Density	$[M/L^3], ppg(kg/m^3)$	
σ	Tension	$[\mathit{ML}/\mathit{T}^2]$, $lbf(N)$	
ϕ	Azimuth	[deg], deg (rad)	
$ au_y$	Yield point	$[M/L^2]$, lbf /100 ft ² (Pa)	
θ	Inclination	[deg], deg (rad)	

Abbreviations

CT	=	Coiled Tubing
ID	=	Inner Diameter
KM	=	Kick Margin
ML	=	Multi Lateral
OD	=	Outer Diameter
PL	=	Production License
SF	=	Safety Factor
TJ	=	Tool Joint
TM	=	Trip Margin

YP = Yield Point BBL = Barrel

BHP = Bottom Hole Pressure
BLF = Buckling Limit Factor

BUR = Build Up Rate

CTD = Coiled Tubing Drilling
DLS = Dog Leg Severity

EOR = Enhanced Oil Recovery

KWM = Kill Weight Mud

LWD = Logging While Drilling
MLT = MultiLateral Technology
MPD = Managed Pressure Drilling
NCS = Norwegian Continental Shelf

NGL = Natural Gas Liquids

NPB = Neutral Point of Buckling P&A = Plugging & Abandonment

RIH = Running In Hole ROP = Rate Of Penetration

RSS = Rotary Steerable drilling Systems

R&D = Research & Development

SCF = Standard Cubic Feet
SPP = Stand Pipe Pressure
TFA = Total Flow Area
TOE = Top of Ekofisk

UBD = Underbalanced Drilling

BSMF = Bending Stress Magnification Factor

IADC = International Association of Drilling Contractors

OPEX = Operational Expenditures

POOH = Pull Out Of Hole

TAML = Technical Advancements of Multi Laterals

CAPEX = Capital Expenditures
COPNO = ConocoPhillips Norway

List of references

- About Geology. 2013. Lamination, California, http://geology.about.com/od/geoprocesses/ig/sedstrucs/lamination.htm (accessed 16 April 2013)
- American Manifacturing. 2013. EMSCO FC-2200, http://www.american manufacturing.com/files/parts-books/emsco-fc-2200-pump-parts.pdf (downloaded 12 May 2013)
- Austad, T., Strand, S. and Madland, M.V et al. 2008. Seawater in Chalk: An EOR and Compaction Fluid. SPE 118431 Res Eval & Eng 11 (4): 648-654. SPE-118431-PA. http://dx.doi.org/10.2118/118431-PA
- Bosworth, S., Ismail, G. and Ohmer, H., et al. 1998. Key Issues in Multilateral Technology, http://www.slb.com/~/media/Files/resources/oilfield_review/ors98/win98/key. pdf (downloaded 20 April 2013).
- Bourgoyne, A.T., Chenevert, M.E., and Millheim, K.K et al. 1986a. *Applied Drilling Engineering*, Vol. 2, 125. Richardson, Texas: Textbook Series, SPE.
- Bourgoyne, A.T., Chenevert, M.E., and Millheim, K.K et al. 1986b. *Applied Drilling Engineering*, Vol. 2, 12 18. Richardson, Texas: Textbook Series, SPE.
- Bourgoyne, A.T., Chenevert, M.E., and Millheim, K.K et al. 1986c. *Applied Drilling Engineering*, Vol. 2, 113 183. Richardson, Texas: Textbook Series, SPE.
- Bourgoyne, A.T., Chenevert, M.E., and Millheim, K.K et al. 1986d. *Applied Drilling Engineering*, Vol. 2, 156 162. Richardson, Texas: Textbook Series, SPE.
- Bourgoyne, A.T., Chenevert, M.E., and Millheim, K.K et al. 1986e. *Applied Drilling Engineering*, Vol. 2, 330. Richardson, Texas: Textbook Series, SPE.
- Celli, A. and Fipke, S. 2007. Unparalleled Success with Multilateral Wells: Venezuela Heavy Oil Producer Uses 100 Level 4 Junctions in the Orinoco Belt. Paper SPE/IADC 104500 presented at the 2007 SPE/IADC Drilling Conference, Amsterdam, The Netherlands, 20-22 February 2007. http://dx.doi.org/10.2118/104500.
- Compass. 2013a. Suite Well Operations Software. Version (EDM 5000.1.10.0 (09.04.07.107) Build 5000.1.10.0.1934). Dubai, UAE: Halliburton Landmark.

- Compass. 2013b. Suite Well Operations Software. Version (EDM 5000.1.10.0 (09.04.07.107) Build 5000.1.10.0.1934) User Guide. Dubai, UAE: Halliburton Landmark.
- ConocoPhillips. 2011. Ekofisk Reservoir Management plan, internal document prepared by Norway Subsurface Organization
- ConocoPhillips. 2013a. Company History, http://www.conocophillips.com/EN/ABOUT/WHO_WE_ARE/HISTORY/Pages/ind ex.aspx (Accessed 10 March 2013)
- ConocoPhillips. 2013b. Phillips Company History, http://www.conocophillips.com/EN/about/who_we_are/history/phillips/Pages/index.aspx (Accessed 10 March 2013)
- ConocoPhillips. 2013c. Worldwide Operations, http://www.conocophillips.com/EN/about/worldwide_ops/Pages/index.aspx (Accessed 10 March 2013)
- ConocoPhillips. 2013d. Norway, http://www.conocophillips.com/EN/about/worldwide_ops/europe/Pages/Norway.aspx (Accessed 11 March 2013)
- ConocoPhillips. 2013e. Ekofisk, http://www.conocophillips.no/EN/Norwegian%20shelf/Ekofisk/EkoEko/Pages/in dex.aspx (Accessed 11 March 2013)
- ConocoPhillips. 2013f. Ekofisk 40 years of history and preparing for 40 more, internal document prepared by Sindre Sørensen
- ConocoPhillips. 2013g. Ekofisk South Plan for Development and Operation, internal document prepared by Sindre Sørensen
- ConocoPhillips. 2013h. Displays for 2/4-Z-26 MLT Junction, internal document prepared by Helen Haneferd
- Colombia University. 2008. An Introduction to Logging While Drilling, http://www.ldeo.columbia.edu/res/div/mgg/lodos/Education/Logging/slides/LW D_Feb_15_2008.pdf (downloaded 10 April 2013).
- Crouse, P.C. 1996. Application and Need for Advanced Multilateral Technologies and Strategies, http://www.netl.doe.gov/kmd/cds/disk28/NG2-5.PDF (downloaded 18 April 2013).

- Dellu, G., Baleanu, I., and Vasillu, G. et al. 1996. Case History of a Low Permeability Creacous Offshore Reservoir Developed Using Horizontal Wells-Lebada East, Romania. Paper SPE 37134 presented at the International Conference on Horizontal Well Technology, Calgary, Alberta, Canada, 18-20 November 1996. http://dx.doi.org/10.2118/37134-MS.
- Dockwise. 2011. Q1 2011 Results Presentation,
 http://www.google.no/url?sa=t&rct=j&q=&esrc=s&source=web&cd=1&cad=rja&ved=0CB4QFjAA&url=http%3A%2F%2Fphx.corporate-ir.net%2FExternal.File%3Fitem%3DUGFyZW50SUQ9OTM2MDd8Q2hpbGRJRD0tMXxUeXBIPTM%3D%26t%3D1&ei=3kKiULz8FtCM4gSn8ICgDA&usg=AFQjCNEym0kPzDzVxHCRZDHInWsB562WEg (downloaded 13 November 2012).
- Drilling Formulas. 2013. Trip Margin Calculation, http://www.drillingformulas.com/trip margincalculation/ (accessed 25 May 2012)
- Economides, M.J., Hill, A.D. and Zhu, D. 2008. *Multilateral Wells*, Richardson, Texas: Textbook Series, SPE.
- ECU. 2006. Drilling Rigs, http://www.scribd.com/doc/29792554/128/Top-Drive VARCO (page 159) (downloaded 03 May 2013)
- E&P Magazine. 2009. Multilateral Wells Come From Russia, With Love, http://www.epmag.com/Production-Drilling/Multilateral-wells-from-Russia-love_44536 (accessed 23 January 2013).
- E&P Magazine. 2007. Multilateral Technology Then and Now, http://www.epmag.com/EP-Magazine/archive/Multilateral-technology-and-now_586 (accessed 10 April 2013).
- Frailja, J., Ohmer, H. and Pulick, T. et al. 2002. New Aspects of Multilateral Well Construction, http://www.slb.com/~/media/Files/resources/oilfield_review/ors02/aut02/p52 69.pdf (downloaded 09 April 2013).
- Gazaniol, D. 1987. Field Data Analysis of Weight and Torque Transmission to the Drill Bit. Paper OTC 5510, presented at the 19th Annual OTC, 27 30 April 1987, Houston, Texas, USA. http://dx.doi.org/10.4043/5510-MS
- Hummus, O., Janwadkar, S. and Powers, J. et al. 2011. Evolution of High Build-Rate RSS Changes the Approach to Unconventional Oil and Gas Drilling. Paper SPE 147455 presented at the SPE Annual Technical Conference and Exhibition, 30 October 2 November 2011, Denver, Colorado, USA. http://dx.doi.org/10.2118/147455-MS

- Hyne, N.J. 1991. *Dictionary of Petroleum Exploration, Drilling and Production*, volume one. Tulsa, Oklahoma, USA. PennWell Publishing Company.
- Inglis, T. 1987. *Directional Drilling*, volume two. Norwell, Massachusetts, USA. Graham & Trotman Inc, Kluwer Academic Publishers Group.
- Johancsik, C.A., Frisen, D.B. and Dawson, R. 1984. Torque and Drag in Directional Wells Prediction and Measurement. Paper SPE 11380 presented at the IADC/SPE Drilling Conference, 20 23 February 1984, New Orleans, Louisiana, USA. http://dx.doi.org/10.2118/11380-MS
- Lawrence, B., Zimmermann, M. and Cuthbert, A. et al. 2010. Multilateral Wells Reduce CAPEX of Offshore, Subsea Development in Australia's Northwest Shelf. Paper SPE/IADC 128314 presented at the 2010 IADC/SPE Drilling Conference and Exhibition, New Orleans, Louisiana, USA, 2-4 February 2010. http://dx.doi.org/10.2118/128314.
- Madla, E. and Haci, M. 2004. Understanding Torque: The Key to Slide-Drilling Directional Wells. Paper IADC/SPE presented at the IADC/SPE Drilling Conference, 2-4 March 2004, Dallas, Texas, USA. http://dx.doi.org/10.2118/87162-MS
- Maxwell. 2013. ConocoPhillips internal database.
- Mohebati, M.H., Maini, T.G. and Harding, T.G. 2010. Optimization of Hydrocarbon Additives with Steam in SAGD for Three Major Canadian Oil Sands Deposits. Paper CSUG/SPE 138151 presented at the Canadian Unconventional Resources & International Petroleum Conference, Calgary, Alberta, Canada, 19-21 October 2010. http://dx.doi.org/10.2118/138151-MS.
- Midtgarden, K. 2010. Advancement of casing- and liner drilling in the Ekofisk field. MS thesis, University of Stavanger, Stavanger, Norway (June 2010).
- Ministry of Petroleum and Energy. 2013. Norway's Oil History in 5 Minutes, http://www.regjeringen.no/en/dep/oed/Subject/Oil-and-Gas/norways-oil-history-in-5-minutes.html?id=440538 (Accessed 11 March 2013)
- Mærsk. 2013. Mærsk Gallant, http://www.maerskdrilling.com/documents/pdf/drillingrigs/specificrigs/maersk-gallant.pdf (downloaded 12 May 2013)
- Nesland, B. 2012. Drilling Parameter Optimization. Project report submitted in the course TPG4520 Drilling Engineering, The Norwegian University of Science and Technology, Trondheim, Norway (December 2012).

- Norwegian Oil and Gas Association. 2013. Norway's Petroleum History, http://www.norskoljeoggass.no/en/Facts/Petroleum-history/ (Accessed 11 March 2013)
- NPD. 2010. Ekofisk, http://www.npd.no/en/Publications/Facts/Facts-2010/Chapter-11/Ekofisk/ (accessed 18 April 2013).
- NPD. 2013a. Tjalve fact pages, http://factpages.npd.no/ReportServer?/FactPages/PageView/discovery&rs:Comm and=Render&rc:Toolbar=false&rc:Parameters=f&NpdId=44066&IpAddress=138 .32.168.34&CultureCode=en (accessed 24 April 2013).
- NPD. 2013b. Tommeliten fact pages, http://factpages.npd.no/ReportServer?/FactPages/PageView/discovery&rs:Comm and=Render&rc:Toolbar=false&rc:Parameters=f&NpdId=43850&IpAddress=138 .32.168.34&CultureCode=en (accessed 24 April 2013).
- NPD. 2013c. Valhall fact pages, http://www.npd.no/en/Publications/Facts/Facts 2012/Chapter-10/Valhall/ (accessed 24 April 2013).
- NY Times. 1987. Jack-Up Project Saves Sinking North Sea Rigs, http://www.nytimes.com/1987/08/19/business/jack-up-project-saves-sinking-north-sea-rigs.html (accessed 25 April 2013).
- Oil Region Alliance. 2013. Oil History Timeline, http://www.oilregion.org/oil-region national-heritage-area/oil-history-timeline/ (accessed 15 April 2013)
- Patricksson, Ø.S. 2012. Semi-Submersible Platform Design to Meet the Uncertainty in Future Operating Scenarios. MS thesis, The Norwegian University of Science and Technology, Trondheim, Norway (June 2012).
- Rigzone. 2012. Offshore Rig Day Rates, http://www.rigzone.com/data/dayrates/ (accessed 12 November 2012)
- Rødland, A. 2012. Borehole Navigation. Lecture notes from 17 September 2012 on borehole navigation. TPG 4215 High Deviation Drilling, NTNU, Trondheim, Norway.
- Saasan, A. Hole Cleaning During Deviated Drilling The Effects of Pump Rate and Rheology. Paper SPE 50582 presented at the SPE European Petroleum Conference, 20 22 October 1998, The Hague, The Netherlands. http://dx.doi.org/10.2118/50582-MS

- Samuel, R. 2010. Friction Factors: What are they for Torque, Drag, Vibration,
 Drill Ahead and Transient Surge/Swab Analysis. Paper IADC/SPE 128059
 presented at the IADC/SPE Drilling Conference and Exhibition, 2-4 February
 2010, New Orleans, Louisiana, USA. http://dx.doi.org/10.2118/128059-MS
- Sangesland, S. 2012. Torque and Drag. Short course and lecture notes from 14
 September 2012 on torque and drag for extended reach wells. TPG4215 High
 Deviation Drilling, The Norwegian University of Science and Technology,
 Trondheim, Norway.
- Scribd. 2013. Top Drive Varco, http://www.scribd.com/doc/29792554/128/Top-Drive VARCO (accessed 2 May 2013)
- Sunry Petro. 2013. Mud Pump, http://sunrypetro.com/mud_pump.html) (Accessed 12 May 2013)
- TAML. 2012. Multilateral Wells Reduce Capex in Subsea Development, http://tamlintl.org/featured/multilateral-wells-reduce-capex-in-subsea-development/(accessed 23 January 2013).
- TAML. 2002. TAML Complexity Ranking, http://taml-intl.org/wp content/uploads/2012/03/tamlcomplexity.pdf (downloaded 11 April 2013)
- Weatherford. 2006. TAML Classifications, http://www.weatherford.com/weatherford/groups/web/documents/weatherfordcorp/WFT041779.pdf (downloaded 10 April 2013).
- Wellplan. 2013a. Suite Well Operations Software. Version (EDM 5000.1.10.0 (09.04.07.107) Build 5000.1.10.0.1934). Dubai, UAE: Halliburton Landmark.
- Wellplan. 2013b. Suite Well Operations Software. Version (EDM 5000.1.10.0 (09.04.07.107) Build 5000.1.10.0.1934) User Guide. Dubai, UAE: Halliburton Landmark.
- WellView®, version 8.1.49.0. 2013. Houston, Texas: Peloton Computer Enterprises Ltd.
- Wojtanowicz, A.K. 2012. *Well Design-Drilling*, 1st edition. Baton Rouge, Louisiana: Louisiana State University internal publication.
- Woodside. 2012. Multilateral Wells Fact Sheet, http://www.woodside.com.au/Our Approach/Documents/Mutilateral%20Wells%20Fact%20Sheet%202012.pdf (downloaded 8 April 2013).

Appendix

For this report the appendix has been used for supporting material of secondary importance, as well as for gathering of graphs and figures not reasonable to include in the main text.

Appendix A: Offshore Daily Rig Rates

Floating Rigs

Table 16: List of average day rates for floating rigs (WD = Water Depth) (Rigzone 2012)

Rig Type	Rigs Working	Total Rig Fleet	Average Day Rate
Drillship <4000' WD	6	8	\$229 000
Drillship 4000'+ WD	63	75	\$457 000
Semisub <1500' WD	9	15	\$267 000
Semisub 1500'+ WD	72	91	\$295 000
Semisub 4000'+ WD	96	112	\$415 000

Jackup Rigs

Table 17: List of average day rates for jackup rigs (Rigzozne, 2012) (IC = Independent Cantilever, IS = Independent Spud, MC = Mat Cantilever, MS = Mat Supported, WD = Water Depth) (Dockwise 2011)

Rig Type	Rigs Working	Total Rig Fleet	Average Day Rate
Jackup IC <250' WD	39	54	\$79 000
Jackup IC 250' WD	46	62	\$84 000
Jackup IC 300' WD	100	134	\$90 000
Jackup IC 300'+ WD	131	157	\$154 000
Jackup IS <250' WD	6	9	
Jackup IS 250' WD	7	9	\$75 000
Jackup IS 300' WD	3	6	\$60 000
Jackup IS 300'+ WD	1	2	\$70 000
Jackup MC <200' WD	2	11	\$40 000
Jackup MC 200'+ WD	11	23	\$72 000
Jackup MS <200' WD	2	3	
Jackup MS 200'+ WD	6	15	\$52 000

Appendix B: A historical perspective of multilateral wells

In 1859 the first well in history deliberately drilled to find oil was created in Titusville, Pennsylvania, by the American Edwin L. Drake. In the years to follow, especially in the 1870's, the oil production in the USA increased rapidly due to the drilling of new wells, mostly in Pennsylvania. With the invention of the internal combustion engine and the manufacturing of the first cars around year 1900 the demand for oil and gas continued to increase (Oil Region Alliance 2013). As a result of this a lot of new techniques and methods in drilling for hydrocarbons were invented and patented over the next couple of decades. Most of these new ideas were rather bold and ambitious at that time and could not be performed in practice due to lack of either skills or technology. This was also the case when the first patent on multilateral technology was filed in 1929 (E&P Magazine 2007).

Although often thought of to be a technology of recent time, the history of multilateral wells with this reaches more than 80 years back. In the years to follow this first patent a range of various versions on this type of well dawned, all on paper, see Figure 66. During the 1930's several attempts to drill multilateral wells were performed, and many credit the Canadian engineer Leo Ranney to be the first to successfully implement the technology to the oilfield. In 1939 he and his men drilled an 8 ft vertical well for then to move equipment and personnel downhole and kick off horizontal sections from the bottom of the initial hole (E&P Magazine 2007).

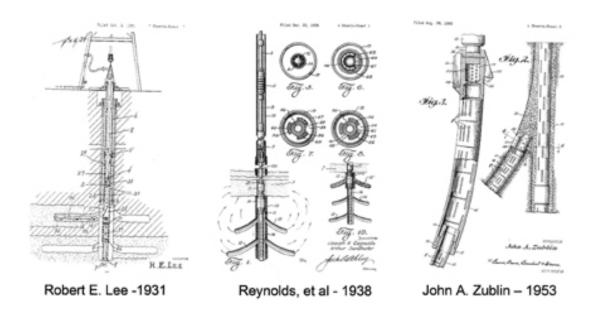


Figure 66: Technical drawings of the first patents on multilateral well technology (E&P Magazine 2007)

Despite the efforts in the 30's the world's first, true multilateral well was not drilled until 1953. That year a nine-branch multilateral well, with laterals reaching from 262.5 ft

to 984 ft, was drilled in Bashkiria, Soviet, now Bashkortostan, Russia, under the supervision of the Soviet petroleum engineer Alexander Grigoryan. His pioneer well, displaced in Figure 67, produced almost 17 times the amount of the single wellbores nearby, while only costing around 1.5 times more. Despite this, however, the well only produced around 700 barrels of oil per day. The main reason for that was the lack of directional drilling technology, and Grigoryan's nine laterals therefore, in reality, were drilled more or less blindfolded as an experiment (E&P Magazine 2009).

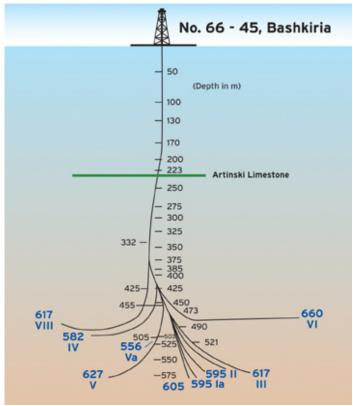


Figure 67: The world's first multilateral well drilled in Soviet in 1953 (E&P Magazine 2007)

B.1 The development of multilateral wells - Introduction of the TAML standard

Even though the multilateral well in Soviet had taken an interest in the global oil industry the wells drilled in the years to follow were mostly conventional single wellbore wells. Commodity prices were low, and it was therefore important to maximize the return on investment on each well slot, especially offshore. The best way of doing this, according to most companies, was to stick with well-known and well-proven technology, and avoid innovative and new methods that possible could result in failure and additional expenditures (E&P Magazine 2007). That, however, changed in the start of the 1970's with the introduction of the Logging While Drilling (LWD) technology. Wireline tools, a method which at that time traditionally had been used for surveying and downhole data acquisition, often failed and were problematic to use at high

deviations. Even though limitations with control and slow telemetry, the real-time data information, possibility of logging in any direction, toughness and finally high deviation and horizontal well capabilities, soon made the LWD tool favorable compared to the more time-consuming and delicate wireline tool (Colombia University 2008). Now the driller had the ability of real-time steering of the bit, and the possibility of navigating and placing the wellbore more precisely close to the targets suddenly made multilateral wells a feasible solution in many cases (E&P Magazine 2009).

Despite the introduction of LWD there was yet a big challenge to overcome in the leap from single wellbores to multi-branched deviated, and even horizontal, wells. This was the junction design, or in other words the technology and strategy tied to the place in the mother wellbore where the different laterals are kicked off and diverge. Not only did the companies face issues and challenges in creating and establishing the junctions, and making them stable and prevent them from failing, they also experienced complications with regulatory authorities in form of safety and integrity approvals (E&P Magazine 2009). As the amount of multilateral wells steadily increased on a worldwide basis during the 80's, an initiative was therefore taken in the early 90's to form a group to share knowledge and creating a classification of different junction types, levels and technologies. The result of this, presented in 1997, was TAML, or Technical Advancements of Multi Laterals, a classification system and set of standards defining the complexity and functionality of different junction types and designs (E&P Magazine 2009). This system divides the complexity of the junctions into six levels, as seen in Figure 9, 1 being the simplest and 6 the most complex (Frailia et al. 2002). In addition the functionality of the junctions is classified, although rarely referenced (Weatherford 2006). Normally the functionality of the junction completion, as well as technical challenges and cost, increases with increased level. The functionality classification can be in terms of whether it is a new or existing well, number of junctions, well type, type of completion above the packer, re-entry possibilities and type of control and monitoring options of the well and junction (E&P Magazine 2007). The different functionality classifications are listed in whole in Appendix C. During the 90's both the industry and different governing authorities accepted TAML as the new classification standard, and since then a common effort has been made to develop and utilize multilateral well technology across companies and countries (E&P Magazine 2009).

Appendix C: TAML functionality classifications for Multilateral Well junctions

The TAML standard lists both the complexity level of the multilateral well junction as well as the functionality level. When describing junctions the latter is rarely used, and most commonly only the complexity level (1-6) define the type of junction used in a multilateral well (Weatherford 2006). Never the less, knowledge about the functionality classification can be useful and, when familiar, will provide a lot of information about both the well and junction. Below follow the TAML functionality classification of a junction in a multilateral well.

Table 18: TAML functionality classification – well description (Weatherford 2006)

New or existing well	N = New
	O = Old
Number of junctions	1,2,3,4 etc.
Type of well	PN = Producer, Natural Lift
	PA = Producer, Artificial Lift
	IN = Injection Well
Completion type above packer	S = Single Bore Completion
	D = Dual Bore Completion

Table 19: TAML functionality classification – junction description (Weatherford 2006)

Tubic 15 t 1111/12 ranceronancy crassification Juni	etion description (; ; entirelior d = 000)
Connectivity number	This is equal to the complexity ranking
	(Level 1 – Level 6) and will describe the
	type of junction.
Accessibility	TR = Tubing Re-entry
Flow control	SEL = Selective Production

These functionality classifications are then put together to form complete description strings of both the multilateral well and the junctions. An example of this can be "Level 3 / O-2-PA-S / 3-TR-SEL". The level of a multilateral well, if more than one junction, corresponds to the junction with the highest level of complexity (TAML 2002). For this example "Level 3" indicates this is a multilateral well with at least one junction of level 3 complexity. The "/" indicates we now are describing the well, and "O" means this is an old well. The "PA" shows the well is a producer on artificial lift, with a Single Bore Completion ("S"). The next "/" then tells us we are shifting from describing the well to describing the junction. "3" should be the same number as the complexity ranking, while "TR" represents Tubing Re-entry. Finally "SEL" indicates this is a junction with possibilities for Selective Production.

Appendix D: Applications of Multilateral Wells

A multilateral well is a type of well design with two, or more, lateral branches tied together to the mother wellbore via one, or more, junctions. A design like this often have additional initial investment, and might also be more technical challenging, require more experience and expertise, and take longer to drill, compared to a single well, but the upsides are in many cases large.

D.1 Maximizing of reservoir exposure and production while reducing drawdown

Although not a new application of multilateral well technology the reservoir exposure and maximizing of production is probably the most common reason for selecting multilaterals in the industry today. Compared to a single-wellbore design a multilateral, via its branches, makes it possible to expose the wells from each slot to larger parts of the reservoir (Crouse 1996). And with more contact between the reservoir and the wellbore the inflow rate in each lateral can be lower, and thus the expected drawdown reduced, compared to single horizontal, deviated or vertical wellbores. This principle is presented in Appendix D. As a result of this water or gas coning can be reduced, and it takes longer before breakthrough from either is experienced, derived in Appendix E, thus increasing the lifetime of the reservoir section ²⁹. In addition, due to this, and with more of the pay zone covered, the recovery factor can be increased (Frailja et al. 2002).

Another element that can make a multilateral well beneficial compared to a single well is the flowing friction. A horizontal well section has limitations when it comes to flowing friction pressure, and if the length is too long the inflow to the wellbore can be limited by friction between the hydrocarbon flow and either borehole or casing, dependent on completion method. The principle behind this is shown in Appendix F. By replacing the horizontal section with a multilateral well with two, or more, shorter, adjacent lateral branches, as shown in Figure 68, with equal total reservoir exposure as the single wellbore section the inflow can be spread and thereby the frictional pressure losses can be reduced (Frailja et al. 2002).

-

²⁹ Personal communication with G. Liland. 2013. Stavanger: Halliburton Scandinavia AS

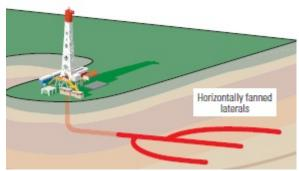


Figure 68: Horizontally fanned laterals can reduce friction pressure drop compared to a single, long horizontal wellbore section (Frailia et al. 2002)

However, if comparing a multilateral with two arms to a system with two, single wells, instead of only one, the production rate, in the North Sea, on average is about 85 %. The reason for this is that the multilateral well can be considered as one well with more reservoir contact than each of the two, single wellbores. The result of this, as mentioned, is reduced drawdown, and thereby a slight reduction in inflow rate. Yet, this way of producing a reservoir, with the benefits with regards to water and gas coning and breakthrough, will in most cases increase both the lifetime and ultimate recovery of a field, as well as yielding more stable production rates³⁰. Two examples of the latter can be seen in Figure 8, both COPNO-wells drilled with MLT from 2004. Both wells show a more stable rate and lower decline than what is expected. The two steep drops in the picture on the right hand side are before acid stimulation³¹.

D.2 Reduction in CAPEX and operating cost

The drilling and completion of a multilateral well with two branches in the North Sea today are on average 1.3 times more expensive than a single well drilled to the same target³². This is also the case for other locations around the world (Woodside 2012). Compared to a single well a multilateral well therefore in almost all cases will yield higher initial investment, but has the potential, in long terms, via more reservoir exposure and longer lifetime, as explained, to be more economical and result in higher return per well slot.

However, multilaterals are in most cases selected and drilled as an alternative to two, or more, single wellbores. The advantages when it comes to reservoir exposure and drawdown reduction with ML's, as presented in Section 4.1.1, might be achieved by doing exactly this, namely drilling more wells to TD. However, by this action, the expenditures, in most cases, are elevated compared to a multilateral system (Crouse 1996). Compared to one single well two wellbores to TD in the North Sea, if drilled without problems, in most cases will result in around two times the cost, as expected

 ^{10 31} Personal communication with G. Liland. 2013. Stavanger: Halliburton Scandinavia AS
 12 13 14 Personal communication with G. Liland. 2013. Stavanger: Halliburton Scandinavia AS

(often, though, this number is more in the area of 1.6-1.8 due to the gaining of experience and possibility of drilling optimization when drilling the second well (Nesland 2012). Compared to a two-branched multilateral, however, at the average of 1.3 times the cost of a single well, that is less cost efficient³³. If the additional necessary drilling and completion equipment, number of risers, casing strings and wellheads and other topside equipment, as well as operating expenditures, needed for two, or more, single wells, compared to a multilateral, is included in the calculation, experience from the North Sea show that ML's on average only require 1.15 times the CAPEX compared to a single wellbore³⁴. Thus, if the desire is to obtain more or less the same reservoir properties in terms of exposure, production, drawdown, recovery factor and lifetime, a multilateral well design in many cases can reduce the capital expenditures, or investment cost, by more than 40 % compared to a single-wellbore system.

D.3 Slot and subsea template utilization

By drilling a multilateral well with for instance two laterals compared to two, single wells, it is quite obvious that one slot space is saved. This second slot on the platform, or in a subsea template for that matter, again can be used to drill another multilateral. This way it is possible to obtain the reservoir exposure, with all the benefits that brings, by using only two, instead of four, slots³⁵.

D.4 Minimizing the environmental impact

For onshore applications fewer wells means less footprint in form of reduction of space requirements for wellheads and other necessary equipment needed per well. Drilling of multilateral wells onshore therefore can help reducing the environmental impact (Crouse 1996). This is, to a certain extent, also valid offshore, where more ML's means less space requirements on the platform, or rig, and thus reduced need for supplies being transported to back and forth from land (Frailja et al. 2002).

D.5 Mitigation of shallow drilling risk

With fewer wells drilled to TD the risk associated with any issues or problems at shallow depths, or in fact above the junction depth, is reduced. With MLT the major part of the drilling to the target is only performed once (Crouse 1996). Using of MLT therefore can help increasing the safety for the operating crew, while minimizing the risk of undesirable events that ultimately can lead to fatalities and/or environmental disasters (Frailja et al. 2002).

³⁵ Personal communication with R. Watts. 2013. Stavanger: ConocoPhillips Norway AS

Appendix E: Modern aspects of Multilateral Well technology

The first patents and theoretical versions of multilateral wells in the 1920's and 1930's were all designed in order to increase the oil production. The engineers and early pioneers understood that by creating branches, or arms, out from the main wellbore into the formation the reservoir exposure would be higher and thus the production would increase. The main issue at that time, however, was the lack of available knowledge and technology to go from paper to practice. That changed with Grigoryan's first true multilateral well in 1953, but the drilling methods and well construction techniques at that time were still so simple that only basic wells could be made (Frailja et al. 2002). In the 1990's, however, especially through the introduction of the TAML standard in 1997, the industry experienced the creation of new well construction techniques and completion methods. Now it was possible to drill and complete complex and previously challenging designs of multilateral wells and thus opening this well construction method to new aspects and applications (Frailja et al. 2002).

E.1 Natural Fractured Reservoirs

With the increased focus on multilateral wells and the introduction of the TAML standard during the 1990's the industry managed to increase the complexity and construct, and complete, more advanced types of laterals. This makes it today possible to drill both the mother-wellbore and the different branches vertical, high-deviated or even horizontal. In addition, the technology on the different downhole steering tools makes it conceivable to place, steer and design the main wellbore and the laterals almost as desired (Frailja et al. 2002).

In natural fractured reservoirs, if the fracture orientation is unknown, this ability to create and design multiple, agile well-branches that to a larger extent can intersect the fractures and more exactly be placed where it is necessary to maximize production, as shown in Figure 69, is often an advantage compared to single wellbores and even hydraulic fracturing methods. On the other hand, if the fracture orientation is known, the interaction between the reservoir and the wellbores can be maximized by placing to branches of a multilateral opposed each other (Frailja et al. 2002).

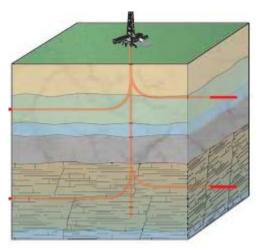


Figure 69: MLT applied in a natural fractured reservoir (Frailja et al. 2002).

E.2 Laminated formations and layered reservoirs

For this type of reservoirs a crucial factor in order to maximize the reservoir contact, and thus production, is vertical and horizontal contact. Lamination, or layering, in a formation means that the pay zones are divided into horizontal divided, adjacent, layers (About Geology 2013), as pictured in Figure 70. In order to effectively drain a reservoir like this there is a need for several vertically stacked, horizontal wellbores. However, the time spent on drilling and completion, as well as the requirement for a large amount of wellheads, separate casing strings and risers and topside equipment, would make a solution with separate main wellbores quire costly. A possible technique in areas like this would be to drill a multilateral well with horizontal branches that diverge into a common main wellbore. This would reduce the investment cost and maximize the reservoir exposure at the same time (Frailja et al. 2002).

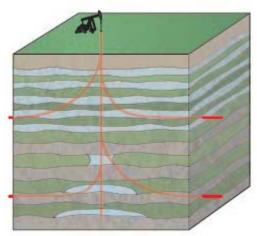


Figure 70: MLT applied in a laminated, or layered, formation (Frailja et al. 2002)

E.3 Low-permeability zones

Reservoirs with low permeability often require a large contact with the wellbore in able to be produced economically. Most often these types of zones are penetrated with horizontal wells, instead of vertical or deviated, due to a higher productivity index (Dellu et al. 1996). Multilateral wells, by larger reservoir exposure from each well slot, therefore can increase the productivity, as well as the economy, of a low-permeability reservoir.

E.4 Distinct, separated reservoir compartments and satellite fields

In some reservoirs, with distinct, separated reservoir compartments, as shown in Figure 71, the drilling of multilateral wells may be the only economic viable solution in order to produce the otherwise bypassed reserves. In addition, in many fields around the world multilateral well technology has made it possible to include small pockets of hydrocarbons and satellite reservoir parts to the mother-wellbore system, as presented in Figure 72. These situations, where an own wellbore from the rig or platform not would be economical due to either too small reserves or a location too far away, will help increasing the recovery rate in a field and thus add valuable return on investment for the project (Frailja et al. 2002).

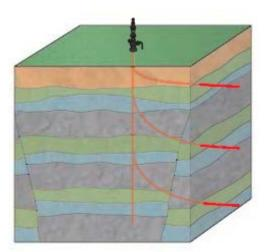


Figure 71: Reservoir with separated reservoir compartments penetrated by a multilateral well with three branches (Frailia et al. 2002)

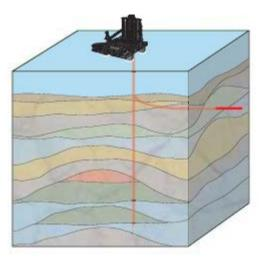


Figure 72: Satellite field being drained by a multilateral well (Frailja et al. 2002)

E.5 Heavy-oil deposits and depleted zones

Heavy oil reservoirs are often produced by injecting steam to the reservoir via horizontal wells. This makes the oil less viscous, and it therefore flows more easily into the producing wellbore (Mohebati et al. 2010). By the utilization of MLT in such areas this enhanced oil recovery (EOR) method is optimized by better reservoir contact, as shown in Figure 73. In addition, other sources of unconventional hydrocarbons, such as shale gas or coal bed methane (CBM), often can be found in thin layers, and multilateral wells therefore can increase the recovery factor by placing of the branches horizontally in these beds (Frailja et al. 2002).

For depleted zones, or mature fields, like the Ekofisk field, multilaterals can help maintaining the production rates and ultimately increase the total recovery. By exploiting each slot to the maximum the remaining, remote reserves can be accessed, and the overall reservoir coverage and contact can be maximized, while keeping the cost at a minimum. In addition, as mentioned before, the gas and water coning, if any, can be reduced to prevent breakthrough of any of these substances to the producing wellbores. This way the lifetime of a field can be extended, often many years beyond what was expected (ConocoPhillips 2013f).

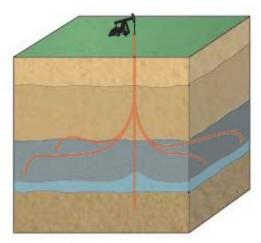


Figure 73: MLT applied in a heavy oil deposit, either as producer or steam injector (Frailja et al. 2002)

E.6 Coiled Tubing Drilling of Multilateral Wells

In 1964 Bowen Tool used a workover coiled tubing unit to drill a new wellbore. At that time this method had only been used for workovers and well interventions, and the event by that marked the beginning of what today is referred to as Coiled Tubing Drilling, or simply just CTD (Crouse 1996). Just like for any other operation using CT the drilling application make use of a thin, long, continuous steel pipe rolled onto a reel at the surface. The pipe cannot be rotated, so downhole mud motors have to provide rotational force to the bit. In addition a large, separate hydraulic workover unit is required in order to install casing strings (Crouse 1996). Some of the advantages of CTD are no need for connections, meaning faster overall ROP, reduced formation damage, improved reservoir contact, improved well control, the possibility for slim- and microhole drilling, and the possibility to drill underbalanced all the time (Patricksson 2012).

Despite the advantages over conventional, jointed pipe drilling, this method is not being used too extensively around the world today. A possible reason for this is the slow-turning oil-industry, that in many cases cling on to existing and old technology that have yielded great success rates for decades³⁶. Development and investment in CTD, however, is continuously ongoing by all the major service companies, and a future, possible application for coiled tubing drilling might be the drilling of multilateral wells (Crouse 1996).

_

³⁶ ¹⁷ Personal communication with G. Liland. 2013. Stavanger: Halliburton Scandinavia AS

Appendix F: Types of Multilateral Wells configurations utilized in the industry today

The dawning of more multilaterals in the industry during the 1990's, as well as the development of the TAML classification in 1997, in many ways revolutionized the multilateral well technology. From pretty simple configurations, often with only one lateral, openhole completed, or with some sort of slotted liner or sand screen, the industry today have a wide variety of multilateral well designs and configurations that can be utilized³⁷.

F.1 Stacked horizontal, or fishbone

A stacked horizontal multilateral well configuration, also called a fishbone well, can be seen in Figure 74. This design consists of a vertical or deviated mother wellbore, with horizontal branches separated vertically ³⁸. Suitable applications for the stacked horizontal ML are layered, or laminated, formations, such as the Austin chalk formation in Texas and Louisiana, USA, where there is a need for exposure in many adjacent, horizontal layers (Bosworth et al. 1996).

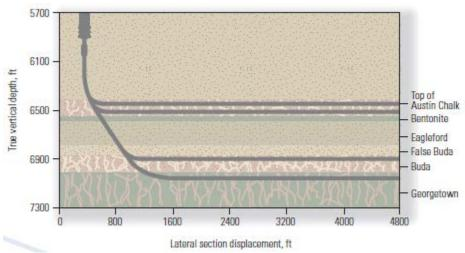


Figure 74: Example of a stacked horizontal well from the Austin chalk formation in Texas, USA (Bosworth et al. 1998)

F.2 Forked, fanned or dual- and tri-lateral

Forked multilaterals are named due to their shape, with two or three, or even more, branches reaching into the reservoir like the prongs of a fork. This type of configuration

³⁸ Personal communication with R. Watts. 2013. Stavanger: ConocoPhillips Norway AS

is beneficial in areas where there is a desire to reduce the flowing friction into the wellbore, and spread the exposure into shorter, parallel wellbore sections instead of one long, as discussed in Section 4.1.1 Examples of forked multilaterals can be seen in Figure 68, Figure 75, Figure 76 and Figure 77. The two latter, as well as the one in Figure 68, are also called planar dual- and planar tri-laterals. This is due to the horizontal landing of the branches (Crouse 1996).

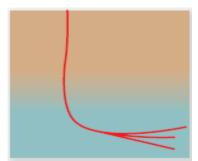


Figure 75: Example of a forked ML (Bosworth et al. 1996)

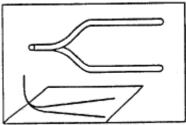


Figure 76: 3D and top view of a forked/planar dual-lateral (Crouse 1996)

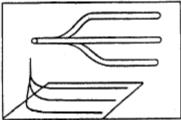


Figure 77: 3D and top view of a forked/planar tri-lateral (Crouse 1996)

F.3 Radial fan, multibranched or chicken foot

The multilateral well configuration known as the radial fan has, in the same way as the forked ML, got its name from the appearance on the drawing table, seen in Figure 78 and Figure 79. From a more or less vertical motherbore the three, or even more, different laterals reach out into the formation like the blades of a fan. Another popular name on this ML well design is chicken foot, where the branches instead are imagined to represent the toes of the animal³⁹. However, most of the vendors in the market today

-

³⁹ Personal communication with R. Watts. 2013. Stavanger: ConocoPhillips Norway AS

more technically describe this as a multibranched well, due to its many arms⁴⁰. This type of ML-design is mostly used in areas where the reservoir has a somewhat flat and circle-shaped form, allowing the chicken foot well to increase the wellbore exposure compared to drilling only one horizontal or deviated well in the area. Another application is heavy oil deposits (Frailja et al. 2002).

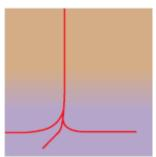


Figure 78: 3D example of a chicken foot, or multibranched, multilateral well (Bosworth et al. 1996)

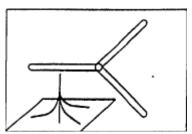


Figure 79: Top and 3D view of a radial tri-lateral, also referred to as a radial fan or chicken foot ML (Crouse 1996)

F.4 Planar opposed

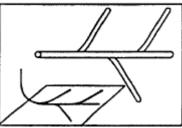


Figure 80: Example of a planar opposed multilateral well, 3D and top view (Crouse 1996)

The planar opposed multilateral is a configuration where the branches are laid out horizontal, facing away from each other, as shown in Figure 80. As for the radial fan, or chicken foot, this design can increase the reservoir-wellbore contact in thin reservoirs with a close to square shape (Crouse 1996).

_

⁴⁰ Personal communication with G. Liland. 2013. Stavanger: Halliburton Scandinavia AS

F.5 Dual opposing laterals

For low permeability or naturally fractured reservoirs a dual opposing lateral configuration, as presented in Figure 81, can be a good solution (Frailja et al. 2002). This type of design to a larger extinct can interact with the fractures thus creating a connecting flow path for the hydrocarbons from reservoir to the surface. The dual opposing lateral, at the same time, just as the radial fan design, also can be utilized in heavy oil deposits where high wellbore exposure are necessary, or flat and circle shaped reservoirs (Crouse 1996).

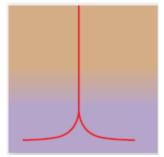


Figure 81: A dual opposing lateral ML design (Bosworth et al. 1996)

F.6 Planar, offset quadrilaterals

The planar, offset quadrilateral (or tri-lateral if only two branches) is a ML design that gathers all the branches in the horizontal plane on the same side of the motherbore. By doing this less directional drilling is required to orient the laterals in the desired direction to effectively spread the wellbores to maximize the reservoir contact. As for the planar opposed design this configuration often is used in quadrangle, but more rectangular-shaped, reservoirs (Crouse 1996).

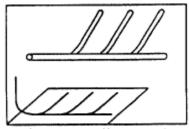


Figure 82: Example of at planar, offset quadrilateral (Crouse 1996)

F.7 Stacked, or inclined, tri-laterals

The design of this type of multilaterals is comparable to the planar, offset tri-lateral, but the branches are facing away from the motherbore in the vertical direction instead of in the horizontal plane. Figure 83 are showing this with the top view in the upper right corner. This configuration can be drilled instead of separate, vertical wellbores in

reservoirs with tall and thin pay zones, where vertical reservoir contact are more important than horizontal exposure⁴¹.

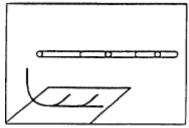


Figure 83: Stacked, or inclined, tri-lateral, 3D view and top view (Crouse 1996)

F.8 Other configurations

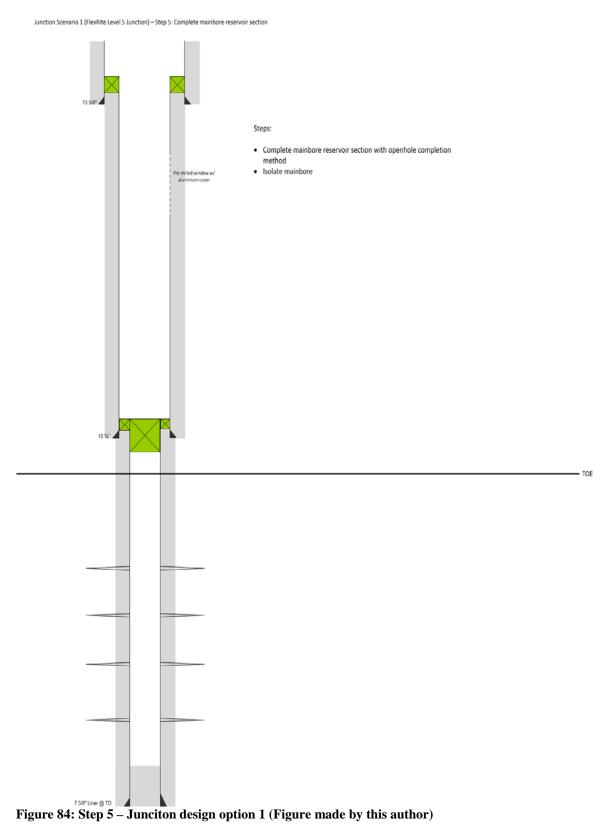
In addition to the multilateral well designs mentioned there are today a large variety of different configurations and shapes. The major service companies all have their own systems and technologies, and in most cases the wells can be customized and designed based on the customer's need. Most of the configurations listed in this thesis have their basis from the late 90's in relationship with the work regarding the TAML standard. New multilateral wells drilled today therefore often fall outside any of the general classifications presented here, but in many cases they still can be somewhat related to one, or more, of the configurations (Crouse 1996). The dawning of the many new, specific configurations was the reason why these presentations of the different old configurations were decided to be put in the appendix rather than in the main report.

_

⁴¹ Personal communication with R.Watts. 2013. Stavanger: ConocoPhillips Norway

Appendix G: Stepwise installation of the Junction design option 1

In this following appendix nine of the total 18 installation steps for the junction design option 1 are presented, see Figure 84 to Figure 92. These nine are carefully selected in order to reduce the number of overall figures, while keeping the necessary information amount.



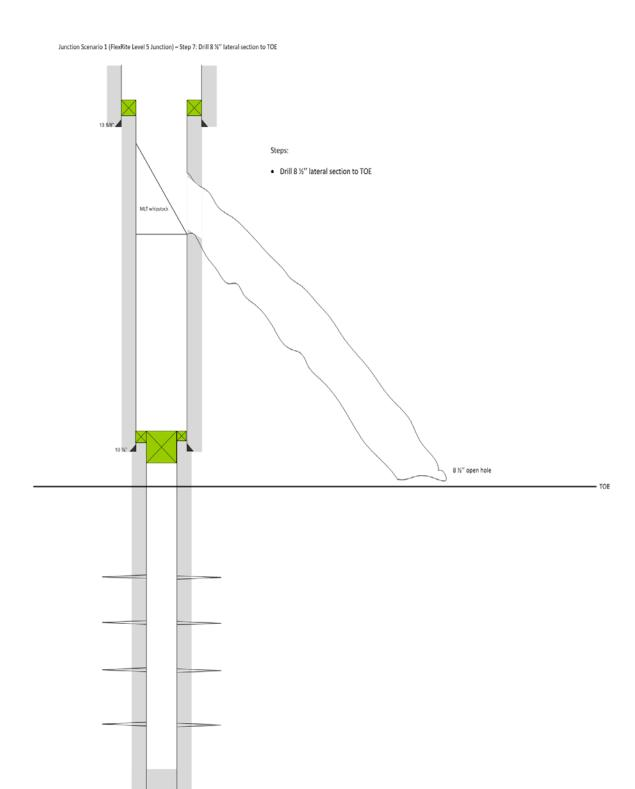


Figure 85: Step 7 – Junciton design option 1 (Figure made by this author)

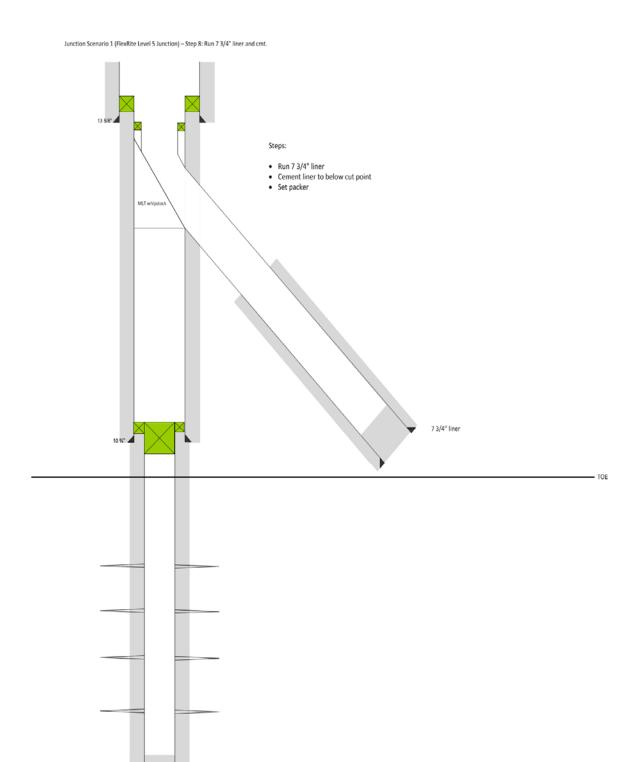


Figure 86: Step 8 – Junciton design option 1 (Figure made by this author)

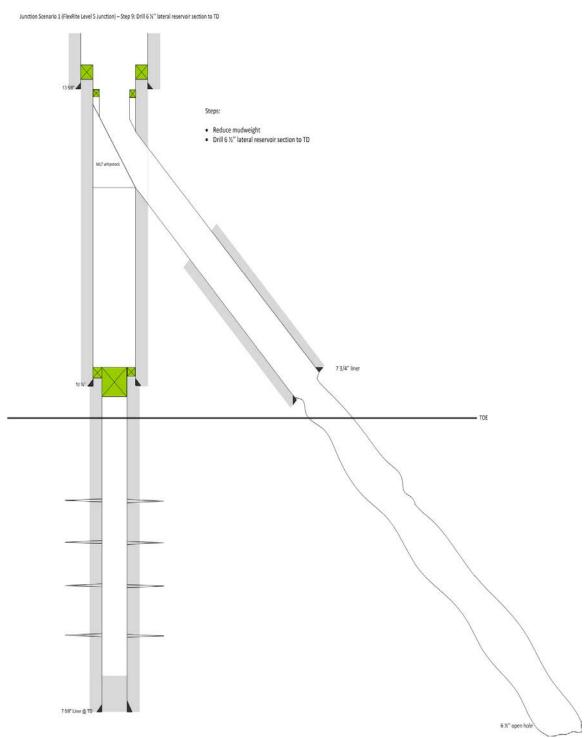


Figure 87: Step 9 – Junciton design option 1 (Figure made by this

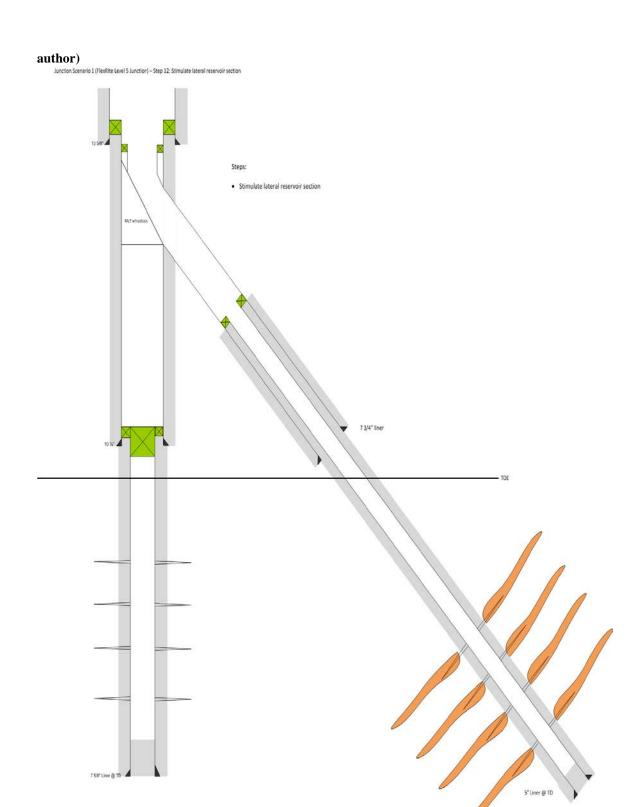


Figure 88: Step 12 – Junciton design option 1 (Figure made by this author)

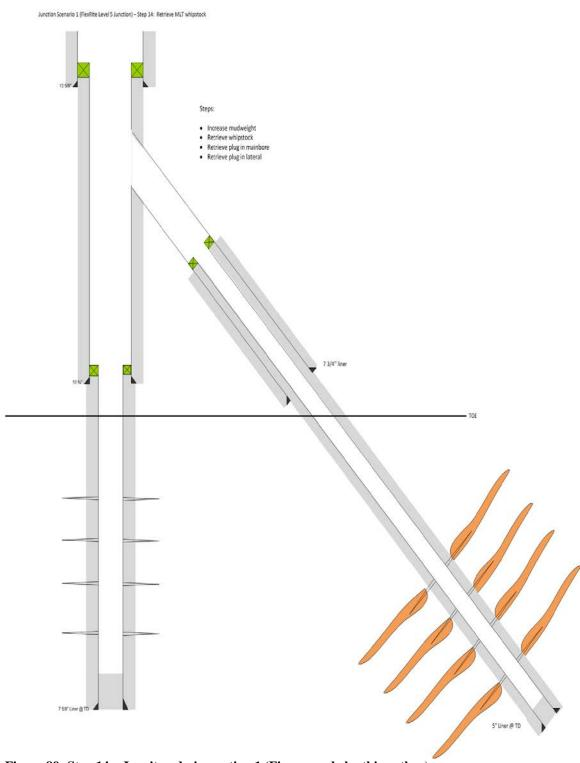


Figure 89: Step 14 – Junciton design option 1 (Figure made by this author)

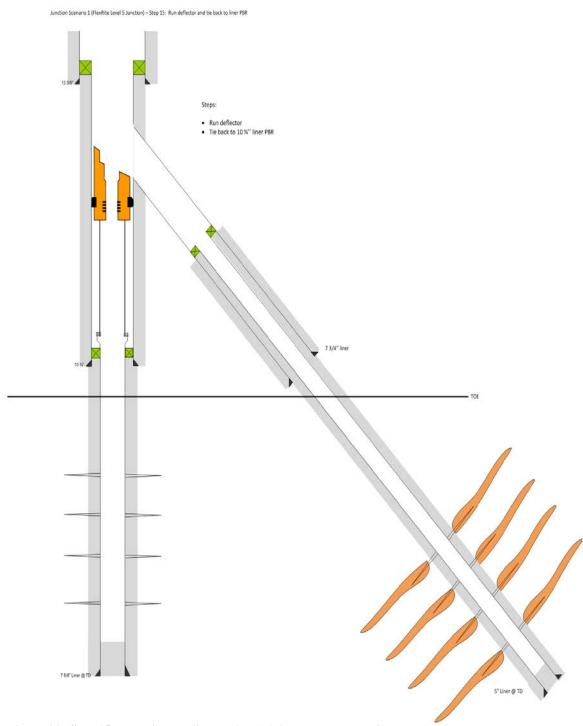


Figure 90: Step 15 – Junciton design option 1 (Figure made by this author)

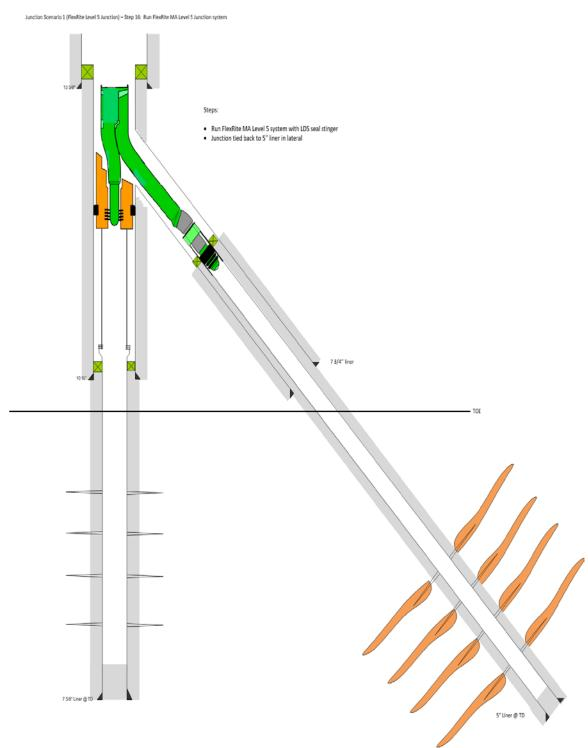


Figure 91: Step 16 – Junciton design option 1 (Figure made by this author)

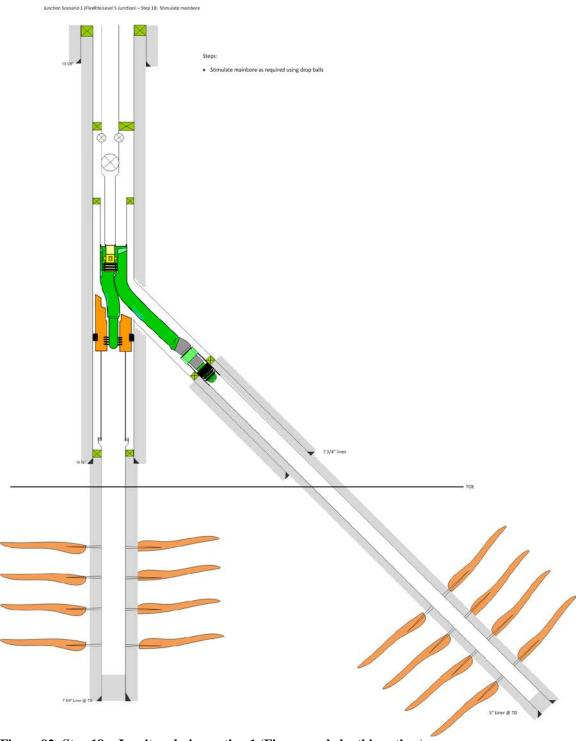
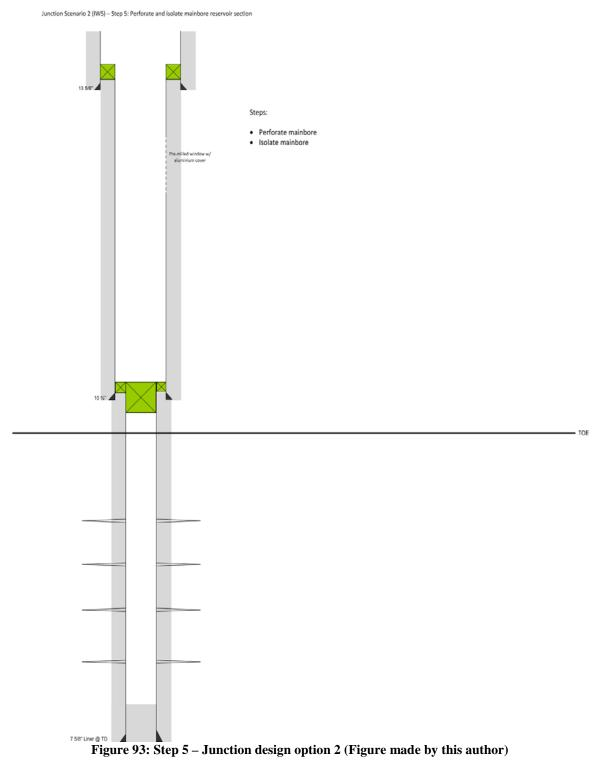
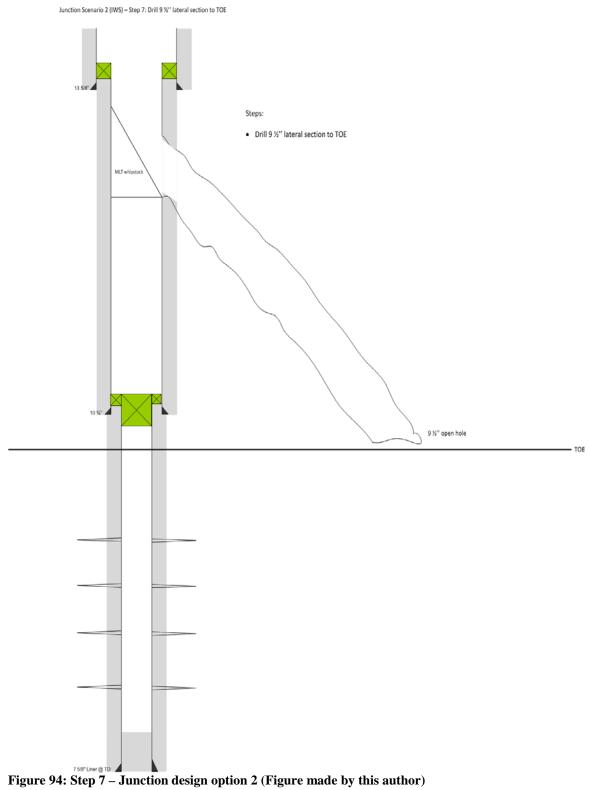


Figure 92: Step 18 – Junciton design option 1 (Figure made by this author)

Appendix H: Stepwise installation of the Junction design option 2

In this following appendix eight of the total 18 installation steps for the junction design option 2 are presented, see Figure 93 to Figure 100. These nine are carefully selected in order to reduce the number of overall figures, while keeping the necessary information amount.





Junction Scenario 2 (IWS) – Step 8: Run 8 5/8" expandable and cmt. Run 8 5/8" expandable (post-exp: Nom OD 9.555", Nom ID 8.6", Drift ID 8.514")
 Cement expandable

Figure 95: Step 8 – Junction design option 2 (Figure made by this author)

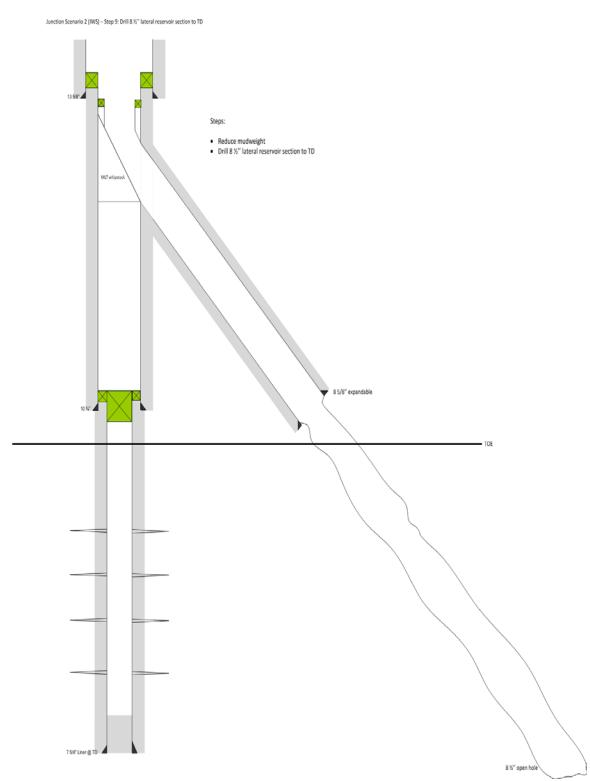


Figure 96: Step 9 – Junction design option 2 (Figure made by this author)

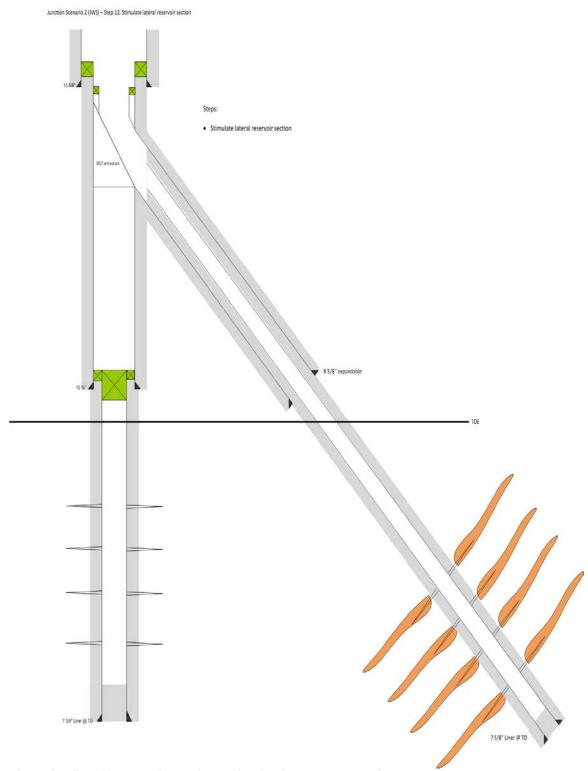


Figure 97: Step 12 – Junction design option 2 (Figure made by this author)

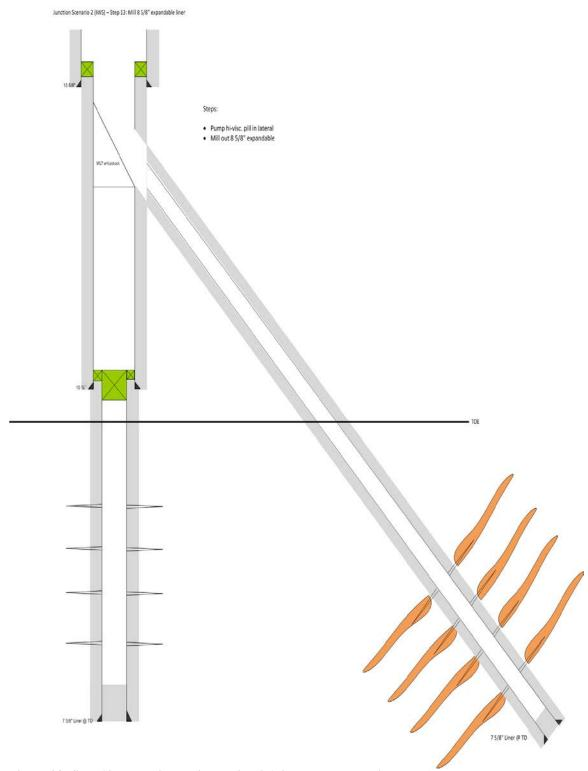


Figure 98: Step 13 – Junction design option 2 (Figure made by this author)

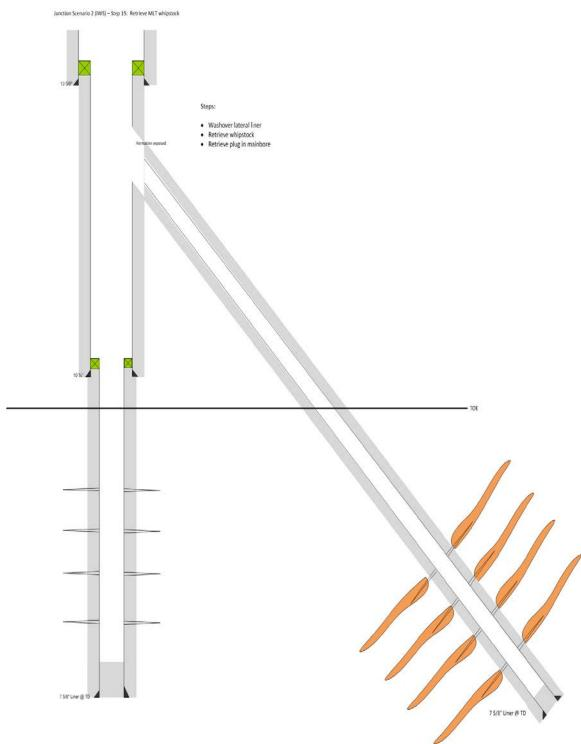


Figure 99: Step 15 – Junction design option 2 (Figure made by this author)

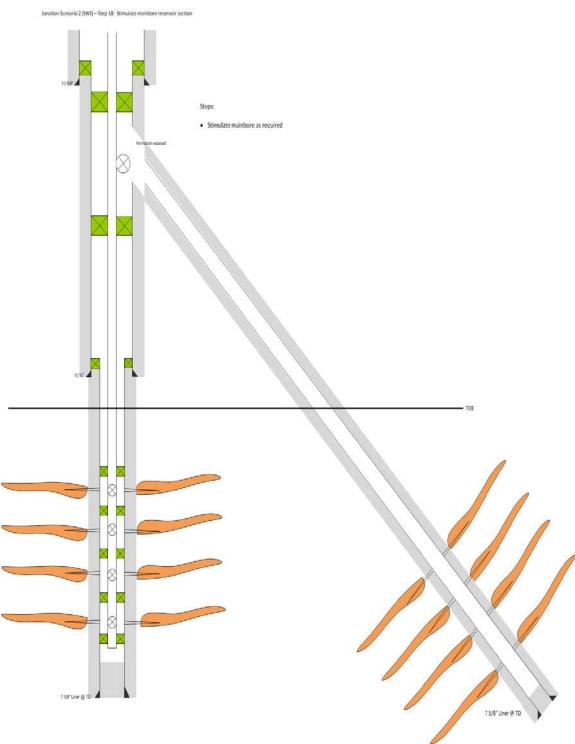


Figure 100: Step 18 – Junction design option 2 (Figure made by this author)

APPENDIX I: Wellplanning on Ekofisk

Note: The following appendix is written purely based on personal communication with Leif Inge Ramsdal, wellplanner in Halliburton, April 2013.

I.1 Introduction

Wellplanning is an integrated task, and different groups within the company will be giving input the well path has to be designed after. The key departments involved in the Wellplanning on Ekofisk is the Wellplanner (WP), Geology Department (GGRE), Drilling Engineers (DE) and the Directional Drilling Coordinators (DD Coordinator).

I.2 Planning procedure

The targets for a wellbore are created based on where the geologist thicks there can be oil. Based on this the wellplanner will be asked to create a well path from a given slot number. By use of the simulation software Compass the targets, for the given wellbore, are then plotted. It is important that the correct height reference is used, for COPNO this is RKB.

I.3 Challenges

Possibly the largest challenge on Ekofisk is the number of wells drilled. The most important is to drill a well that is both drillable and that will avoid other wells. The avoiding of other wells is called anticollision. Other challenges in the Greater Ekofisk area is to ensure that the tangent section will be casing drilling (Ekofisk kilo have casing drilling from $\sim 4800'\text{TVD}$ to $\sim 5200'\text{TVD}$), and there is a max inclination of 75 degrees to hit the top Ekofisk formation. There is also a need of around 500 ft down to the top Ekofisk formation, as a string has to be set 2/3 into Våle, which is the formation above top Ekofisk.

I.4 The concept of Anticollision

The definition of anticollision is given by Compass (2013b) as: "Anticollision can be used to check the separation of surveyed and planned Wellbores from offset wells. Anticollision provides spider plots, ladder plots, traveling cylinder, and printouts of well proximity scans. Any anticollision scans may be run interactively with planning, surveying or projecting ahead. All anticollision calculations are integrated with Wellbore uncertainties that are shown on graphs or reported as separation ratios. Warnings may be configured to alert the user when the Wellbores converge within a minimum ratio or distance specified by company policy."

For any new well on Ekofisk the anticollision is the first to be checked. The accuracy of a scan is based on the tools used (Gyro, MWD). The uncertainty is higher in old wells, as

outdated survey tools were used then. For these old surveys the ellipsis of uncertainty is larger, and the wellbore will for a longer section be within the scanned anticollision value.

The separation factor, given by Figure 101, is important for the scanning of anticollision. Based on this factor a separation factor view plot can be calculated, as showed in Figure 102. The area the scan will cover is pre-defined before scanning, and is usually decided by company regulations. SF = 1.0 means that the uncertainty ellipses of the reference well (plan) and offset well is intersecting each other. The intersected area becomes larger and larger with decreasing SF below 1.0.

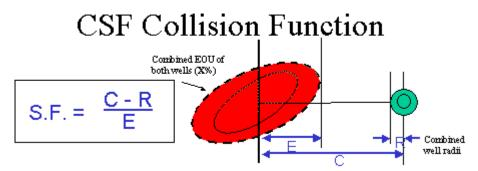


Figure 101: Separation Factor (SF) (Compass 2013b)

The guidelines for different values of separation factors for COPNO are presented in Table 20 and Table 21 for major and minor collision risks, respectively.

Table 20: Major collision risk based on separation factor (SF)

Proximity Ratio, Rp	Planning	Drilling	Notes		
			Drilling operations must cease until one of the below requirements is met:		
No.		Drilling operations must cease until of the below requirements is met: Plug back drilling well to a safe point where Rp>1.0 Take immediate action to increase Rother than drilling ahead Redefine potential collision to "Minor Collision Risk" and follow QRA procedures. Drilling operations should take swift, positive action to change drilling direction, increase survey accuracy other actions to increase Rp>1.5 Caution Continuously monitor Rp both onshould the suit of the positive action to change drilling direction, increase Rp>1.5			
Less than 1.0		Stop	Drilling operations must cease until one of the below requirements is met: Plug back drilling well to a safe point where Rp>1.0 Take immediate action to increase Rp other than drilling ahead Redefine potential collision to "Minor Collision Risk" and follow QRA procedures. Drilling operations should take swift, positive action to change drilling direction, increase survey accuracy or		
	Not permitted		Collision Risk" and follow QRA		
Between 1.0 and 1.5		Act	positive action to change drilling direction, increase survey accuracy or		
Between 1.5 and 2.5	Acceptable	Caution			
Between 2.5 and 3.0	Acceptable	Monitor			
Up to and including 4.0	Include in Collision Scan	IVIOTIILOI	j –		

Major risk elements are defined as producers and injectors (collision may lead to a catastrophe for environment and humans)

Table 21: Minor collision risk based on separation factor (SF)

Proximity Ratio. Rp Planning Drilling Notes								
Proximity Ratio, Rp.	Planning	Drilling						
Less than 1.0	Acceptable but only permitted when there is full risk analysis performed	Caution	Full Risk analysis is performed: Riskit meeting performed Mitigation agreed Signed approval by Chief engineer or delegate. A deviation must be entered into SAP Mitigation: Well is not producing or injecting Well in question is satisfactorily plugged and abandoned around zone of interest. (Also the case when sidetracking from original well) Well is in another clearly definable formation than the drilled well. Error models for wells in question have been checked and verified. HSE and financial risk is deemed minor after discussions and agreed mitigation in Riskit meeting					
Between 1.0 and 1.5	Acceptable but only permitted when there is full risk analysis performed	Monitor	Continuously monitor Rp including project ahead. There is a risk of magnetic interference if well in question is cased or that a fish exists, so the magnetic parameters need to be monitored.					
Between 1.5 and 2.5 Greater than 2.5	Acceptable	Monitor	There is a risk of magnetic interference if well in question is cased or that a fish exists, so the magnetic parameters need to be monitored.					
Greater than 2.5	Acceptable	Acceptable						

Minor risks are wells that are P&A-ed or shut-in (collision will only cause mechanical damage).

Figure 102: Separation plot (Compass 2013a)

APPENDIX J: Mærsk Gallant specifications

Below is the specification for the rig Mærsk Gallant listed in Table 22. A picture of Mærsk Gallant can be seen in Figure 103.

Table 22: List of specifications for Mærsk Gallant (Mærsk 2013)

Table 22: List of specifications for Mærsk Gahant (Mærsk 2013)						
Year of Construction	1993					
Class	Lloyd's Register of Shipping					
Work area	North Sea					
Hull dimension	78.2 m x 90.3 m x 10.8 m (257 ft x 296 ft x 35					
	ft)					
Length of legs	175.3 m (575 ft)					
Rated water depth	up to 125 m (410 ft)					
Rated drilling depth	7,620 m (25,000 ft)					
Variable load	5,000 t including hook load					
Cantilever reach	19.3 m x 4.6 m x 4.6 m (63.3 ft x 15 ft x 15 ft)					
Power supply	5 Caterpillar 3516 DITA					
Well control equipment	15,000 psi hp/ht					
Cranes	2 Liebherr BOS 50/1100, 1 BOS 34/930					
Cement pump	15,000 PSI (on free placement)					
Hoisting equipment capacity	1,650,000 lb (static hook load)					
Drawworks	1 LTV Emsco C-3, type II, 3,000 hp					
Top drive	1 Varco TDS-6S					
Mud pumps	3 Emsco FC-2200 triplex pumps					
Bulk mud capacity	260 m ³ (9,100 ft ³)					
Bulk cement capacity	160 m ³ (5,650 ft ³)					
Liquid mud capacity	5,035 bbl, slurry 1,880 bbl					
Accommodation	100 people					



Figure 103: Picture of Mærsk Gallant (Mærsk 2013)

The top drive on Mærsk Gallant is of the type Varco TDS-6S. At rotational speed of 195 RPM (max) the maximum torque is 60000 ft-lbf (Scribd 2013).

Appendix K: Setup for the mother wellbore

As mentioned in chapter 5 a common mother wellbore was assumed for all the three MLT options. In order to perform any simulations on the nine wellbore sections for thre three options the mother wellbore had to be established in Wellplan. As mentioned, it was early in the project face determined that this base case had to be realistic, meaning it had to be as identical as possible to the designated area in the Ekofisk South where the simulated multilaterals were decided to be placed. The creation of the mother wellbore was based on the actual nearby well 2/4-Z-17.

The vertical section of the well path for the mother wellbore down to the junction point can be seen in Figure 104, with the geothermal gradient in Figure 105.

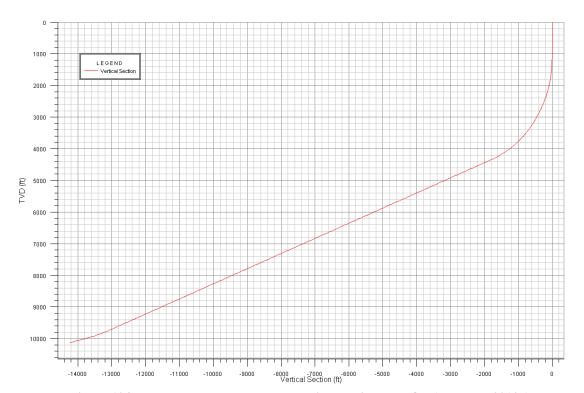


Figure 104: Mother wellbore well path vertical sections to TOE (Wellplan 2013a)

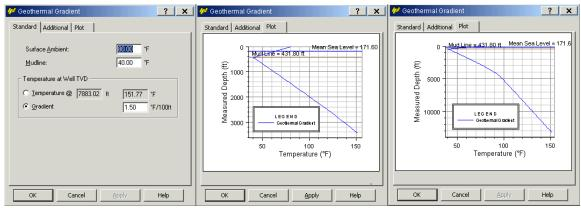


Figure 105: Geothermal gradient input in Wellplan for the mainbore (Wellplan 2013a)

To ease the required flow rate to achieve appropriate hole cleaning a booster pump was decided to be installed at the bottom of the riser. This would have an injection rate of 100 gpm. By doing this the minimum pump rate for cuttings transport would not be limited by the riser annulus, but by downhole sections. The booster pump setup can be seen in Figure 106. For the rest of the appendix, for simplicity, only the figures from the hole sections, pipe schematic, wellbore schematic and mud data are presented. In Wellplan no simulations were performed on the mother wellbore, and therefore only the setup, by using of the input modes shown in the figures in this appendix, were used.

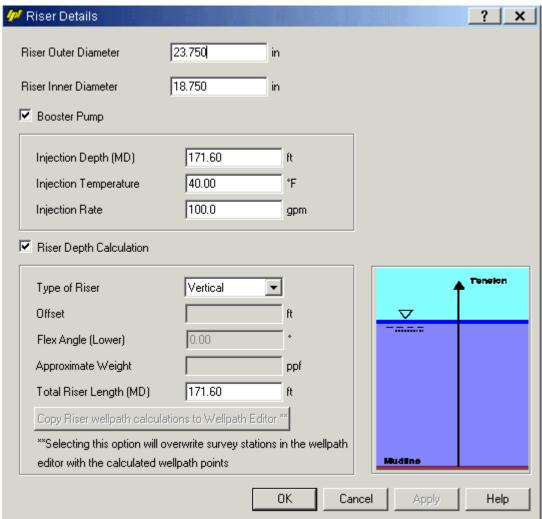


Figure 106: Riser booster pump configuration for both Scenario 1 and Scenario 2 (Wellplan 2013)

K.1 Drilling of the 20" x 17 1/2" hole section

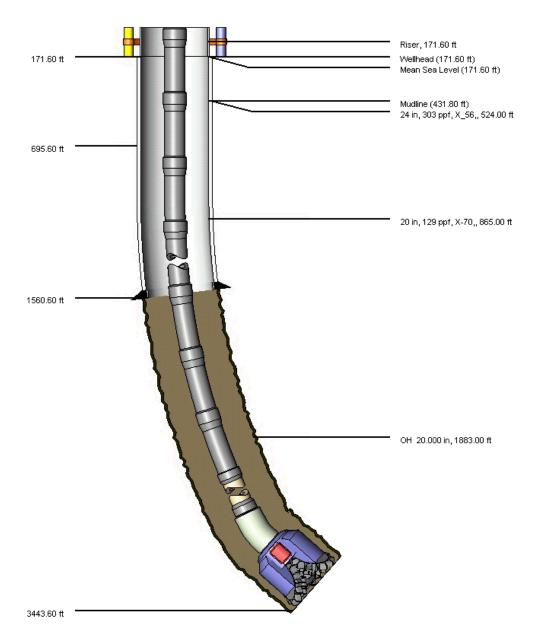


Figure 107: Schematic of hole sections with drillstring for the 20" x 17 $\frac{1}{2}$ " drilling in mainbore (to scale) (Wellplan 2013a)

Hole Section Editor									
Hole Na	ame: 17.17	2" Hole Section	Im	port Hole Section	on				
Hole Section Depth (MD): 3443.60 ft Additional Columns									
	Section Type	Measured Depth (ft)	Length (ft)	6.251 ID (in)	Drift (in)	Effective Hole Diameter (in)	Friction Factor	Linear Capacity (bbl/ft)	Item Description
1	Riser	171.60	171.60	18.750				0.3415	Riser
2	Casing	695.60	524.00	21.500	21.500	21.500		0.4490	24 in, 303 ppf, X_56,
3	Casing	1560.60	865.00	ן 18.750	18.750	18.750		0.3415	20 in, 129 ppf, X-70,
4	Open Hole	3443.60	1883.00	20.000		20.000		0.3886	
5									

Figure 108: Overview of the hole sections at the input page in Wellplan for 20" x 17 $^1\!/\!^2$ drilling in mainbore (Wellplan 2013a)

String Editor							
String	Initialization		Library				
String	Name Z-26 17 1/2" x 20" GP assembly		Export				
String	(MD): 3443.60 ft Specify: Top to B	ottom 🔻 Import String	Import				
	Section Type	Length	Measured Depth	OD	ID	Weight	Item Description
		(ft)	(ft)	(in)	(in)	(ppf)	
1	Drill Pipe	2631.79	2631.79	6.625	5.901		Drill Pipe, 6.625 in, 26.44 ppf, S-135, FH
2	Heavy Weight	270.00	2901.79	6.625	4.500		Heavy Weight Drill Pipe, 6.625 in, 64.43 ppf, S,
3	Drill Collar	4.00	2905.79	8.000	2.812		Drill Collar, 8.000 in, 146.15 ppf, S,
4	Drill Collar	89.00	2994.79	8.250	2.812		Drill Collar, 8.250 in, 146.15 ppf, S,
5	Jar	34.00	3028.79	8.000	3.000		Accelerator
6	Drill Collar	89.00	3117.79	8.250	2.812		Drill Collar, 8.250 in, 146.15 ppf, S,
7	Jar	33.00	3150.79	8.000	3.000	132.58	
8	Drill Collar	122.00	3272.79	8.250	2.812		Drill Collar, 8.250 in, 146.15 ppf, S,
9	Drill Collar	3.90	3276.69	9.500	2.810		Drill Collar, 9.500 in, 146.15 ppf, S,
10	Drill Collar	30.00	3306.69	9.500	3.000		9 1/2 × 3 - 216.9# Drill Collar
11	Drill Collar	3.00	3309.69	9.500	3.000		Float Sub w/non ported flapper
12	Drill Collar	8.90	3318.59	9.500	3.375		Split Flow Circ Sub (40 : 60 split)
13	Stabilizer	8.29	3326.88	9.500	2.810		Integral Blade
14	MWD	7.90	3334.78	9.500	2.375		Downhole Screen
15	MWD	10.20	3344.98	9.500	4.000		9 1/2 HOC
16	MWD	5.41	3350.39	9.500	2.375		9 1/2 HCIM Collar
17	Stabilizer	4.00	3354.39	9.500	2.375		Inline Stabilizer (ILS)
18	MWD	4.37	3358.77	9.500	2.375		9 1/2 PWD
19	MWD	7.64	3366.41	9.500	2.375		9 1/2 EWR-P4 Collar
20	MWD	5.04	3371.45	9.500	2.375		9 1/2 DGR Collar
21	MWD	25.00	3396.45	9.500	4.125		9 1/2 Evader Gyro
22	Underreamer	13.43	3409.88	9.500	2.800		Underreamer, 9.500 in, 267.00 ppf, V-150, 3 1/2 Reg. Pin
23	Drill Collar	9.20	3419.08	6.750	3.500		Geo-Pilot 9600 Flex Collar
24	Stabilizer	3.51	3422.59	9.625	2.375		Geo-Pilot 9600_0
25	Stabilizer	4.51	3427.10	9.625	2.375		Geo-Pilot 9600_1
26	Drill Collar	13.69	3440.79	9.625	2.375		Geo-Pilot 9600_2
27	Bit	2.81	3443.60	17.500		795.63	Tricone - (w/restrictor plate in sleeve)

Figure 109: Drillstring design for the drilling of the 20" x 17 ½" hole section in the mainbore (Wellplan 2013a)

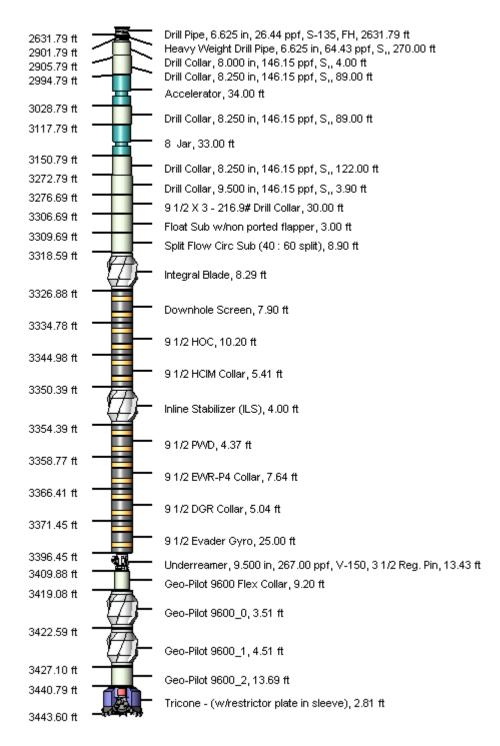


Figure 110: BHA Schematic for the drilling of 20" x 17 ½" hole section in mainbore (non-deviated, not to scale) (Wellplan 2013a)

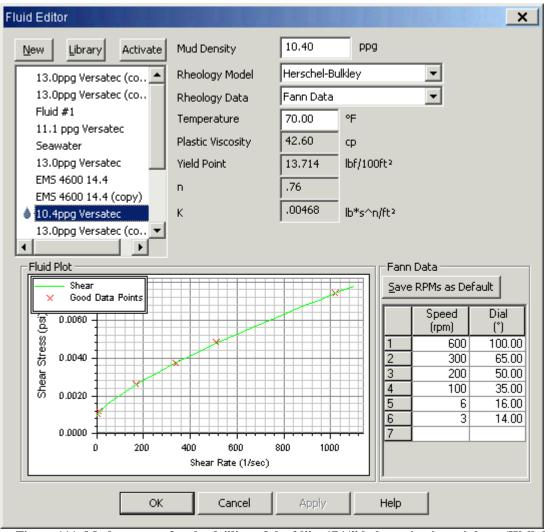


Figure 111: Mud program for the drilling of the 20" x 17 ½" hole section in mainbore (Wellplan 2013a)

K.2 RIH with 17" liner

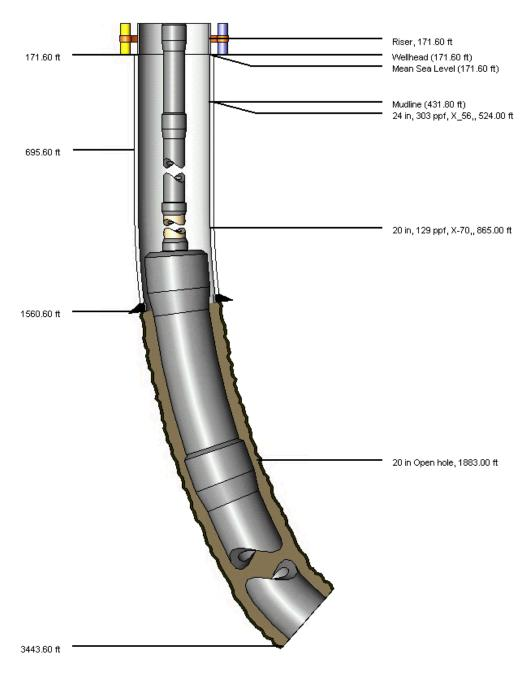


Figure 112: Schematic of hole sections with string for running of the 17" liner in mainbore (to scale) (Wellplan 2013a)

Hole sections presented in Figure 108 for the 17" liner.

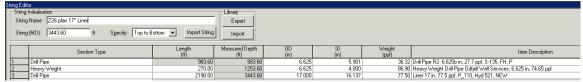


Figure 113: String design for the running of the 17" liner in the mainbore (Wellplan 2013a)

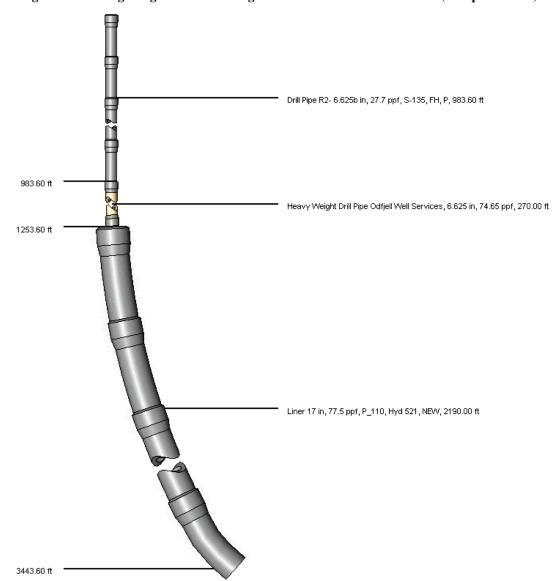


Figure 114: Component schematic for the running of 17" liner in mainbore (to scale) (Wellplan 2013a)

Mud as presented in Figure 111.

K.3 Drilling of the 16" hole section

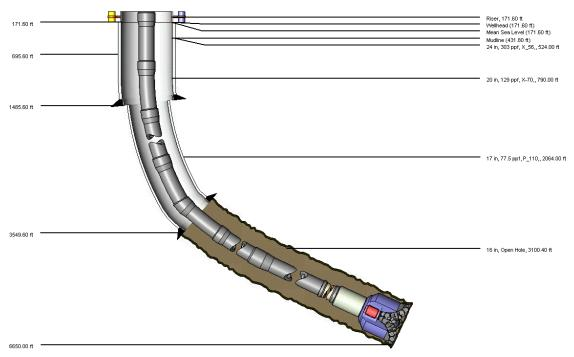


Figure 115: Schematic of hole sections with drillstring for the 16" drilling in mainbore (to scale) (Wellplan 2013a)



Figure 116: Overview of the hole sections at the input page in Wellplan for 16" drilling in mainbore (Wellplan 2013a)

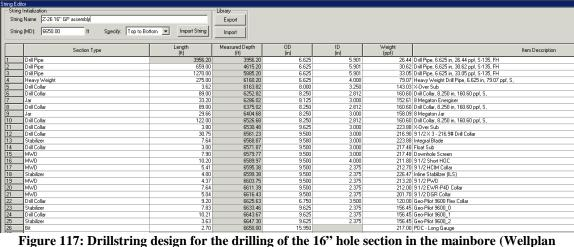


Figure 117: Drillstring design for the drilling of the 16" hole section in the mainbore (Wellplan 2013a)

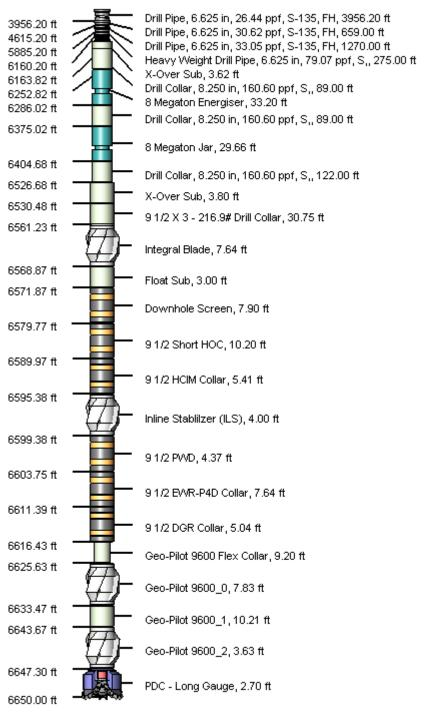


Figure 118: BHA Schematic for the drilling of 16" hole section in mainbore (non-deviated, not to scale) (Wellplan 2013a)

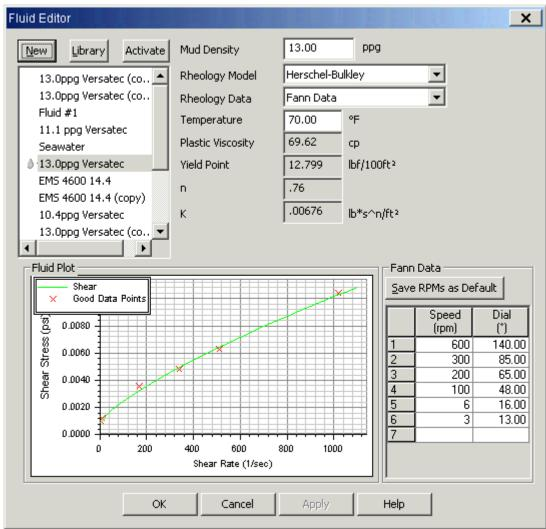


Figure 119: Mud program for the drilling of the 16" hole section in mainbore (Wellplan 2013a)

K.4 RIH with 13 5/8" casing

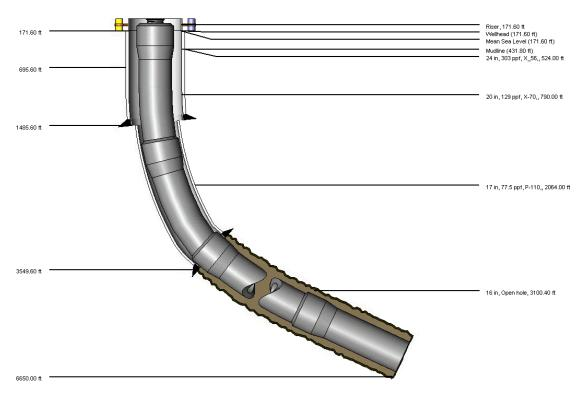


Figure 120: Schematic of hole sections with string for running of 13 5/8" casing in mainbore (to scale) (Wellplan 2013a)

Hole sections presented in Figure 112.

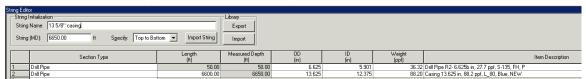


Figure 121: String design for the running of the 13 5/8" casing in the mainbore (Wellplan 2013a)

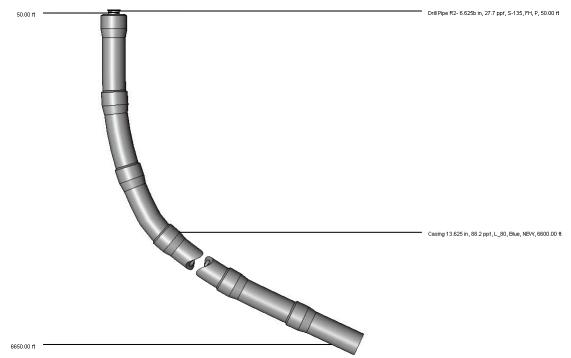


Figure 122: Component schematic for the running of 13 5/8" casing in mainbore (to scale) (Wellplan 2013a)

Mud as presented in Figure 119.

K.5 Drilling of the 12 1/4" hole section

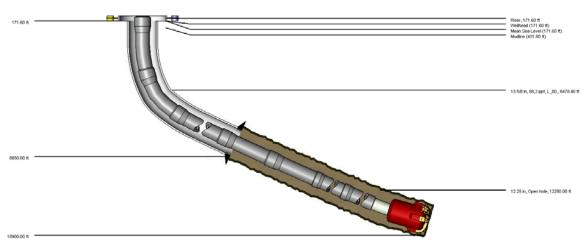


Figure 123: Schematic of hole sections with drillstring for the 12 $^{1}\!\!4$ " drilling in mainbore (to scale) (Wellplan 2013a)

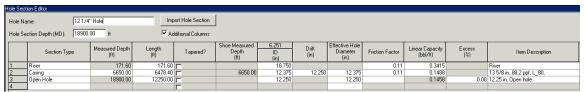


Figure 124: Overview of the hole sections at the input page in Wellplan for 12 $\frac{1}{4}$ " drilling in mainbore (Wellplan 2013a)

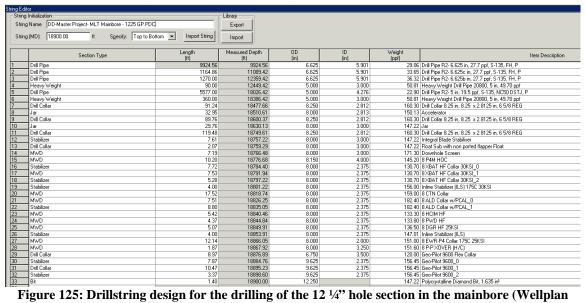


Figure 125: Drillstring design for the drilling of the 12 1/4" hole section in the mainbore (Wellplan 2013a)

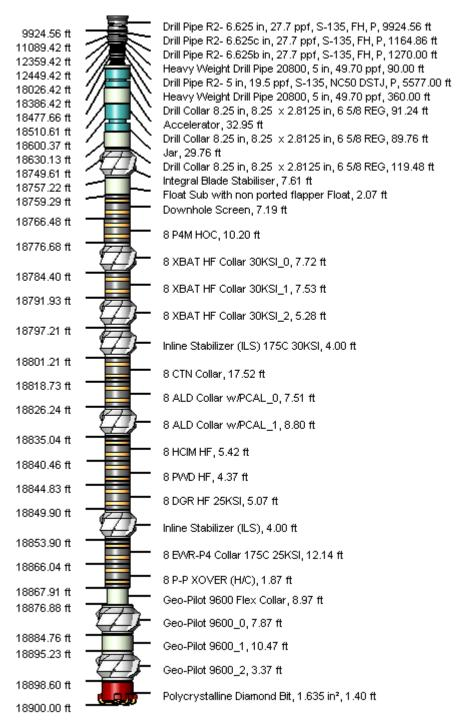


Figure 126: BHA Schematic for the drilling of $12\,\%$ hole section in mainbore (non-deviated, not to scale) (Wellplan 2013a)

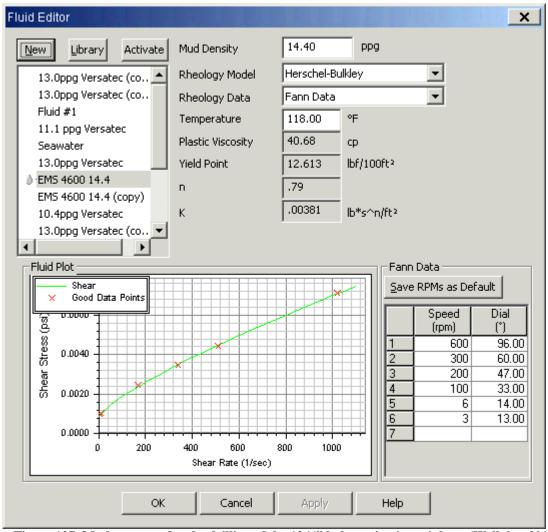


Figure 127: Mud program for the drilling of the 12 1/4" hole section in mainbore (Wellplan 2013a)

K.6 RIH with 10 ¾" liner

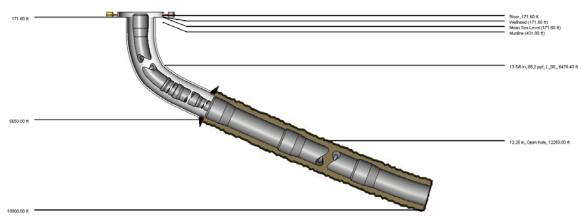


Figure 128: Schematic of hole sections with string for running of 10 $^{3}4$ " liner in mainbore (to scale) (Wellplan 2013a)

Hole sections presented in Figure 124.

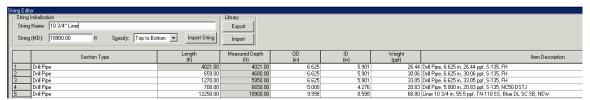


Figure 129: String design for the running of the 10 ¾" liner in the mainbore (Wellplan 2013a)

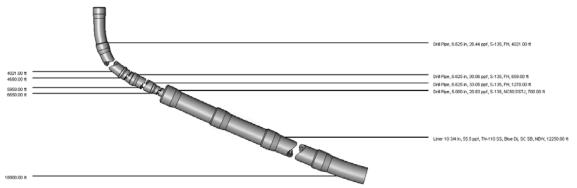


Figure 130: Component schematic for the running of $10\,\%$ " liner in mainbore (to scale) (Wellplan 2013a)

Mud as presented in Figure 127. As presented in chapter 4, the 10 $\frac{3}{4}$ " liner for the mother wellbore would be sat 2/3 into Våle at TOE. The junction would be placed at 18150 ft MD in this liner.

Appendix L: Setup for each of the nine wellbore sections in the MLT option

L.1 Making of the simulation base for MLT1 L1 for junction option 1

From the junction point in the mother wellbore the MLT1 option would split into two separate wellbores, making it a multilateral well, with Lateral 1 being the mainbore and Lateral 2 being the side branch. The motherbore from surface, as described in Appendix K, would be drilled with a 12 ½" bit to TOE, and a 10 ¾" liner would be installed 2/3 into Våle at TOE. The mainbore, or Lateral 1, would from there be drilled with an 9 ½" PCD long gauge bit down to TD at 24280 ft MD in Ekofisk. The hole sections were created in Wellplan according to this, as presented in Figure 131.

Section Type	Measured Depth	Length		Shoe Measured	6.251	777	Effective Hole						-
	(0)	(H)	Tapered?	Depth (b)	ID (in)	Drift (in)	Diameter (in)	Friction Factor	Linear Capacity (bbl/ft)	Excess (%)	Item Description	Manufacturer	Model
ier	171.60	171.60		4	18.750	~~~		1 3000	0.3415	- 2	Ripet		
sing	6650.00	6478.40		6650.00	12.375	12,250	12.375	0.18	0.1488		13 5/8 in, 88.2 ppf, L. 80.		
ising	19600.00	11950.00		19600.00	9.760	9.625	9.760	0.18	0.0925		10 3/4 in. 55.5 ppf, TN-110 SS, Blue DL S		
en Hole	24290.00	5680.00			9.500		9.500	0.18	0.0877	0.00	9 1/2 in openhole		
sin	9	9 6650.00 9 19600.00	9 6650.00 6478.40 9 19600.00 11950.00	9 6650.00 6478.40 (***) 1 10600.00 11950.00 (***)	9 6650.00 6470.40 F 6650.00 10600.00 11950.00 F 10600.00	9 6650.00 6470.40 (*** 6650.00 12.375 10600.00 11950.00 (*** 10600.00 9.760	9 6650.00 6478.40 F 6650.00 12.375 12.250 16600.00 11950.00 F 18600.00 9.760 9.625	9 6650.00 6478.40 (** 6650.00 12.375 12.250 12.375 16600.00 11950.00 (** 16600.00 9.760 9.625 9.760	9 6650.00 6470.40 T 6650.00 12.375 12.250 12.375 0.18 9 10600.00 11950.00 T 10600.00 2.760 2.625 2.760 0.19	9 6650.00 6478.40	9 6650.00 6476.40 6650.00 12.375 12.250 12.375 0.18 0.1400 16600.00 11560.00 10600.00 9.760 9.625 9.760 0.19 0.0025	g 6650.00 6476.40 (* 6650.00 12.375 12.570 12.375 0.16 0.1486 13.596.00.25 0.24.1,00. 1960.00 (* 1550.00 (* 1560.00 (* 2.375 0.25 0.276 0.16 0.005 10.24.6.155.5.84e.0.L.S	9 6650.00 6478.40 (* 6650.00 12.375 12.250 12.375 0.18 0.1488 13.549.6,88.2 cpt, L,00. 1800.00 11950.00 (* 1800.000) 3 760 9 625 9 730 0.19 0.0025 10.324 8.55 562.TN 10195.5,8 las 0.15

Figure 131: Hole sections for drilling of the 9 ½" hole from junction to TD for MLT1 Lateral 1 (Wellplan 2013a)

Then the drillstring for this section had to be created. A challenge for the simulation of the drilling of the multilateral wells from Z-26 to be investigated in this thesis was that there were little, or no, information about the underground in the specific area planned to place the wells. It was therefore assumed that the properties for the area where these multilateral wells would be drilled could be compared to the properties in the area where the actual well from the neighboring slot Z-17 had been drilled. This well was drilled in April 2013 (Maxwell 2013). All the six different wellbores simulated in this thesis would therefore identical BHA for equal hole sizes, with basis in the actual string used when COPNO drilled Z-17, and in after advise from both Halliburton and drilling engineer in ConocoPhillips Gunnar Namtvedt. The drillstring for MLT1 Lateral 1 can be seen in Figure 132. This drillstring would be unique for MLT1 L1 in the way that the length of the top DP section would be designed in order to reach TD, but otherwise similar to all the other 9 ½" sections drilled in the eight other wellbores.

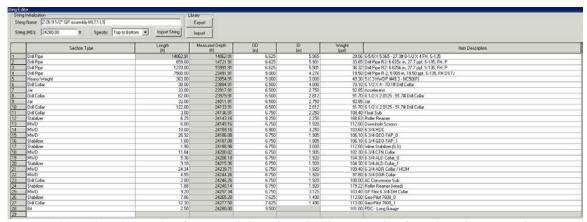


Figure 132: Drillstring design for the drilling of the 9 ½" hole section from junction to TD for MLT1 Lateral 1 (Wellplan 2013a)

Overview of the well schematic and BHA for the drilling of the 9 ½" section from junction to Ekofisk TD for MLT1 Lateral 1 are shown in Figure 133 and Figure 134, respectively.

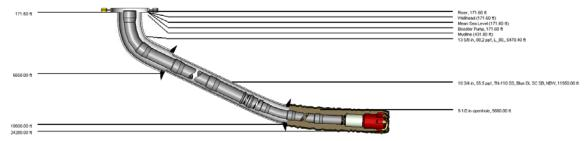


Figure 133: Well schematic for the drilling of the 9 $\frac{1}{2}$ " hole section from junction to TD for MLT1 Lateral 1 (Wellplan 2013a)

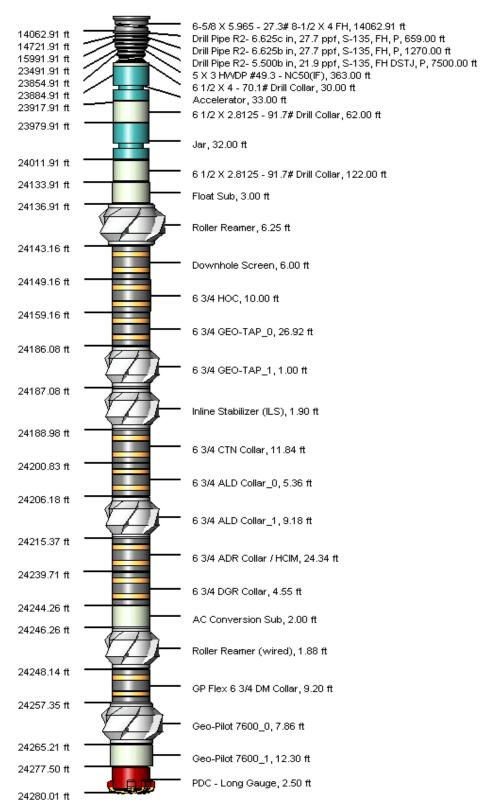


Figure 134: Initial BHA schematic for the drilling of the 9 ½" hole section from junction to TD for MLT1 Lateral 1 (Wellplan 2013a)

The well path for the wellbore from surface to junction point, presented more in detail in Appendix L, is shown in Figure 104. For the drilling of the 9 ½" section from the junction point to TD in Ekofisk for MLT1 Lateral 1 the path is, naturally, identical down to the junction point. From there on the well path is unique for this lateral down to total depth in the reservoir. In cooperation with Leif Inge Ramsvik in Halliburton the well path from the junction point to TD for Lateral 1 in the MLT1 option was created in the Compass software based on the target specified in Figure 17. The vertical section is presented in Figure 135 and the plan view in Figure 136. The tortuosity applied to the well path is shown in Figure 137. The sine wave configuration, with top at 12500 ft MD, magnitude of 0.5 degree, angle change period of 500 ft and depth interval of 30 ft are all default inputs in Wellplan and assumed to be valid for the simulations to be performed for the drilling of the 8 ½" section for MLT1 Lateral 1. The inclination and azimuth plotted against measured depth for the whole well path from surface to TD for the drilling of the 9 ½" section for MLT1 Lateral 1 are presented in Figure 138 and Figure 139, respectively.

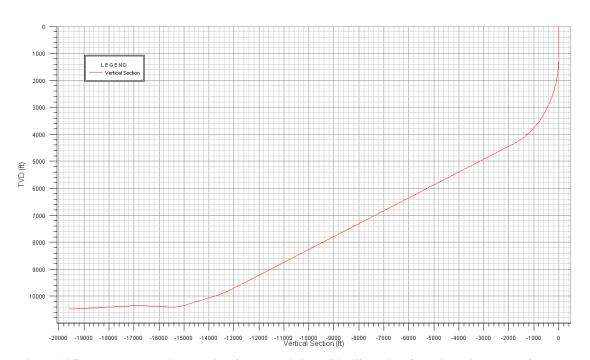


Figure 135: Well path vertical section for the drilling of 9 ½" section from junction to TD for MLT1 Lateral 1 (Wellplan 2013)

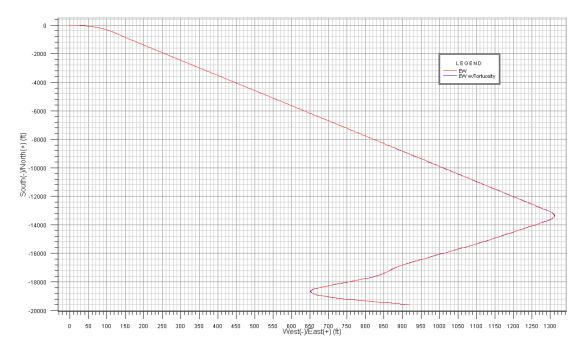


Figure 136: Well path plan view for the drilling of $9\frac{1}{2}$ " section from junction to TD for MLT1 Lateral 1 (Wellplan 2013)

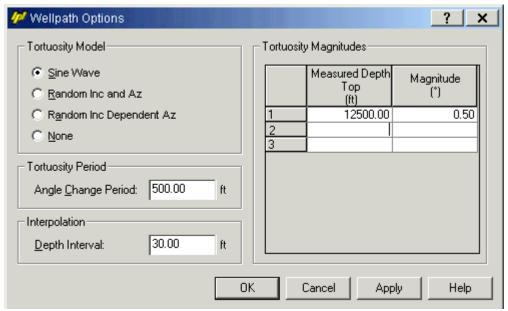


Figure 137: Well path tortuosity input for the drilling of 9 1/2" section from junction to TD for MLT1 Lateral 1 (Wellplan 2013)

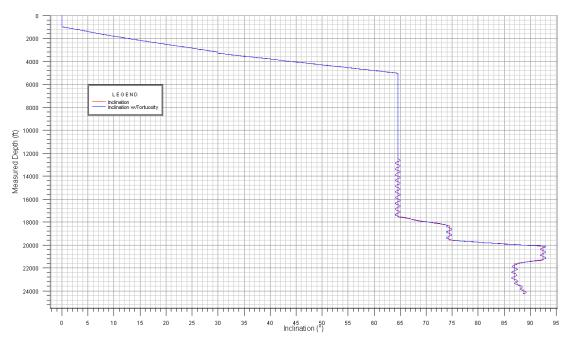


Figure 138: Well path inclination with tortuosity for the drilling of the $9\frac{1}{2}$ " section from junction to TD for MLT1 Lateral 1 (Wellplan 2013)

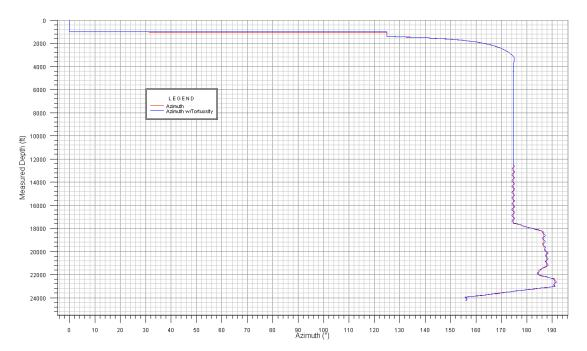


Figure 139: Well path azimuth with tortuosity for the drilling of the $9\frac{1}{2}$ section from junction to TD for MLT1 Lateral 1 (Wellplan 2013)

The geothermal gradient for the section to be drilled is presented in Figure 140. As no data collection had been done in the area at the time of simulation the underground temperature was assumed to be equal to the measurements from Z-17.

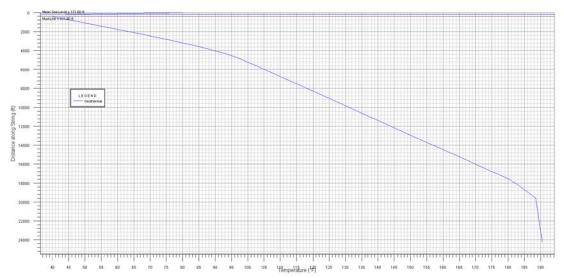


Figure 140: Geothermal gradient for the underground for drilling of the $9\frac{1}{2}$'s section from junction to TD for MLT1 Lateral 1 (Wellplan 2013a)

L.2 Making of the simulation base for the eight remaining wellbore sections

The creation of the simulation bases were done in the same manner for each of the nine different wellbore sections making up the three different MLT options. For simplicity, only the figures from the creation for MLT1 L1 was, as shown in Appendix L.1, were decided to include in this report. The process of setting up the setup were, however, quite similar for all the remaning eight wellbore sections. The desired figures for the eight remaining wellbores not showed here can be provided by the author upon request.

Appendix M: The Wellplan software

Wellplan, as described by Nesland (2012), is made up of, and based around, seven different modules, as seen in Figure 141. These are Torque and Drag analysis, Hydraulics analysis, Surge and Swab analysis, Well Control analysis, Critical Speed analysis, Bottomhole Assembly analysis and Stuck Pipe analysis. In addition there is a module for input of general well data, as shown in Figure 142. A list of features of what is covered in the modules can be found in Appendix N.

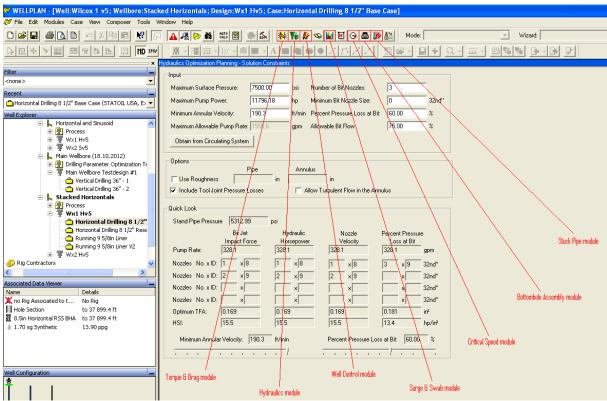


Figure 141: Overview of the different modules in Wellplan (Wellplan 2012)

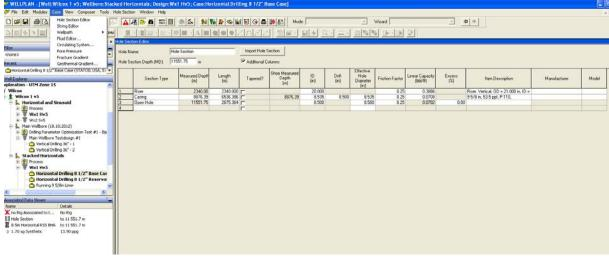


Figure 142: Wellplan interface showing the general well input module. The dropdown curtain under "case" is different from when other modules are selected allowing the user to input general data (Wellplan 2012)

M.1 Torque and Drag Analysis

This module focuses mainly on the measured weights and torques in different aspects of drilling and at different depths in the well. Results from tripping in and out, slide drilling, backreaming and rotating on and off bottom is then used to determine whether a well, or a portion of the well, is drillable or not. In addition buckling, and type of buckling (helical, sinusoidal, transitional or lockup), can be analyzed. Based on these results consideration must be done if it is necessary, or desired, to change the design of the well. These changes can be in the drillstring, casing strings, tieback strings, tubing strings, coiled tubing strings or liners (Halliburton/Landmark 2008).

M.2 Hydraulics Analysis

The hydraulics of a well can be analyzed using the Hydraulics module. Based on the selection of one of the rheological models (Bingham, Plastic, Power Law, Newtonian or Herschel Bulkley, the pressure losses in the well will be calculated. From this the selection of bit and jets will be made for optimum bit hydraulics, the minimum flow rate for cleaning of the hole and the maximum flow rate for avoiding turbulent flow is determined, as well as surge and swab hydraulic pressures. In addition an evaluation of the rig operational hydraulics can be done (Halliburton/Landmark 2008).

M.3 Well Control Analysis

Based on oil, water or gas influx (gas being default) Well Control analysis can be done. The influx volumes are calculated, and evaluations of the results from an influx are presented. Both maximum inflow volumes and maximum safe drilling depths are determined. From this the user are guided in the selection of casing setting depths and kill sheets are automatically generated. A weakness of this module is the lack of

dispersed gas modeling as only single bubble methane influx can be analyzed (Halliburton/Landmark 2008).

M.4 Critical Speed Analysis

In this module, by evaluating the resonant rotational speeds in revolutions per minute (RPM) by use of the Forced Frequency Response (FFR) technique, the critical rotating speeds are determined. Several features are considered in this analysis to more accurately represent the downhole environment and determine the areas of high stress concentration in the well, including intermittent contact/friction, buoyancy, finite displacement, 3D lateral bending vibrational response of the Bottomhole Assembly (BHA), axial, lateral and torsional vibrations, damping and mass effects (Halliburton/Landmark 2008).

M.5 Bottomhole Assembly Analysis

This module, made up of a static "in-place" condition and a "drillahead" non-static condition, is used to predict build and drop in the BHA. By including factors as WOB, sizes in the drillstring and formation type, the behavior of the BHA is analyzed. Due to the complexity of the many non-controllable parameters affecting the BHA, these predictions are very complex. As a result of this the Bottomhole Assembly modules uses Finite Element Analysis (FEA), a method that breaks the overall calculations into tiny elements solving each one separately (Halliburton/Landmark 2008).

M.6 Stuck Pipe Analysis

The stuck point is determined using this module. At this location in the well the forces acting on the drillstring are calculated, and both the overpull without yielding the pipe, as well as the measured weight necessary to set the jars, are analyzed. Based on these results suggestions of how to react, and what actions to do topside, in order to achieve the conditions desired at the back-off point are given. A limitation in this module is in the yield strength analysis where fatigue is not considered (Halliburton/Landmark 2008).

Appendix N: List of features in the Wellplan modules

Table 23: List of features in the Wellplan modules (Halliburton/Landmark 2008)

Table 23: List of features in the Wellpla	
General Well Data Input Module	 Integration between Wellplan software
	modules
	Defining the hole section
	 Defining the drillstring and
	components
	Defining well path and tortuosity
	 Defining wellbore fluids
Torque and Drag Module	Analytical methods of T&D
	Stiff string and soft string models
	Mechanical limitations
	Tripping and drilling modes
	 Defining friction factors
	Analyze T&D at TD
	Analyze T&D at other depths
	 Examine effective and true tension
	Examine fatigue
	 Determine the torque acting on the
	string
	 Investigate the buckling possibilities
	 Investigate solution to T&D issues
Hydraulics Module	Examine hole cleaning at various pump rates
	 Investigate effects of ROP on hole
	cleaning
	 Determine pressure losses
	 Determine annular velocity
	 Input of circulating system information
	Investigate required horsepower
	■ ECD check
	 Hydraulics optimization
Surge and Swab Module	Analyze transient surge/swab
	pressures and ECD's
	 Generation of a trip schedule
Well Control Module	Investigate well control
	 Determine predicted kick type
	Estimate influx volume and kick
	tolerance
	Evaluate pressures as a kick is
	circulated out
	 Predict a safe drilling depth
	Generate a kill sheet

Critical Speed Module	 Determine critical rotational speeds Examine the stresses acting on the workstring at various ROP's Determine type of stress and where it occurs Examine string displacements Review bending moments
Bottom Hole Assembly Module	 Predict BHA build and drop Evaluate BHA contact points along the wellbore Analyze the effect of various WOB and ROP combinations on BHA performance
Stuck Pipe Module	 Estimate a stuck point for specified surface conditions and string sketch Determine loads required to set and trip a jar Determine load required to yield the pipe

Appendix O: Setting up initial drilling parameter values, Scenario 1 and Scenario 2, for input in Wellplan

O.1 Common setup values valid for both Scenario 1 and Scenario 2

BHA

It was assumed that equal hole sizes would have equal BHA, bases on the actual BHA used when drilling the neighboring well Z-17. The difference in the drillstring for each of the six possible wellbores would be length of the drill pipe in order to get to TD. The BHA used for each of the wellbores is presented in the making of each simulation base in Appendix L.

Drilling fluid properties

The drilling fluid properties for both Scenario 1 and Scenario 2 for the initial simulations were set based on the underground data from well 2/4-A-21, a closely offset well, as well as experience from the drilling of Z- 17^{42} , and a mud weight of 12.4 ppg was selected as the initial suggestion for the simulations to be performed, as presented in Figure 143. The other properties of the drilling fluid were all extracted from the drilling of Z-17.

233

⁴² Personal communication with G. Namtvedt. 2013. Stavanger: ConocoPhillips Norway

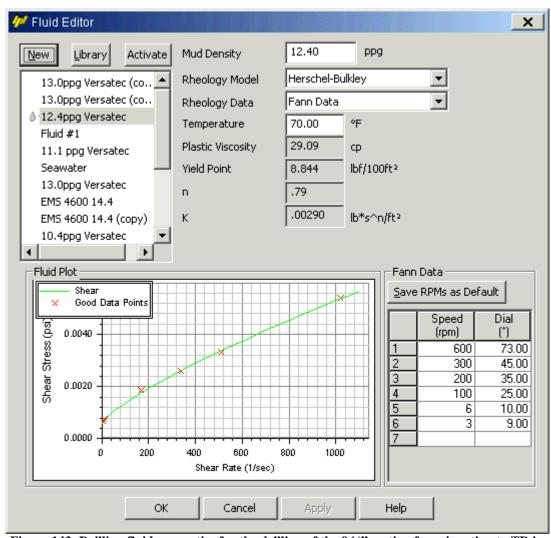


Figure 143: Drilling fluid properties for the drilling of the $9\,1\!/2$ ' section from junction to TD in Ekofisk for MLT1 Lateral 1 (Wellpan 2013)

Rig specific setup and pipe modeling

The traveling assembly weight was set to 24.7 klbf, which corresponds to the actual weight rating at Mærsk Gallant, the rig planned to drill all the wells on Ekofisk Zulu⁴³. Then the buckling limit and contact force normalization length were determined to be 1.0 and 31.0 ft, respectively. The Buckling Limit Factor, or BLF, is a multiplier applied to the buckling Eq. used in Wellplan. A BLF of 1.0, as was assumed for these simulations, means that the buckling conditions will follow the Eq., while a higher or lower value than 1.0 will increase or reduce, respectively, the buckling limit of the material investigated (Wellplan 2013b). The contact force normalization is the length of the reported contact forces in the well (Wellplan 2013b). For both scenarios this length was set to be 31 ft to report the force per length of pipe. Further the "use bending stress magnification" box was checked off. The Bending Stress Magnification Factor, or simply

_

⁴³ Personal communication with T. Gaup. 2013. Stavanger: ConocoPhillips Norway

BSFM, presented in 45, is defined as the absolute curvature value in the pipe body divided by the curvature of the hole axis.

$$BSFM = \frac{\left| Curvature_{pipebody} \right|}{Curvature_{hole\,axis}} \tag{45}$$

To more accurately calculate the bending stresses in a pipe with a TJ larger than the OD of the body of the pipe the BSFM can be applied as a multiplier. For such a case, when the string is subjected to compressional or axial load, the hole axis curvature will be less than the maximum curvature of the DP. Therefore local max curvatures, represented through the BSFM, can be input to yield more accurate calculations of the bending stresses of the pipe body. With the BSFM box checked off the magnifier will be applied to the calculation of the von Mises stress off the pipe in the Wellplan analysis (Wellplan 2013b). The sheave friction correction was ignored and assumed to be irrelevant for the total torque and drag calculations. The same was the case for the viscous torque and drag. This is the additional drag force applied to the system due to the downhole hydraulic effect of the drilling fluid on the pipe. Further was the soft string model used, and therefore was the stiff string model box left unchecked. The soft string models the drillstring as a cable, rather than a stiff pipe. This modeling makes the soft string able to carry axial loads, but not bending moments. As a result of this the cable is assumed to constantly be in contact with the wellbore at all times, thus ignoring the bending moments and radial clearance. The cable is divided into sections, where each section contributes to increased weight, drag and torque. The ignored moments in soft string model resulting from bending will impact the total tension indicated in the string (Midtgarden 2010). The stiff string model, on the other hand, accounts for tubular stiffness in bending, stiffness modified for compressive forces, single point weight concentrations and tubular joint to hole wall clearance. It models the string in 30 ft sections and calculates the force on the side at the center, which again is transformed into the torque and drag computations. Compared to the soft string model the stiff string model typically yields a slightly lower drag value due to the straightening out of the pipe and wellbore through doglegs. At the same time, for wellbores with many, and especially high, doglegs, the stiff string model often can increase the drag output due to more pipe being modeled to move against the borehole (Wellplan 2013b).

The block and torque ratings are rig specific, see Figure 144. For Mærsk Gallant the hoisting capacity is 1 650 klbf and max torque, given by the rotary table (Varco TDS-6S) is 60000 ft-lbf. Neither of the values are used in any calculations in Wellplan, but will be present in result graphs to easier see the constraints. A detailed presentation of Mærsk Gallant is presented in Appendix J. The three last boxes, maximum WOB rotating (no sinusoidal buckling), maximum WOB rotating (no helical buckling) and maximum overpull using % of yield, were all checked off. The first of these is used to calculate the largest WOB the string can handle before sinusoidal buckling occurs, as described in

chapter 5.7. The second is for helical buckling. The last, the maximum overpull using % yield, is used to compute the maximum drag weight, or overpull, the rig will encounter during tripping out before yielding the pipe. The percentage indicated gives the maximum extra weight above the static hook load that can be accepted (Wellplan 2013b). In this case it was assumed that a 10 % safety margin was needed, so the maximum allowable overpull would be 90 % of the yield strength of any section of the pipe at a given depth.

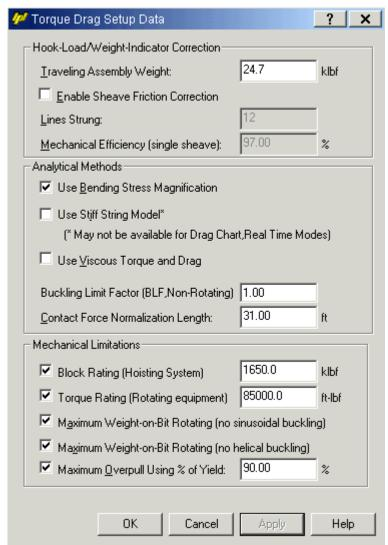


Figure 144: Torque and Drag Setup Data used for both Scenario 1 and Scenario 2 (Wellplan 2013a)

Torque at bit

Based on measurements performed by Midtgarden (2010) a constant torque at bit of 2500 ft-lbf was assumed, as presented in chapter 6.

Tripping speeds and friction factors

The tripping in and tripping out speed was set to 60 ft/min, based on default settings in the Wellplan software. The friction factors for both openhole and casing were set based on work performed by Midtgarden (2010), where it was showed, via reverse-calculations data from actual drilling on Ekofisk, that a friction factor of 0.18 was appropriate for both cases.

Circulating System

The circulation system was set up based on the actual mud pumps on Mærsk Gallant. A total of three ESCO FC-2200 triplex pumps are installed on the rig, each with a maximum discharge pressure of 5000 psi at speed 105 spm and 3.907 gal/stroke. A volumetric efficiency of 85 % was assumed, resulting in a maximum pump rate of 348.7 gpm per pump. Further it was assumed that the three pumps would be installed in parallel, so that total max horsepower rating and total maximum pump rate would increase to 6600 hp and 1046.1 gpm, respectively. The maximum SPP on Mærsk Gallant is 5500 psi⁴⁴. The rig specifications and details regarding the pumps there are found in Appendix AAAAA and Appendix BBBBB, correspondingly. It was further assumed a surface equipment pressure loss of 100 psi. This value was set based on typical pressure losses in surface equipment, but will in real-life vary with total length, number of bends and sizes of the equipment⁴⁵. The simulations would therefore not calculate the pressure loss in the surface equipment, but instead add this pre-determined value to the total system loss.

_

⁴⁴ Personal communication with T. Gaup. 2013. Stavanger: ConocoPhillips Norway

⁴⁵ Personal communication with S. Tørressen. 2012. Lindesnes: Acona Wellpro

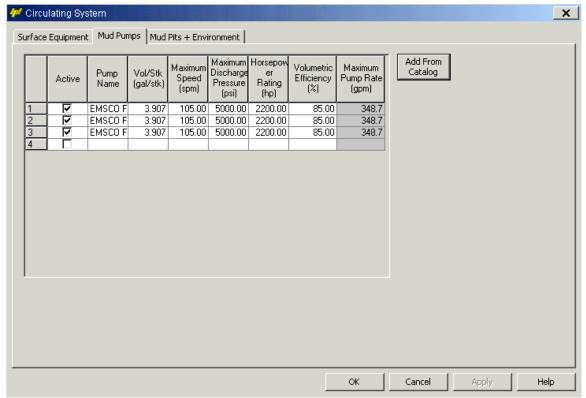


Figure 145: Circulating system setup for both Scenario 1 and Scenario 2 based on Mærsk Gallant specifications (Wellplan 2013)

Run Parameters for Torque and Drag at Other Depths than TD analysis

The run parameters were determined to be divided into 100 ft sections, with start at surface and end at TD for each respectable wellbore section for the three MLT options.

Bit data

The bit data for the drilling of all the 9 %" sections in the six different wellbores, with nozzle count and size giving the Total Flow Area (TFA), was specified based on the bit used for drilling of the 8 %" section on Z-17. This would of course represent a source of error. Further was the same bit used for the three 8 %" section for the MLT options. The input page, with a print screen from the Z-17 Well Report in Maxwell, is presented in Figure 146. By copying the bit configuration from the Z-17 it was assumed, as an initial consideration, that these values could be valid and usable also for all the 8 %" and all the 9 %" section to be drilled.

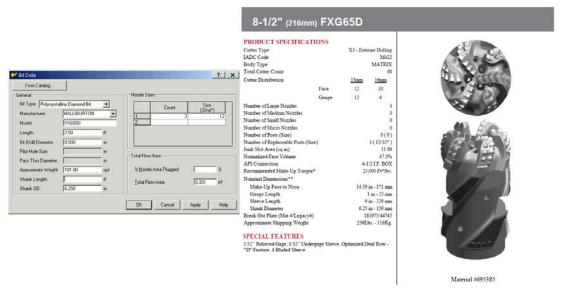


Figure 146: Initial bit and nozzle configuration for the drilling of all the $8 \frac{1}{2}$ " sections in the MLT options. For the $9 \frac{1}{2}$ " section the BHA had the same design, but larger bit diameter, naturally (Wellplan 2013; Maxwell 2013)

Rock properties

The cuttings diameter and density were both assumed to be equal to the Wellplan default input of 0.125'' and 2.5 sg, respectively. The bed porosity was selected to 36.0 %, an assumed value within the actual Ekofisk rock porosity range of 25-45 %, as mentioned in Chapter 2.

Transport analysis data for hydraulic effects

For both Scenario 1 and Scenario 2 a calculation interval was set to 100 ft MD, with start at surface and end at each of the six wellbores respective TD's.

Riser setup with booster pump

For both scenarios a booster pump would be installed in the riser to ease the cuttings transport in this section. For the 9 $\frac{1}{2}$ " section and scenario 1 parameter values in MLT1 L1 the minimum pump rate for hole cleaning was 618.4 gpm in the riser annulus. With a booster pump of 100 gpm installed the requirement to lift the cuttings would be reduced leading to sufficient hole cleaning in the 13 5/8" annulus. The booster pump configuration can be seen in Figure 106.

O.2 Scenario 1 parameter input values

WOB and Torque at bit for Torque and Drag analysis

The WOB for Scenario 1 was the lower limit in the Halliburton recommendations when drilling Z-17. For all sections this would mean a WOB of 10 klbf. The torque at bit and tripping in/out values, as discussed, would be equal for both Scenario 1 and 2, at 2500 ft-lbf and 60 ft/hr, respectively. For the slide drilling the WOB for Scenario 1 is also 10 klbf, even though not likely to a utilized method for the drilling of the MLT options. Backreaming overpull was determined to be 8 klbf. A summary of the WOB and Torque at bit values for Scenario 1 for all sections to be simulated is shown in Figure 147.

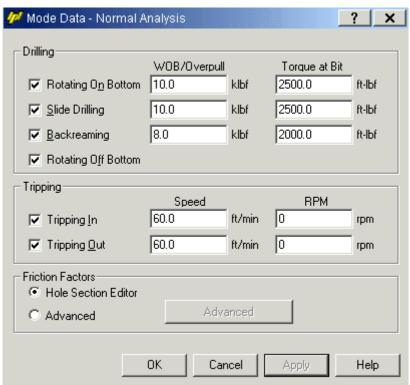


Figure 147: Torque and Drag Setup with WOB, torque at bit and tripping speed for Scenario 1 (Wellplan 2013)

Transport analysis data for Hydraulic simulations

For both Scenarios a calculation interval of 100 ft MD was set. For scenario 1 the pump rate would be 450 gpm and ROP 25 ft/hr. The rotary speed would be 140 rpm, as mentioned. The initial 450 gpm was based on the lowest value in the Z-17 recommendations from Halliburton of pump rate between 450 - 650 gpm for the drilling of the 8 ½" section there (Maxwell 2013). In Wellplan ROP is an input variable rather than an output variable. This means that instead of getting a penetration rate based on other input values, a desired ROP is set and then Wellplan gives an output of what the other input values have to be in order to be able to achieve the set ROP, which may lead to challenges (Nesland 2012). For the drilling of the reservoir section on Ekofisk the ROP

most often varies between 30 and 40 ft/hr⁴⁶. As an conservative value an ROP of 25 ft/hr was therefore set for Scenario 1. These initial transport analysis input data for Scenario 1 are shown in Figure 148.

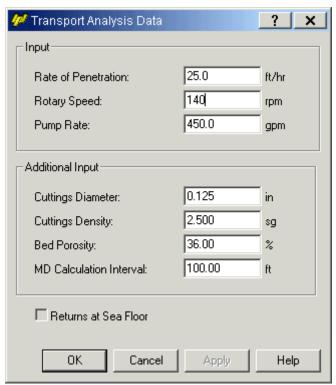


Figure 148: Transport analysis data initial setup for Scenario 1 (Wellplan 2013)

O.3 Scenario 2 parameter input values

WOB and Torque at bit for Torque and Drag analysis

For Scenario 2 the WOB would be 25 klbf, presented in Figure 149, the higher limit of the interval Halliburton recommended for the actual drilling of Z-17. The torque at bit for each operation would be the same as for Scenario 1.

⁴⁶ Personal communication with G. Namtvedt. 2013. Stavanger: ConocoPhillips Norway

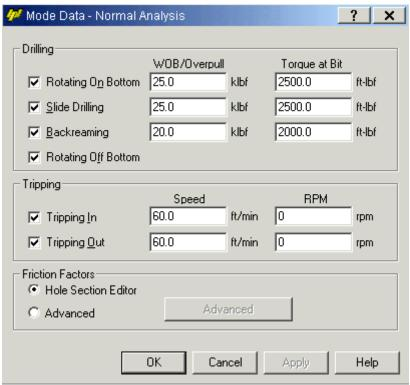


Figure 149: Torque and Drag Setup with WOB, torque at bit and tripping speed for Scenario 2 (Wellplan 2013)

Transport analysis data for Hydraulic simulations

A pump rate of 650 gpm was selected for Scenario 2. The ROP was set to 40 ft/hr, with a rotary speed of 195 rpm, see Figure 150. The rotational speed while drilling was recommended to be between 140 and 250 rpm for well Z-17 (Maxwell 2013). However, the maximum rotary speed for the topdrive on Mærsk Gallant is 195 rpm, and for Scenario 2 this value was selected instead of 250 rpm. As for Scenario 1 the calculation interval would be 100 ft.

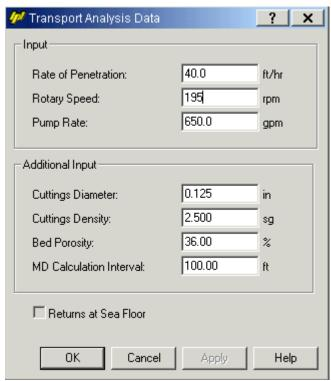


Figure 150: Transport analysis data initial setup for Scenario 2 (Wellplan 2013)

Appendix P: Iteration processes in Wellplan to find the suggested parameter input values

In this appendix a rough presentation of the iteration processes performed in Wellplan for each of the nine wellbore sections in order to end up with a set of suggested parameter values. As it can be seen the iteration process presentation here is quite rough, and only takes into account the major steps that were performed. In addition only short form of language has been used, rather than writing the whole sentence as one. This is not good practice for a report, but for the presentation of the iterations in this Appendix is was assumed to be of no larger significance, and equally well point out the important results as whole sentences.

P.1 MLT1 L1

For MLT1 L1 the suggested parameters are as listed in Table 24.

Table 24: Suggested parameter values for MLT1 L1

Table 24. Suggested parameter values for WILTI LT
WOB = 25 klbf
RPM = 195
ROP = 25 ft/hr
Flowrate = 680 gpm
MW = 11.20 ppg
New bit nozzle config: 3x(18/32) instead of 3x(12/32)
(Contingency: Tieback 10 3/4" Liner to surface without changing BHA)

The iteration process from the start parameters equal to scenario 1 values were as given below:

- 1) Startet off with scenario 1 values.
- ECD above frac limit. Decide to reduce MW.
- 2) Set MW at 11.10 ppg.
- ECD just below PP at last csg shoe.
- 3) Check hole cleaning requirement. 717.1 gpm needed to clean 13 5/8" annulus. Set pump rate to 680 gpm. Increase RPM from 140 to 195 to improve hole cleaning.
- Min flowrate for hole cleaning is now 674.8 gpm.
- 4) Check ECD again. ECD within the drilling window, however close to the PP at last csg shoe (a bit too close).
- 5) Check SPP. SPP is 7664.77 psi, above the max of 5000 psi surface pressure.
- 6) Change from 3x12 bit nozzles to 3x18 bit nozzles to reduce SPP.
- SPP is now 4210.42 psi.
- 7) Increase MW to 11.20 ppg to not go UB just below last csg shoe.
- MIn flowrate is now 667 gpm. I have set pumprate of 680 gpm.
- 8) Check summary loads for WOB 10.

No issues.

9) Increase WOB to 25.

S-buckling for slide drilling. No other issues. Set WOB for slide drilling to 15 klbf. WOB for rot on bottom (which is what is investigated) is set to 25 klbf.

P.2 MLT1 L2 9 1/2"

Table 25: Suggested parameter values for MLT1 L2 9 1/2"

The iteration process for the MLT1 L2 9 ½" section was as following:

- 1) Started off at Scenario 1 parameters.
- 2) Check ECD.

The ECD is within the drilling window, quite in the middle. So for faster ROP the overbalance should be less, so more optimum would be if the ECD was closer to the PP line. However, a trip margin should be added to the PP to take prevent UB due to surge pressures when tripping out. The TM is often 0.5 ppg above pore pressure. Estimates vary from 1 - 2% of the MW added to the PP⁴⁷.

3) Check hole cleaing requirements.

Min flowrate is 618 gpm.

4) Increase pumprate to 620 gpm. Increase ROP to 195 to help cleaning the hole.

Min flowrate is now 581 gpm.

5) Check ECD again.

ECD can be reduced more for faster ROP. At last csg shoe ECD is 13.18 ppg, could be reduced to 12.80 ppg.

Reduce MW to 12.1 ppg. ECD is now good.

6) Check min flowrate.

This is now 602 gpm, less than pumprate set to 620 gpm.

7) Check SPP.

This is 6656 psi, higher than the max surface pressure of 5000 psi.

8) Choose 3x18 nozzles instead of 3x12.

SPP is now 3526 psi.

-

⁴⁷ Personal communication with S. Tørressen. 2013. Lindesnes: Acona Wellpro

9) Check Load Summary.

For WOB 10 klbf no issues. Increase WOB rot on bot to 25 klbf. Still no issues.

P.3 MLT1 L2 8 1/2"

Table 26: Suggested parameter values for MLT1 L2 8 1/2"

Table 20. Suggested parameter values for WETT 12 0 /2
WOB = 25 klbf
RPM = 195
ROP = 25 ft/hr
Flowrate = 640gpm
MW = 11.1ppg
New bit nozzle config: 3x(18/32) instead of 3x(12/32)
(Contingency: Tieback 10 3/4" Liner to surface without changing BHA)
WOB slide: 15 klbf
WOB back: 20 klbf.
Trippin in/out: 60 ft/min, 0 RPM

The iteration process for the MLT1 L2 8 ½" section was as following:

- 1) Start off with Scenario 1 parameters.
- 2) Check ECD. It is too high, as the FG line is crossed towards bottom.
- 3) Check min flowrate.

This is 614 gpm.

4) Increase pump rate to 600 gpm. Set RPM to 195 for help cleaning hole. Decrease MW to 10.4 ppg.

Min flowrate now 629 gpm.

5) Check ECD again.

ECD now a bit too low at last csg show. UB by ca 0.4ppg.

6) Increase pump rate to 640 gpm.

ECD still a bit too low at last casing shoe.

7) Increase MW to 11.1 ppg.

Min flowrate now 582.6 gpm. ECD is totally within the drilling window, with a clearance above PP at last csg shoe of around 0.3 ppg.

8) Check load summary.

No issues at WOB 10 klbf.

9) Increase WOB to Scenario 2 values.

Now S-buckling for slide drilling.

- 10) Decrease WOB for slide to 15 klbf. Now no issues.
- 11) Check SPP.

With 3x12 nozzles it's 7666 psi, above max surface of 5000 psi.

12) Select 3x18 nozzles.

Now SPP is 4606 psi.

P.4 MLT2 L1

Table 27: Suggested parameter values for MLT2 L1

Table 27. Suggested parameter values for ME12 E1
WOB = 25 klbf
RPM = 195
ROP = 25 ft/hr
Flowrate = 640 gpm
MW = 10.5 ppg
New bit nozzle config: 3x(18/32)
(Contingency: Tieback 10 3/4" Liner to surface without changing BHA)
Tripping out RPM: 120
WOB slide: 10 klbf
WOB back: 20 klbf

The iteration process for the MLT2 L1 section was as following:

1) started off at Scenario 1 parameters. Check ECD.

The ECD is too high, and will frac the formation below around 26000 ft MD.

2) Select MW 11.1 ppg.

ECD now looks fine, except crossing the frac line towards TD around 28000 ft MD.

- 3) Check min flowrate. This is 623.5 gpm for selected MW.
- 4) Set pumprate to 620 gpm. Increase RPM to 195 to improve hole cleaning.

Min flowrate is now 585.5gpm, given by the 13 5/8" annulus.

- 5) Check ECD again. Too high towards TD.
- 6) Reduce pumprate to 580 gpm and MW to 10.9ppg.

ECD looks better, but still above frac limit towards TD.

7) Reduce MW to 10.6 ppg.

Now ECD is more or less within the drilling window, but appears to just go UB just below last csg shoe (BAD), and just above the frac limit in the bend at around 28500 ft MD (BAD).

- 8) Check min flowrate. Min flowrate is 618.7 gpm.
- 9) A trend is that the ECD becomes more "vertical" if the MW is reduced and the pump rate is increased. End up with MW 10.5ppg and pumprate 640 gpm.

ECD is now below FG at all times, and just on the limit of PP at last csg shoe (risky, but OK for now).

10) Check SPP.

This is 7380 psi with 3x12 nozzles, above max surface pressure of 5000 psi.

11) Change to 3x18 bit nozzles.

SPP is now 4485 psi.

- 12) Check min flowrate. This is 625.5 gpm. The set pumprate of 640 gpm will clean the hole sufficiently.
- 13) Check Load summary. WOB is 10 klbf fot rot on bottom (From Scenario 1).

For tripping out the yield strenght and the maximum overpull using % of yield is exceeded.

14) Set rotaional speed while tripping out to be 120 RPM.

Now the issue is gone. The rotary while tripping out reduces the drag force (vis med ligning, jf høyaviksboring)

15) Increase the WOB from 10 to 25 klbf.

S-buckling for slide drilling. Reduce WOB for slide drilling to 10 klbf. No issues.

P.5 MLT2 L2 9 1/2"

Table 28: Suggested parameter values for MLT2 L2 9 1/2"

Table 20. Buggested parameter values for WILT2 IL2 / /2
WOB = 25 klbf
RPM = 195
ROP = 25 ft/hr
Flowrate = 620gpm
MW = 12.1 ppg
New bit nozzle config: 3x(18/32) instead of 3x(12/32)
(Contingency: Tieback 10 3/4" Liner to surface without changing BHA)
Scenario 2 values for slide, back osv.

The iteration process for the MLT2 L2 9 ½" section was as following:

1) Check ECD.

ECD is within drilling window, but could be lower for faster ROP.

2) Check min flowrate.

Min flowrate er 618 gpm.

- 3) Increase pumprate to 600 gpm. Increase RPM to 195 to help cleaning.
- 4) Check ECD again.

Still within drilling window, but a big high.

- 5) Decrease MW to 12.0ppg.
- 6) Check min flowrate.

Min flowrate is 609.3 gpm.

- 7) Increase pumprate to 620 gpm.
- 8) Check ECD.

ECD look fine, but a bit low at last csg shoe. Only 0.05 ppg above PP.

- 9) Increase MW to 12.1 ppg.
- 10) NOw ECD is OK, around 0.15 ppg above PP line.
- 11) Min flowrate is 600.2 gpm, lower than set pumprate of 620 gpm.
- 12) SPP with 3x12 nozzles is 6653.26 psi, higher than max surface pressure of 5000 psi.
- 13) Change to 3x18 nozzles.

Now SPP is 3522.9 psi.

14) Check Load Summary.

No issues for Scenario 1 parameters.

15) Increase to Parameter 2 values.

No issues.

P.6 MLT2 L2 8 1/2"

Table 29: Suggested parameter values for MLT2 L2 8 1/2"

Table 23. Suggested parameter values for WL12 L2 8 72
WOB = 25 klbf
RPM = 195
ROP = 25 ft/hr
Flowrate = 640gpm
MW = 10.8 ppg
Changed BHA.
New bit nozzle config: 6x(18/32) instead of 3x(12/32)
(Contingency: Tieback 10 3/4" Liner to surface without changing BHA)
WOD slide: 3 klbf
Rest WOB parameters Scenario 2.

The iteration process for the MLT2 L2 8 ½" section was as following:

- 1) Start off with Scenario 1 values
- 2) Check ECD

ECD too high, crosses FG line around 25500 ft MD.

3) Reduce MW to 11.1 ppg.

ECD still too high. Crosses the frac limit around 26500 ft MD now.

4) Reduce MW to 10.4 ppg.

Now ECD almost within drilling window, but still a bit too high and crosses the FG towards the bottom.

5) Reduce MW to 9.8 ppg.

Now ECD does not cross the FG line, but will be UB contra the PP line at last csg shoe.

6) Check the min flowrate.

This is 713.3 gpm.

7) Increase pumprate to 680 gpm. Increase RPM to 195 to clean the hole better.

Min flowrate is now 671.5 gpm.

8) Check ECD.

Within for most of the openhole section, but UB below last csg shoe and above the FG towards TD (See figure).

9) Decided to change BHA for this MLT2 L2 8.5in Section.

Conclusion: Should change BHA to get down the rapid changes in the EDC, or underream the hole to 9 1/2". Not suggested to drill this section.

- 10) BHA changed to 8 1/2" assembly in Wellpan library. NOT checked if DP can be delivered by Mærsk Gallant. Not suggested to drill this section.
- 11) Check ECD.

Now there is no sudden jump in the ECD line due to shorter BHA, with 6.5" OD instead of 6.75" OD, reducing the ECD.

Now ECD a bit too low.

12) Increase MW to 10.8 ppg. Flowrate reduced to 640 gpm. Min flowrate needed is 630 gpm.

ECD now within drilling window for most of openhole. Never crosses the FG line, but is UB just below last csg shoe, but better than for last BHA.

Not to recommend still due to UB at last csg shoe.

13) Check SPP.

This is 8251psi with string nozzles 3x12. Too high with respect to max surface pressure of 5000 psi.

14) Change to 3x18nozzles.

Still too high, now SPP of 5274 psi.

15) Change to 6x18 nozzles.

NOw SPP is 4724 psi.

16) Check Load Summary.

With Scenario 1 parameters there is S-buckling for slide drilling.

17) Increase all the parameters to Scenario 2, except slide drilling, which is reduced to 3 klbf (small). No issues.

P.7 MLT3 L1

Table 30: Suggested parameter values for MLT3 L1

Table 50: Suggested parameter values for ML15 L1
WOB = 25 klbf
RPM = 195
ROP = 25 ft/hr
Flowrate = 640 gpm
MW = 10.5 ppg
New bit nozzle config: 3x18
(Contingency: Tieback 10 3/4" Liner to surface without changing BHA)
WOB slide: 5 klbf
WOB back: 20 klbf
Tripping in/out rotation: 0 RPM

The iteration process for the MLT3 L1 section was as following:

- 1) Start off with parameters from Scenario 1.
- 2) Check ECD.

ECD too high. Falls above FG below around 19800 ft MD.

3) Reduce MW to 10.5 ppg.

Now ECD is within the drilling window, but too close to the PP at just below last csg shoe.

- 4) Check min flowrate. Min flowrate is 665.6 gpm for MW 10.5ppg.
- 5) Increase pumprate to 620 gpm. Increase RPM to 195 to increase hole cleaning.

Min flowrate now is 625.5 gpm.

- 6) Check ECD again. Better now. Within the drilling window, with some small margins (too small) at each side.
- 7) Increase pumprate to 630 gpm.

ECD is totally within the drilling window. Margin at TD to FG is around 0.03 ppg (a bit small). Margin to PP at last csg shoe around 0.22 ppg (OK?)

8) Check SPP.

This is 7445 psi with 3x12 nozzles, higher than max surface pressure of 5000 psi.

9) Select 3x18 bit nozzles.

SPP is now 4551 psi.

10) Check load summary.

S-buckling for slide drilling with WOB 10 klbf. Reduce to 5 klbf WOB for slide drilling to remove issue.

11) Increase WOB rot on bot from 10 klbf to 25 kblf.

No issues.

P.8 MLT3 L2 9 1/2"

Table 31: Suggested parameter values for MLT3 L2 9 1/2"

Table 31: Suggested parameter values for ML13 L2 9 ½
WOB = 25 klbf
RPM = 195
ROP = 25 ft/hr
Flowrate = 610 gpm
MW = 12.1 ppg
New bit nozzle config: 3x(18/32) instead of 3x(12/32)
(Contingency: Tieback 10 3/4" Liner to surface without changing BHA)
WOB values: Scenario 2

The iteration process for the MLT3 L2 9 ½" section was as following:

- 1) Start off with Scenario 1 values.
- 2) Check ECD.

ECD within drilling window, but could be closer to PP for faster ROP.

3) Reduce MW to 12.1 ppg.

Now ECD better and closer to PP for faster ROP.

4) Check min flowrate.

This is 640.5 gpm.

5) Increase pumprate to 610 gpm. Increase RPM to 195 for better cleaning.

Min flowrate is now 602 gpm.

6) Check ECD.

Look fine. A margin (trip) of 0.16 ppg above PP at last casing shoe.

7) Check SPP.

This is 6475 psi for 3x12 nozzles, which is above the max of 5000 psi.

8) Change to 3x18 nozzles.

SPP is now 3444 psi.

9) Check Load Summary.

No issues for Scenario 1 WOB values.

10) Increase to Scenario 2 WOB values.

No issues.

P.9 MLT3 L2 8 1/2"

Table 32: Suggested parameter values for MLT3 L2 8 ½"

Table 32: Suggested parameter values for ML13 L2 8 ½
WOB = 25 klbf
RPM = 195
ROP = 25 ft/hr
Flowrate = 500 gpm
MW = 10.7 ppg
New BHA to overcome ECD.
New bit nozzle config: 3x(18/32) instead of 3x(12/32)
(Contingency: Tieback 10 3/4" Liner to surface without changing BHA)
Tripping in RPM: 120 RPM (to overcome S-buckle)
Slide WOB: 0 (not possible)

The iteration process for the MLT3 L2 98 ½" section was as following:

- 1) Start off with Scenario 1 values.
- 2) Check ECD.

The ECD is way too high. Due to the long horizontal section the ECD rises dramatically after the last csg shoe.

3) Reduce MW to 10.8 ppg.

ECD is now around 0.2 ppg above PP at last csg shoe, but rises to cross the FG line around 22000 ft MD.

4) Check min flowrate.

This is 640 gpm.

5) Increase pumprate to 610 gpm and RPM to 195 to help cleaning.

Min flowrate is now 602.3 gpm.

6) Check ECD.

Again ECD is fine from last csg shoe down to around 21800 ft, where the FG is crossed. Recommend NOT to drill this section with this BHA.

- 7) Decided to change BHA. Change to same as for MLT2 L2 8.5in.
- 8) Check ECD. Now better. Almost within drilling window for whole openhole section. Just above FG at TD, and just below PP at last csg shoe.
- 9) Set MW at 10.7 ppg. Set pumprate at 500 gpm. This to get ECD within drilling window. 10) Check ECD.

NOw ECD more or less within drilling window. Never exceed the FG, but no kick margin at TD. At last casing shoe just UB compared to PP (BAD).

However, in order to get this a pumprate of 500 gpm had to be set. Min flowrate is 637.7 gpm, so bed height over 2 inches outside 13 5/8" annulus.

11) Check SPP.

This is 5721 psi, more than max of 5000 psi.

12) Change to 3x18 nozzles.

Now SPP is 3921 psi.

13) Check Load Summary.

S-buckle for borth trip-in and slide.

Set RPM for tripping in to 120 RPM. Set WOB for slide to 0.5 klbf. Still S-buckle. Slide drilling not possible for this section! Uncheck slide drilling.

14) Rest of WOB set to Scenario 2.

No issues.

As it could be seen both MLT2 L2 8 ½" and MLT3 L2 8 ½" showed indications of issues with regards to the circulating pressures and ECD, and the BHA was changed for both wellbores. With the new BHA, due to shorter length and average smaller OD, the challenges partly disappeared, but not fully. In addition, the pipe selected to in Wellplan had not been validaded towards the possible drilling equipment on the rig, Mærsk Gallant.

Appendix Q: Simulation results

In this appendix chapter all the simulations results from all the comparison cases are presented. The evaluation of each of the graphs shown here lead to the evaluation summary sheets displayed and discussed in chapter 8.

Q.1 Effective Tension

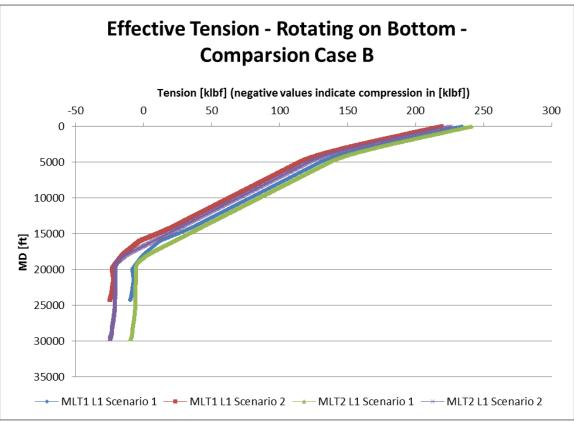


Figure 151: Effective tension scenario 1 and 2 comparison case B (Wellplan 2013a)

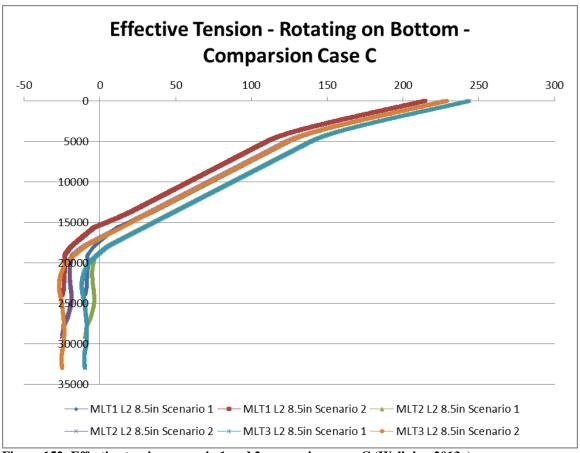


Figure 152: Effective tension scenario 1 and 2 comparison case C (Wellplan 2013a)

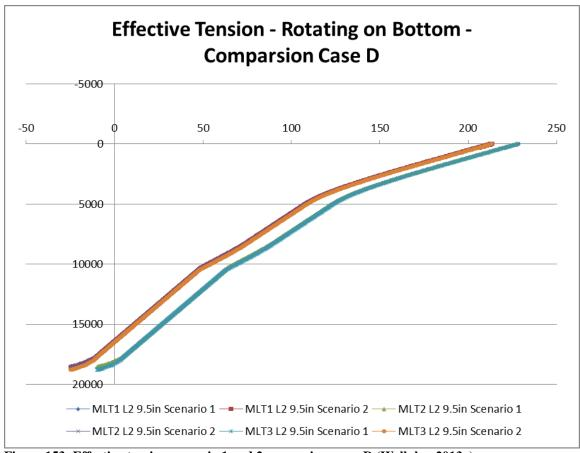


Figure 153: Effective tension scenario 1 and 2 comparison case D (Wellplan 2013a)

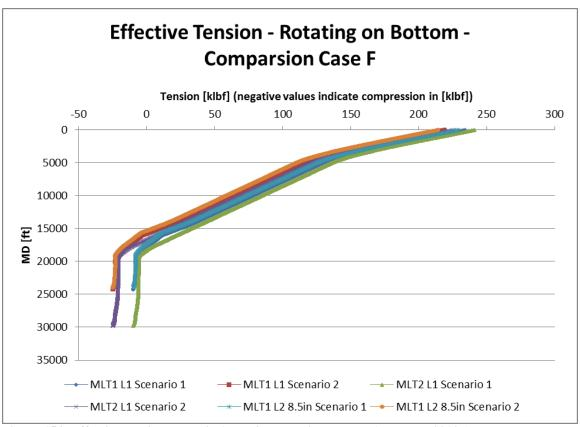


Figure 154: Effective tension scenario 1 and 2 comparison case F (Wellplan 2013a)

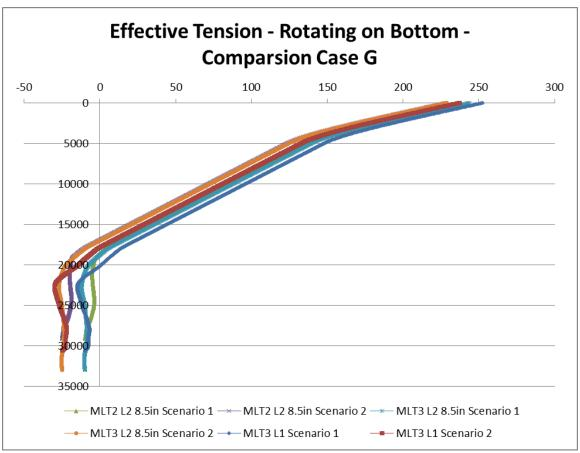


Figure 155: Effective tension scenario 1 and 2 comparison case G (Wellplan 2013a)

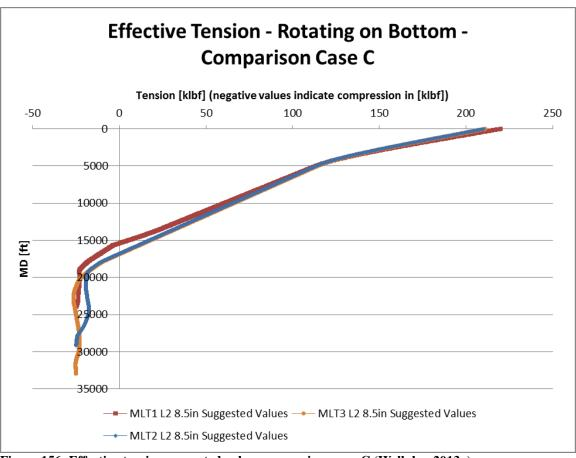


Figure 156: Effective tension suggested values comparison case C (Wellplan 2013a)

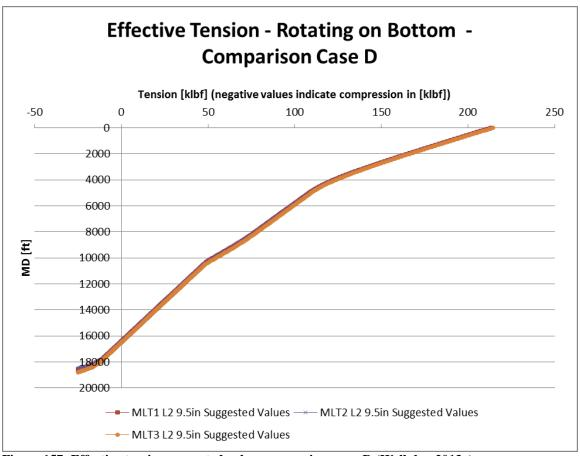


Figure 157: Effective tension suggested values comparison case D (Wellplan 2013a)

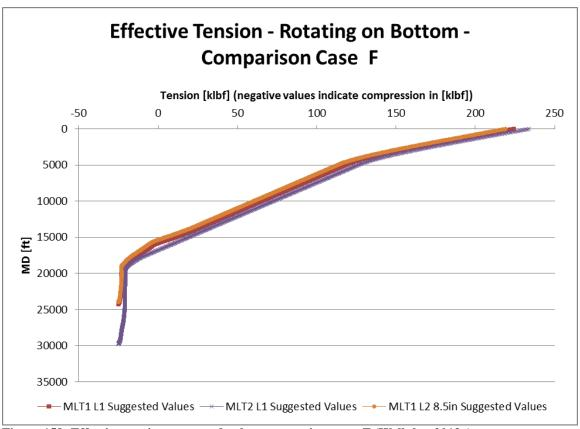


Figure 158: Effective tension suggested values comparison case F (Wellplan 2013a)

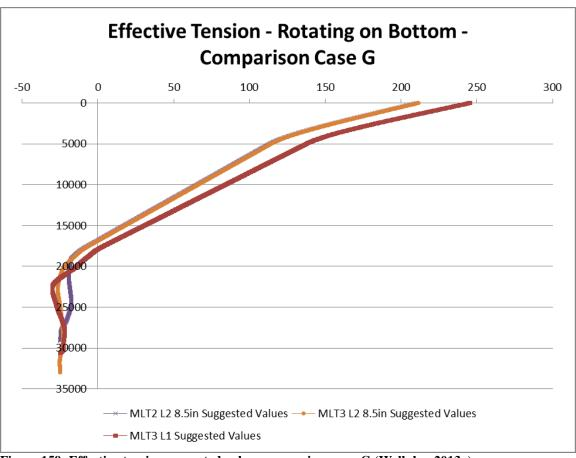


Figure 159: Effective tension suggested values comparison case G (Wellplan 2013a)

Q.2 Torque

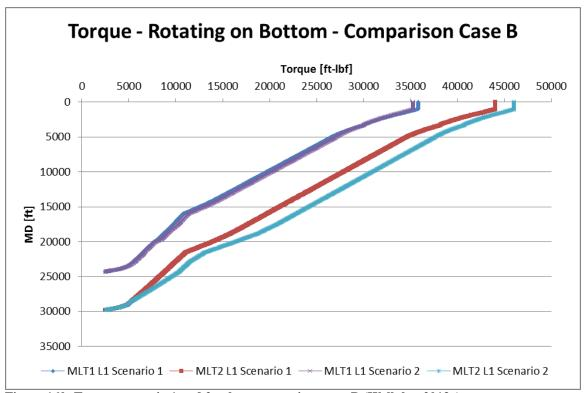


Figure 160: Torque scenario 1 and 2 values comparison case B (Wellplan 2013a)

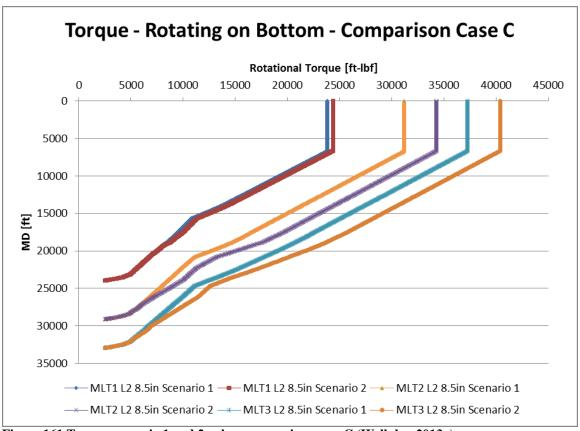


Figure 161 Torque scenario 1 and 2 values comparison case C (Wellplan 2013a)

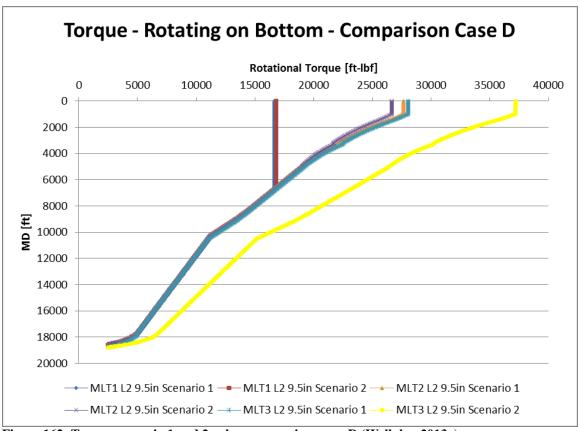


Figure 162: Torque scenario 1 and 2 values comparison case D (Wellplan 2013a)

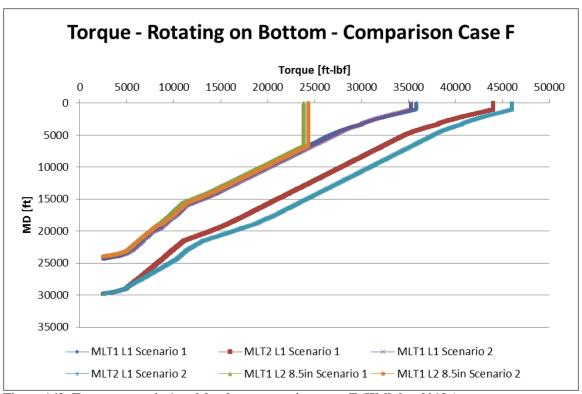


Figure 163: Torque scenario 1 and 2 values comparison case F (Wellplan 2013a)

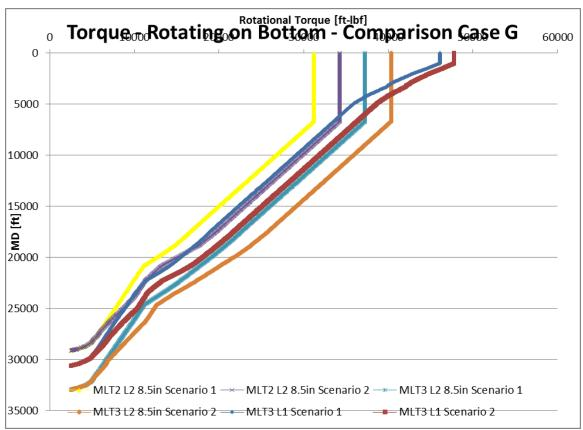


Figure 164: Torque scenario 1 and 2 values comparison case G (Wellplan 2013a)

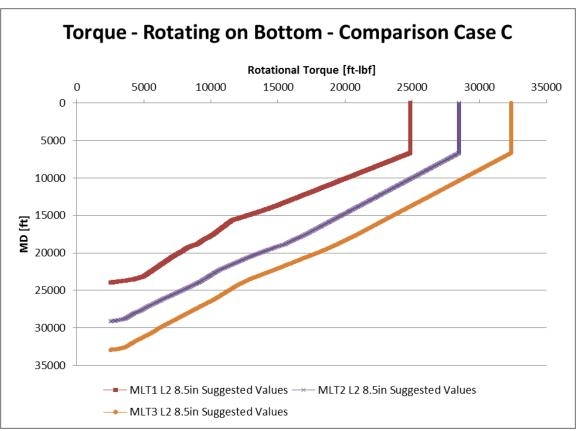


Figure 165: Torque suggested values comparison case C (Wellplan 2013a)

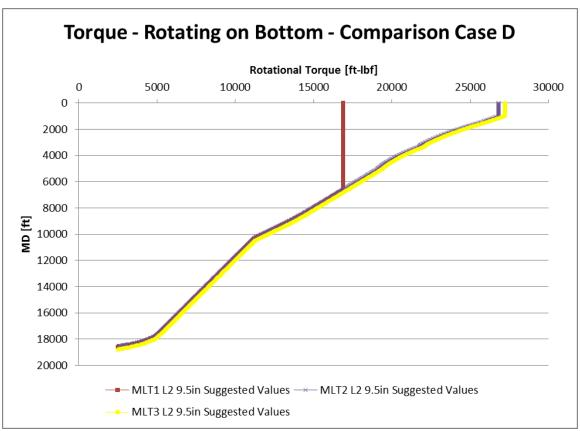


Figure 166: Torque suggested values comparison case D (Wellplan 2013a)

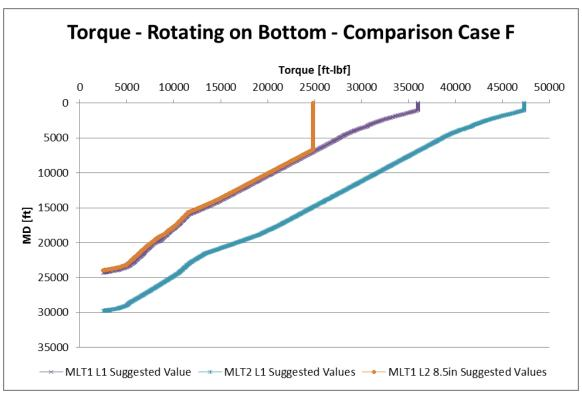


Figure 167: Torque suggested values comparison case F (Wellplan 2013a)

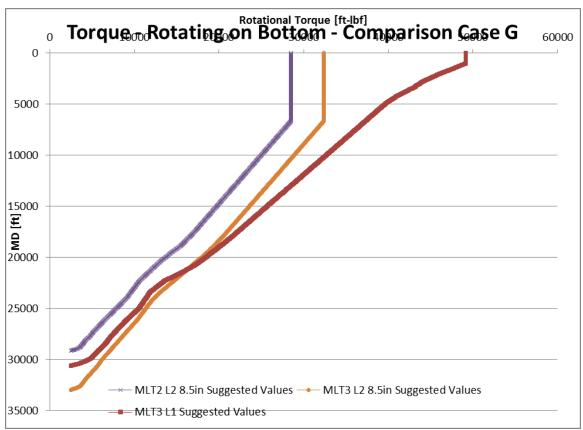


Figure 168: Torque suggested values comparison case G (Wellplan 2013a)

Q.3 Fatigue Ratio

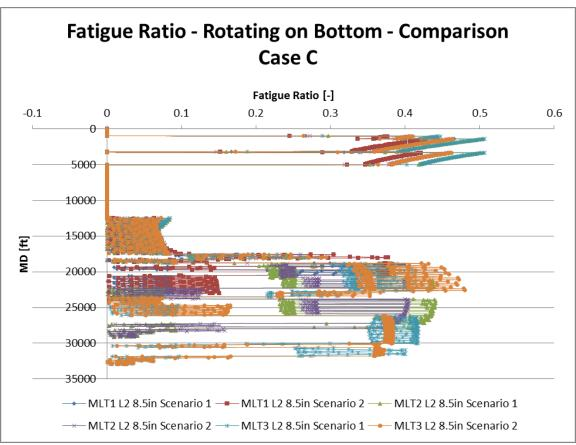


Figure 169: Fatigue ratio scenario 1 and 2 values comparison case C (Wellplan 2013a)

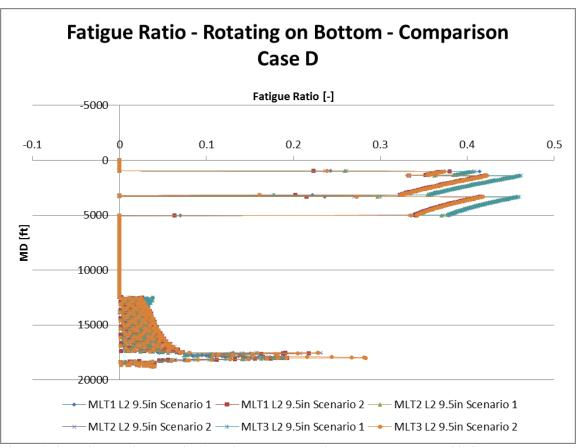


Figure 170: Fatigue ratio scenario 1 and 2 values comparison case D (Wellplan 2013a)

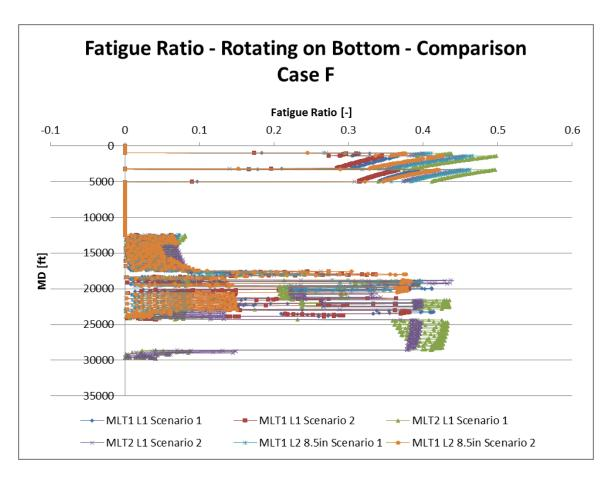


Figure 171: Fatigue ratio scenario 1 and 2 values comparison case F (Wellplan 2013a)

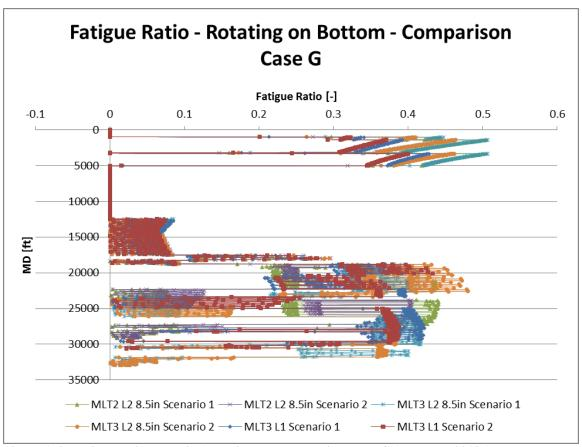


Figure 172: Fatigue ratio scenario 1 and 2 values comparison case G (Wellplan 2013a)

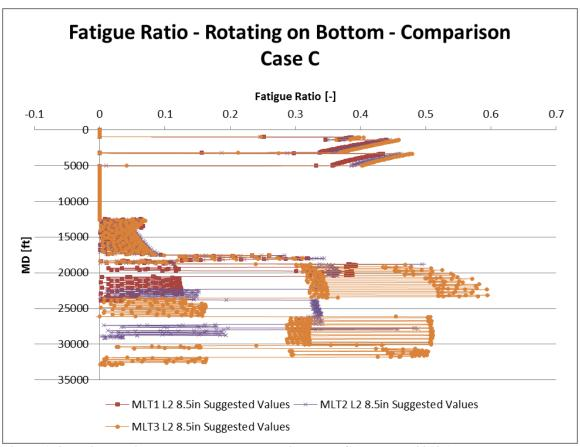


Figure 173: Fatigue ratio suggested values comparison case C (Wellplan 2013a)

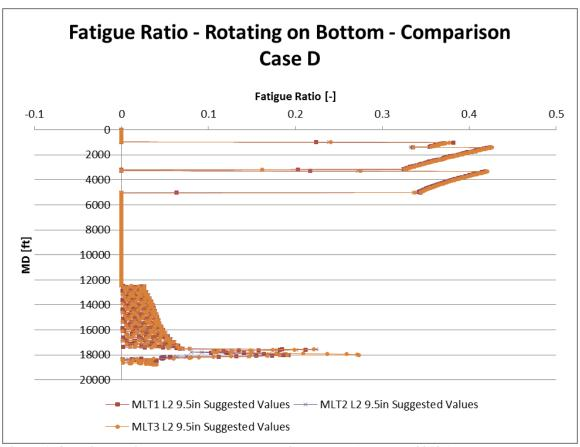


Figure 174: Fatigue ratio suggested values comparison case D (Wellplan 2013a)

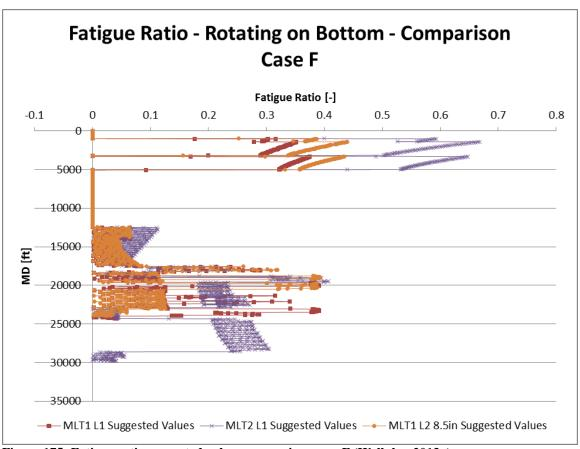


Figure 175: Fatigue ratio suggested values comparison case F (Wellplan 2013a)

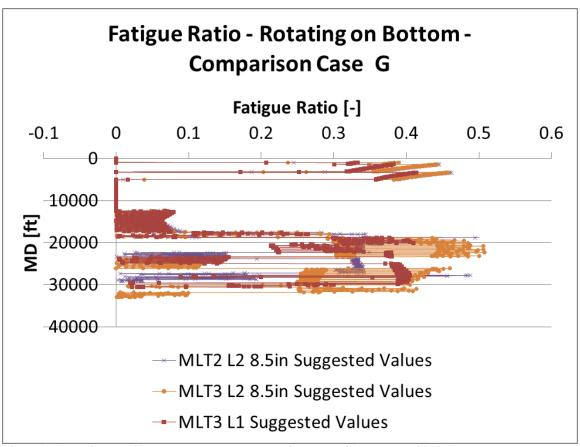


Figure 176: Fatigue ratio suggested values comparison case G (Wellplan 2013a)

Q.4 Hook Load

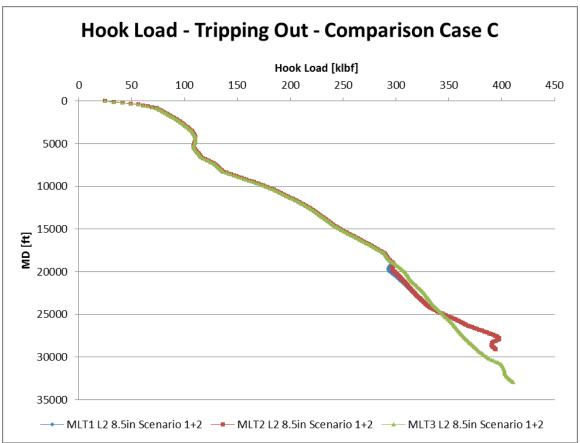


Figure 177: Hook load scenario 1 and 2 values comparison case C (Wellplan 2013a)

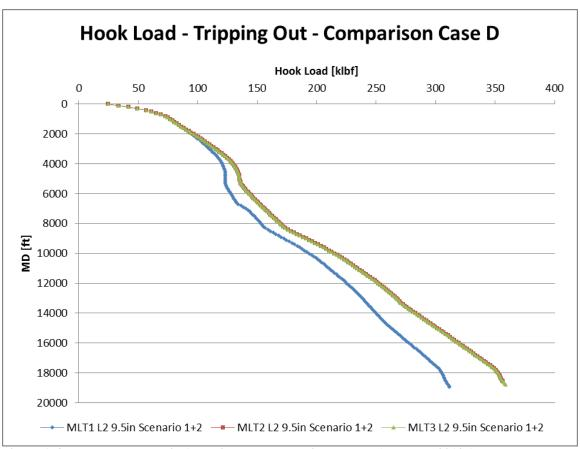


Figure 178: Hook load scenario 1 and 2 values comparison case D (Wellplan 2013a)

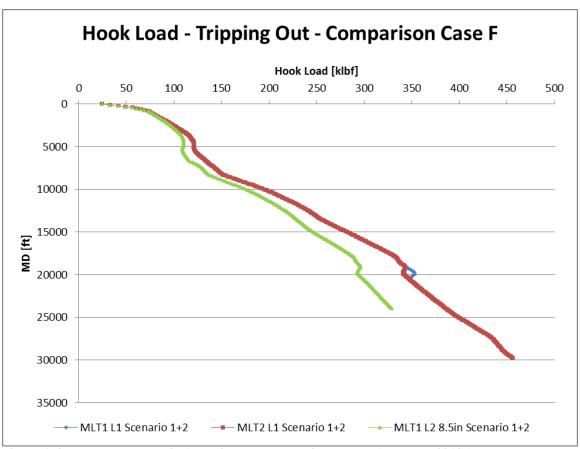


Figure 179: Hook load scenario 1 and 2 values comparison case F (Wellplan 2013a)

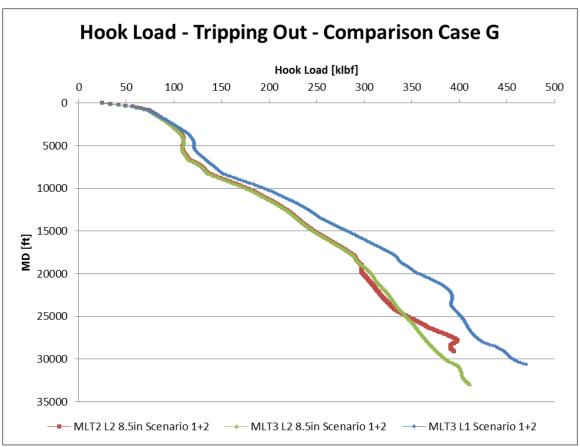


Figure 180: Hook load scenario 1 and 2 values comparison case G (Wellplan 2013a)

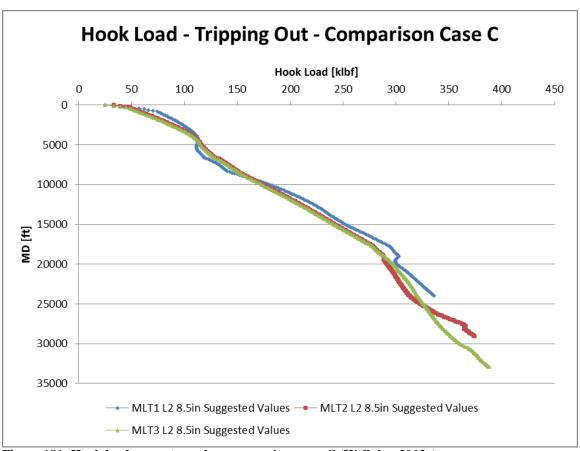


Figure 181: Hook load suggestev values comparison case C (Wellplan 2013a)

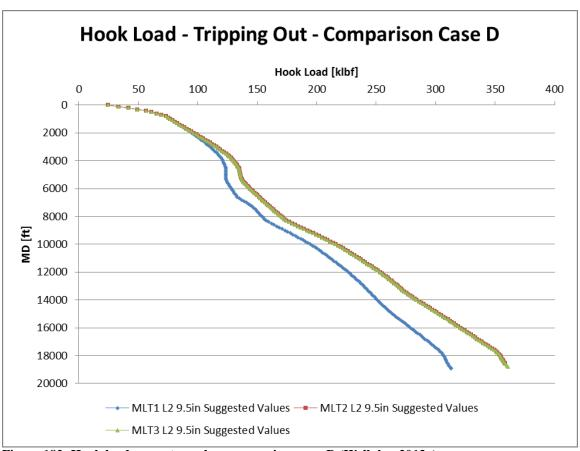


Figure 182: Hook load suggestev values comparison case D (Wellplan 2013a)

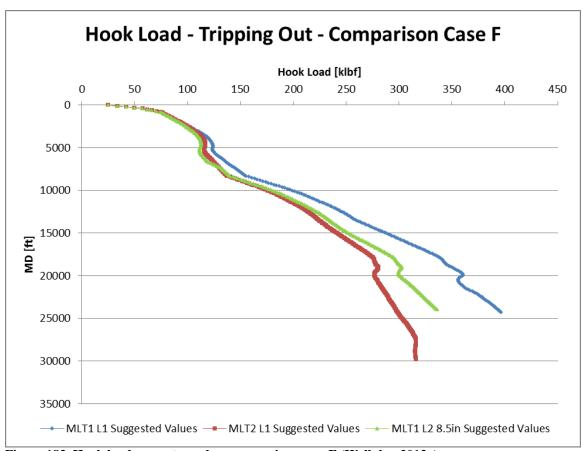
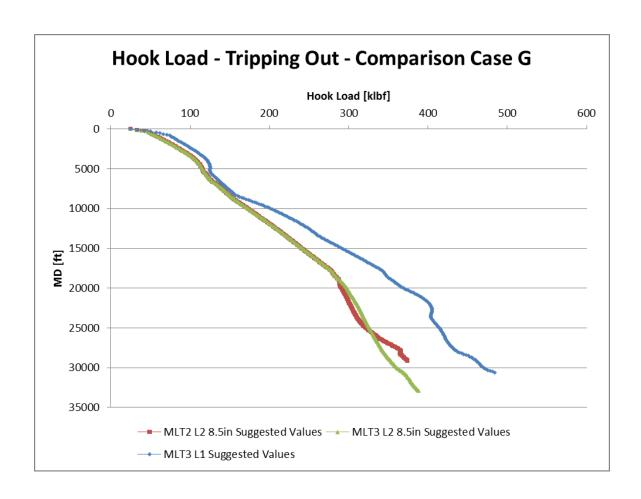


Figure 183. Hook load suggestev values comparison case E (Wellplan 2013a)



Q.5 Torque vs MD, Minimum WOB and Hole Cleaning

Based on the amount of figures in this report the simulation results for these effects were decided to taken out. The Torque is already given in Q.2, the minimum WOB not indicated to be an issue for any of the wellbores for rotating on bottm and the hole cleaning given by the 13 5/8" annulus in all wellbore sections. Due to this all of these drilling effects were not presented in this appendix. All graphs, however, can be given based upon request.

Q.6 Pressure Losses

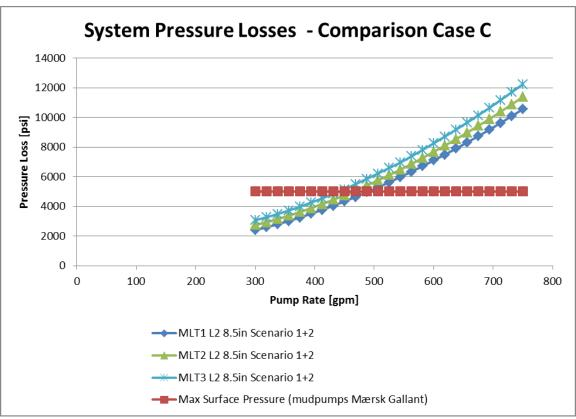


Figure 184: Pressure losses scenario 1 and 2 values comparison case C (Wellplan 2013a)

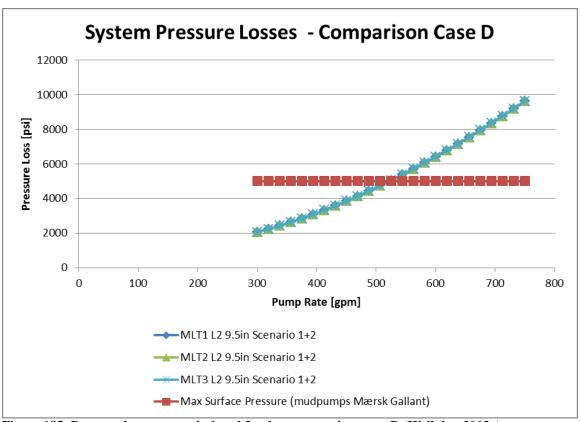


Figure 185: Pressure losses scenario 1 and 2 values comparison case D (Wellplan 2013a)

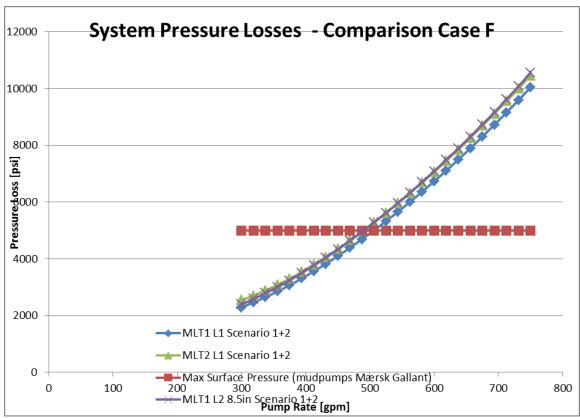


Figure 186: Pressure losses scenario 1 and 2 values comparison case F (Wellplan 2013a)

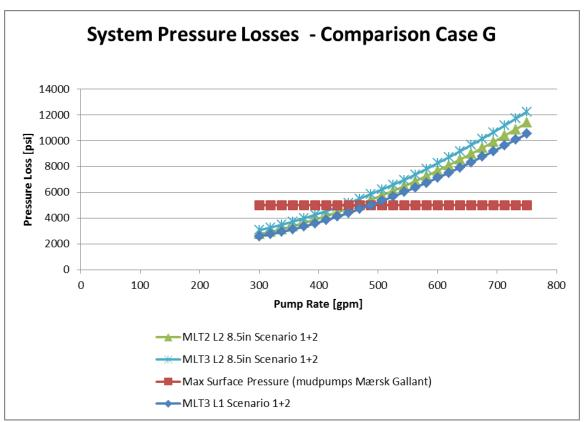


Figure 187: Pressure losses scenario 1 and 2 values comparison case G (Wellplan 2013a)

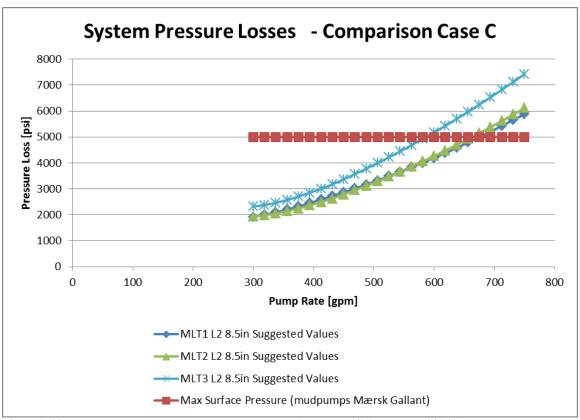


Figure 188: Pressure losses suggested values comparison case C (Wellplan 2013a)

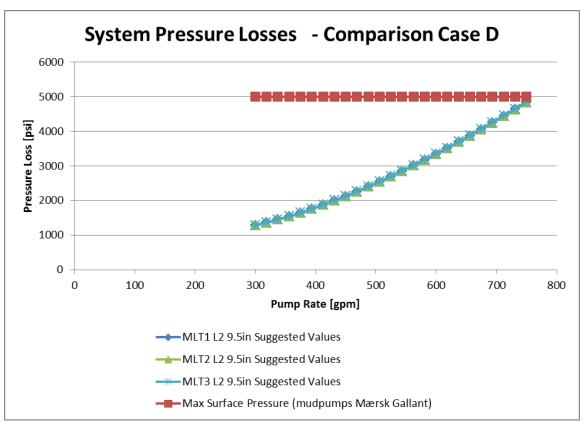


Figure 189: Pressure losses suggested values comparison case D (Wellplan 2013a)

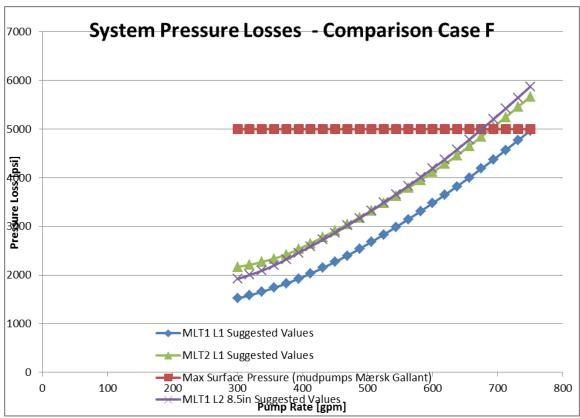


Figure 190: Pressure losses suggested values comparison case F (Wellplan 2013a)

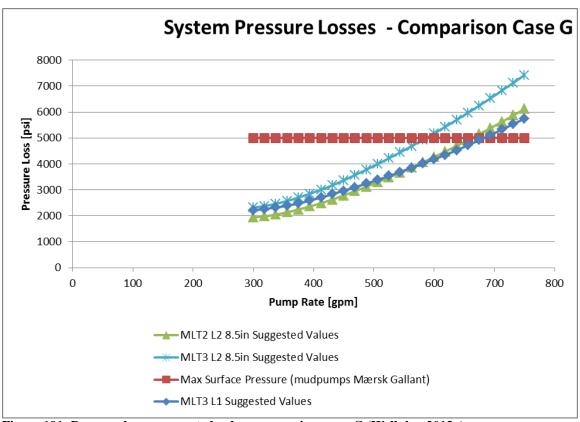


Figure 191: Pressure losses suggested values comparison case G (Wellplan 2013a)

Q.7 ECD and Circulating Pressures

In order to reduce the number of figures in the report only ECD effects are shown in this Appendix.

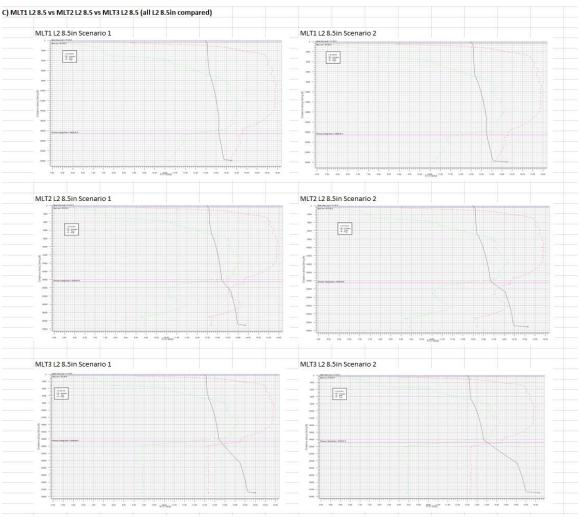


Figure 192: ECD for scenario 1 and 2 values comparison case C (Wellplan 2013a)

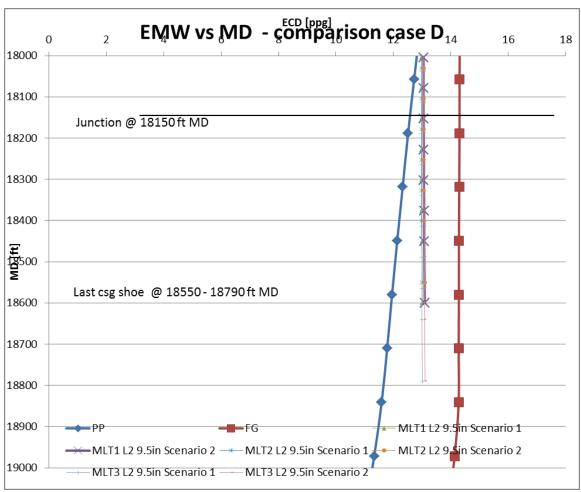


Figure 193: ECD for scenario 1 and 2 values comparison case D (Wellplan 2013a)

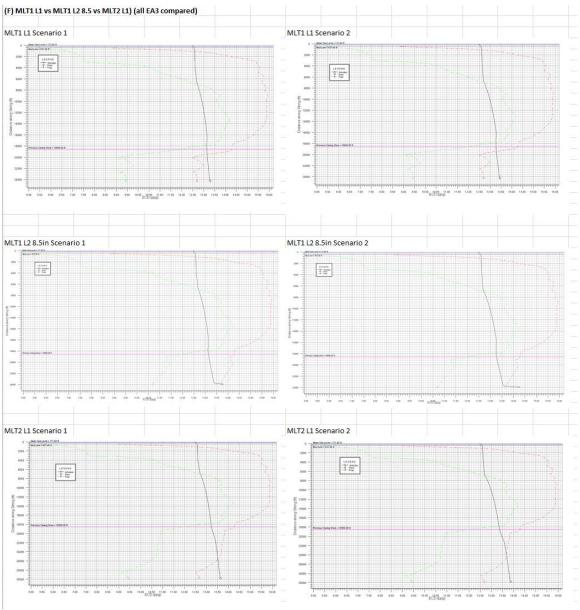


Figure 194: ECD for scenario 1 and 2 values comparison case F (Wellplan 2013a)

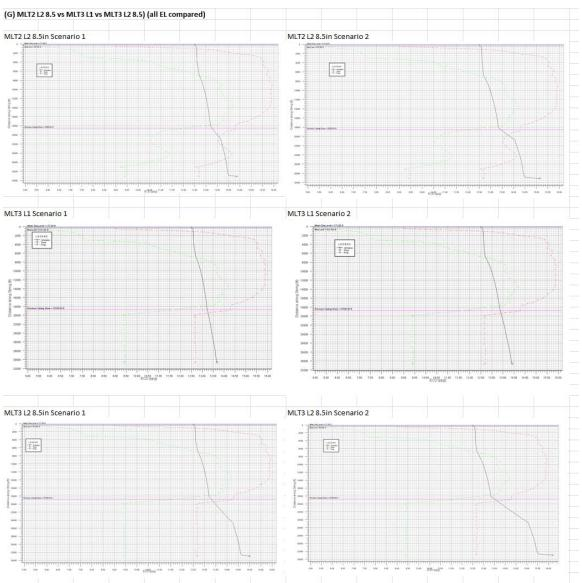


Figure 195: ECD for scenario 1 and 2 values comparison case G (Wellplan 2013a)

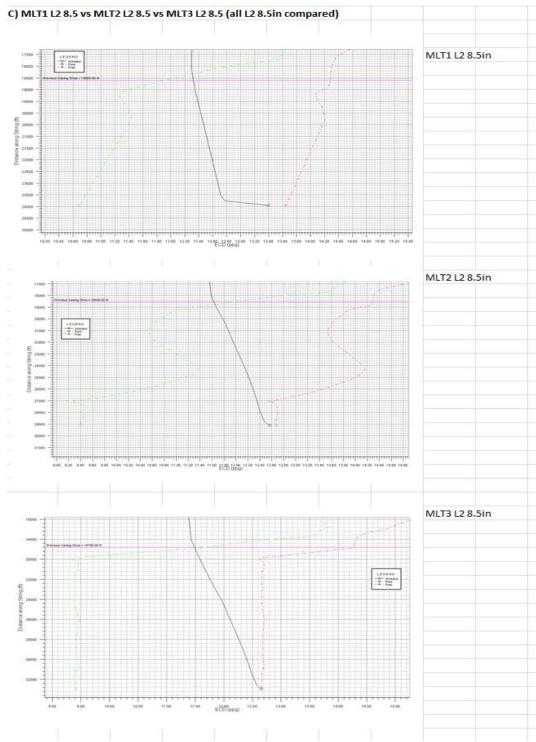


Figure 196: ECD for suggested values comparison case C (Wellplan 2013a)

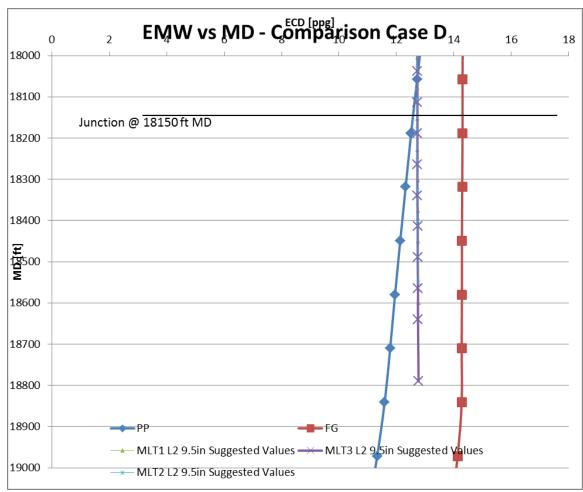


Figure 197: ECD for suggested values comparison case D (Wellplan 2013a)

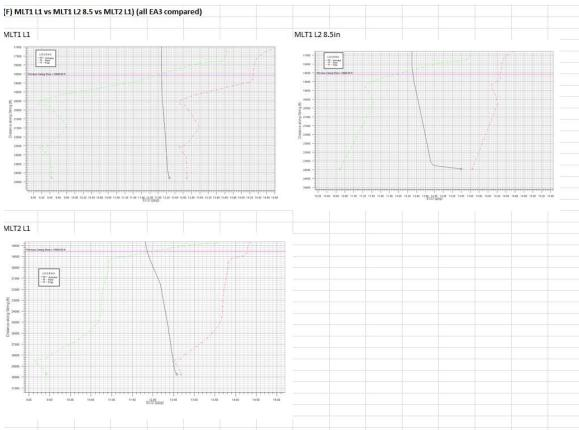


Figure 198: ECD for suggested values comparison case F (Wellplan 2013a)

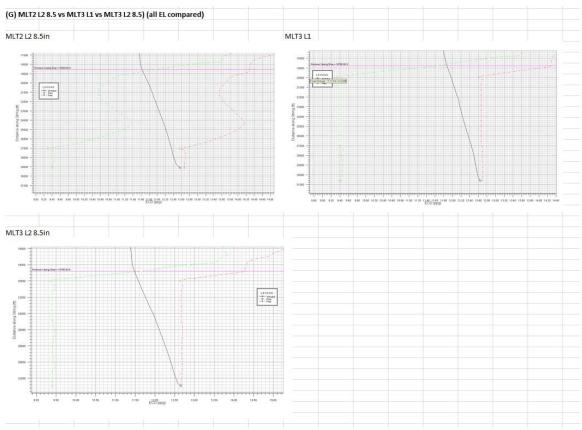


Figure 199: ECD for suggested values comparison case G (Wellplan 2013a)

Appendix R: Ekofisk South

The Ekofisk south project has a net present value of 29 050 million NOK. The first production in the area is expected in December 2013, while the first water injection, via the 2/4-VB, came in June 2013, although not scheduled until September 2013 (Maxwell 2013). The licence in the area expires in 2028, but the estimated have showed production until 2049. In order to ensure optimal long-term development and hydrocarbon recovery, the PL 018 licensees have designed the Ekofisk South facilities to maximize resources and value over the field life without regard for short-term value maximization within the current license period (ConocoPhillips 2013f).

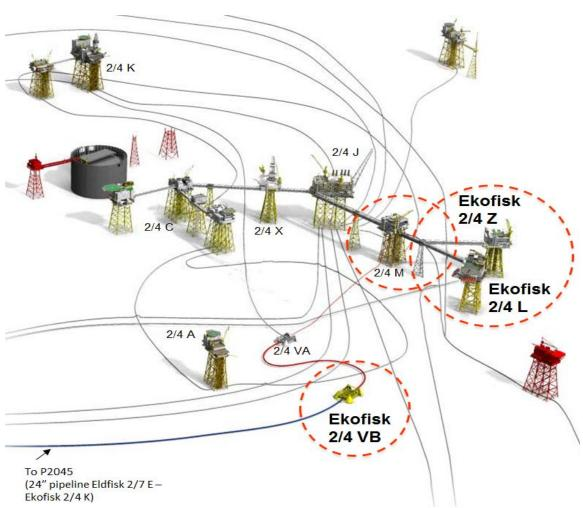


Figure 200: Project scope of the current ongoing development of the Ekofisk South area (ConocoPhillips 2013f)

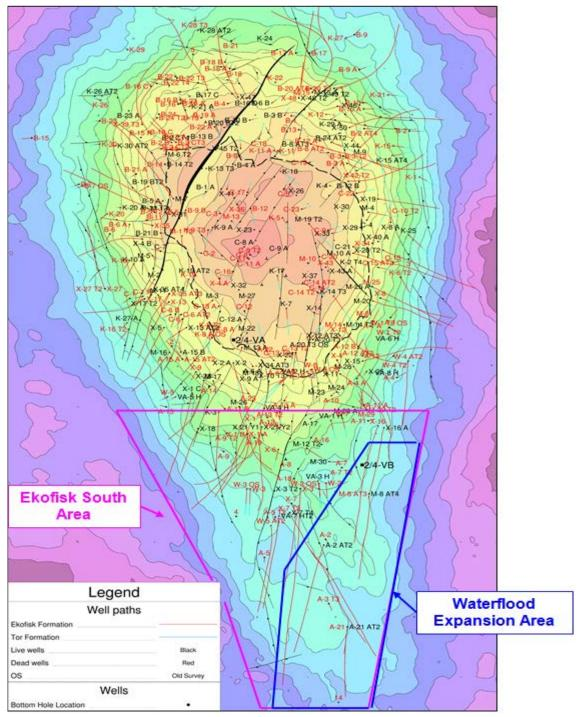


Figure 201: Map showing the Ekofisk south area, with the waterflood expansion area marked in blue (ConocoPhillips 2013f)

APPENDIX S: Mudpump configurations

The mud pump currently available on Mærsk Gallant is marked with bold letters in the table below. The maximum mud pump pressure is 5000 psi, with a maximum displacement of 1.215 gpm with liner of 9" (American Manufacturing 2012).

Table 33: The F-series mudpumps for the manufacturer EMSCO (Sunry Petro)

Table 35. The 1-series madpaints for the manufacturer EMSCO (Sum y 1 ctro)						
Model	F-500	F-800	F-1000	F-1300	F-1600	FC-2200
Max. liner size x	170x191	170x229	170x254	180x305	180x305	203x356
stroke (mm)						
Rating strokes	165	150	140	120	120	105
(rpm)						
Rating Power	373(500)	596(800)	746(1000)	969(1300)	1193(1600)	1640(2200)
KW (HP)						
Gear Ratio	4.286 : 1	4.185 : 1	4.207 : 1	4.206 : 1	4.206 : 1	3.521:1
Lubricating	Pressure and Splash					
System						
Suction Inlet	8"	10"	12"	12"	12"	12"
Flange						
Discharge	4"	5"	5"	5"	5"	5"
Outlet Flange						
Diameter of	139.7	177.8	196.9	215.9	215.9	254
Pinion Shaft						
mm						
Weight (Kg)	9770	14500	18790	24572	24791	38460